QUANTITATIVE MAGNETIC RESONANCE IMAGING AND NEUROPATHOLOGY OF THE HIPPOCAMPUS IN TEMPORAL LOBE EPILEPSY

Wim Van Paesschen, MRCP(UK)

EPILEPSY RESEARCH GROUP,
UNIVERSITY DEPARTMENT OF CLINICAL NEUROLOGY,
NATIONAL HOSPITAL FOR NEUROLOGY AND NEUROSURGERY,
QUEEN SQUARE,

DEPARTMENT OF NEUROPATHOLOGY,
INSTITUTE OF NEUROLOGY,

NMR UNIT,
GREAT ORMOND STREET HOSPITAL FOR CHILDREN,
GUILFORD STREET,

LONDON.

THESIS SUBMITTED TO THE UNIVERSITY OF LONDON FOR THE DEGREE OF DOCTOR IN PHILOSOPHY, 1997

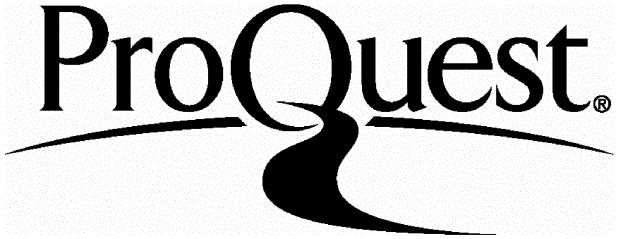

Errata.

- p 19: list of abbreviations: CSE: convulsive status epilepticus
- p 76, table 5, number 33: HCVR should be 0.83 and not 1
- p 155, legend to Figure 43, second paragraph, 15th line: "E compares RHC_B..." should read "F compares RHC_B..."
- p 207, reference: "Grünewald, R.A., Farrow, T.F.D., Mundy, J.V.B., Rittey, C., and Sagar, H.J. Preliminary results of university of Sheffield study of complicated early childhood convulsion. *Epilepsia* 37:125, 1996. (Abstract)" should read: "Grünewald, R.A., Farrow, T.F.D., Mundy, J.V.B., Rittey, C., and Sagar, H.J. Preliminary results of university of Sheffield study of complicated early childhood convulsion. *Epilepsia* 37 (suppl 5):125, 1996. (Abstract).
- p 219, reference: " VanLandingham, K.E., Tien, R.D., Cavazos, J.E., Heinz, E.R., and Lewis, D.V. MRI hippocampal volume and signal abnormalities following complex febrile convulsions. *Epilepsia* 37:113, 1996. (Abstract)" should read: "VanLandingham, K.E., Tien, R.D., Cavazos, J.E., Heinz, E.R., and Lewis, D.V. MRI hippocampal volume and signal abnormalities following complex febrile convulsions. *Epilepsia* 37 (suppl 5):113, 1996. (Abstract).

Addendum: My own contribution to the present work.

The initial aim of the present work was to validate hippocampal T2 relaxation time measurements of the hippocampus with quantitative neuropathology, and to correlate hippocampal T2 relaxation time measurement with hippocampal volumetry. My own contribution was to work out the methodology of the quantitative neuropathological study, and to work out a systematic approach for the study of the hippocampus combining hippocampal volume ratios, absolute hippocampal volumes corrected for intracranial volume, hippocampal T2 relaxation time measurements and an hippocampal volume distribution graph. My idea was to study the hippocampi in a large group of patients and to correlate these findings with clinical data in addition to the neuropathological validation. It was my idea to work out the amygdala T2 mapping, to integrate this with the rest of the work and to correlate this with clinical data. I suggested to study patients with intractable temporal lobe epilepsy with normal hippocampi and amygdala with magnetic resonance spectroscopy. I planned to correlate quantitative MRI of hippocampus and amygdala with pathology and clinical data as much as possible. The correlation of the auras with amygdala pathology (not presented in this work) was my idea. I also worked out the methodology of the longitudinal study.

The following papers have been published or accepted for publication since the time of submission of the thesis in February 1997.

1. Van Paesschen W, Duncan JS, Stevens JM, Connelly A. A quantitative hippocampal MRI study of newly diagnosed partial seizures in adults: worse early prognosis for patients with hippocampal sclerosis. **Neurology**: in Press.

2. Van Paesschen W, Revesz T, Duncan JS. Corpora amylacea in hippocampal sclerosis. **J Neurol Neurosurg Psychiatry**: in Press.

3. Van Paesschen W. Quantitative magnetic resonance imaging of mesial temporal structures in temporal lobe epilepsy. **Epilepsia**: in Press.

4. Van Paesschen W, Duncan JS, Connelly A. A comparison of the neuropathological effects of vigabatrin and carbamazepine in patients with newly diagnosed localization-related epilepsy using MR-based cerebral T2 relaxation time measurements. **Epilepsy Res**: in Press.

5. Van Paesschen W, Revesz T, Duncan JS, King MD, Connelly A. Quantitative neuropathology and quantitative magnetic resonance imaging of the hippocampus in temporal lobe epilepsy. **Ann Neurol** 1998; 43: in Press.

6. Vargha-Khadem F, Gadian DG, Watkins KE, Connelly A, Van Paesschen W, Mishkin M. Differential effects of early hippocampal pathology on episodic and semantic memory. **Science** 1997; 277: 376-380.

7. Baxendale SA, Van Paesschen W, Thompson PJ, Duncan JS, Harkness WF, Shorvon SD. Hippocampal cell loss and gliosis: relationship to pre and postoperative memory function. **Neuropsychiatry, neuropsychology and behavioral neurology**: in Press.

8. Baxendale SA, Van Paesschen W, Thompson PJ, Connelly A, Duncan JS, Shorvon SD. Quantitative MRI measures of hippocampal structure as predictors of sodium amytal test performance. **Epilepsia**: in Press.

9. Koepp MJ, Richardson MP, Labbe C, Cunningham VJ, Ashburner J, Van Paesschen W, Revesz T, Brooks DJ, Duncan JS. 11C-Flumazenil PET, volumetric MRI and quantitative pathology in mesial temporal lobe epilepsy. **Neurology** 1997: in press.

10. Koepp MJ, Richardson MP, Brooks DJ, Van Paesschen W, Labbe C, Duncan JS. Regional hippocampal 11C-flumazenil PET in temporal lobe epilepsy with unilateral and bilateral hippocampal sclerosis. **Brain** 1997: in press.

11. Hand K, Baird V, Bowery NG, Duncan JS, Revesz T, Van Paesschen W. Quantitative hippocampal neuropathology and central benzodiazepine receptor autoradiography. **Br J Pharmacol**: in press.

Antwerpen, 24/8/97.

ABSTRACT.

Background. Hippocampal sclerosis (HS) is the most common cause of intractable temporal lobe epilepsy (TLE). Hippocampal atrophy and an increased T2-weighted signal are MRI characteristics of HS. MRI-based hippocampal volume (HCV) and hippocampal T2 (HCT2) measurement allow a quantitative description of HS.

Aims. 1. to establish a 3-D microscopic counting technique to quantify neuronal and glial cell densities of hippocampal neuronal cell layers, 2. to correlate these densities with HCT2 and HCV, 3. to describe the spectrum of HS, 4. to establish amygdala T2 (AT2) mapping and its clinical correlations, 5. to evaluate single voxel proton magnetic resonance spectroscopy in MRI-negative intractable TLE, 6. to establish MRI-based etiologies of newly diagnosed localization-related epilepsy, 7. to conduct a prospective, longitudinal quantitative MRI study of the patients with newly diagnosed epilepsy to elucidate the etiology and pathogenesis of HS.

Methods. A total of 207 patients with localization-related epilepsy and 39 control subjects were studied. Seventy-nine of these patients underwent surgery for intractable localization-related epilepsy. MR imaging, including HCT2 and AT2 maps, images for HCV studies, FLAIR, and MR spectroscopy (MRS) were obtained on a 1.5 T Siemens SP63 Magnetom scanner. For the neuropathological studies, a 3-D counting technique was used.

Results. HCT2 was related to damage in the CA1 and the hilus, and HCV to damage in CA1-CA3 and the hilus. In a group of 100 patients with intractable TLE (foreign tissue lesions excluded), 5% had anterior HS, about 50% unilateral diffuse HS, 10% bilateral diffuse HS, 20% an isolated amygdala abnormality and 6 of 7 patients with apparent MRI-negative TLE had an abnormality on MRS. Ten percent of 63 patients with newly diagnosed localization-related epilepsy had HS, and 14% had other MRI abnormalities. The early prognosis of patients with HS was worse with respect to seizures compared with patients with other MRI findings. Progressive MRI-based hippocampal changes were detected in 3 patients after one year.

Conclusion. This study validates the neuropathological basis of quantitative hippocampal MRI and its use in the study of patients with epilepsy.

ACKNOWLEDGMENTS

The work for this thesis was conducted under the supervision of Dr John S Duncan, MA, DM, FRCP, Reader in Neurology at the National Hospital for Neurology, Alan Connelly, PhD, Senior Lecturer in MR physics at the Great Ormond Street Hospital for Children and Tamas Revesz, MRCPath, consultant neuropathologist at the Institute of Neurology. I am deeply grateful for their direction, expert advice, motivation and friendship.

I would like to thank Cheryl L Johnson, radiographer at the Great Ormond Street Hospital for Children, for her outstanding work in scanning all patients in this study, for her wonderful dedication, the several Saturdays of additional scanning, and her friendship; Martin D King, PhD, MR physicist at the Royal College of Surgeons Unit of Biophysics at the Institute of Child Health for his thorough and outstanding statistical advice; Dr John M Stevens, FRCR, consultant neuroradiologist, for his contribution in the visual assessment of several of the MRI scan as part of this work; Dr Graeme D Jackson, consultant neurologist, for his advice and enthusiasm, and for his work that forms a large part of the background of the present work; Dr RA Grünewald, senior registrar in neurology, who was my predecessor and whose work was also part of the background of this work; Steve Durr for his help with the photographic reproductions, Robert and Lillian for their contribution in the histopathological processing of the hippocampal sections, Prof JJ Martin for providing a control hippocampus, Dr Clifford Jack for his advice on the MR-based intracranial volume measurement, Irene Buvat and Chloe Hutton for their help with the Sun Workstation, and all the members of the Epilepsy Research Group at the National Hospital for Neurology.

This work was made possible by grants of Action Research and the Wellcome Trust, whose support is gratefully acknowledged.

Last but not least, I thank my parents for their love and support and my wife Nadine for her love, understanding, patience and encouragement.

AWARDS

Founders Award of the American Academy of Neurology to the value of $1,000 for the manuscript :"Amygdala T2 mapping in intractable temporal lobe epilepsy: a quantitative MRI study", San Francisco, 1996.

GRANTS

Travel grant of the Guarantors of Brain to the value of £500 to present the paper "Quantitative MRI in temporal lobe epilepsy and hippocampal sclerosis" at the American Academy of Neurology meeting, Washington, 1994.

Travel Grant of the European Neurological Society to the value of 500 SFr to present the paper "T2 relaxometry and volumetrics of the hippocampus in the preoperative evaluation of intractable temporal lobe epilepsy" at the European Neurological Society meeting, Barcelona, 1994.

Travel grant of the Guarantors of Brain to the value of £300 to present the paper "Amygdala T2 mapping in intractable temporal lobe epilepsy: a quantitative MRI study" at the American Academy of Neurology meeting, San Francisco, 1996.

ORIGINAL ARTICLES

1. Van Paesschen W, Sisodiya S, Connelly A, Duncan JS, Free SL, Raymond AA, Grünewald RA, Revesz T, Shorvon SD, Fish DR, Stevens JM, Johnson CL, Scaravilli F, Harkness WFJ, Jackson GD. Quantitative hippocampal MRI and intractable temporal lobe epilepsy. **Neurology** 1995; 45: 2233-2240.

2. Van Paesschen W, Connelly A, Johnson CL, Duncan JS. The amygdala and intractable temporal lobe epilepsy. A quantitative magnetic resonance imaging study. **Neurology** 1996; 47: 1021-1031.

3. Van Paesschen W. Magnetisch Resonantie Imaging en epilepsie chirurgie. **Neurone** 1996; 1: 15-22.

4. Van Paesschen W, Connelly A, King MD, Jackson GD, Duncan JS. The spectrum of hippocampal sclerosis: a quantitative magnetic resonance imaging study. **Ann Neurol** 1997; 41: 41-51.

5. Van Paesschen W, Revesz T, Duncan JS, King MD, Connelly A. Quantitative neuropathology and quantitative magnetic resonance imaging of the hippocampus in temporal lobe epilepsy. Submitted.

6. Koepp MJ, Richardson MP, Brooks DJ, Poline JB, Van Paesschen W, Friston KJ, Duncan JS. Cerebral benzodiazepine receptors in hippocampal sclerosis: an objective in vivo analysis. **Brain** 1996: 119; 1677-1687.

7. Van Paesschen W, Duncan JS, Stevens JM, Connelly A. A quantitative hippocampal MRI study of newly diagnosed localization-related epilepsies in adults: worse early prognosis for patients with hippocampal sclerosis. Submitted.

8. Van Paesschen W, Connelly A, Stevens JM, Duncan JS. A quantitative hippocampal MRI study of newly diagnosed localization-related epilepsies in adults: one year follow-up results. Submitted.

9. Van Paesschen W, Connelly A, Duncan JS. Sampling strategies for MR hippocampal volumetry. Submitted.

ABSTRACTS

1. Van Paesschen W, Grünewald RA, Duncan JS, Connelly A, Jackson GD, Sisodiya S, Raymond AA, Shorvon SD, Fish DR, Stevens JM. Quantitative MRI in temporal lobe epilepsy and hippocampal sclerosis [abstract]. **Neurology** 1994; 44 (suppl 2): 350. American Academy of Neurology meeting, Washington DC., 1994.

2. Van Paesschen W, Grünewald R, Duncan JS, Connelly A, Jackson GD, Sisodiya S, Raymond AA, Shorvon SD, Fish DR, Stevens JM. T2 relaxometry and volumetrics of hippocampus in the preoperative evaluation of intractable temporal epilepsy [abstract]. **J Neurol** 1994; 241 (suppl 1): S87. European Neurological Society meeting, Barcelona, 1994.

3. Van Paesschen W, Jackson GD, Grünewald R, Connelly A, Duncan JS. T2 mapping can provide quantitative information on both T2 signal change and atrophy in the hippocampus of patients with intractable temporal lobe epilepsy [abstract]. **Epilepsia** 1994; 35 (suppl 7): 30. European Congress of Epileptology, Oporto, 1994.

4. Van Paesschen W, Sisodiya S, Raymond AA, Grünewald RA, Duncan JS, Connelly A, Jackson GD, Shorvon SD, Fish DR, Stevens JM. The combination of T2 relaxometry and volumetrics of the hippocampus identifies clinically useful subgroups of patients with intractable temporal lobe epilepsy [abstract]. **Epilepsia** 1994; 35 (suppl 7): 30. European Congress of Epileptology, Oporto, 1994.

5. Van Paesschen W, Baxendale S, Thompson PJ, Duncan JS. Carotid amobarbital memory test in a patient with bilateral hippocampal sclerosis [abstract]. **Epilepsia** 1994; 35 (suppl 7): 49. European Congress of Epileptology, Oporto, 1994.

6. Van Paesschen W, Revesz T, Duncan JS, Connelly A, Harkness WFJ, Sisodiya S, Raymond AA, Jackson GD, Alsanjari N, Shorvon SD, Fish DR. Quantitative neuropathology and quantitative MRI of hippocampal sclerosis [abstract]. **Epilepsia** 1994; 35 (suppl 8): 19. American Epilepsy Society meeting, New Orleans, 1994.

7. Duncan JS, Van Paesschen W, Johnson CL, Connelly A. T2 relaxometry of the amygdala in temporal lobe epilepsy [abstract]. **Epilepsia** 1994; 35 (suppl 8): 22. American Epilepsy Society meeting, New Orleans, 1994.

8. Van Paesschen W, Revesz T, Sisodiya S, Connelly A, Jackson GD, Duncan JS. Quantitative neuropathology and quantitative magnetic resonance imaging of the hippocampus of patients with intractable temporal lobe epilepsy [abstract]. **Epilepsia** 1995; 36 (suppl 3): 96. International Epilepsy congress, Sidney, 1995.

9. Van Paesschen W, Connelly A, Johnson CL, Duncan JS. Clinical and pathological correlations of amygdala T2 mapping [abstract]. **Epilepsia** 1995; 36 (suppl 3): 247. International Epilepsy congress, Sidney, 1995.

10. Van Paesschen W, Connelly A, Johnson CL, Duncan JS. Bilateral hippocampal sclerosis: a quantitative MRI study [abstract]. **Proc. Soc. Magn. Res.** 1995; 2: 1231. SMR-ESMRMB meeting, Nice, 1995.

11. Van Paesschen W, Connelly A, Johnson CL, Duncan JS. Amygdala T2 mapping in patients with MRI-negative intractable temporal lobe epilepsy [abstract]. **Proc. Soc. Magn. Res.** 1995; 1: 7. SMR-ESMRMB meeting, Nice, 1995.

12. Van Paesschen W, Connelly A, Duncan JS, Johnson CL, Porter DA, Gadian DG. Single voxel 1H Magnetic Resonance Spectroscopy in patients with MRI-negative intractable temporal lobe epilepsy. **Proc. Soc. Magn. Res.** 1996; 1: 139. SMR meeting, New York, 1996.

13. Van Paesschen W, Duncan JS, Johnson CL, Connelly A. Vigabatrin (Sabril) as first-line monotherapy in newly diagnosed epilepsy: no evidence of neuropathological changes on quantitative MRI using T2 relaxation time mapping [abstract]. **Epilepsia** 1996; 37 (suppl 4): 163. European Congress of Epileptology, Den Haag, 1996.

14. Van Paesschen W, Revesz T, Connelly A, Duncan JS. Quantitative MRI of the hippocampus: neuropathological validation [abstract]. **Epilepsia** 1996; 37 (suppl 4): 24. European Congress of Epileptology, Den Haag, 1996.

15. Van Paesschen W, Connelly A, Duncan JS, Johnson CL, Porter DA, Gadian DG. Single voxel ^{1}H Magnetic Resonance Spectroscopy in MRI-negative temporal lobe epilepsy patients compared with those with hippocampal sclerosis [abstract]. **Epilepsia** 1996; 37 (suppl 4): 37. European Congress of Epileptology, Den Haag, 1996.

16. Van Paesschen W, Duncan JS, Connelly A. Progression of hippocampal disease in newly diagnosed localisation-related epilepsy: a longitudinal quantitative MRI study [abstract]. **Epilepsia** 1996; 37 (suppl 5): 191. American Epilepsy Society meeting, San Francisco 1996.

17. Connelly A, Van Paesschen W, Stevens JM, Duncan JS. Aetiology and early prognosis of newly diagnosed localisation-related epilepsies in adults: a quantitative MRI study [abstract]. **Epilepsia** 1996; 37 (suppl 5): 124. American Epilepsy Society meeting, San Francisco 1996.

18. Koepp MJ, Richardson MP, Brooks DJ, Van Paesschen W, Duncan JS. [^{11}C] Flumazenil PET in temporal lobe epilepsy with normal or nondiagnostic MRI. **Epilepsia** 1996; 37 (suppl 4): 153. European Congress of Epileptology, Den Haag, 1996.

19. Baxendale S, Van Paesschen W, Thompson PJ, Duncan JS, Connelly A, Shorvon SD. Role of neuropsychology in the presurgical evaluation of patients for temporal lobectomy. **Epilepsia** 1996; 37 (suppl 4): 31. European Congress of Epileptology, Den Haag, 1996.

20. Baxendale SA, Van Paesschen W, Thompson PJ, Duncan JS, Harkness WF, Shorvon SD. Prediction of postoperative memory decline in temporal lobectomy: a multivariate approach [abstract]. **Epilepsia** 1996; 37 (suppl 5): 181. American Epilepsy Society meeting, San Francisco 1996.

21. Cross HJ, Duncan JS, Fish DR, Harkness W, Harper A, Neville BGR, Taylor D, Van Paesschen W. The range of presentation of drug-resistant temporal lobe epilepsy in adults and children. **Epilepsia** 1996; 37 (suppl 5): 103. American Epilepsy Society meeting, San Francisco 1996.

22. Hand KS, Bowery NG, Baird VH, Van Paesschen W, Revesz T, Harkness W, Duncan JS. Central benzodiazepine receptor autoradiography in hippocampal sclerosis. **Epilepsia** 1996; 37 (suppl 5): 43. American Epilepsy Society meeting, San Francisco 1996.

23. Koepp MJ, Richardson MP, Brooks DJ, Van Paesschen W, Duncan JS. Comparison of quantitative ^{11}C-Flumazenil PET, MRI and neuropathology in mesial temporal lobe epilepsy. **Epilepsia** 1996; 37 (suppl 5): 200. American Epilepsy Society meeting, San Francisco 1996.

TABLE OF CONTENTS.

FIGURES.

TABLES

ABBREVIATIONS.

AED:	antiepileptic drug
AMPA:	α-amino-3-hydroxy-5-methyl-4-isoxazole-propionic acid
AT2:	amygdala T2
AS:	amygdala sclerosis
CA:	Cornu Ammonis
Ca^{2+}:	calcium
CD:	cortical dysgenesis
Cho:	choline-containing compounds
CP:	Carr-Purcell
CPMG:	Carr-Purcell-Meiboom-Gill
CPS:	complex partial seizure
Cr:	creatine and phosphocreatine
CSF:	cerebrospinal fluid
DNET:	dysembryoplastic neuroepithelial tumor
EEG:	electroencephalogram
EFS:	end folium sclerosis
FC:	febrile convulsion
FLAIR:	fluid attenuated inversion recovery
FOV:	field of view
FTL:	foreign tissue lesion
GABA:	γ-amino-butyric-acid
GCDG:	granule cell layer of the dentate gyrus
GD:	glial cell density
GFAP:	glial fibrillary acidic protein
H&E:	haematoxylin and eosin
HS:	hippocampal sclerosis
HCT2:	hippocampal T2
HCV:	hippocampal volume
ICV:	intracranial volume
IR:	inversion recovery
LFB/CV:	Luxol fast blue/cresyl violet
mm:	millimeter
MPRAGE:	Magnetization Prepared Rapid Gradient Echo
MRI:	magnetic resonance imaging
MRS:	Magnetic Resonance Spectroscopy
msec:	millisecond

NAA:	N-acetylaspartate
ND:	neuronal cell density
NEX:	number of excitations
NMDA:	N-methyl-D-aspartate
PHAPS:	phase alternating-phase shift sequence
RC:	repeatability coefficient
ROI:	region of interest
SC:	solochrome cyanin
SD:	standard deviation
SGS:	secondary generalized seizure
SPGR:	Spoiled Gradient Echo
SPS:	simple partial seizure
TE:	echo time
TI:	inversion time
TLE:	temporal lobe epilepsy
TR:	repetition time

I. CHAPTER I. INTRODUCTION.

1.1. THE HIPPOCAMPUS: STRUCTURAL AND FUNCTIONAL ASPECTS.

1.1.1. INTRODUCTION.

The hippocampus is an arch-shaped 4-4.5 cm long gray matter structure lying in the medial temporal lobe (Lorente de Nó, 1934; Duvernoy, 1988; Amaral, Insausti, 1990; Carpenter, 1991; Van Hoesen, 1995). The hippocampal formation includes the dentate gyrus, the hippocampus proper (Ammon's horn or cornu Ammonis [CA]), and also the subicular complex and entorhinal cortex. The hippocampus, i.e. hippocampus proper and dentate gyrus, belongs to the archipallium or allocortex ("other cortex") and has a three-layered structure, which consists of the stratum oriens, stratum pyramidale and molecular zone (the stratum radiatum, lacunosum and moleculare). This three-layered cortex is different from the six-layered neocortex, also called neopallium or isocortex. The subiculum has a cortical structure which is a transition between allo- and isocortex, which is called peri-allocortex.

1.1.2. HIPPOCAMPUS PROPER.

1.1.2.1. LAYERS OF THE HIPPOCAMPUS PROPER *(Figure 1, p 22).*

1.1.2.1.1. The alveus covers the intraventricular surface and contains the axons of the hippocampal and subicular neurons, which enter the fimbria as the main efferent path of these structures.

1.1.2.1.2. The stratum oriens is composed of scattered neuronal cells, called basket cells, is crossed by pyramidal cell axons, and is rather poorly defined as it is blended with the underlying stratum pyramidale or pyramidal cell layer. Basket cells are regulatory interneurons and form basket arborizations around the pyramidal cell bodies. They receive impulses from pyramidal neurons and inhibit pyramidal cells via their gamma-amino-butyric acid (GABA) -ergic axons.

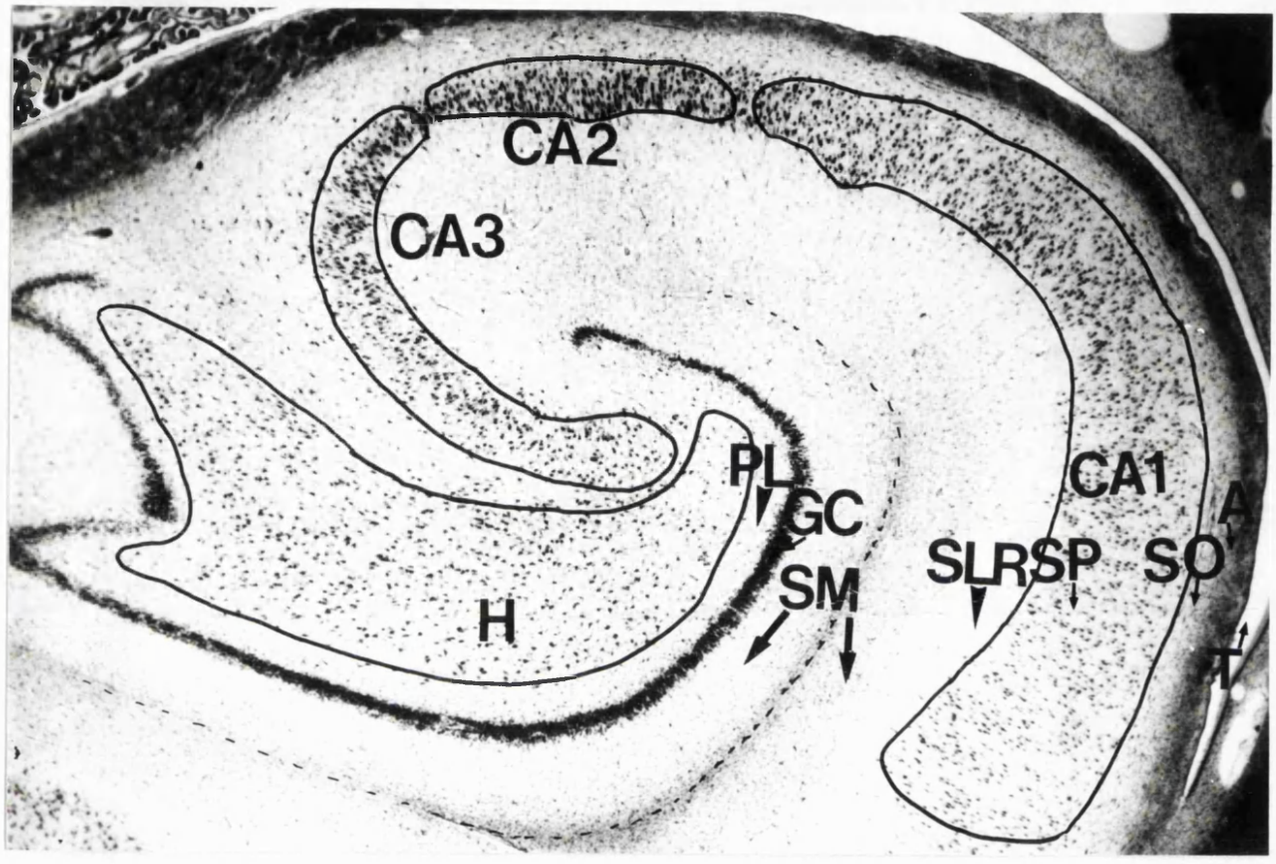

Figure 1. Microscopic anatomy of a control hippocampal body. The photograph shows a transverse section of the hippocampal body of a control subject (obtained at autopsy) (Luxol fast blue/cresyl violet [LFB/CV] stain; magnification: x22; section thickness: 20 μm). The layers of the hippocampus from the temporal horn of the lateral ventricle (T) towards the hilus (H) are the alveus (A), stratum oriens (SO), stratum pyramidale (SP), stratum lacunosum-radiatum (SLR), stratum moleculare (SM) of the hippocampus proper, hippocampal sulcus (which is a virtual sulcus indicated by dashed line), stratum moleculare (SM) of the dentate gyrus, GCDG (GC), and the polymorphic layer of the dentate gyrus (PL). The neuronal cell layers of the hippocampus are the CA1, CA2, CA3, hilus and GCDG. The boundaries of these hippocampal subregions which were used in this study are outlined in black.

1.1.2.1.3. The stratum pyramidale or pyramidal cell layer contains the pyramidal neuronal cells. The body of a pyramidal cell is triangular, its base with the axon facing the alveus and its apex with an apical dendrite towards the hippocampal sulcus. The basal axon traverse the stratum oriens and via the alveus and fimbria projects to the septal nuclei, thalamus and mammillary bodies. The apical dendrite projects to the stratum moleculare. In addition, there are basal dendrites, some of which arborize in the stratum oriens.

1.1.2.1.4. The stratum radiatum has a radiated appearance because it consists mainly of apical dendrites of the pyramidal neuronal cells. Schaffer collaterals from the CA3 hippocampal subregion and dentate hilar neuronal cell axons synapse with the apical dendrites in the stratum radiatum of CA2 and CA1. In the CA3 hippocampal subregion, the stratum lucidum can be found between the pyramidal cell layer and the stratum radiatum and contains the mossy fibers of the GCDG which synapse in this region with the dendrites of the CA3 pyramidal cells.

1.1.2.1.5. The stratum lacunosum contains Schaffer collaterals and perforant fibers.

1.1.2.1.6. The stratum moleculare contains the arborizations of the apical dendrites of the pyramidal neuronal cells, and few interneurons. Because the hippocampal sulcus disappears during development, it blends with that of the molecular layer of the dentate gyrus.

1.1.2.2. HIPPOCAMPAL SUBREGIONS *(Figure 1, p 22; Figure 19, p 80; Figure 38, p 126).* The hippocampus proper can be divided into three distinct fields which have been labeled CA1, CA2 and CA3 in classification scheme of the hippocampal subregions described by Lorente de Nó (Lorente de Nó, 1934). This classification was based on the microscopic structure of neuronal cells and connections between these cells assessed on Golgi-stained hippocampal specimens.

1.1.2.2.1. CA1. The limit between prosubiculum and CA1 is given by the appearance of the stratum radiatum in the CA1. In CA1, superficial and deep pyramidal cell are recognized. The deeper a pyramidal cell, the lesser contact it has with the basket plexus. The dendrites of the CA1 pyramidal cells have side branches in the stratum radiatum which are not seen in the CA2 or CA3. Projections of CA2 and CA3, the so-called Schaffer collaterals, terminate in the stratum radiatum and stratum oriens of CA1. CA1 also receives input from the alvear and perforant path of the

entorhinal region in the stratum lacunosum-moleculare. The axons of the pyramidal cells of CA1 are thin, and go towards the fimbria. Some of these axons of the CA1 pyramidal cells have a long recurrent collateral towards the prosubiculum.

1.1.2.2.2. CA2. The CA2 pyramidal neuronal cells are the giant pyramidal cells of the hippocampus, together with those of the CA3. The pyramidal cells of this region are densely packed and the stratum pyramidale of the CA2 is the thinnest of the hippocampus. The apical dendrites are similar to those of the CA3, but without thorns i.e. input form the mossy fibers. The basal axons of the CA2 pyramidal cells give collaterals for the longitudinal association path, and together with those of the CA3 form a system which can act upon CA1, CA2 and CA3 of other segments of the hippocampus *(see the functional organization of the hippocampus, p 31)*.

1.1.2.2.3. CA3. The pyramidal cells of the CA3 are giant pyramidal cells. The hallmark of CA3 are the synapses between the apical dendrites of the CA3 pyramidal cells and the mossy fibers of the dentate granule cells in the stratum lucidum, which has the appearance of a thorny excrescence. The basal axon is thick, goes to the fimbria and gives off a very thick collateral which is called the Schaffer collateral, which crosses the stratum pyramidale and radiatum and enters the stratum lacunosum, and innervates pyramidal cells of the CA1 hippocampal subregion. Those pyramidal cells which have no Schaffer collateral have one or two collaterals which ascend to the stratum radiatum and constitute immediately above the stratum pyramidale of CA2 and CA3 an association path which runs parallel to the long axis of the hippocampus. This path which runs in the long axis of the hippocampus therefore associates different segments of the hippocampus, in contrast to the Schaffer collaterals which associate the fields of the same segment of the hippocampus. Part of the CA3 is enclosed by the GCDG. Here, the pyramidal cell layer typically makes a sharp bend and folds back on itself, i.e. the so-called end-blade.

1.1.3. THE DENTATE GYRUS.

The dentate gyrus can be divided into the following three layers: 1. the GCDG, 2. the polymorphic layer or hilus of the dentate gyrus, and 3. the molecular layer.

1.1.3.1. THE STRATUM GRANULOSUM OR GRANULE CELL LAYER has a characteristic C-shape at the level of the body of the hippocampus and consists of the bodies of the granule cells, which are rounded, small, and densely packed. The axons are the mossy fibers, which are glutaminergic, and contact neuronal cells of the hilus and CA3.

Because of their large zinc content, they are best visualized with the Timm's stain. A single dendrite innervates the stratum moleculare.

1.1.3.2. THE STRATUM MOLECULARE OR MOLECULAR LAYER is thick and separated from the molecular layer of the hippocampus by the hippocampal sulcus. Its external two thirds near the hippocampal sulcus receive fibers from the perforant path, whereas the inner one third near the stratum granulosum is occupied by commissural and septal fibers. GABA-ergic basket cells in the molecular and polymorphic layers inhibit granule cells.

1.1.3.3. THE POLYMORPHIC LAYER OR HILUS OF THE DENTATE GYRUS. Lorente de Nó (Lorente de Nó, 1934) considered the neuronal cells in the hilus of the dentate gyrus as part of the hippocampus proper and described it as the CA4 hippocampal subregion, separated by a thin polymorphic layer from the GCDG. This is a very complex region, and recent evidence suggests that this CA4 hippocampal subregion may be a part of the dentate gyrus rather than the hippocampus proper, and a better name therefore may be hilus of the dentate gyrus (Blackstad, 1956; Amaral, 1978; Duvernoy, 1988; Amaral, Insausti, 1990). Several neuronal cell types have been recognized in the hilus of the dentate gyrus (Amaral, 1978). One of these is the mossy cell (Ribak *et al.* 1985), with a triangular or multipolar shaped body, extensive dendritic arborizations restricted to the hilus, thorny excrescences on its body and proximal dendrites and spines on distal dendrites (due to innervation with mossy fibers of the granule cells), and bifurcating axons which are directed toward fimbria and molecular layer of dentate gyrus. Other neuronal cells in the hilus contain neuropeptide Y, somatostatin, etc.

1.1.4. MACROSCOPIC HIPPOCAMPAL ANATOMY ON MR IMAGES.

The macroscopic anatomy of the hippocampus can be assessed in vivo using magnetic resonance images. An inversion recovery (IR) T1-weighted 3-D volume set has a high signal-to-noise ratio, a high contrast resolution, which is important for the disarticulation of amygdala from hippocampus, and can be reformatted along the axes of the hippocampus *(Figure 11, p 58)*, which reduces partial volume effects, and therefore an ideal sequence to study the hippocampal anatomy.

1.1.4.1. AXIAL IMAGE ALONG THE LONG AXIS OF THE HIPPOCAMPUS. An axial image along the long axis of the hippocampus shows the typical sea-horse appearance

of the hippocampi *(Figure 2, p 27)*. The hippocampal length is between 4 and 4.5 cm. The hippocampus lies medial from the temporal horn of the lateral ventricle, lateral from the mesencephalon and the crus cerebri, and postero-caudal of the amygdala. The hippocampus can be described in three parts: 1. a posterior part or tail, 2. a middle part or body, and 3. an anterior part or head.

1.1.4.2. POSTERIOR ASPECT OF THE HIPPOCAMPUS. The posterior limit for MR-based hippocampal volume (HCV) measurement is usually taken as the crus fornicis seen in its full profile *(Figure 3, p 29)*. The fornix is the main efferent system of the hippocampal formation. It contains both projection and commissural fibers. It is composed of axons of cells in the subiculum and pyramidal cells of the hippocampus, which spread over the ventricular surface as the alveus and converge to form the fimbria. Proceeding backward, the fimbriae of the two sides increase in thickness. At the tail of the hippocampus, they arch under the splenium of the corpus callosum as the crura of the fornix, at the same time converging toward each other. The fornix projects to the septal nuclei, thalamus and mammillary bodies.

1.1.4.3. THE TAIL OF THE HIPPOCAMPUS can be seen at the level of the cerebellum on an oblique coronal section which is oriented at 90 degrees to the long axis of the hippocampus *(Figure 3, p 29)*. The tail has an intraventricular part which forms the medial wall of the atrium of the lateral ventricle, which contains the choroid plexus, and an extraventricular part. Between the parahippocampal gyrus and the hippocampus lies the isthmus and anterior calcarine sulcus. Anatomical details such as fasciola cinerea (i.e. continuation of margo denticulatus), gyrus fasciolaris (composed of CA3 covered with alveus), and gyri of Andreas Retzius (i.e. folding of the CA1 hippocampal subregion which may be visible at the surface of the parahippocampal gyrus) *(see Figures 22 and 23 of* (Duvernoy, 1988)*)* are not clearly visible on magnetic resonance imaging (MRI) images used in this study.

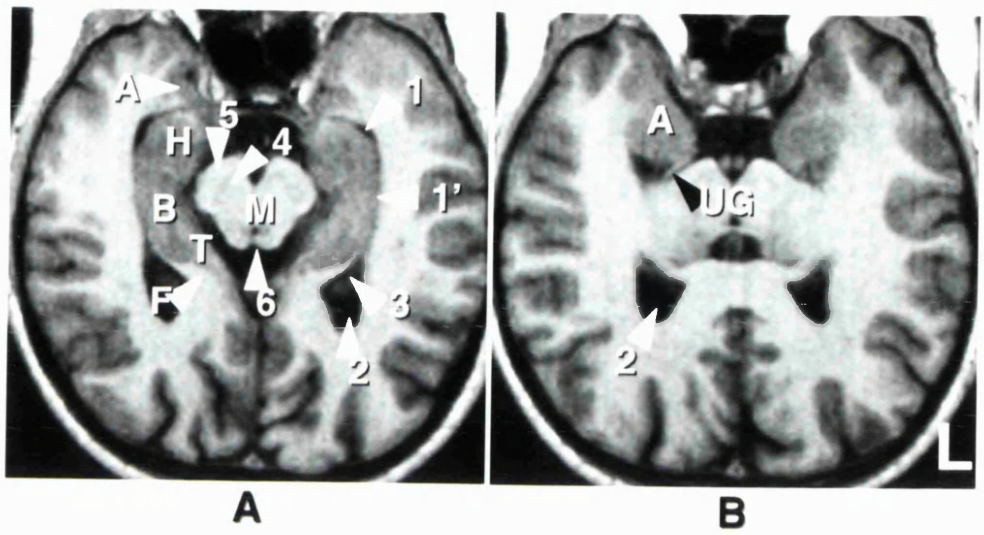

Figure 2. Axial view of the hippocampi. Reformatted control MPRAGE images (1mm thick sections). A. View of the hippocampi in a tilted axial plane along the long axis of the hippocampus. The hippocampi can be divided into the hippocampal head (H), body (B) and tail (T). At this level, the hippocampal head is separated from the amygdala (A) by the uncal recess of the lateral ventricle (1). The lateral border of the hippocampal body is the temporal horn of the lateral ventricle (1'). The medial border is the ambient cistern and the mesencephalon (M) with crus cerebri (5) and substantia nigra (4). Posteriorly, the fornix (F) can be seen, which is an important landmark for reformatting the MPRAGE volumeset *(Figure 11, p 58)*. The atrium of the lateral ventricle (2), choroid plexus (3) and quadrigeminal cistern (6) are indicated. B. Axial view of the amygdalae (A). The orientation of this image is parallel to that of A, but 4 mm higher. This orientation was used for amygdala T2 (AT2) mapping *(see AT2 mapping, p 68, and Chapter 8)*. Uncinate gyrus (UG), and atrium of the lateral ventricle (2) are indicated.

1.1.4.4. THE HIPPOCAMPAL BODY can be seen at the level of the anterior brainstem on an oblique coronal section which is oriented at 90 degrees to the long axis of the hippocampus *(Figure 3, p 29)*. The hippocampus forms the medial aspect of the temporal horn of the lateral ventricle. The convex protrusion in the ventricle corresponds to the CA1, CA2 and CA3 hippocampal subregions, which are covered by the alveus. The hippocampal body is bordered laterally by the collateral eminence, which is the intraventricular protrusion of the collateral sulcus. The hippocampus lies superior to the parahippocampal gyrus. The distinction between hippocampus and subiculum is not visible. The fimbria is visible on the supero-medial aspect of the hippocampus.

1.1.4.5. THE HIPPOCAMPAL HEAD can be seen at the level of the amygdala on an oblique coronal section which is oriented at 90 degrees to the long axis of the hippocampus *(Figure 4, p 30)*. The intraventricular part of the head of the hippocampus is characterized by digitationes hippocampi, which are transverse foldings of the hippocampus. The hippocampus at this level is covered by a thick alveus, which is an important landmark for the disarticulation of the hippocampus from the amygdala. The hippocampus is separated from the amygdala by the uncal recess of the temporal horn. The extraventricular part of the hippocampal head is called the uncal part. The uncus can be divided in a posterior segment which belongs to the hippocampus, and an anterior segment which belongs to the parahippocampal gyrus. In the posterior segment of the uncus, the uncal sulcus separates the uncinate gyrus form the parahippocampal gyrus.

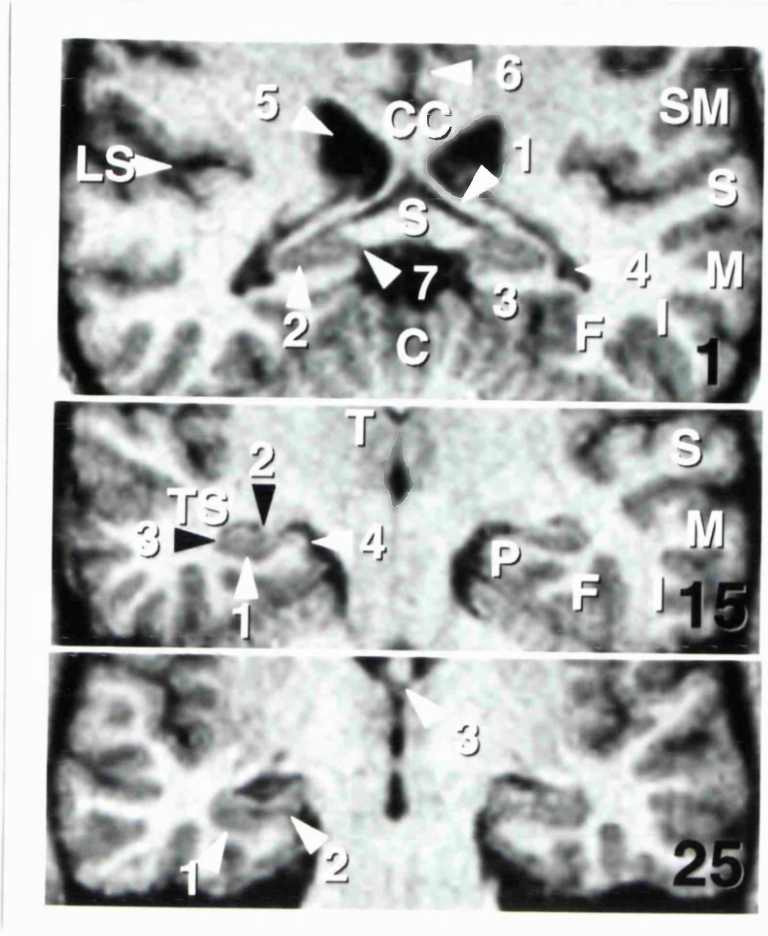

Figure 3. Hippocampal tail, body and head. MPRAGE images of a control subject were reformatted into 1 mm thick contiguous sections. The black numbers in the right lower corner are the section numbers. The MRI section in which the crus fornicis is seen in its full profile is defined as the first section for hippocampal volumetry *(see hippocampal volumetry, p 57)*. Section 15 and 25 are 15 and 25 mm more anteriorly than section 1. Section 1. The crus fornicis is seen in its full profile (1). The hippocampal tail (2) is bordered laterally by the temporal horn of the lateral ventricle (4), caudally by the isthmus (3), medially by the splenium (S) of the corpus callosum (CC), and superiorly by the crus fornicis (1). The gyrus of Andreas Retzius, fasciola cinerea and gyrus fasciolaris (7) are not visible on these MR images. Cingulate gyrus (6), atrium of lateral ventricle (5), supramarginal gyrus (SM), superior temporal gyrus (S), middle temporal gyrus (M), inferior temporal gyrus (I), fusiform gyrus (F), cerebellum (C), lateral sulcus (LS). Section 15. The hippocampal body (1) gives rise to the fimbria (2) and is bordered laterally by the temporal horn of the lateral ventricle (3) and medially by the ambient cistern (4). Temporal stem (TS), parahippocampal gyrus (P), thalamus (T). Other abbreviations see section 1. Section 25. In the posterior part of the hippocampal head (1), the intralimbic gyrus (2) can be seen. Body of fornix (3).

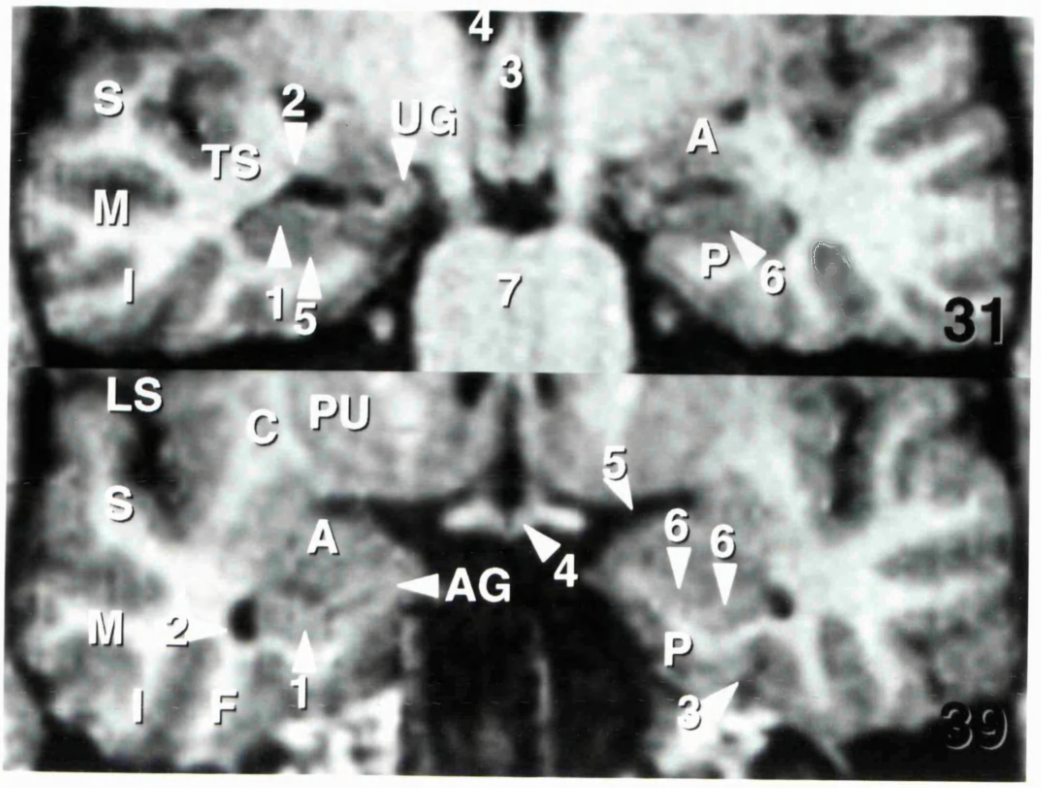

Figure 4. The hippocampal head. Section 31 and 39 of the same reformatted control MPRAGE as the previous Figure. Section 31. The hippocampal head (1) with digitationes hippocampi is separated from the subiculum (5) by the uncal sulcus (6), and from the amygdala (A) by the uncal recess of the temporal horn (2). The uncinate gyrus (UG) connects the medial hippocampus with the amygdala (A). Third ventricle (3), body of lateral ventricle (4), brainstem (7), superior temporal gyrus (S), middle temporal gyrus (M), inferior temporal gyrus (I), fusiform gyrus (F), parahippocampal gyrus (P). Section 39. The hippocampal head (1) is smaller compared with section 31, and is bordered laterally by the temporal horn of the lateral ventricle (2), medially by the ambient gyrus (AG), superiorly by the uncal recess of the temporal horn and amygdala (A), and caudally by the parahippocampal gyrus (P). The hippocampus can be disarticulated from the amygdala by the uncal recess of the temporal horn or by the alveus, which is white on a T1-weighted image (6). Putamen (PU), claustrum (C), lateral sulcus (LS), superior temporal gyrus (S), middle temporal gyrus (M), inferior temporal gyrus (I), fusiform gyrus (F), optic chiasm (4), endorhinal sulcus (5), collateral sulcus.

1.1.5. THE FUNCTIONAL ORGANIZATION OF THE DENTATE GYRUS AND HIPPOCAMPUS.

The activation of the hippocampus involves a trisynaptic unidirectional circuit i.e. entorhinal cortex (via perforant path) → dentate granule cell (via mossy fiber) → CA3 pyramidal cell (via Schaffer collateral) → CA1 pyramidal cell which sends its axon towards the alveus and fimbria (Duvernoy, 1988; Amaral, Insausti, 1990; Carpenter, 1991). The neurotransmitter at these three excitatory synapses is glutamate. These trisynaptic circuits are organized in functional thin parallel sections or lamellae which are oriented transversely to the long axis of the hippocampus (Andersen *et al.* 1971). Extensive longitudinal association pathways have been shown to exist in hippocampus and dentate gyrus (Amaral, Witter, 1989). Only the mossy fiber projection form the dentate granule cells to the CA3 pyramidal cells has an anatomical distribution that is strictly lamellar (Blackstad, 1956). GABA-mediated lateral inhibition keeps these transverse hippocampal lamellae functionally separated (Sloviter, 1994; Sloviter, Brisman, 1995) *(see dentate lamellar hypothesis, p 50).*

Numerous local hippocampal circuits regulate and inhibit this main excitatory trisynaptic circuit. Basket cells are GABA-ergic interneurons which are found largely in the stratum oriens of the hippocampus proper, and the molecular and polymorphic layer of the dentate gyrus (Lorente de Nó, 1934). The basket cells receive input from pyramidal and granule cells and their axons form arborizations around these cells, which are inhibitory. Neurons producing substance P, VIP, CCK, somatostatin, CRF and neuropeptide Y have been described in the hippocampus. They have an intervening role in local inhibitory and excitatory circuits. Also, granule cells of the dentate gyrus may produce enkephalin and dynorphin which may reach the hippocampus through mossy fibers.

The hippocampus and dentate gyrus receive external input. Septal neurons innervate the granule cells of the dentate gyrus and pyramidal cells of the hippocampus. These fibers are cholinergic and excitatory. Noradrenergic fibers arising from the locus coeruleus may reach the hippocampus via the fornix or longitudinal striae. Serotonergic fibers of the raphe nuclei reach the hippocampus via the longitudinal striae. There also exist direct connections between hippocampus and neocortex, such as cingulate gyrus, temporal and prefrontal lobes.

1.2. HIPPOCAMPAL SCLEROSIS.

1.2.1. QUALITATIVE DESCRIPTION OF HIPPOCAMPAL SCLEROSIS

1.2.1.1. HIPPOCAMPAL SCLEROSIS *(Figure 5, p 33; Figure 38, p 126; Figure 39, p 128)*. Hippocampal sclerosis (HS) has a pattern of damage which is characterized by severe neuronal cell loss in the CA1 (vulnerable or Sommer's sector (Sommer, 1880)) and the CA3 hippocampal subregion, and the hilus of the dentate gyrus (Bratz sector (Bratz, 1899)), and less severe neuronal cell loss in the CA2 hippocampal subregion (resistant sector of Spielmeyer (Spielmeyer, 1927)) and dentate gyrus (Earle *et al.* 1953; Sano, Malamud, 1953; Falconer *et al.* 1964; Green, Scheetz, 1964; Margerison, Corsellis, 1966; Corsellis, 1970; Jensen, Klinken, 1976; Armstrong, Bruton, 1987; Babb, Brown, 1987; Bruton, 1988; Babb, 1991; Meencke, Veith, 1991; Plate et al. 1993; Wolf, Wiestler, 1993; Vital *et al.* 1994b). This distribution of hippocampal damage is typical of HS and suggests selective vulnerability of the different hippocampal subregions *(see glutamate mediated excitotoxicity, p 46)*. There is concomitant dense and chronic reactive astrogliosis. Frequently, the GCDG shows dispersion. It is not clear whether this granule cell dispersion represents cortical dysgenesis (CD) (Houser *et al.* 1992) or whether this is a secondary effect of the seizures and hippocampal damage (Mello *et al.* 1992). There is mossy fiber sprouting and synaptic reorganization in the inner molecular layer as revealed by Timm's stain *(Figure 6, p 35)* (Sutula *et al.* 1989; Babb *et al.* 1991; Mathern *et al.* 1995b), or dynorphin immunoreactivity (Houser *et al.* 1990). Focal anterior, diffuse unilateral and bilateral HS have been observed pathologically. Autopsy studies have reported that classical HS is bilateral in 18-60% of cases (Sano, Malamud, 1953; Margerison, Corsellis, 1966; Meencke, Veith, 1991). The combination of HS with another lesion is frequently found *(see dual pathology, p 41)*.

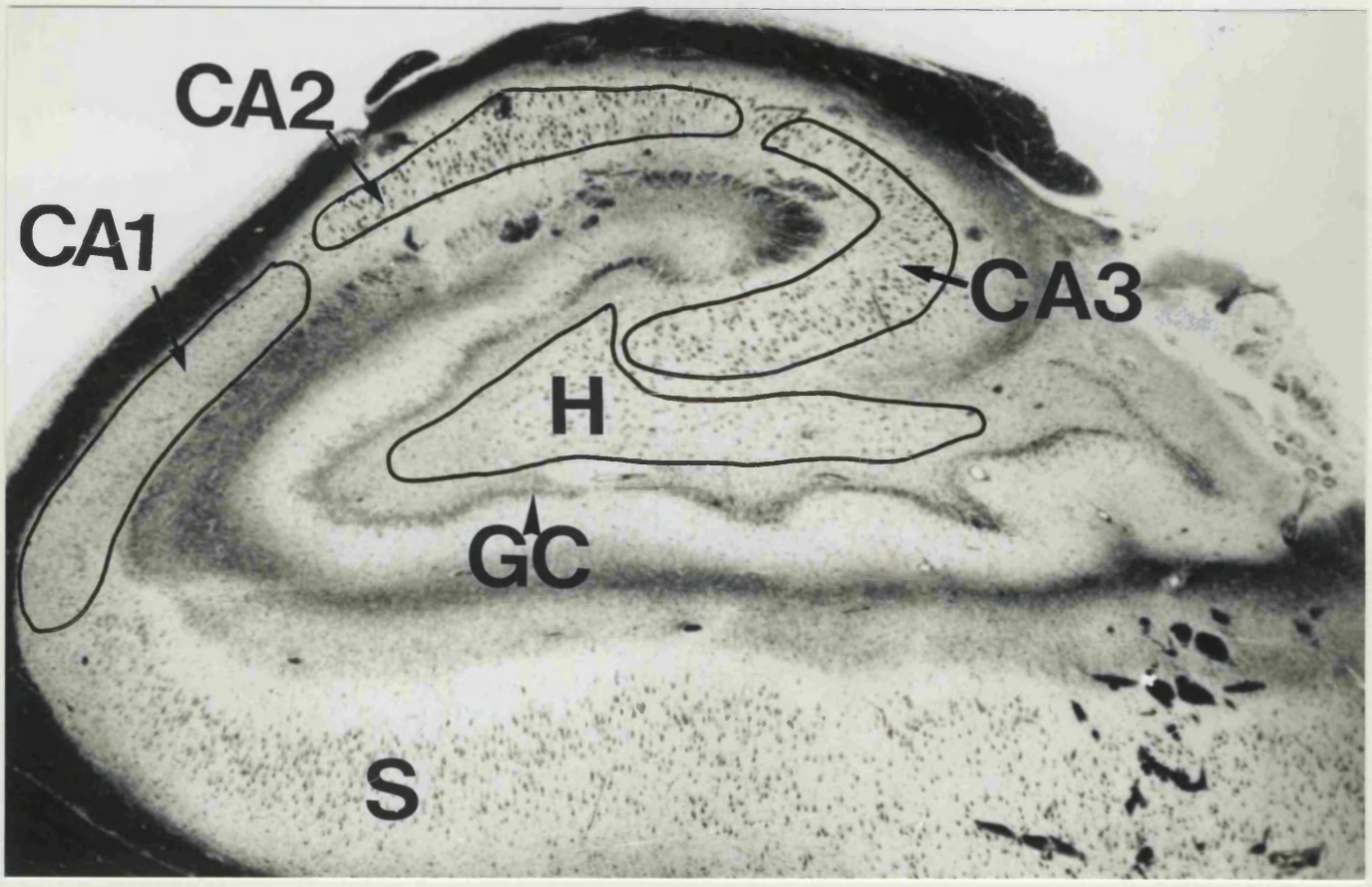

Figure 5. Microscopic anatomy of HS. Transverse section of the body of the hippocampus affected by HS (LFB/CV, 20 μm thick section, magnification: x22). There is severe pyramidal cell loss of the CA1 hippocampal subregion, i.e. the vulnerable or Sommer's sector, and the hilus (H). In this example, the CA2 and CA3 hippocampal subregion and the GCDG (GC) were less severely affected. Granule cell dispersion was present. The subiculum (S) was well preserved. The borders of the CA1, CA2, CA3 and hilus as defined in this study are outlined in black.

1.2.1.2. SCLEROSIS OF OTHER AREAS OF THE HIPPOCAMPUS *(Figure 20, p 81; Figure 38, p 126, EFS: a clinicopathological entity ?, p 136).* Sclerosis affecting the hippocampus in a distribution which is different from that of "classical" HS has been described by several authors (for summary of a workshop discussion see (Armstrong, Bruton, 1987)). Sano and Malamud (Sano, Malamud, 1953) described sclerosis confined to the dentate gyrus and also to the end plate (i.e. dentate hilar region). Margerison and Corsellis (Margerison, Corsellis, 1966) and Bruton (Bruton, 1988) described end folium sclerosis (EFS), Sagar and Oxbury (Sagar, Oxbury, 1987) and Duncan and Sagar (Duncan, Sagar, 1987) described non-specific HS. Age at onset of habitual epilepsy of patients with these forms of sclerosis is later compared to those with classical HS, seizure discharges are not primarily localized in the anterior hippocampus alone, pathology is not localized in the anterior part of the hippocampus and it is associated with a less favorable outcome after temporal lobe resection than classical HS. In contrast, classical HS is associated with prolonged febrile convulsions (FC), may be associated with early onset of habitual epilepsy, is associated with seizure discharges in the hippocampal formation, and with a good prognosis after temporal lobe resection (Armstrong, Bruton, 1987).

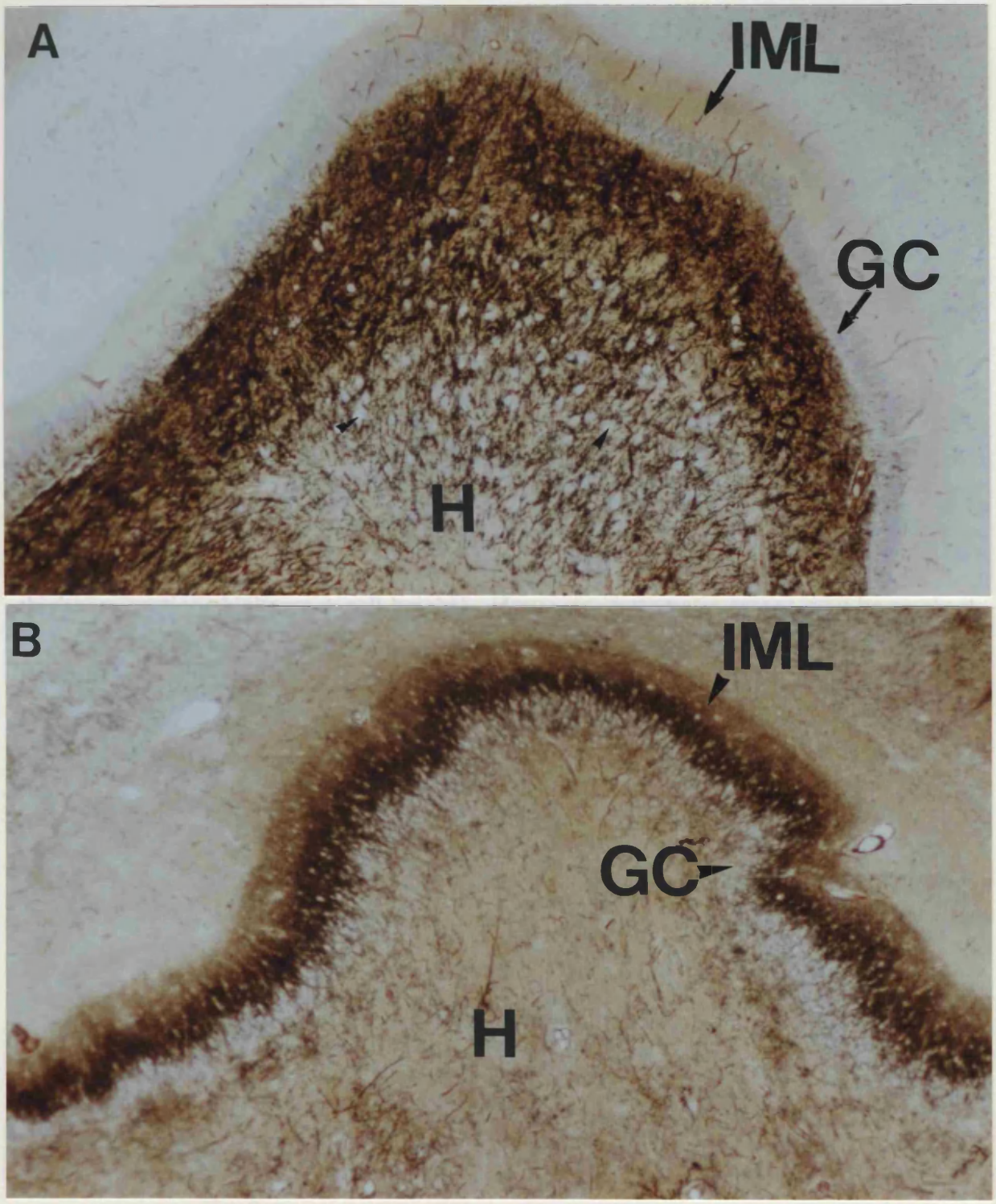

Figure 6. Mossy fiber sprouting. Hippocampus of patients with EFS (A) and HS (B). Timm's stain. Magnification approximately x80. The two sections show a part of the dentate hilar region (H), the GCDG and the inner molecular layer (IML). The Timm's method stains mossy fibers black. In A, the normal pattern is observed, i.e. the mossy fibers are seen only on the hilar side of the GCDG. The hilar neuronal cells are readily observed as translucent areas (two arrowheads as an example). In B, there is severe hilar neuronal cell depletion. Compared to A, there is little black staining in the hilar area, but staining is now observed in the IML (arrowhead). This indicates loss of mossy fibers in the dentate hilar area and new axon formation from granule cells towards the IML, i.e. synaptic reorganization.

1.2.2. QUANTITATIVE DESCRIPTION OF HIPPOCAMPAL SCLEROSIS

1.2.2.1. 2-D MICROSCOPIC COUNTING METHODS. Previous quantitative neuropathological studies of HS have determined ND using 2-D counting techniques. In a 2-D counting technique, all cells of a tissue section that fall in a square and those that intersect two of the four sides of the square are counted. The area in which cells are counted is then multiplied by the estimated section thickness to give the reference volume, i.e. the volume in which the cells are counted. This technique introduces bias because the probability that the nucleus, i.e. the structure that is counted, appears in the tissue section is related to its size, shape and orientation. Also, the cell fragments of cells that were split by the knife at the cut surfaces of the tissue sections are counted as if they were entire cells, which gives an overestimate of the density, which is the split cell error. To correct for this overestimate, Abercrombie described a correction factor: corrected number of cells = counted number of cells x (section thickness/section thickness + cell height). However, systematic errors may be made if the size, shape and orientation of cells are not taken into account. The cell height is difficult to measure, and substitution of cell diameter for cell height may not be correct. Also, it is assumed that the knife splits the cells in its path, which may not be correct, because cells may be pushed aside. Further, variation in the thickness of individual sections may cause sampling error and correct identification of fragments of cells located at the top and bottom of sections may be difficult. Despite these considerations, the 2-D counting methods have been used extensively to quantitate ND in hippocampal subregions (Dam, 1979; Dam, 1980; Dam, 1982; Babb *et al.* 1984a; Babb *et al.* 1984b; Meencke, 1985; Sagar, Oxbury, 1987; Kim *et al.* 1990; Bronen *et al.* 1991; Lencz *et al.* 1992; Lee *et al.* 1995), and may have yielded accurate data in those cases where the assumptions were reasonably fulfilled (Oorschot, 1994).

1.2.2.2. 3-D MICROSCOPIC COUNTING METHODS. Three-dimensional counting techniques use a counting box within a tissue section (Sterio, 1984; Brændgaard, Gundersen, 1986; Gundersen *et al.* 1988; Williams, Rakic, 1988; West, Gundersen, 1990; Mayhew, 1992; Oorschot, 1994). The sides of the counting box are defined by a grid, and the top and bottom planes of the counting box by focal planes within the tissue section, which require a narrow field of depth and a digital length gauge for accurate determination (Williams, Rakic, 1988). This technique does not require Abercrombie's correction factor, and overcomes problems caused by irregular cell shape and size, non random orientation, splitting of cells by the knife during sectioning, and variations in section thickness.

1.2.2.3. THE USE OF NEURONAL DENSITY AS PRINCIPAL MEASURE. The use of density measures as definitive data is of greater scientific concern than the method used (i.e. 2-D versus 3-D) to calculate absolute numbers (Brændgaard, Gundersen, 1986; West, Gundersen, 1990; Oorschot, 1994; Saper, 1996; Coggeshall, Lekan, 1996). The neuronal density (ND) as a measure of neuronal cell loss may be of limited value because changes in the hippocampal reference volume (i.e. the volume in which the cells are counted) due to disease processes such as HS and tissue distortion during histopathological processing (Haug, 1986) affect ND independent of neuronal cell loss. Therefore, the total number of neuronal cells in a hippocampal subregion would be the ideal outcome measure (West, Gundersen, 1990). Determination of total number of neuronal cells in a hippocampal subregion however requires the availability of the full hippocampus, and can therefore not be obtained in patients undergoing temporal lobe resection for TLE since the hippocampus is removed only partially. In the present study, ND and glial cell densities (GD) were determined and the ratio of GD/ND of hippocampal subregions was used as the main outcome measures. The GD/ND ratio is independent of HCV changes due to disease processes and tissue distortion during histopathological processing. GD in HS using GFAP-stained sections have not been reported before.

1.2.3. MRI OF HIPPOCAMPAL SCLEROSIS.

1.2.3.1. VISUAL ASSESSMENT OF HIPPOCAMPAL SCLEROSIS ON MR IMAGES. Initial MR studies of the brain of patients with epilepsy did not detect HS (Sperling *et al.* 1986; Brooks *et al.* 1990; Forsgren *et al.* 1991). Improvements in scanning techniques have made it possible to detect HS reliably on visual inspection of MR images. These improvements include scanning perpendicular to the long axis of the hippocampus and use of thin (i.e. 1-3 millimeter [mm]) sections to reduce partial volume effects, the use of IR T1-weighted images which have an increased contrast between gray and white matter, which is important for reliable disarticulation of amygdala from hippocampus (Kuzniecky *et al.* 1987; Jackson *et al.* 1990; Berkovic *et al.* 1991; Jackson *et al.* 1993a), and more recently the use of surface MR coil phased-array imaging which improves the signal-to-noise ratio (Hayes *et al.* 1993). MRI features of HS include hippocampal atrophy, an increased T2 signal, hypodensity on a T1-weighted image, and disruption of the internal structure (Kuzniecky *et al.* 1987; Jackson *et al.* 1990; Berkovic *et al.* 1991; Jackson *et al.* 1993a) *(Figure 7, p 38)*. In 18 patients with unilateral HS, Jackson et al (Jackson *et al.* 1993a) reported disrupted internal structure in 16 (89%), atrophy and decreased T1-weighted signal in 15 (83%) and increased T2-weighted signal in 14 (77%).

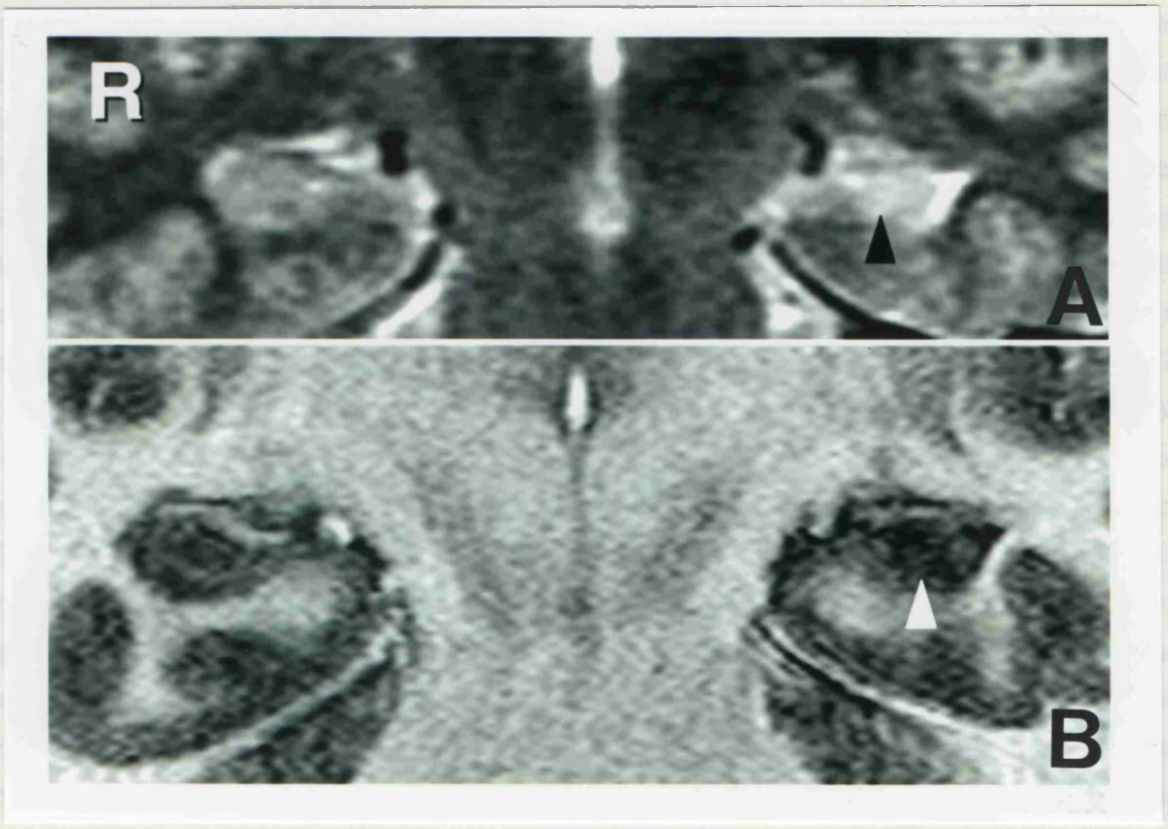

Figure 7. The MRI features of HS. Left HS. A. The T2-weighted image (TE=118msec) shows an increased signal in an atrophic left hippocampus (black arrow). B. An IR-T1 weighted image shows a hypodense, atrophic left hippocampus (white arrow), in which the normal layers of the hippocampus can no longer be observed (compare with normal right [R] side).

1.2.3.2. QUANTITATIVE MRI OF THE HIPPOCAMPUS.

1.2.3.2.1. Hippocampal T2 mapping. Jackson et al have reported that the measurement of hippocampal T2 (HCT2) relaxation time increased both sensitivity and objectivity of assessing HCT2-related signal change associated with hippocampal pathology (Jackson *et al.* 1993b). HCT2 maps were calculated from 16 identical images obtained at echo times ranging from 22 to 262 milliseconds (msec) using a phase alternating-phase shift (PHAPS) sequence (Graumann *et al.* 1986), a Carr-Purcell-Meiboom-Gill (CPMG) sequence followed by a Carr-Purcell (CP) sequence, and were generated by fitting single exponentials to the image data of corresponding pixels from these 16 echoes. The thickness of this HCT2 map was 8 mm and its orientation was in a tilted coronal plane along the anterior border of the brainstem perpendicular to and at the level of the body of the hippocampus. The HCT2 relaxation time was measured by placing the largest possible circle as a region of interest (ROI) within the hippocampus while avoiding boundaries where partial volume effects with cerebrospinal fluid (CSF) might occur, and was expressed in msec. Interobserver variation was reported as minimal (Jackson *et al.* 1993b). HCT2 in control subjects ranged from 99-106 msec and HCT2 $\geq$ 116 msec was always associated with HS. In 29% of patients with TLE and HS, the contralateral T2 was also outside the normal range, although the higher value was always on the side of the seizure focus. In 23 patients with intractable localization-related epilepsy, the mean difference of HCT2 measured on repeated HCT2 maps (median interval between the two HCT2 maps was 169 days) was -1.1 msec with a standard deviation (SD) of 6.4 msec. The conclusion that these values were not affected by recent seizure activity and were stable over time may not be warranted, since the repeatability coefficient (RC) (Bland, Altman, 1986) of repeated HCT2 maps in control subjects was not reported (Grünewald *et al.* 1994a). Neuropathological correlations with HCT2 have not been reported, and correlations with HCV not established.

1.2.3.2.2. Hippocampal volumetry. Hippocampal volumetry is the most frequently used MR method to study the hippocampus quantitatively (Jack, Jr. *et al.* 1988; Jack, Jr. *et al.* 1990; Cook *et al.* 1992; Bhatia *et al.* 1993; Cendes *et al.* 1993b; Reutens *et al.* 1993; Spencer *et al.* 1993; Adam *et al.* 1994; Jack, Jr. 1994). Initial studies used thick (e.g. 5 mm thick slices) and non-contiguous slices to measure HCV and did not measure the full length of the hippocampus, and were therefore biased (Jack, Jr. *et al.* 1988; Jack, Jr. *et al.* 1990). The reported asymmetry in HCV with the right hippocampus being slightly larger than the left was probably a result of this bias, and has not been reproduced in studies using contiguous thin slices with measurement

of the full length of the hippocampus (Cook *et al.* 1992; Watson *et al.* 1992; Bhatia *et al.* 1993; Cendes *et al.* 1993b; Kuks *et al.* 1993; Free *et al.* 1995; Kim *et al.* 1995b; Lee *et al.* 1995; Van Paesschen *et al.* 1997). Initial studies used an SPGR 3-D volume acquisition, which has a contrast resolution which makes disarticulation of hippocampus form amygdala difficult. Several investigators have therefore limited measurement of the hippocampus to the hippocampal bodies, which introduces bias (Kim *et al.* 1994). Also, comparing HCV ratio or difference in HCV may be of limited value in the detection of bilateral HS (Jack *et al.* 1995; King *et al.* 1995; Van Paesschen *et al.* 1995b). A significant difference in HCV expressed as a difference or ratio has been shown to indicate the presence of HS on the smaller side on neuropathological examination and to correlate with its severity (Cascino *et al.* 1991; Lencz *et al.* 1992; Cendes *et al.* 1993a; Kim *et al.* 1995b; Lee *et al.* 1995). Several studies have shown that these patients do well after surgery (Berkovic *et al.* 1991; Jack, Jr. *et al.* 1992; Garcia *et al.* 1994; Berkovic *et al.* 1995), and demonstration of unilateral HS with concordant functional tests obviates the need for invasive electroencephalographic (EEG) studies (Baulac *et al.* 1994; Thadani *et al.* 1995). HCV of men as a group are larger than those of women. Correcting HCV for ICV has been reported to abolish differences in HCV between genders (Jack, Jr. *et al.* 1990; Bhatia *et al.* 1993; Cendes *et al.* 1993b; Free *et al.* 1995). Plotting of HCV cross-sectional areas as a function of section position allows the assessment of the presence of focal and diffuse hippocampal atrophies (Cook *et al.* 1992; Kuks *et al.* 1993; Kim *et al.* 1995b). An ideal MR-based HCV measurement protocol should make use of thin slices, high resolution images, an inversion prepulse to increase contrast, measure the full length of the hippocampus, correct for ICV, and plot a HCV distribution graph which should be compared against a control graph to detect focal and diffuse hippocampal atrophies (Van Paesschen *et al.* 1997).

1.2.4. HIPPOCAMPAL SCLEROSIS AND OTHER PATHOLOGICAL LESIONS IN TEMPORAL LOBE EPILEPSY.

1.2.4.1. HIPPOCAMPAL SCLEROSIS. Several surgical series and autopsy studies of patients with TLE have reported that HS is the single most common pathology found in the resected specimen or at autopsy accounting for around 40% of cases *(Table 1, p 41)* (Falconer *et al.* 1964; Green, Scheetz, 1964; Corsellis, 1970; Jensen, Klinken, 1976; Babb, Brown, 1987; Duncan, Sagar, 1987; Bruton, 1988; Meldrum, Bruton, 1992; Armstrong, 1993). Several surgical series which used MRI for the selection of patients reported similar figures, with HS as the most common single pathological lesion (Plate *et al.* 1993; Wolf, Wiestler, 1993; Vital *et al.* 1994b; Kim *et al.* 1995a;

Zentner *et al.* 1995). A few studies however reported that neoplastic lesions as a group were a more frequent cause of intractable TLE, but patients in these studies might have been selected with imaging techniques before HS could be reliably detected with high resolution MRI (Plate *et al.* 1993; Zentner *et al.* 1995).

1.2.4.2. LESIONS OTHER THAN HIPPOCAMPAL SCLEROSIS.
Other lesions which are found in resected temporal lobe of patients with intractable TLE include neoplasms and benign tumors, vascular malformations, scars (post traumatic or post ischemic), CD and microdysgenesis, inflammatory lesions, developmental lesions (e.g. arachnoid or epidermoid cyst) and indefinite lesions. No pathology is found in around 13% *(Table 1, p 41)*. The neoplastic lesions as a group are the second most frequently found pathology after HS in resected temporal lobe of patients with TLE accounting for around 28% of cases *(Table1, p 41)* (Falconer, Cavanagh, 1959; Falconer *et al.* 1964; Green, Scheetz, 1964; Corsellis, 1970; Jensen, Klinken, 1976; Armstrong, Bruton, 1987; Babb, Brown, 1987; Duncan, Sagar, 1987; Bruton, 1988; Armstrong, 1993; Plate *et al.* 1993; Wolf *et al.* 1993; Vital *et al.* 1994b; Berkovic *et al.* 1995; Kim *et al.* 1995a).

Study	n	HS	Neoplasm	Other	Normal
(Falconer *et al.* 1964)[1]	94	41 (47%)	21 (24%)	10 (13%)	22 (22%)
(Green, Scheetz, 1964)	78	36 (46%)	14 (18%)	14 (18%)	14 (18%)
(Jensen, Klinken, 1976)	61	21 (34%)	4 (7%)	19 (31%)	17 (28%)
(Duncan, Sagar, 1987)	58	19 (33%)	15 (26%)	17 (29%)	7 (12%)
(Babb, Brown, 1987)	129	79 (61%)	15 (12%)	35 (27%)	0 (0%)
(Bruton, 1988)[2]	231	107 (46%)	38 (16%)	20 (9%)	66 (29%)[3]
(Plate *et al.* 1993)	247	49 (22%)	126 (56%)	68 (20%)	4 (2%)
(Berkovic *et al.* 1995)[4]	135	85 (63%)	20 (15%)	6 (4%)	24 (18%)
(Zentner *et al.* 1995)	178	39 (22%)	79 (44%)	55 (31%)	5 (3%)
Total	**1211**	**476 (39%)**	**332 (28%)**	**244 (20%)**	**159 (13%)**

Table 1. Pathological lesions in surgical series of temporal lobe epilepsy (TLE)
1: Six cases with dual pathology not included in this table
2: Eighteen patients with dual pathology not included in this table
3: Twenty-five patients (10%) with indefinite pathology and 41 patients (17%) with no apparent pathology
4: MRI-based study

1.2.4.3. DUAL PATHOLOGY. Dual pathology is the combination of two pathological lesions in patients with TLE (Sano, Malamud, 1953; Falconer *et al.* 1964; Bruton,

1988; Fried *et al.* 1992; Cascino *et al.* 1993; Raymond *et al.* 1994; Vital *et al.* 1994b; Cendes *et al.* 1995c). In the vast majority of patients one of the two lesions is HS. Sano and Malamud (Sano, Malamud, 1953) described the association of bilateral HS and congenitally malformed brains in 11 patients. This association could explain why up to 30% of a pediatric population with severe intractable epilepsy has bilateral HS, not typically seen in adult studies (Jackson *et al.* 1994b). Falconer (Falconer *et al.* 1964) and later Bruton (Bruton, 1988) described 18 of 249 patients (7%) who underwent temporal lobe resection for intractable TLE and had dual pathology, most often HS with another lesion. Lévesque et al (Lévesque *et al.* 1991) reported that 54 of 178 patients (30%) who underwent en bloc temporal lobe resection had dual pathology i.e. an extrahippocampal temporal foreign tissue lesion (FTL) in addition to neuronal cell loss within the hippocampus. Twelve patients with a glioma had only a mild decrease in hippocampal ND, whereas all 13 patients with neuronal heterotopia had a more severe decrease in hippocampal ND, consistent with a diagnosis of HS. Fish et al (Fish *et al.* 1991) found HS in 7 of 20 patients (36%) with inaccessible posterior temporal or extratemporal lesions. Fried et al (Fried *et al.* 1992) reported that NDs of hippocampal subregions in patients with TLE and mass lesions on imaging are lower than in control subjects. Patients with earlier onset seizures, and mass lesions in the medial temporal region compared to those with lesions in the lateral temporal lobe had lower NDs, suggesting an increased vulnerability of the hippocampus to lesions close to the hippocampus, and early onset seizures.

MRI has made it possible to study the occurrence of dual pathology systematically and to diagnose it pre-operatively. Raymond et al (Raymond *et al.* 1994) described the occurrence of CD in 15% of patients with HS *(Figure 8, p 49)*. This corroborates the observation that microdysgenesis or neuronal heterotopia is frequently found in association with HS (Armstrong *et al.* 1987; Lévesque *et al.* 1991) *(see etiopathogenesis of HS, p 45)*. Cendes et al (Cendes *et al.* 1995c) reported that hippocampal atrophy was found in 25% of cases with CD independent of the distance between the lesion and the hippocampus. In patients with other types of lesions, such as vascular malformations, dual pathology tended to be found when the lesion was in the vicinity of the hippocampus. However, only one of 52 patients (2%) with tumors had hippocampal atrophy, which suggested that proximity to the lesion may not be an important factor for the occurrence of dual pathology, as suggested by Fried et al (Fried *et al.* 1992). These studies stress the importance of obtaining high quality imaging in all patients with HS to exclude the possibility of dual pathology, which may be subtle and easily overlooked, and may have prognostic implications with respect to seizure outcome after surgery.

1.2.4.4. PATHOLOGY AND SURGICAL OUTCOME WITH RESPECT TO SEIZURES. The nature of the underlying pathology is a key determinant of seizure outcome after surgery. The absence of pathology in the resected temporal lobe is prognostically unfavorable (Falconer, Serafetinides, 1963; Green, Scheetz, 1964; Falconer, Taylor, 1968; Jensen, Klinken, 1976; Armstrong, Bruton, 1987; Duncan, Sagar, 1987; Bruton, 1988; NIH consensus panel. 1990; Berkovic *et al.* 1991; Jack, Jr. *et al.* 1992; Engel, Shewmon, 1993; Engel, 1993; Kuzniecky *et al.* 1993; Fish, 1994a; Garcia *et al.* 1994; Berkovic *et al.* 1995; Duncan *et al.* 1995). The extent of resection of a lesion is also important with respect to seizure outcome. Patients with a lesion that was resected only partially do worse than those in whom the resection removed the lesion completely (Babb *et al.* 1984a; Awad *et al.* 1991). Good surgical outcome with respect to seizure (i.e. seizure free or aura only) and social outcome is seen in around 60-70% of patients who underwent temporal lobe resection including the hippocampus for unilateral HS. Jack et al (Jack *et al.* 1995) reported that three of seven patients (43%) with bilateral HS became seizure free after unilateral temporal lobe resection. Little is known about surgical outcome in patients with dual pathology. Bruton (Bruton, 1988) described 15 patients with HS and a second lesion and reported that seizure frequency was not altered and that the effect on personality and social adjustment was disastrous. Postoperative outcomes on a small number of patients reported by Raymond et al (Raymond *et al.* 1994) seem to corroborate Bruton's observations. It appears that the second lesion modifies the clinical response and should be considered in the decision to operate.

1.2.5. ETIOLOGY OF SEIZURES IN PATIENTS WITH HIPPOCAMPAL SCLEROSIS

Since the description of HS more than a century ago, it has been debated whether HS is the cause or consequence of seizures, or both. Arguments in favor of HS being a cause of epileptic seizures are 1.) the association of HS with intractable TLE (Bouchet, Cazauvieilh, 1825; Sommer, 1880; Sano, Malamud, 1953; Falconer, Cavanagh, 1959; Margerison, Corsellis, 1966; Glaser, 1987; Commission on classification and terminology of the International League Against Epilepsy, 1981; Delgado-Escueta, Walsh, 1985; Quesney, 1986; Wieser, 1988; Commission on classification and terminology of the International League Against Epilepsy, 1989; Wieser, 1991; French *et al.* 1993; Duncan *et al.* 1995), and not other types of epilepsy such as idiopathic generalized epilepsy, 2.) the ictal onset in medial temporal structures on the side of the affected hippocampus on depth-EEG studies (Delgado-Escueta *et al.* 1979; Babb *et al.* 1984b; Quesney, 1986; Wieser, 1988; Spencer *et al.* 1993; Baulac *et*

al. 1994; Cascino *et al.* 1995), and 3.) the remission of the epilepsy and improvement of social adjustment after surgical removal of the affected hippocampus. Several studies have shown that around 60-80% of patients with HS have a good surgical outcome with respect to seizure outcome (Falconer, Serafetinides, 1963; Green, Scheetz, 1964; Jensen, Klinken, 1976; Babb *et al.* 1984a; Armstrong, Bruton, 1987; Duncan, Sagar, 1987; Bruton, 1988; Berkovic *et al.* 1991; Jack, Jr. *et al.* 1992; Kuzniecky *et al.* 1993; Garcia *et al.* 1994; Berkovic *et al.* 1995; Thadani *et al.* 1995). Babb et al (Babb *et al.* 1984b) showed that anterior HS (assessed pathologically) correlated with anterior hippocampal ictal onset on depth-EEG, and good seizure outcome probably because the epileptogenic lesion was removed completely. On the other hand, evidence of diffuse HS affecting both the anterior and posterior segments of the resected hippocampus correlated with regional (i.e. in anterior and posterior hippocampus at the same time) ictal onset on depth-EEG. Patients who were not rendered seizure free after surgery had diffuse HS, and most likely the seizure focus extended beyond the resection line. Williamson et al (Williamson *et al.* 1993) described 67 patients who were selected on the basis of intractable TLE not due to mass lesions, in whom medial temporal seizure origin was documented on depth-EEG and who obtained a class 1 outcome as defined by Engel et al (Engel *et al.* 1993) after temporal lobe resection. Forty-eight of the 59 pathological specimens (81%) that were adequate for neuropathological examination showed HS. Baulac et al (Baulac *et al.* 1994) reported 18 patients who were selected on the basis of mesiotemporal seizure onset on depth-EEG. Ictal onset was on the side of the hippocampus that was small on MR-based hippocampal volumetry in 16 of the 18 patients.

Several authors, however, have postulated that the amygdala might be an important structure for epileptogenesis in mesial temporal sclerosis (Falconer *et al.* 1964; Wieser, 1988; Feindel *et al.* 1991; Gloor, 1992a; Gloor, 1992b). Firstly, the amygdala is gliotic on the side of HS in 50-76% of cases (Sano, Malamud, 1953; Falconer *et al.* 1964; Margerison, Corsellis, 1966; Bruton, 1988). Secondly, depth-EEG studies in patients with mediobasal limbic epilepsy have documented focal ictal onset in the amygdala in about 10%, in the hippocampus in 25% and regional ictal onset in the amygdala and hippocampus at the same time in about 65% of seizures in patients with intractable TLE, i.e. in the majority of cases it can not be decided whether mesiobasal seizures have their onset in the amygdala or hippocampus (Quesney, 1986; Maldonado *et al.* 1988; Wieser, 1988; So *et al.* 1989). Further, the amygdala has the lowest threshold of all the mesial temporal structures to give rise to an epileptic seizure in response to electrical stimulation (Falconer *et al.* 1964; Falconer, Taylor, 1968), and kindles more readily than the hippocampus (Goddard *et al.* 1969).

Also, Feindel and Rasmussen (Feindel, Rasmussen, 1991; Rasmussen, Feindel, 1991) noted that seizure outcome was similar for patients who underwent temporal lobe resection with amygdalectomy and minimal hippocampal resection as for those who underwent a standard temporal lobe resection with major hippocampectomy. They concluded that resection of the amygdala might be crucial for a good seizure outcome. Finally, the amygdala has been shown to play a key role in the animal model of kainate-induced epilepsy (Ben-Ari, 1985), a mechanism of epileptogenesis which may occur in humans (Cendes *et al.* 1995a) *(see domoic acid intoxication, p 46).*

1.2.6. ETIOPATHOGENESIS OF HIPPOCAMPAL SCLEROSIS.

1.2.6.1. ETIOLOGY OF HIPPOCAMPAL SCLEROSIS.

1.2.6.1.1. Association of prolonged early childhood convulsions and status epilepticus with hippocampal sclerosis. Status epilepticus and more particularly prolonged early childhood or FCs have been associated with hippocampal damage and unilateral HS in about 50-80% of cases (Cavanagh, Meyer, 1956; Falconer *et al.* 1964; Falconer, 1974; Annegers *et al.* 1987; Rocca *et al.* 1987; Sagar, Oxbury, 1987; Bruton, 1988; Cendes *et al.* 1993a; Kuks *et al.* 1993; Harvey *et al.* 1995; Maher, McLachlan, 1995; Mathern *et al.* 1995a). Acute hippocampal pathological changes after convulsive status epilepticus (CSE) observed at autopsy in patients who died in CSE include pyramidal cell necrosis in a pattern which is typical for HS, with maximal damage of the CA1 hippocampal subregion, and edema (Spielmeyer, 1927; Corsellis, Bruton, 1983). Chronic changes are hippocampal atrophy, gliosis and mossy fiber sprouting. Progression from these acute hippocampal changes associated with CSE to HS, and its time course have been documented with MRI in a total of six patients (Nohria *et al.* 1994; Jackson *et al.* 1995; Tien, Felsberg, 1995). In the acute stages, the affected hippocampus was enlarged or appeared normal in size and had an increased T2 signal, consistent with edema, which resolved over weeks to months. In one of these patients, the hyperintense signal corresponded to the CA1 hippocampal subregion. Several months after CSE, hippocampal atrophy with normal or increased T2 signal was observed. Two of these 6 patients developed complex partial seizures (CPS), one immediately after CSE, the second with a delay of one year. Serial MRI studies in cats showed high HCT2 signals during kainic acid-induced limbic seizures which correlated with edema, isointense signals after 1-2 weeks, and high HCT2 signals after 1-3 months which correlated with gliosis and atrophic changes in the hippocampi (Tanaka *et al.* 1993).

1.2.6.1.1.1. Glutamate-mediated excitotoxicity. The typical distribution of hippocampal damage in HS suggests selective vulnerability of the hippocampal subregions or pathoclisis, i.e. different susceptibilities of nerve cells to a variety of pathogenic agents due to differences in physicochemical properties (Vogt, 1925; Gloor, 1992b). This selective vulnerability could be explained by glutamate receptor-mediated excitotoxicity (Olney, 1978; Olney *et al.* 1986). Glutamate toxicity is believed to result predominantly from excessive inflow of Ca^{2+} , which may be toxic to the cell, through glutamate-gated ion channels as a result of overstimulation (Dubinsky, 1993). Sustained CPS activity in animals, whether induced by kainic acid (Olney *et al.* 1974; Nadler *et al.* 1978; Sperk *et al.* 1983; Ben-Ari, 1985), perforant path stimulation (Sloviter, 1987; Sloviter, 1991) or other means (Olney *et al.* 1983), consistently results in HS if allowed to continue for longer than 1 hour. Glutamate acts on three classes of glutamate-gated ion channels, namely N-methyl-D-aspartate (NMDA), α-amino-3-hydroxy-5-methyl-4-isoxazole-propionic acid (AMPA), and kainate receptors, and on metabotropic receptors, which are linked to G proteins. These excitatory amino acid receptors and their pathways have different anatomical distributions in the hippocampus (Monaghan *et al.* 1983; Cotman *et al.* 1987; Hollmann, Heinemann, 1994; Bettler, Mulle, 1995), which could explain the selective vulnerability of some of the hippocampal subregions. NMDA receptors are highly permeable to Ca^{2+} (Kandel, Schwartz, 1991), are found in high concentration in the termination fields of the Schaffer collaterals i.e. CA1 stratum radiatum and stratum oriens (Monaghan *et al.* 1983), and are believed to mediate excitotoxicity (Greenamyre, Porter, 1994). Kainate receptors on the other hand are found in highest concentration in the stratum lucidum of the CA3 hippocampal subregion, i.e. the region innervated by the mossy fibers (Monaghan *et al.* 1983; Hollmann, Heinemann, 1994; Bettler, Mulle, 1995). Also, calbindin (Sloviter *et al.* 1991) and chromogranin A (Munoz, 1990), which are Ca^{2+}-binding proteins which confer protection against Ca^{2+}, are present mainly in CA2 hippocampal subregion and dentate gyrus. The distribution of hippocampal damage can therefore be explained by the distribution of glutamate receptors which mediate excitotoxic damage during periods of overstimulation such as status epilepticus in neuronal subpopulations that are relatively unprotected against Ca^{2+} due to the absence of Ca^{2+}-binding proteins.

1.2.6.1.1.2. Domoic acid intoxication in humans A glutamate receptor-mediated excitotoxic mechanism as a cause of HS and epileptogenesis has been suggested in humans. Intoxication with domoic acid, which is an excitotoxin analogous to kainic acid and structurally related to glutamate, has been reported to cause generalized convulsions and complex partial status epilepticus causing severe

memory difficulties most likely due to bilateral HS which has been documented at autopsy in 4 patients who died within a few months of intoxication (Teitelbaum *et al.* 1990). One patient with domoic acid intoxication developed TLE due to bilateral HS after a silent period of 1 year (Cendes *et al.* 1995a). These observations are consistent with the animal model of kainic acid-induced TLE. In this animal model, there is evidence that the HS is a direct effect of the prolonged seizures and not due to a neurotoxic effects of kainic acid (Olney *et al.* 1974; Nadler *et al.* 1978; Ben-Ari, 1985; Olney *et al.* 1986).

1.2.6.1.2. Infections. Infections such as meningitis or encephalitis have been reported to be associated with unilateral or bilateral HS (Ounsted *et al.* 1985; Marks *et al.* 1992; Gambardella *et al.* 1993; Free *et al.* 1995). It is not clear whether HS is caused by a direct neurotoxic, ischemic or excitotoxic mechanism.

1.2.6.1.3. Cerebral trauma. French et al (French *et al.* 1993) obtained a history of cerebral trauma as the sole risk factor in 5 of 67 patients (7.5%) with mesial TLE, most of whom had HS. Mathern et al (Mathern *et al.* 1995a) reported 26 of 162 patients (16%) with intractable TLE who had a history of cerebral trauma. It is unclear however from these studies what the inclusion criteria for cerebral trauma were. Post traumatic scars as a cause of intractable TLE have been reported in only 3% of patients with intractable TLE in a large surgical series, which was not associated with HS (Bruton, 1988). The association of cerebral trauma and HS therefore may not be a causal one.

1.2.6.1.4. Genetic factors. Genetic factors may predispose individuals to seizures, which may cause HS. In humans, FCs probably have a genetic basis (Maher, McLachlan, 1995). Also, familial TLE has recently been recognized, but these patients do not have HS on MRI (Berkovic *et al.* 1996). The genetic defects underlying FCs and familial TLE however have not been found. Research in animals has been targeting epilepsy genes (Noebels, 1996). Several genetic defects have been associated with the occurrence of limbic and hippocampal seizures in mice, and may be of relevance to the human epileptic condition.

AMPA-sensitive glutamate receptor channels are impermeable to Ca^{2+}. Mice with an editing-deficient GluR-B allele express AMPA receptors with increased Ca^{2+} permeability in neuronal cells and interneurons, and develop spontaneous and recurrent seizures probably due to this aberrant excitatory signaling. Animals that had prolonged

seizures had neuronal cell loss in the CA3 hippocampal subregion, reminiscent of kainate-induced hippocampal lesions (Brusa *et al.* 1995).

Mice carrying a Ca^{2+}/calmodulin-dependent kinase II α-subunit mutation have limbic epilepsy and evidence of mossy fiber sprouting of the dentate granule cells on Timm-stained sections of the hippocampus (Butler *et al.* 1995).

Finally, mice lacking neuropeptide Y, which has been shown to inhibit glutamate release in the hippocampus (Greber *et al.* 1994), are susceptible to seizures (Erickson *et al.* 1996). Neuropeptide Y positive neuronal cells in the human dentate hilar region may play an role in the epileptogenesis, since these cells are selectively depleted with sprouting of remaining neuropeptide Y hilar neurons in the dentate molecular layer in HS (de Lanerolle *et al.* 1989). It has been postulated that these neuropeptide Y positive neurons may have an intralamellar inhibitory role *(see dentate lamellar hypothesis, p 50)* (Sloviter, 1994).

1.2.6.1.5. Dual pathology. As discussed above, HS frequently occurs in association with a second lesion. There appears an important association between HS and CD *(Figure 8, p 49)* or neuronal heterotopia (Babb, Brown, 1987; Lévesque *et al.* 1991; Rush, Morrell, 1993; Raymond *et al.* 1994; Cendes *et al.* 1995c; Raymond *et al.* 1995). These patients have a history of prolonged FCs less often than patients without CD (Raymond *et al.* 1994). Rush and Morrell (Rush, Morrell, 1993) described four patients with CD and HS who developed clinically a second seizure type after 1-15 years, and postulated that the HS was a secondary lesion induced by kindling responsible for this second seizure type. Cendes et al (Cendes *et al.* 1995c) however found a low frequency (2%) of HS in patients with tumors and a high frequency (25%) of HS in patients with CD, and argued that kindling is therefore not a likely pathogenic mechanism. A common pathogenic mechanism during early development could explain the combination of HS and CD (Raymond *et al.* 1994; Cendes *et al.* 1995c).

1.2.6.1.6. Cryptogenic hippocampal sclerosis. A history of FC, status epilepticus or meningo-encephalitis may not be obtained in patients with isolated HS. The etiopathogenesis of these cryptogenic cases remains to be established.

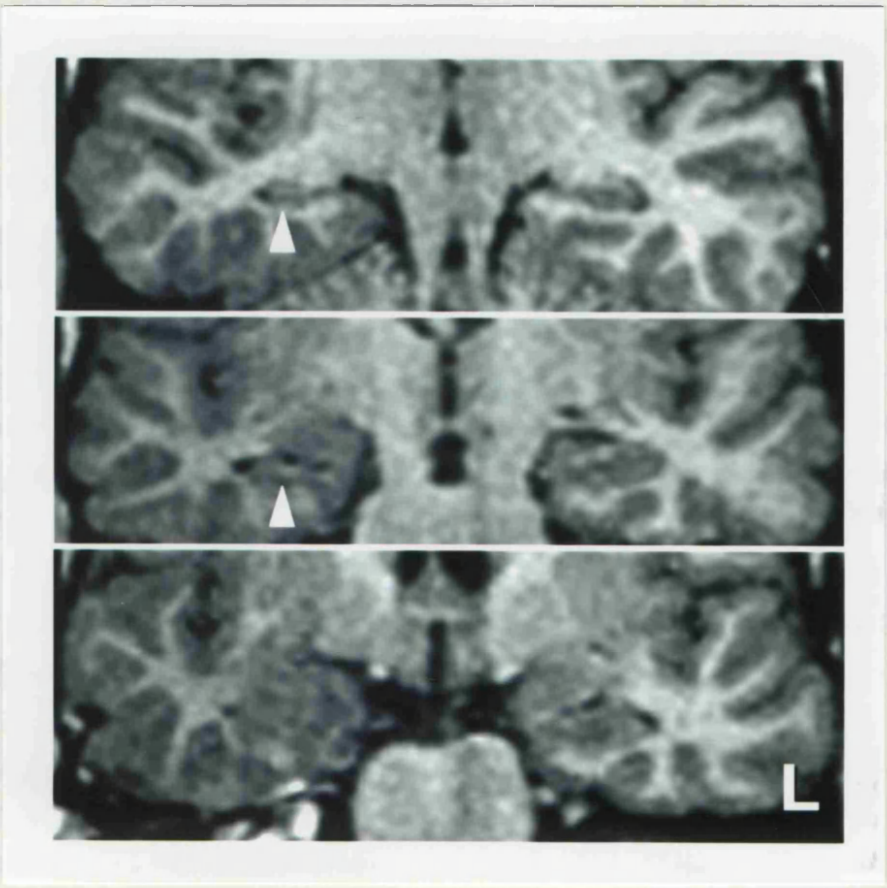

Figure 8. Dual pathology: the combination of HS and CD. Patient was a 31 year old man with intractable TLE. He had a history of prolonged FC at the age of 2 years. MRI showed dual pathology, i.e. right HS (white arrows) and marked CD of the right temporal lobe. The right temporal neocortex was thickened, and the white matter had an abnormal appearance compared with the left (L) side.

1.2.6.2. DENTATE LAMELLAR HYPOTHESIS. The dentate lamellar hypothesis (Sloviter, 1987; Sloviter, 1991; Sloviter, 1994; Sloviter, Brisman, 1995) states that a decreased GABA-mediated lateral inhibition in the dentate gyrus due to dentate hilar cell dysfunction abolishes the functional lamellar organization of hippocampal excitatory pathways and results in a hyperexcitable GCDG, which has a tendency to generate synchronous repetitive discharges, i.e. hippocampal seizures. The damage to the dentate hilar cells could be caused by prolonged FC, status epilepticus, cerebral trauma, infections or genetic factors. Sloviter (Sloviter, 1994) hypothesized that the silent period between initial insult such as FC and onset of habitual epilepsy, i.e. the time during which the scar "ripens" might be inversely proportional to the degree of damage to the hippocampus. He hypothesized that an initial small insult would take longer to develop into an epileptogenic lesion. However, the postulated progression of HS in humans has never been observed or documented. He also postulated that an individual's seizure threshold is inversely proportional with the extent of hippocampal damage.

1.2.6.3. PROGRESSIVE HIPPOCAMPAL CHANGES.

1.2.6.3.1. Human studies. It is unclear whether HS is always present from the outset of habitual epilepsy, whether HS can be the consequence of repeated seizures, or whether HS can progress as a consequence of repeated seizures.

There is clinical evidence that some patients with TLE have a progressive history. Glaser (Glaser, 1987) and French et al (French *et al.* 1993) observed that seizures in mesial TLE may progressively become worse and suggested that this may be indicative of a progressive disease. Hauser (Hauser, 1992) estimated that between 5-10% of patients with newly identified CPSs will not be controlled on antiepileptic drugs (AED) and may progress. Elwes et al (Elwes *et al.* 1984; Elwes *et al.* 1988) reported a declining interval between SGS in patients who had presented with between two and five untreated SGS, in keeping with an escalating process of epilepsy in the early stages. None of these studies however has implicated the hippocampus or HS in this progressive course.

Several previous quantitative neuropathological and MRI studies have addressed the issue of progression of HS. Due to the cross-sectional and retrospective character of these studies however the direction of an association was not clear (Mathern *et al.* 1995a; Meencke, 1995), i.e. did more seizures results in more hippocampal damage or vice versa, and the absence of an association did not rule out

the possibility of progressive changes (Cendes *et al.* 1993c; Trenerry *et al.* 1993b). It is therefore not established in humans that isolated seizures which are recurrent over years cause progressive hippocampal damage.

1.2.6.3.2. Kindling. Kindling refers to a progressive increase in electrographic and behavioral seizures evoked by periodic electrical or chemical activation of neural pathways that eventually evolve into spontaneous seizures and a permanent epileptic state (Goddard *et al.* 1969). Kindling studies in animals have provided evidence that rapidly recurring hippocampal seizures and limbic status epilepticus (Bertram *et al.* 1990), and also repeated brief seizures (Cavazos *et al.* 1994) may induce HS. The destruction of the GCDG slows the rate of development of kindling (Sutula *et al.* 1986), and kainic acid-induced HS facilitates kindling (Feldblum, Ackermann, 1987), implicating the hippocampus as an important structure for kindling-induced epileptogenesis. Morphologic alterations induced by kindling include hippocampal neuronal loss (Bertram *et al.* 1990; Cavazos, Sutula, 1990; Cavazos *et al.* 1994) and a reorganization of the axons of the granule cells, the mossy fibers, i.e. synaptic reorganization (Sutula, 1990; Cavazos *et al.* 1991). These mossy fibers normally project to hippocampal neurons in CA3 and hilus, but during kindling sprout into the inner molecular layer of the dentate gyrus and are believed to establish excitatory synapses (Cavazos *et al.* 1991). The mossy fibers and the synaptic reorganization can be visualized using Timm histochemistry and dynorphin immunoreactivity (Houser *et al.* 1990). This synaptic reorganization is observed early in the course of kindling, progresses with the evolution of kindling and is permanent (Cavazos *et al.* 1991). In resected hippocampi of patients with TLE and HS, a similar pattern of mossy fiber synaptic reorganization has been observed (Sutula *et al.* 1989; Houser *et al.* 1990; Babb *et al.* 1991; Babb *et al.* 1992; Mathern *et al.* 1995b). Although the relevance of the animal kindling model has not been established for human TLE, these observations raise the possibility that kindling could be a mechanism in the progression of HS and could explain a progressive worsening of the epileptic condition, a history often obtained from patients with TLE (Gowers, 1881; Glaser, 1987; Elwes *et al.* 1984; Elwes *et al.* 1988; Hauser, 1992; French *et al.* 1993).

1.2.6.4 CONCLUSION. The current hypothesis of the etiopathogenesis of HS postulates that HS may be both the cause and consequence of seizures that originate in the temporal lobe (Pringle *et al.* 1993; Sloviter, 1994).

CHAPTER II. METHODOLOGY.

In this chapter, methodologies which have been used in several chapters are discussed. In subsequent chapters, reference is made to sections of this chapter. The methodology of the neuropathological studies is discussed in chapter 5.

2.1. SUBJECTS.

2.1.1. CONTROL SUBJECTS.

Thirty-nine control subjects (22 women and 17 men, median age: 29 years, range: 21-38 years) underwent HCT2 mapping *(Chapter 3 and 4)*. Twenty-two of these control subjects had MR-based HCV measurements *(Chapter 4)*. For the longitudinal MRI study, 12 control subjects were rescanned with a median interval between baseline and follow-up scan of 643 days (range: 385 to 1024) *(Chapter 7)*. Twenty control subjects had AT2 maps *(Chapter 8)*. For the pathology study, 6 control hippocampi of persons (three men and three women; median age = 31 years, range: 14 to 52) who had died form non-neurological causes were obtained at autopsy *(Chapter 5)*.

2.1.2. PATIENTS.

A total of 207 patients (115 women and 92 men) with median age of 29 years (range: 14 to 64) with localization-related epilepsy were studied and included in the present work. Sixty-three of these patients (30%) had newly-diagnosed localization-related epilepsy *(Chapter 6)* and 144 (70%) had intractable TLE *(Chapter 3,4,5 and 8 and 9)*. The overlap of patients in the different studies is shown in Appendix A (p 222).

2.2. EVALUATION OF PATIENTS AND DATA COLLECTION.

All patients were assessed clinically by the author and data collection was prospective and systematic. The following data were entered in a database (Filemaker Pro 2.0, Macintosh II si): gender, age, date of birth, age at the time of study, handedness, age of onset of habitual epilepsy, duration of epilepsy, a history of FCs and meningo-encephalitis, age at the time of these events, family history of FC and epilepsy, seizure types and description, average frequency of each seizure type during the year preceding the scan, and total number of secondary generalized seizures (SGS) in their lifetime, findings of physical and neurological examination, results of interictal and ictal

video-EEG, results of standard qualitative MR imaging, quantitative hippocampal and amygdala MRI (see below), and quantitative hippocampal neuropathology.

2.3. STANDARD QUALITATIVE MR IMAGING AND VISUAL ASSESSMENT OF MR IMAGES.

2.3.1. STANDARD MR IMAGING.

For patients with chronic epilepsy standard MR images were obtained on a GE Signa 1.5 T, and included a 3-D Spoiled Gradient Echo (SPGR) sequence (35/8/0.75 (repetition time [TR]/echo time [TE]/number of excitations [NEX]), flip angle 30 degrees, matrix size 256x192, 200 mm field of view (FOV), 124 1.5 mm contiguous coronal sections), and proton density and T2-weighted images in the coronal plane perpendicular to the long axis of the hippocampus (5 mm thick sections with intersection gap of 1.5 mm, 3100/30-90/0.75 (TR/TE/NEX), 220 mm FOV, matrix size 256x256).

In the longitudinal study of adult patients with newly diagnosed localization-related epilepsy, the standard images were obtained on a 1.5 T Siemens SP63 Magnetom scanner. The standard protocol included a 3-D Magnetization Prepared Rapid Gradient Echo (MPRAGE) sequence 10/4/200/1 (TR/TE/inversion time [TI]/NEX), flip angle 12 degrees, matrix size 256x256, and 128 sagittal partitions in the third dimension with partition thickness of 1.25 mm, that was reformatted into 2 mm thick sections in a tilted coronal plane at right angles to the long axis of the hippocampus, and in a tilted axial plane parallel to the long axis of the hippocampus, and T2-weighted images in the coronal plane perpendicular to the long axis of the hippocampus (5 mm thick sections with intersection gap of 0.5 mm, 4600/90/1 (TR/TE/NEX), 220 mm FOV, matrix size 192x256), and IR T1-weighted images in the coronal plane perpendicular to the long axis of the hippocampus (5 mm thick sections with intersection gap of 0.5 mm, 3500/20/300/1 (TR/TE/TI/NEX), 220 mm FOV, matrix size 135x256) *(Chapter 6)*.

2.3.2. VISUAL ASSESSMENT OF HCT2 SIGNAL AND ATROPHY.

To assess sensitivity of visual inspection to detect an increased HCT2 signal and atrophy, two observers, who were blinded to patient's data, assessed hard copies of MR images of 40 patients with intractable TLE for the presence of atrophy and increased T2 signal. Atrophy was assessed using 1.5 mm contiguous SPGR coronal

images of the hippocampi. Increased signal was assessed from the image with TE of 118 msec from the 16 echo data set used to calculate the HCT2 map. A HCT2 ≥ 115 msec and a HCVR ≤ 0.85 were consistently detected on visual inspection *(see Chapter 3, p 79)*.

2.3.3. VISUAL ASSESSMENT OF AMYGDALA T2 SIGNAL.

Three observers blinded to the AT2 values measured on AT2 maps rated the presence or absence of an increased AT2 signal on visual inspection of a hard copy of the image with TE =118 msec (from the set of images used to calculate the AT2 map). Agreement between two or three observers was used as outcome measure (i.e. presence or absence of increased AT2 signal). The sensitivity of detecting an abnormal amygdala signal on visual inspection compared to the quantitative measurement was 38% *(see Chapter 8, p 180)*.

2.4. QUANTITATIVE MR IMAGING.

For both control subjects and patients, all imaging to enable HCT2 mapping and HCV measurements described in this present work was performed on a 1.5 T Siemens SP63 Magnetom Scanner.

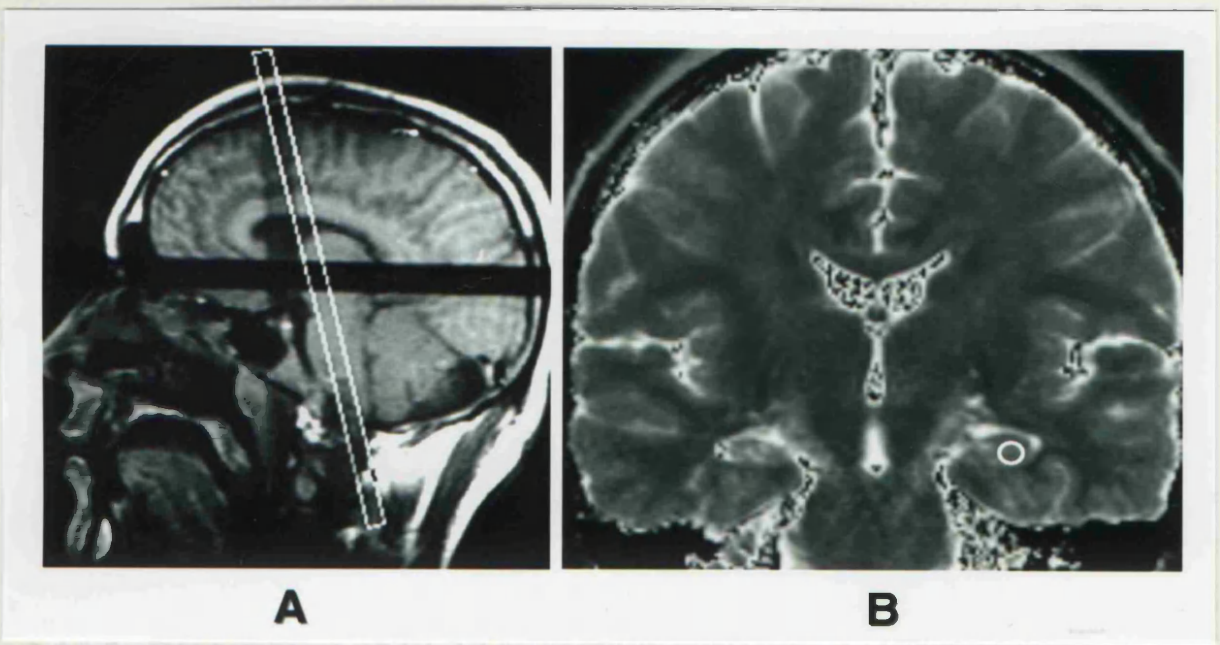

Figure 9. HCT2 map. A. The orientation of the 8 mm thick HCT2 map is determined on a sagittal scout. The HCT2 map is aligned along the anterior border of the brainstem, which results in an orientation at right angles to the long axis of the hippocampus. B. HCT2 map with circular ROI in which T2 relaxation time was measured in the left hippocampus.

2.4.1. HIPPOCAMPAL T2 (HCT2) MAPPING.

HCT2 maps *(Figure 9, p 55)* were calculated from 16 identical images obtained at echo times ranging from 22 to 262 msec using a PHAPS sequence (Graumann *et al.* 1986) which is made up of a combination of a CPMG sequence followed by a CP sequence, and were generated by fitting single exponentials to the image data of corresponding pixels from these 16 echoes, as described previously (Jackson *et al.* 1993b; Grünewald *et al.* 1994a). The thickness of this HCT2 map was 8 mm and its orientation was in a tilted coronal plane along the anterior border of the brainstem perpendicular to and at the level of the body of the hippocampus. The HCT2 relaxation time as used in this study was measured by placing the largest possible circle as a ROI within the hippocampus while avoiding boundaries where partial volume effects with CSF might occur, and is expressed in msec. In the first study of the present work *(Chapter 3)*, the measurements were done by two observers, who were blinded to patient's data, and who agreed on the ROI within the hippocampus in which HCT2 was measured. In the later studies *(Chapter 4-9)*, measurements were done by one person. Mean HCT2 of 39 control subjects including the 12 previously described (Jackson *et al.* 1993b) was 101.7 msec with a SD of 3.1 msec (range: 93-107 msec). The upper limit of normal was 108 msec, which is 2 SDs above mean control HCT2 in

Chapter 3-5, 8 and 9, and 111 msec, which is 3 SD above mean control in Chapter 6 and 7. The latter was done to increase the specificity of the test in patients with newly diagnosed localization-related epilepsy.

2.4.1.1. REPEATABILITY STUDIES OF HIPPOCAMPAL T2 MAPPING. In the longitudinal quantitative hippocampal MRI study of patients with newly-diagnosed localization-related epilepsy, it was important to know the RC and limits of agreement of repeated HCT2 maps in control subjects for the correct interpretation of results in the patient group. HCT2 maps were therefore repeated in 12 control subjects. The mean difference d_{T2} (± SD) between baseline and follow-up HCT2 (n=22) was 0 ± 3 msec. The limits of agreement for HCT2 mapping defined as d_{T2} ± 3 SD were therefore ± 9 msec *(see Chapter 7, p 153)*

2.4.1.2. DEPENDENCE OF HCT2 ON SECTION POSITION. T2 values as measured with the PHAPS sequence have been reported to show a variation of up to 18% as a function of section position in the MR scanner in particular circumstances, e.g. long T2 and low number of echoes (Rimmington, Porter, 1996). In this study, a PHAPS sequence with 16 echoes was used. HCT2 values (n=280) obtained from 140 persons were plotted as a function of the position of the HCT2 map in the MR scanner. No systematic deviations in HCT2 values obtained from 16 echoes were observed as a function of section position in the MRI scanner *(Figure 10, p 57).*

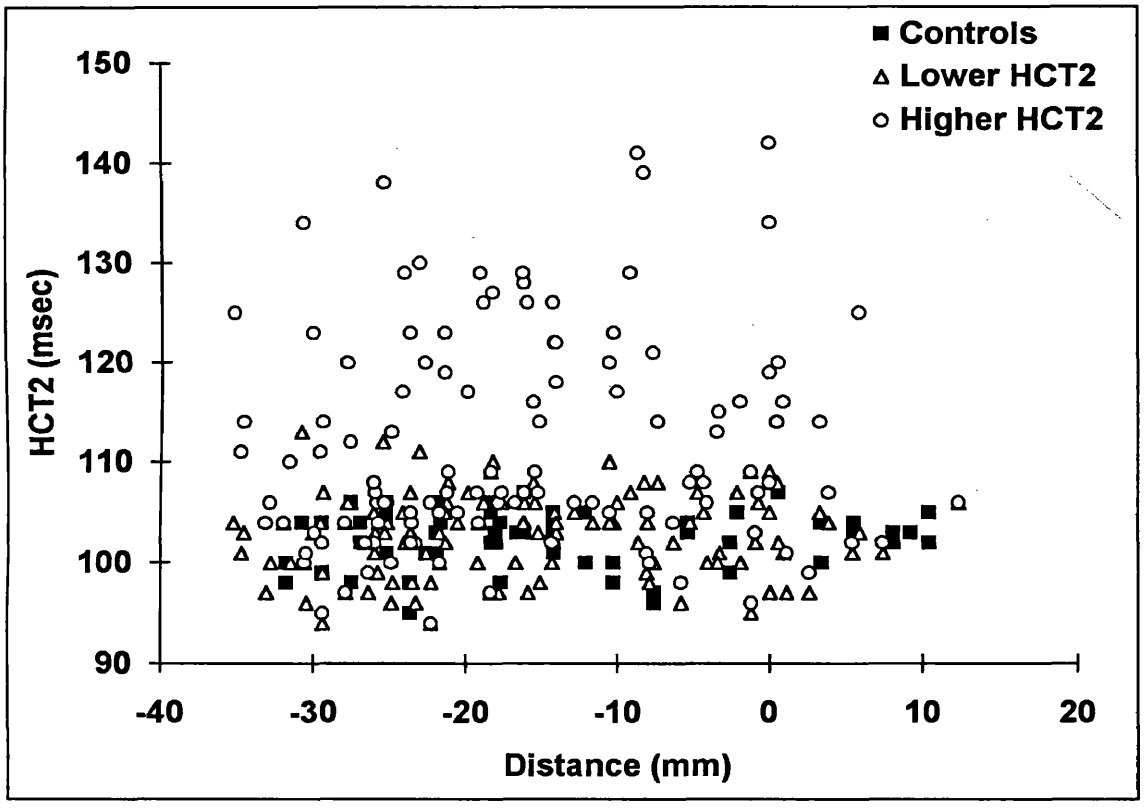

Figure 10. HCT2 as a function of the position of the HCT2 map in the MRI scanner. HCT2 values of 32 control subjects, and 108 patients with epilepsy were plotted as a function of section position (expressed in millimeter [mm]) in the MRI scanner. There was no obvious dependence of HCT2 on the position in the MR scanner.

2.4.2. HIPPOCAMPAL VOLUMETRY.

2.4.2.1. DESCRIPTION OF MR-BASED HIPPOCAMPAL VOLUMETRY. The volume of the hippocampus can be estimated from parallel sections separated by a known distance h, by summing the cross-sectional hippocampal areas and multiplying this figure by the distance h (Cavalieri's principle) (Gundersen *et al.* 1988; Mayhew, Olsen, 1991; Cook *et al.* 1992; Oorschot, 1994). Images for hippocampal volumetric studies were obtained using a 3-D MPRAGE sequence 10/4/200/1 (TR/TE/TI/NEX), flip angle 12 degrees, matrix size 256x256, and 128 sagittal partitions in the third dimension with partition thickness of 1.25 mm. In the longitudinal follow-up study, the same FOV was used for baseline and follow-up MPRAGE. The MPRAGE dataset was reformatted into 1 mm thick contiguous sections in a tilted coronal plane that was perpendicular to the long axis of the hippocampus *(Figure 11, p 58)*. In the longitudinal follow-up study *(Chapter 7)*, the baseline and follow-up MPRAGE datasets were reformatted in an identical way during the same session. The reformatted images were transferred to a SUN workstation and analyzed using

Xdispim (Plummer, 1992). Hippocampal boundaries were as described by Watson et al (Watson *et al.* 1992). The hippocampus proper, dentate gyrus, fimbria, subiculum, intralimbic gyrus and uncinate gyrus were included in the HCV measurements *(see macroscopic hippocampal anatomy on MR images, p 25 and following pages)*. The first section was defined as the one in which the fornix was seen in its full profile. The full length of the hippocampus was measured. For comparison of two datasets of one individual in the longitudinal study *(Chapter 7)*, a one-in-one sampling strategy (i.e. hippocampal cross-sectional areas on all 1 mm sections were measured) was used. Otherwise, a one-in-three sampling strategy was used which was random and systematic i.e. from the first three sections one was chosen randomly and from that section every third section was measured systematically *(see optimal sampling strategies, p 59)*. The HCV was calculated by summing the hippocampal cross-sectional areas and multiplying this figure by the distance between two sections i.e. 1 or 3 mm, depending on the sampling strategy (Cavalieri's principle) (Gundersen *et al.* 1988; Mayhew, Olsen, 1991; Cook *et al.* 1992; Oorschot, 1994).

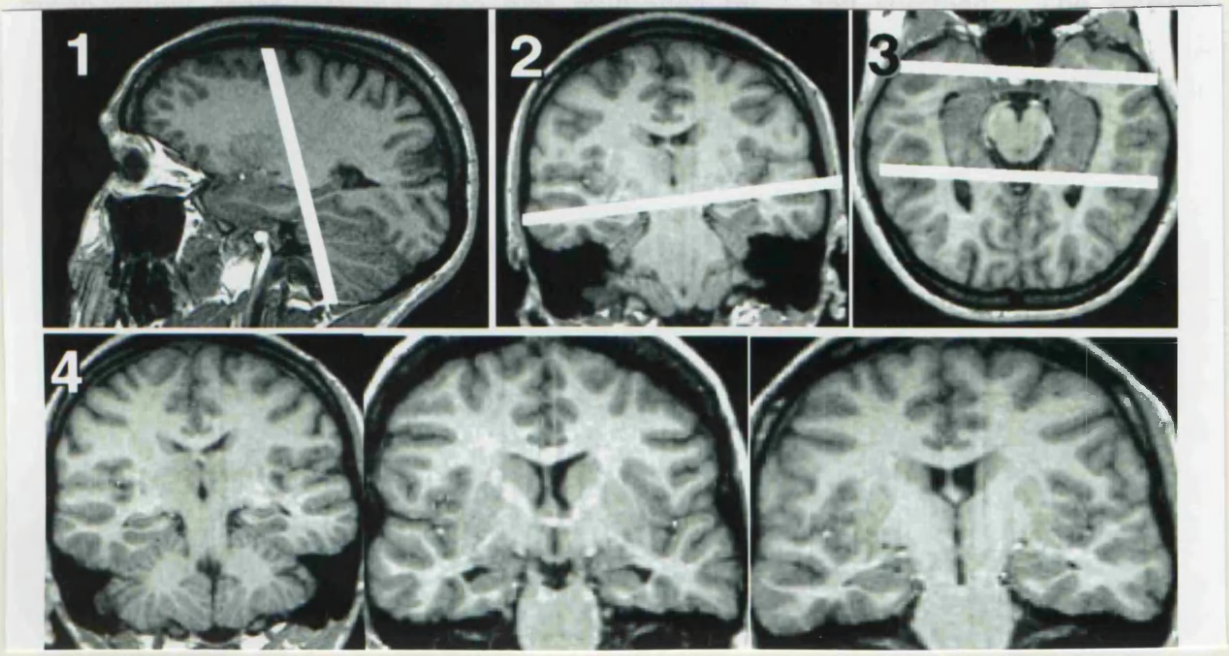

Figure 11. Reformatting of MPRAGE dataset for hippocampal volumetry. The unreformatted MPRAGE volume set consists of 128 1.25 mm contiguous sagittal sections. A section in which the hippocampus is visible is selected (1). On this image, a section is selected at the level of the body of the hippocampus, at right angles to the long axis of the hippocampus. This results in an image in a tilted coronal plane through the hippocampi (2). On this image, a section is selected through both hippocampi, which corrects for headtilt. This results in a tilted axial image in which the full length of both hippocampi are visible (3). On this image, a set of 1 mm contiguous sections are selected with alignment at the fornices posteriorly (*see Figure 2, p 27*). This results in a set of 1 mm contiguous sections at right angles to the long axis of the hippocampus with alignment of the fornices and correction for headtilt.

2.4.2.2. REPEATABILITY STUDIES.

2.4.2.2.1. Repeatability studies of MR-based hippocampal volumetry using the same dataset and determination of optimal sampling strategies.

2.4.2.2.1.1. Design of repeatability studies to determine optimal sampling strategies. Hippocampi of control subjects (n=22) were measured three times. The first and second measurements were carried out in the same session and the third measurement with a delay of several months. The HCV for the three sets of measurements were calculated in five different ways. Firstly, using Cavalieri's principle (Gundersen *et al.* 1988; Mayhew, Olsen, 1991; Cook *et al.* 1992; Oorschot, 1994), the hippocampal cross-sectional areas of all measurements were multiplied by the section thickness i.e. 1 mm and summed. Secondly, every second section was selected and the hippocampal cross-sectional area was multiplied by 2 and summed. The starting section position (i.e. either section 1 or 2) was chosen randomly. The HCVs were also calculated using every third, fourth and fifth section with random start from section 1 to x (x being 3, 4 or 5 respectively). The mean, mean difference and RC between the first measurement and subsequent remeasurements were calculated for each of the 5 sampling strategies. The RC is 2 SD of the mean difference between two measurements and has been suggested to be the best method to assess agreement between two methods of clinical measurement (Bland, Altman, 1986).

2.4.2.2.1.2. Results of repeatability studies for MR-based hippocampal volumetry. The mean number of sections covering the hippocampus in the tilted coronal plane was 42 ±2. Results are shown in Table 2. The mean HCVs were identical for all sampling strategies with SDs that were not significantly different. The mean differences between measurements were small and within 2.2 % of the mean HCV in all cases. For the immediate remeasurements *(Table 2, section A, p 60)*, the sampling strategy using all 1 mm sections had the lowest RC of 221 mm^3 (= 4.2% of mean HCV). This means that 95% of remeasurements were within 4.2% of the first measurement. The RC increased as the sampling interval increased. For the delayed remeasurement *(Table 2, section B, p 60)*, the RC for the one-in-one sampling strategy was identical to that of the one-in-two and one-in-three sampling strategies. The agreement was less good for the one-in-four and one-in-five sampling strategies.

	Section selection	Mean	SD	Mean difference	RC (% of mean)
A	one-in-one	5271	622	46	221 (4.2%)
	one-in-two	5262	637	116	345 (6.9%)
	one-in-three	5235	626	94	459 (8.8%)
	one-in-four	5280	664	83	553 (10.5%)
	one-in-five	5284	659	18	803 (15.2%)
B	one-in-one	5272	609	44	529 (10.0%)
	one-in-two	5294	610	51	576 (10.9%)
	one-in-three	5262	627	39	530 (10.1%)
	one-in-four	5305	653	33	818 (15.4%)
	one-in-five	5238	656	109	757 (14.5%)

Table 2. Repeatability of MR-based HCV measurement using the same dataset. A: Immediate (in same session) remeasurement of HCVs. B: Delayed (months) remeasurement of HCVs. Mean, SD and RC are expressed in mm^3. Mean = $\Sigma(x_1/2 + x_2/2)/n$ and mean difference = $\Sigma(x_1 - x_2)/n$ with x_1 = HCV on first measurement and x_2 = HCV on repeat measurement and n = number of hippocampi measured i.e. 42. SD is standard deviation of mean HCV.

*2.4.2.2.1.3. **Optimal sampling strategies and conclusion of repeatability studies using the same dataset.*** The results of delayed remeasurements indicate that a one-in-three sampling scheme is optimal for routine measurement of HCV. It has a better agreement than a one-in-four scheme and has the same RC as the more exhaustive sampling strategies, reducing measuring time by a factor 2 or 3, to 15 minutes. For a longitudinal study of HCV, the lowest RC can be obtained by measuring scans from different time points in a single session using one-in-one section sampling. The better results of the immediate remeasurement are explained by visual memory of the boundaries traced on the first set of scans.

2.4.2.2.2. Repeatability studies of MR-based hippocampal volumetry using different datasets of the same person. In the longitudinal follow-up study *(Chapter 7)*, patients were rescanned after around 1 year. It was therefore necessary to establish the RC of HCV measurement using two different dataset in control subjects. Twelve control subjects were rescanned. The mean difference d_{HCV} (± SD) between baseline and follow-up HCV (n=24) was 91 ± 151 mm^3. The limits of agreement for the HCV defined as d_{HCV} ± 3 SD were therefore +554 and -362 mm^3 *(see Chapter 7, p 153).*

2.4.2.3. CORRECTION OF HIPPOCAMPAL VOLUMES FOR INTRACRANIAL VOLUME. Intracranial volume (ICV) was measured on the sagittal unreformatted MPRAGE dataset with a 1-in-10 random and systematic sampling strategy of the 1.25 mm thick sections. Landmarks for ICV were the dura mater (which was easily visible over the

convexities of the cerebral and cerebellar hemispheres) or the inside of the skull if the dura was not visible; the undersurface of frontal and temporal lobes excluding the petrous bone; the clivus; at the craniovertebral junction, the attachment of the dura to the anterior and posterior arch of C1 *(Figure 12, p 62)* [C. Jack, personal communication]. Test-retest repeatability studies for all control subjects showed a mean difference between first and repeated measurement of 15 cm^3 (1%) and a RC (Bland, Altman, 1986) of 32 cm^3 (2%). The Pearson's correlation coefficient between HCV and ICV was 0.62 ($p < 0.001$) *(Figure 13, p 63)*. HCV was corrected for ICV using the covariance method described by Jack et al (Jack, Jr. *et al.* 1990), and Free et al (Free *et al.* 1995). This method derives a HCV corrected for ICV via the following equation: $HCV_{corrected} = HCV_{measured}$ - gradient x ($ICV_{measured} - ICV_{mean}$) (HCV and ICV expressed in mm^3). Gradient is the slope of the regression line of control HCV versus ICV, which was calculated using a linear regression analysis. In this study, the gradient was 0.00241. Mean control uncorrected HCV was 5180 ± 532 mm^3 and corrected for ICV 5180 ± 416 mm^3. The lower limit of the corrected control HCV reference range was defined by 2 SD below the mean control value and was 4348 mm^3 in Chapter 4, 5, 8 and 9, and by 3 SD below the mean control value, i.e. 3932 mm^3 in Chapter 6 and 7. In the remainder of the text, HCV will always refer to HCV corrected for ICV. *(see also discussion of correcting HCV for ICV, p 110)*. Mean (±SD) HCVR was 0.96 ± 0.03. The smallest HCVR of the controls was 0.92. A cut-off value of 0.87 was used which is 3 SD below mean control HCVR.

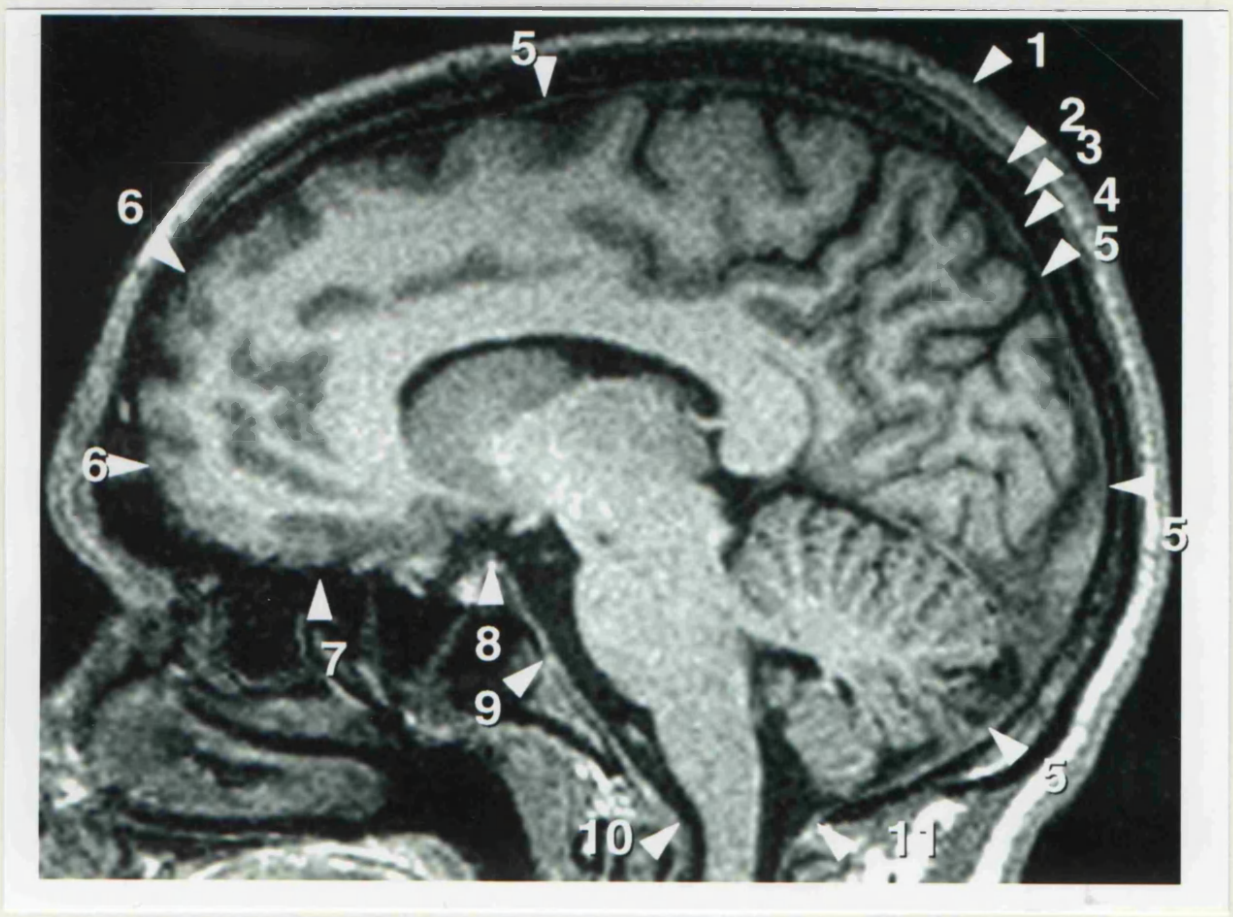

Figure 12. Landmarks for ICV measurement. ICV was measured on the unreformatted 1.25 mm sagittal sections of the MPRAGE. Over the cerebral convexity, the dura mater was used as landmark. The dura is easily visible on thin T1-weighted images as a white line (5). The scalp (1) is visible as a bright white line. The outer table of the skull (2) is seen as a black line immediately below the scalp. The diploë (3) is the white line between outer table (2) and inner table (4), the second black line, of the skull. The dura mater (5) lies immediately below the inner table (4). Over the frontal convexity, the dura may be difficult to visualize, in which case the cerebral contour is outlined (6). Caudally, the undersurfaces of frontal lobe (7), and temporal lobe (not shown) are used as landmarks. The petrous bone is excluded from the measurements (not shown). Other landmarks are the dorsum sellae (8), clivus (9), and at the craniovertebral junction the attachment of the dura to the anterior (10) and posterior arch (11) of C1.

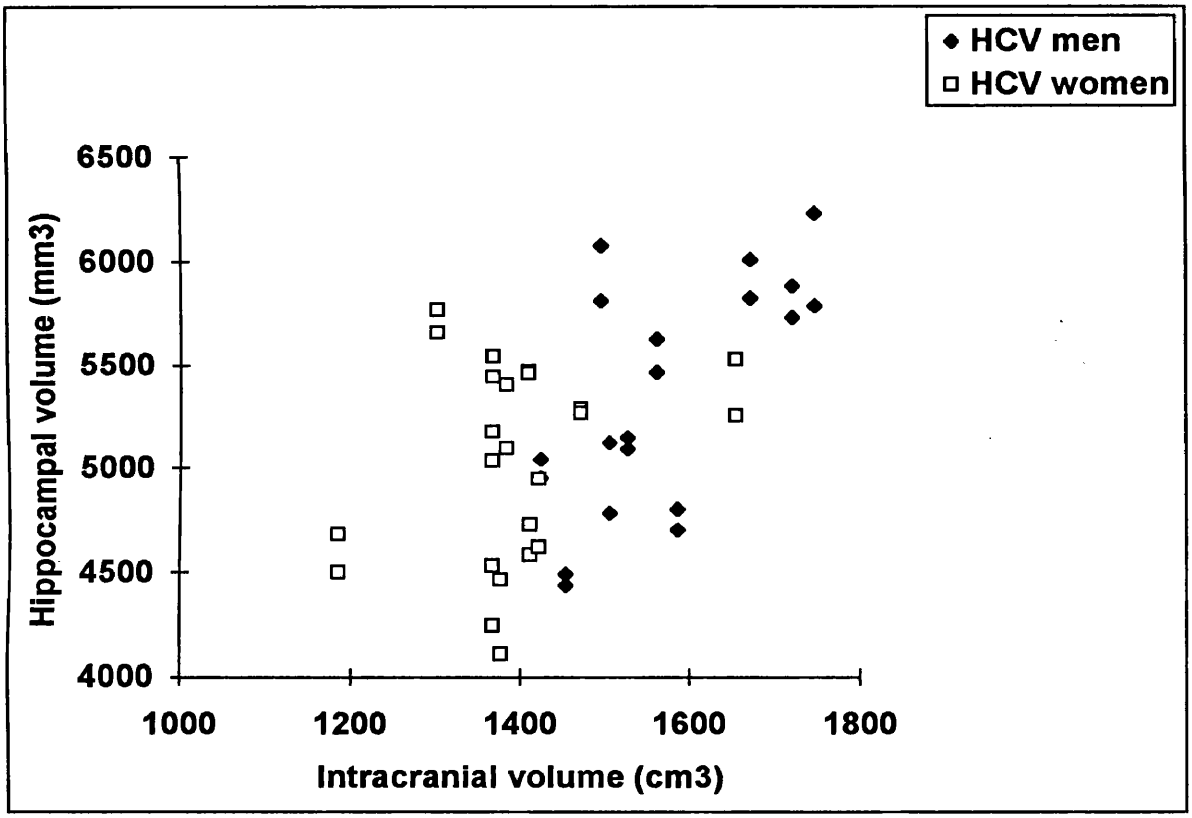

Figure 13. HCV as a function of ICV. The graph plots control HCV (mm^3) as a function of ICV (cm^3). The graph shows that men (black diamonds) tend to have larger HCV and ICV than women (open squares). The HCV correlates with ICV ($r= 0.62$, $p< 0.001$).

2.4.2.4. HIPPOCAMPAL VOLUME DISTRIBUTION GRAPHS. The hippocampal cross-sectional areas were plotted in a graph as a function of section position, as described by Cook et al (Cook *et al.* 1992) *(Table 3, p 64; Table 4, p 65; Figure 14, p 66)*. For a one-in-three sampling strategy, all datapoints were plotted. For a one-in-one sampling strategy, one datapoint represented the average hippocampal cross-sectional area of three consecutive sections. A control graph plotting mean control hippocampal cross-sectional area for each section position was constructed as described by Kim et al (Kim *et al.* 1995b), with 2 graphs covering a total volume which was 2 SDs above and below the mean control HCV. These two graphs were drawn at a distance from the mean control graph which was proportional to the SD of the mean control value for each section position. In the current work only these calculated graphs (± 2 SD) are shown in the figures. In Chapter 7, the graphs are drawn at 3 SD. HCV distribution was assessed qualitatively by visual assessment of the graphs, and atrophy was classified as anterior, posterior or diffuse.

n	S1	S2	S3	S4	S5	S6	S7	S8	S9	S10	S11	S12	S13	S14	S15	S16
h1	87	75	103	80	98	87	105	111	152	190	194	163	153	87	70	0
h2	57	83	82	111	94	80	104	112	116	151	209	220	168	139	108	49
h3	38	95	94	89	85	97	104	101	166	211	210	178	135	67	0	0
h4	36	94	89	93	99	95	86	113	155	180	192	181	112	32	0	0
h5	93	93	98	92	97	95	117	134	203	243	234	198	98	0	0	0
h6	86	94	108	103	102	107	127	171	199	218	156	159	62	0	0	0
h7	82	84	108	79	105	76	104	128	164	233	212	220	186	108	24	0
h8	76	87	98	113	102	100	101	133	182	196	228	211	154	106	0	0
h9	99	86	94	82	92	97	107	99	111	172	209	166	151	48	0	0
h10	95	109	97	82	72	110	112	84	114	127	191	187	150	71	0	0
h11	67	76	67	80	73	80	85	101	132	153	187	182	137	86	0	0
h12	66	73	79	85	87	88	89	87	121	141	172	167	133	83	0	0
h13	71	91	86	87	88	98	113	114	138	179	212	202	141	58	0	0
h14	99	79	77	98	97	99	108	129	170	176	195	151	122	58	0	0
h15	82	75	90	96	83	84	113	119	131	196	205	185	174	127	70	25
h16	102	106	82	92	81	89	90	109	107	176	221	221	167	164	73	22
h17	50	86	93	85	86	107	111	111	175	193	221	228	187	93	0	0
h18	61	104	94	96	110	106	116	127	161	213	227	215	107	27	0	0
h19	100	67	80	97	87	92	83	103	116	126	199	227	210	162	112	0
h20	60	108	86	91	100	86	102	112	111	123	194	249	217	161	58	0
h21	100	70	82	82	82	91	109	87	178	187	194	193	127	91	0	0
h22	92	73	76	86	102	95	95	104	160	196	190	188	133	103	40	0
h23	114	104	100	105	92	115	135	209	230	166	143	70	0	0	0	0
h24	121	103	120	110	95	102	116	170	183	173	116	56	0	0	0	0
h25	67	80	80	62	77	82	96	103	91	103	184	197	175	133	127	47
h26	34	93	64	90	76	77	90	95	93	102	146	219	186	152	94	0
h27	106	84	80	101	110	105	123	121	177	179	208	158	123	46	0	0
h28	97	100	102	105	92	95	105	135	161	162	201	171	126	42	0	0
h29	93	79	97	77	114	94	122	107	161	169	190	145	71	0	0	0
h30	95	98	93	91	104	113	113	112	166	180	185	177	86	0	0	0
h31	106	101	109	92	104	99	118	106	152	193	209	182	117	41	0	0
h32	107	126	89	110	92	101	118	118	179	184	201	142	55	0	0	0
h33	82	107	106	124	124	131	128	130	159	172	159	141	118	52	0	0
h34	97	114	107	105	105	123	116	121	146	180	195	170	130	86	0	0
h35	82	115	92	90	115	114	110	122	170	176	194	201	162	59	0	0
h36	104	114	92	98	106	94	123	131	168	184	202	226	155	136	41	0
h37	88	96	102	82	95	93	98	124	156	192	199	163	91	0	0	0
h38	97	102	87	92	93	81	129	130	179	195	199	166	78	0	0	0
h39	65	82	84	75	98	103	109	113	118	158	180	207	194	190	86	25
h40	86	103	90	76	104	97	128	124	129	152	208	201	169	169	84	0
h41	84	74	91	86	101	109	111	127	170	209	205	192	162	58	0	0
h42	88	76	99	104	104	98	100	123	194	230	208	199	145	0	0	0
h43	101	71	88	96	118	110	120	141	204	234	204	186	80	0	0	0
h44	116	106	101	110	115	96	107	123	160	230	195	173	105	65	0	0
mean	85	92	92	93	97	98	109	120	155	180	195	183	131	70	22	4
SD	21	15	11	12	12	12	13	22	32	33	23	37	48	57	39	12

Table 3. Control hippocampal cross-sectional area (mm^2) as a function of section position. Hippocampal cross-sectional area (mm^2) is given for each section position (S) of 44 control hippocampi (h) (n=22). Notice that cross-sectional area is the same as the volume of the 1 mm thick section on which it was measured. Section position 1 is the section in which the fornix is seen in its full profile *(see Figure 3, p 29)*. The mean cross-sectional area for each section position and its SD are given.

Section position	Mean cross-sectional area (*)	SD	SD/mean SD	52x (SD/ mean SD)	52x (SD/ mean SD)/3	mean cross-sectional area - 2SD	mean cross-sectional area + 2SD
1	84.75	21.12	0.85	44.11	14.70	70.05	99.45
2	91.73	14.65	0.59	30.60	10.20	81.53	101.93
3	91.73	11.46	0.46	23.94	7.98	83.75	99.71
4	92.73	12.31	0.49	25.71	8.57	84.16	101.30
5	96.73	12.15	0.49	25.38	8.46	88.27	105.19
6	97.52	11.97	0.48	25.00	8.33	89.19	105.85
7	109.00	12.71	0.51	26.55	8.85	100.15	117.85
8	119.86	22.49	0.90	46.98	15.66	104.20	135.52
9	154.73	31.53	1.27	65.86	21.95	132.78	176.68
10	179.61	33.02	1.33	68.97	22.99	156.62	202.60
11	195.07	22.93	0.92	47.90	15.97	179.10	211.04
12	182.57	36.75	1.48	76.76	25.59	156.98	208.16
13	130.73	48.24	1.94	100.76	33.59	97.14	164.32
14	70.45	56.94	2.29	118.93	39.64	30.81	110.09
15	22.43	38.53	1.55	80.48	26.83	-4.40	49.26
16	3.82	11.52	0.46	24.06	8.02	-4.20	11.84

Table 4. Construction of control graph. The mean control cross sectional area (mm^2) and its SD for each section position are given in the first three columns. (*) Notice that this cross-sectional area is the same as the volume since section thickness was 1 mm. The fourth column gives the SD of each section position divided by the mean SD, i.e. 24.89 mm^2. The mean control HCV was 5180 ± 416 mm^3. Two SD of the mean control HCV is therefore 832 mm^3. This volume divided over the 16-three mm sections is 52 mm^3. This volume of 52 mm^3 multiplied by SD/mean SD (column 5) and divided by the distance between section, i.e. 3 mm, gives the 2 SD for each section position, which allows the construction of a HCV distribution graph ± 2SD *(see Figure 14, p 66)*.

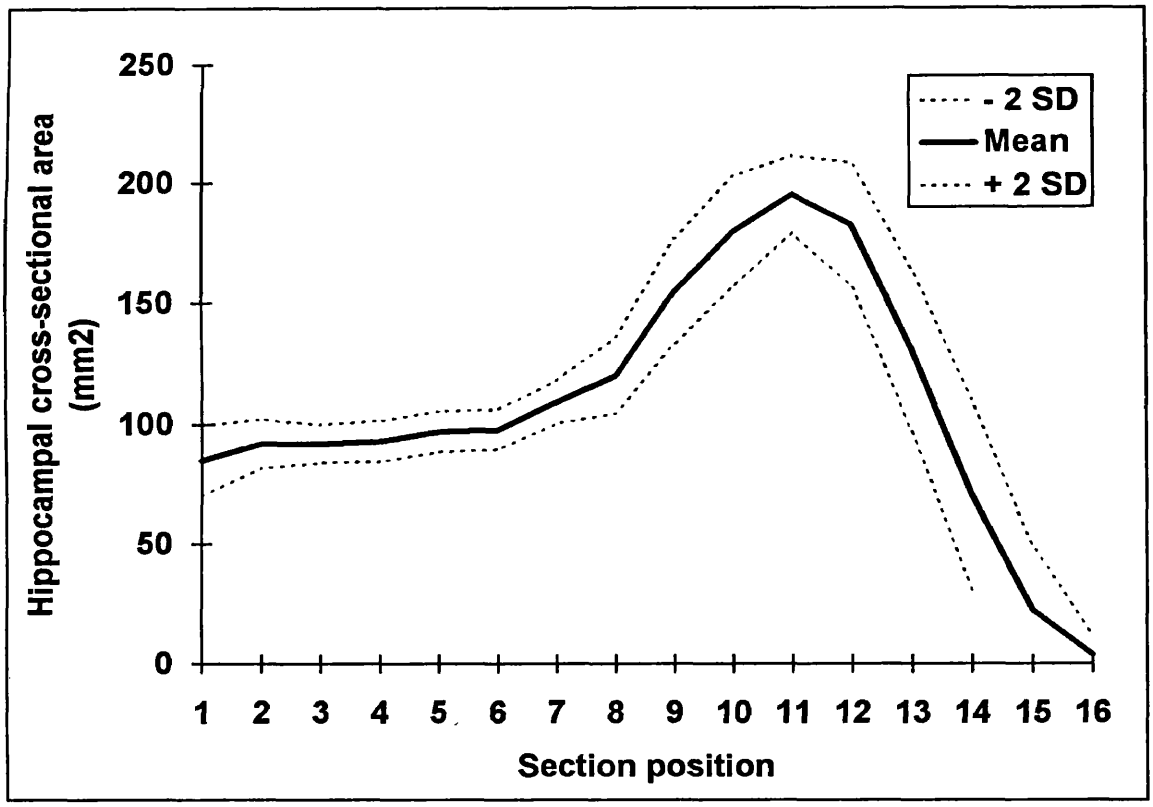

Figure 14. Construction of control HCV distribution graph. The graph plots the mean control cross-sectional area (mm^2) for each section position (in bold), and 2 graphs (in broken lines) representing a HCV which is ± 2 SD of the mean control HCV *(see Table 4, p 65)* Notice that these 2 SD represent values corrected for ICV. The plots of HCV cross-sectional area of an individual patient should be corrected for ICV, which can be done by adding the following correction factor to each hippocampal cross-sectional area: (measured area x [corrected HCV - measured HCV]/mean HCV).

2.4.2.5. SPGR-BASED HIPPOCAMPAL VOLUMETRY PROTOCOL. In the initial study (Chapter 3), MR-based HCVs were measured by others (Cook *et al.* 1992; Bergin *et al.* 1994). The images for these studies were obtained on a 1.5 T GE Signa MR scanner using a 3-D SPGR sequence 35/5/1 (TR/TE/NEX), flip angle 35 degrees, matrix size 256x128, and 128 coronal partitions in the third dimension with partition thickness of 1.5 mm. Hippocampal cross-sectional areas were outlined manually and measured on consecutive images. The sum of the hippocampal cross-sectional areas multiplied by partition thickness gave total HCV. HCV ratio (HCVR) of 32 control subjects were measured by one observer using the protocol of Cook et al (Cook *et al.* 1992). Nineteen controls were men and 13 women (median age 27 years, range: 20-53 years). Mean HCVR was 0.97 ± 0.02. For that study, a HCVR of 0.91 was used as the lower limit of normal, which is 3 SDs below the mean control value of the HCVR. HCV and HCVR of patients were measured by 2 observers, who were blind to the patient's data. Interrater variability for HCVR was less than 3% (Bergin *et al.* 1994). The HCV distribution graphs did not use a control group, and HCV was not corrected for ICV in this protocol *(for examples of these SPGR-based graphs, see Figures 20, p 81; Figure 21, p 82; and Figure 22, p 83).*

2.4.3. AMYGDALA T2 MAPPING *(see chapter 8).*

An AT2 map 2000/22-262/1 (TR/TE/NEX), 16 echoes, matrix 135x256, FOV 220x165 mm, thickness 5 mm was oriented in a tilted axial plane parallel to and above the long axis of the hippocampus *(Figure 2, p 27; Figure 15, p 68).*

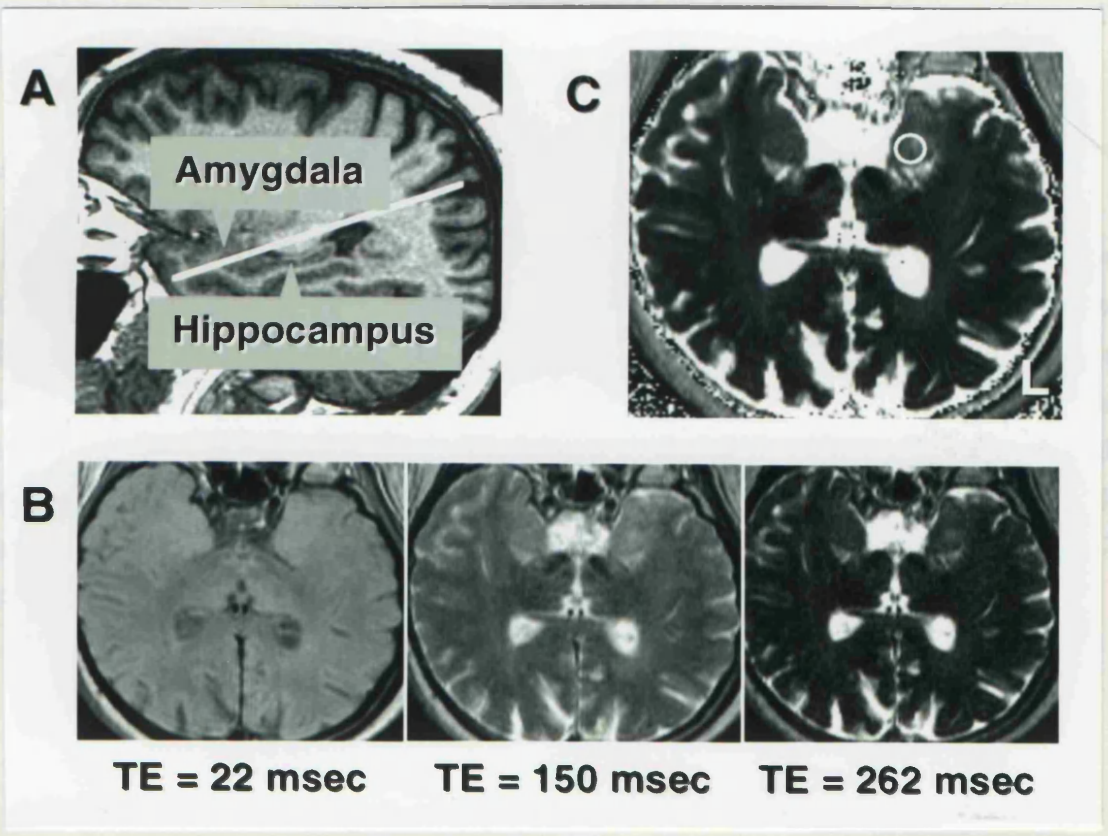

Figure 15. AT2 mapping. A. Sagittal 1.25 mm section of the unreformatted MPRAGE 3-D volume acquisition showing the right hippocampus and amygdala (indicated with text and arrows). The orientation of the AT2 map is shown by the white line. The AT2 map lies parallel and superior to the long axis of the hippocampus. The coordinates for the AT2 map were determined on the MPRAGE 3-D volume dataset after reformatting in the coronal and axial plane, while the patient was still on the table. B. Sixteen images through the amygdalae, all with the same coordinates and section thickness of 5 mm, but with different echo times (TE) ranging from TE of 22 msec to TE of 262 msec were obtained. Three such images with TE of 22, 150 and 262 msec respectively are shown. C. From these 16 images with different TE, T2 values were calculated for each pixel and displayed as an AT2 map. The AT2 signal (expressed in msec), as defined in this study, was measured by placing the largest possible circle within the amygdala as a ROI, while avoiding the boundaries with CSF, as demonstrated for the left (L) amygdala.

This plane has been suggested by Kuzniecky and Jackson for the study of the amygdalae (Kuzniecky, Jackson, 1995). The coordinates of the AT2 map were determined on the reformatted MPRAGE dataset during the scanning session. A section through the amygdala at right angles to the long axis of the hippocampus was

selected on the unreformatted sagittal MPRAGE image of the right amygdala and hippocampus. On this tilted coronal section a set of 1 mm horizontal sections symmetrically through the amygdalae was chosen. Five sections which covered the amygdalae optimally were selected and the coordinates of the middle section was taken for the AT2 map. AT2 was measured by placing a ROI in the largest possible circular area within the amygdala while avoiding boundaries with CSF, and was expressed in msec.

2.4.4. A FLUID ATTENUATED INVERSION RECOVERY (FLAIR) IMAGE.

A FLAIR image [4200/90/ 2010/1 (TR/TE/TI/NEX)] was obtained in patients who had a focal increased AT2 signal, to rule out the possibility that this was the result of CSF. (This is not a quantitative MRI technique, but is described here because it was used in conjunction with AT2 mapping in this study). The FLAIR scan was obtained in the same scanning session, with the same coordinates as the AT2 map to enable comparison between the AT2 map and the FLAIR image *(for examples of FLAIR images in combination with AT2 maps, see Figure 48, p 170; Figure 49, p 173; Figure 50; p 175; Figure 51, p 176; and Figure 52, p 177*

2.4.5. SINGLE VOXEL ^{1}H MAGNETIC RESONANCE SPECTROSCOPY *(see Chapter 9)*.

^{1}H MR spectra were obtained from 2x2x2 cm cubes in the medial portions of the left and right temporal lobes (i.e. from two regions, one region in each side). The regions were selected in a standardized way with the aid of scout images. In the axial view the 2 cm voxel was centered on the brainstem. In the coronal view, the voxel included the lateral part of the hippocampus. The volume included only temporal lobe structures and CSF *(Figure 16, p 70)*.

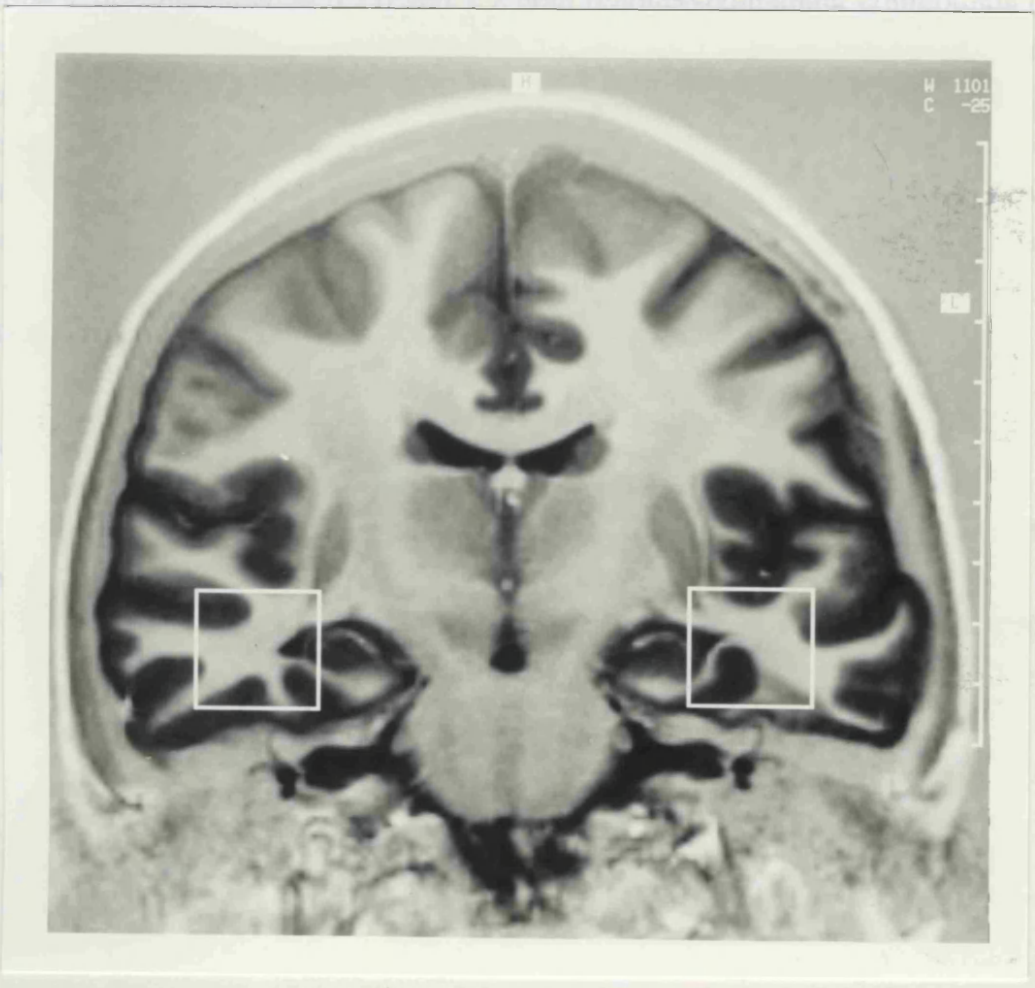

Figure 16. Position of regions of interest in ^{1}H MRS of the temporal lobes. Coronal IR image showing the positions in the temporal lobes of the 2x2x2 cm regions from which ^{1}H MR spectra were obtained.

Spatial localization was achieved using a 90°-180°-180° spin echo technique with the three selective radiofrequency pulses applied in the presence of orthogonal gradients of 2mT/m. Water suppression was effected by pre-irradiation of the water

resonance using a 90° Gaussian pulse with a 60Hz bandwidth, followed by a spoiler gradient. TR was 1600ms and TE was 135ms. After global and local shimming, and optimization of the water suppression pulse, data were collected in 2 to 4 blocks of 128 scans. The time domain data were corrected for eddy-current induced phase modulation using non-water-suppressed data as a reference. Exponential multiplication corresponding to 1Hz line broadening was carried out prior to Fourier transformation, and a cubic spline baseline correction was performed.

Signal intensities at 2.0 ppm (primarily N-acetylaspartate [NAA]), 3.0 ppm (creatine + phosphocreatine [Cr]) and 3.2 ppm (choline-containing compounds [Cho]) were measured from the peak areas by integration. The effects of T1 and T2 relaxation were not determined, and therefore it was not possible to convert these intensities to concentration measurements. Data are presented in the form of the dimensionless intensity ratio NAA/(Cho+Cr). NAA/(Cho+Cr) < 0.72 was considered abnormally low, and the ratio was regarded as lateralizing if it was abnormally low and also if it was lower than the contralateral ratio by more than 0.05 (Connelly *et al.* 1994) *(For examples of spectra, see Figure 53, p 190).*

2.5. NEUROPATHOLOGY.

The methodology of the neuropathology is described in Chapter 5, p 115 and following pages.

2.6. STATISTICS.

Statistical analysis was performed using SAS release 6.04 (DOS version) and SPSS for Windows, release 6 (SPSS Inc., Chicago, Ill., USA). Pearson's correlation coefficients (r), partial correlation coefficients, Fisher's Exact test, Student's t-test, Mann-Whitney U test, Kruskal-Wallis test, ANOVA and linear regression analysis were used where indicated.

Where appropriate, contingency table analysis has included a partitioning of the chi-square statistic and a calculation of the adjusted residuals, as outlined by Everitt (Everitt, 1992). Computer simulation was used to obtain probability values from the t-ratio in those instances in which the underlying distribution assumptions were violated *(Chapter 4)*.

The multivariate method of analysis described by Gabriel (Gabriel, 1968; Hand, Taylor, 1987) *(Chapter 5)* was used to examine all possible patterns of differences between the five hippocampal subregions of control, EFS and HS specimens simultaneously. Accordingly the maximum characteristic root statistic (θ) was calculated using $\theta = \lambda_1/(1+\lambda_1)$ where λ_1 is the largest eigenvalue of $H.E^{-1}$. H is the hypothesis sums-of-squares and cross products matrix and E the all groups errors sums-of-squares and cross products matrix. These were obtained using the MANOVA statement within the SAS GLM procedure. The values thus obtained were compared with a critical value of 0.22, which was derived from tables of the greatest characteristic root distribution. Only the single variable results are shown in Table 10, p 130 because all patterns of differences between the three groups achieved significance in at least one single variable.

CHAPTER III. HIPPOCAMPAL T2 AND MR-BASED HIPPOCAMPAL VOLUMETRY, AND QUALITATIVE NEUROPATHOLOGICAL ASSESSMENT OF THE HIPPOCAMPUS.

3.1. ABSTRACT.

The aim of this initial study was to evaluate and compare HCT2 measurement and MR-based HCV measurement in the presurgical evaluation of patients with intractable TLE, and to correlate these quantitative MRI measures with qualitative. pathology of the resected hippocampi. Forty patients with intractable TLE underwent presurgical evaluation and subsequent temporal lobe resection. HCT2, SPGR-based HCV and HCVR (defined in this chapter as the volume of hippocampus with higher HCT2 divided by volume of hippocampus with lower HCT2), and qualitative hippocampal pathology were the main outcome measures. Thirty-two patients had HS, three patients had EFS, one patient had amygdala sclerosis (AS), and four patients had a FTL in the temporal lobe. HCT2 ratio (R/L) correlated inversely with HCVR (R/L) ($r= -0.90$; $p < 0.0001$). A high HCT2 signal in an atrophic hippocampus was characteristic of HS. All patients with HS had a HCVR below control values, and only one of these had a HCT2 in the normal range. Visual assessment of SPGR-reformatted images and SPGR-based HCVR produced one false-positive result, i.e. a preoperative diagnosis of classical HS was not confirmed on neuropathological examination. The patients with EFS had a normal HCT2 and HCVR. The patient with AS had a normal hippocampus on qualitative and quantitative assessment. Of the four patients with a lesion, one had a mildly increased HCT2, and one a mild volume asymmetry. HCV asymmetry could be reliably detected on visual inspection of the MRI with a HCVR of 0.85 or less, and an increase of HCT2 with a T2 of 115 msec or higher. It was concluded that quantitative MRI combining HCT2 and HCVR is a reliable method to diagnose HS non-invasively.

3.2. INTRODUCTION.

HS is the most common cause of intractable TLE . Characteristic MRI features of HS are atrophy, an increased T2 signal, a decreased T1 signal and disruption of the internal structure *(Figure 7, p 38)*. The aim of this study was to evaluate and compare quantitative HCT2 and HCVs in patients with intractable TLE and to correlate these measures with the pathology of the resected hippocampus (Van Paesschen *et al.* 1995d).

3.3. METHODS.

3.3.1. DESCRIPTION OF STUDY POPULATION.

Forty patients (16 men and 24 women) with median age of 27 years (range: 16 to 47 years) who underwent presurgical evaluation for intractable TLE and subsequent temporal lobe resection. Median age at onset of habitual epilepsy was 7 years (range: 0 to 26 years). Median duration of epilepsy was 20 years (range: 7 to 40 years). Presurgical evaluation included interictal EEG, video-telemetry with ictal EEG recordings in 37 (93%), neuropsychological assessment, standard MRI, MR-based HCV measurement and HCT2 mapping. Three patients (8%) had depth EEG. Thirty-one patients had a carotid amobarbital test (78%).

3.3.2. QUANTITATIVE HIPPOCAMPAL MRI PROTOCOL.

3.3.2.1. HIPPOCAMPAL T2 MAPPING: *see p 55.*

3.3.2.2. SPGR-BASED HIPPOCAMPAL VOLUMETRY: *see p 67.* Thirteen patients of this SPGR-based HCV study overlapped with a study using an MPRAGE-based HCV protocol *(see MPRAGE-based HCV measurement protocol, p 57; Chapter 4; and Appendix A, p 222).* These MPRAGE-based HCVs were measured after surgery and used for the study described in Chapter 4. The HCVR of one of these 13 patient differed by 17% and changed category from abnormal using SPGR to normal using MPRAGE; this finding and its implications are therefore discussed in more detail in this chapter *(see Figure 23, p 84).*

3.3.3. NEUROSURGICAL PROCEDURES.

Thirty-five patients (87.5%) underwent anterior temporal lobe resection including hippocampus and amygdala, four patients (10%) had a lesionectomy and one patient (2.5%) had an amygdalectomy.

3.3.4. NEUROPATHOLOGY.

HS was defined by neuronal cell loss and reactive gliosis affecting the hippocampal subregions in a typical distribution. EFS was defined as (mild) pyramidal cell loss and reactive gliosis confined to the hilus with preservation of the pyramidal cell layer of the CA1, CA2 and CA3 (Margerison, Corsellis, 1966; Armstrong, Bruton,

1987; Babb, Brown, 1987; Sagar, Oxbury, 1987; Bruton, 1988; Wyler *et al.* 1992) *(see also p 116).*

3.3.5. STATISTICS: *see Statistics, p 72.*

3.4. RESULTS.

No	HCT2 right	HCT2 left	HCV right	HCV left	HCVR	Side surgery	Patho-logy	MRI: visual assessment	NHNN Hospital number
1	142	109	1983	2556	0.77	R	HS	RHS	MVP13421
2	139	108	1526	2876	0.53	R	HS	RHS	QSB85154
3	130	111	1779	2269	0.78	R	HS	RHS	QSB89363
4	129	104	2385	2855	0.84	R	HS	RHS	QSC00388
5	129	107	1568	2988	0.52	R	HS	RHS	MVP24607
6	126	97	2023	2818	0.72	R	HS	RHS	MVC05847
7	126	102	1169	3171	0.37	R	HS	RHS	QSB82506
8	125	103	2130	2931	0.73	R	HS	RHS	MVP06823
9	123	104	1912	2836	0.67	R	HS	RHS	MV95228
10	123	107	1883	2903	0.65	R	HS	RHS	QSB64404
11	123	102	2390	3195	0.75	R	HS	RHS	MVC11255
12	121	100	1785	2409	0.74	R	HS	RHS	QSB93870
13	120	110	1806	2589	0.7	R	HS	RHS	QSB36531
14	119	105	1887	2980	0.63	R	HS	RHS	MVC09566
15	118	103	2054	2657	0.77	R	HS	RHS	MVP21487
16	116	101	1889	2708	0.7	R	HS	RHS	MVC06063
17	116	100	1722	2267	0.76	R	HS	RHS	QSC04082
18	114	108	1843	3022	0.61	R	HS	RHS	QSB92544
19	113	100	2595	3087	0.86	R	HS	RHS	MVP20497
20	112	138	2457	1680	0.68	L	HS	LHS	MVC14609
21	110	127	2717	1765	0.65	L	HS +	LHS	QSC10954
22	108	116	2801	1992	0.71	L	HS +	LHS	QSB91555
23	107	114	1781	1417	0.8	L	HS	LHS	QSB00779
24	106	117	3424	1906	0.56	L	HS	LHS	QSB71679
25	105	122	2387	1581	0.66	L	HS	LHS	QSB92230
26	104	106	2906	1928	0.66	L	HS	LHS	QSC13829
27	104	128	3556	1999	0.56	L	HS	LHS	MVP23055
28	104	122	2724	1442	0.53	L	HS	LHS	QSC13498
29	102	120	2885	1815	0.63	L	HS	LHS	MVC20080
30	102	141	2736	1299	0.47	L	HS	LHS	QSB48898
31	101	120	3054	1557	0.51	L	HS	LHS	MVC07277
32	101	115	2583	1693	0.66	L	HS	LHS	MVP24605
33	107	103	2333	2802	1	R	EFS	RHS	QSA83367
34	106	107	2603	2522	0.97	L	EFS	normal	MV99857
35	103	103	2729	2565	0.94	L	EFS	normal	QSB36976
36	99	97	3060	2781	1.1	L	AS	normal	QSC22940
37	109	109	2688	2402	1.12	R	glioma	RTL cort.les.	QSB76280
38	105	104	2220	1950	1.14	L	non-	mass L PHG	QSC02138
39	104	106	4035	4252	1.05	R	cav.hae	cav.haem.	QSB99878
40	104	104	2667	2555	0.96	R	DNET	DNET	QSB97295

Table 5. HCT2 relaxation times (msec), MR-based hippocampal volumes (mm^3) and qualitative neuropathological assessment of the hippocampus of 40 patients who underwent surgery for intractable TLE. RTL cort.les.: right temporal lobe cortical lesion; non-spec.ch.: non-specific changes; mass L PHG: mass left parahippocampal gyrus; cav.haem.: cavernous haemangioma; NHNN: National Hospital for Neurology and Neurosurgery.

3.4.1. SURGERY AND PATHOLOGY.

Thirty-five of the 40 patients (87.5%) underwent temporal lobe resection including the hippocampus and amygdala. Thirty-two of these patients had HS. Two of these patients with HS also had microdysgenesis. Three patients had EFS. One patient (2.5%) had an amygdalectomy for AS. Four patients (10%) had a temporal FTL and underwent a lesionectomy without resection of the hippocampus. One patient had a low-grade glioma, one a cavernous angioma, one a dysembryoplastic neuroepithelial tumor (DNET), and one patient had non-specific changes only on pathological examination *(Table 5, p 76)*.

3.4.2. CORRELATIONS BETWEEN HIPPOCAMPAL VOLUME AND T2.

HCT2 correlated inversely with HCV ($r = -0.70$; $p<0.0001$). HCT2 ratio (R/L) correlated inversely with the ratio of HCVs (R/L) ($r= -0.91$; $p<0.0001$) *(Figure 17, p 77)*. Higher HCT2 correlated inversely with HCVR (volume of hippocampus with higher T2 divided by volume of hippocampus with lower T2) ($r = -0.63$; $p<0.0001$) *(Figure 18, p 78)*.

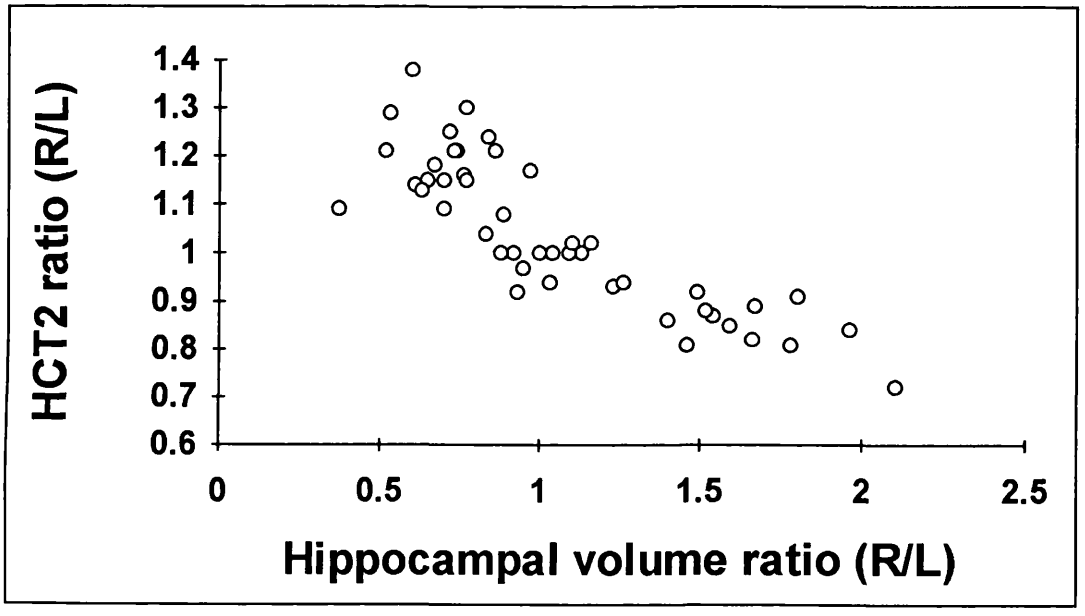

Figure 17. HCT2 ratio (R/L) as a function of HCVR (R/L). A high inverse correlation exists between the HCT2 ratio (R/L) and the HCV ratio (R/L) [$r = -0.91$; $p < 0.0001$).

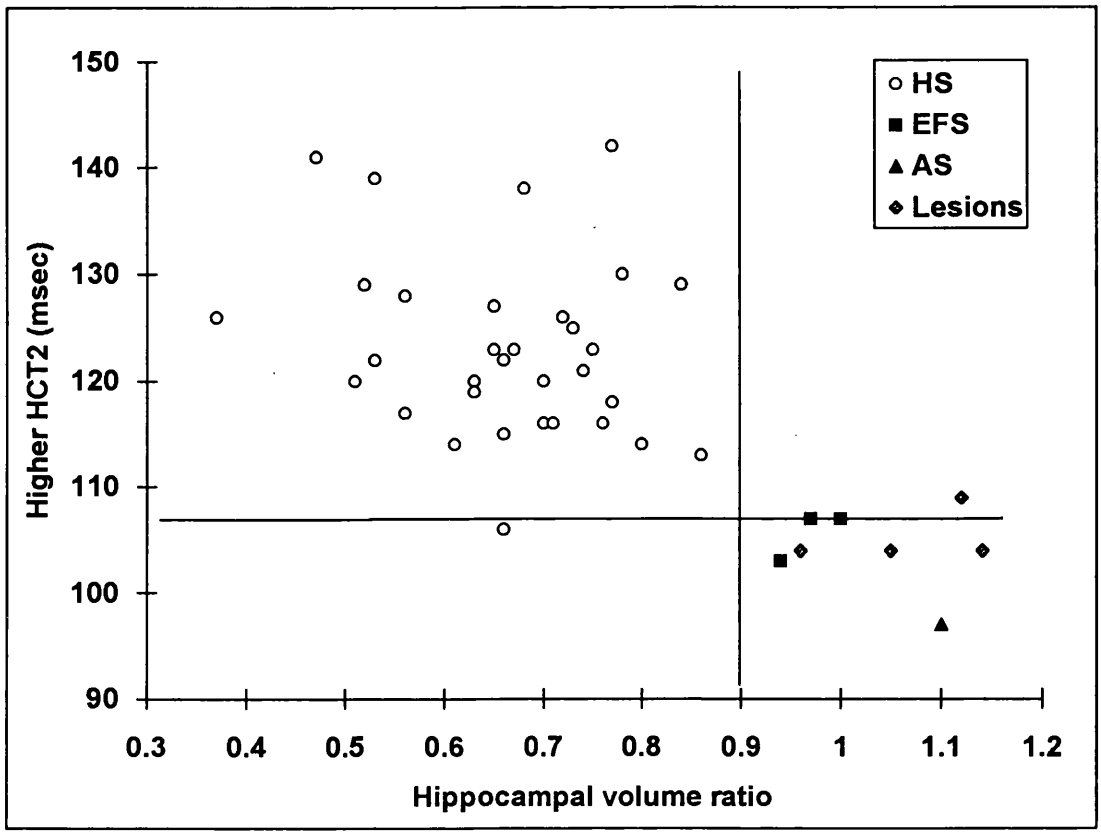

Figure 18. Higher HCT2 as a function of the HCVR (volume of hippocampus with higher T2 divided by volume of hippocampus with lower T2). The horizontal line drawn at a HCT2 of 108 msec represents the upper limit of normal. The vertical line drawn at a HCVR of 0.91 represents the lower limit of normal. HS: patients with HS. EFS: patients with end folium sclerosis. AS: patient with amygdala sclerosis. Lesion: patients with temporal FTL. The patient with HS and normal HCT2 is discussed in detail *(Figure 37, p 123)*.

3.4.3. QUANTITATIVE HIPPOCAMPAL MRI IN HIPPOCAMPAL SCLEROSIS.

Thirty-two patients had HS *(Figure 18, p 78; Figure 21, p 82; Figure 22, p 83)*. Mean higher HCT2 was 123 ± 9 msec (range: 106-142). Mean HCVR was 0.66 ± 0.11 (range: 0.37 - 0.86). All patients with HS had a HCVR below control values and only one had a HCT2 in the normal range *(Figure 37, p 123, and for discussion of HCT2 mapping, p 109)*. The higher HCT2 and atrophy was always on the side of seizure onset and resection. Five patients (16%) had an increased signal in the contralateral hippocampus (median: 110 msec; range: 109 to 112 msec).

3.4.4. QUANTITATIVE HIPPOCAMPAL MRI IN PATIENTS WITH END FOLIUM SCLEROSIS.

Three patients had EFS. HCT2 and HCVR were normal in all three *(Figure 20, p 81)*. In another of these patients, the right hippocampus was positioned asymmetrically compared to the left *(Figure 23, p 84)*. Reliable disarticulation of the hippocampus from the amygdala proved not possible in this particular patient using SPGR image data, and led to a spuriously low HCVR (R/L) of 0.83. MPRAGE data which were acquired preoperatively were analyzed after surgery. These allowed visualization of the hippocampi at the level of the amygdala and measurement of the full length of the hippocampi showed that the HCVR was 1.

3.4.5. QUANTITATIVE HIPPOCAMPAL MRI IN PATIENTS WITH A TEMPORAL FOREIGN TISSUE LESION.

Four patients had a temporal FTL. All underwent lesionectomy without resection of the hippocampus. One had bilateral mildly increased HCT2 (HCT2 = 109 msec) and the bigger hippocampus on the side of the lesion (HCVR = 1.12). One had a smaller hippocampus on the side of the lesion (HCVR = 1.14; ipsilateral HCT2 = 104 msec; contralateral HCT2 = 105 msec).

3.4.6. QUANTITATIVE HIPPOCAMPAL MRI IN AMYGDALA SCLEROSIS (AS).

One patient had AS. The HCT2 and HCVR were within normal limits *(see Chapter 8)*.

3.4.7. VISUAL ASSESSMENT OF HIPPOCAMPI AND QUANTITATIVE HIPPOCAMPAL MEASURES.

Two observers always agreed on the presence of hippocampal asymmetry when HCVR was 0.85 or lower. They thought there was significant unilateral atrophy in a patient with EFS, whose HCVR on MPRAGE proved to be 1. They agreed on the presence of an increased hippocampal signal when HCT2 was 115 msec or higher. However, they disagreed on the interpretation of a high signal in 2 patients, i.e. one observer thought that the high signal was caused by partial volume effects with CSF. They did not detect a high T2 signal in a patient with a HCT2 of 114 msec.

A

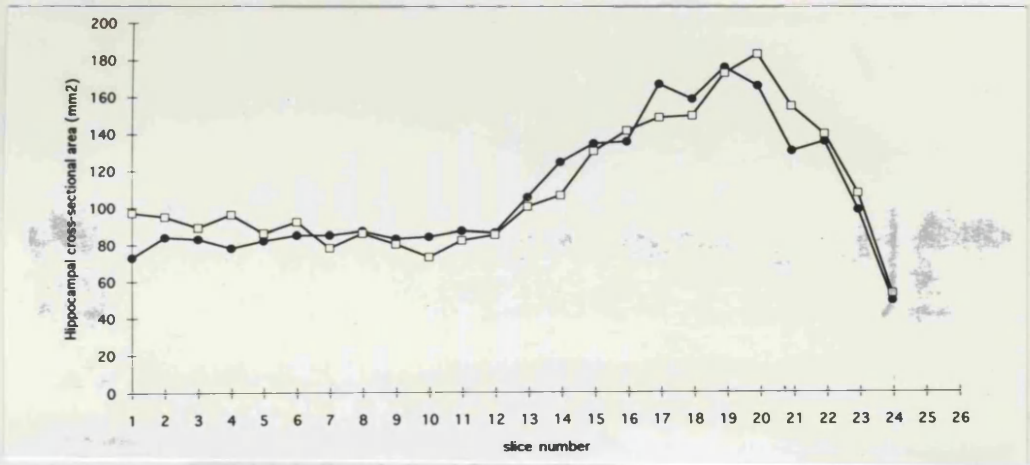

B

C

Figure 19: Quantitative hippocampal MRI and qualitative pathology of a normal control. A.: HCT2 map. The right hippocampus is on the left side of the photograph. Hippocampi are symmetric and of normal size on visual inspection, with no evidence of an increased signal. HCT2 is 105 msec on the right and 99 msec on the left (Nl ≤ 108 msec). B.: HCV studies. The right hippocampus is represented by the dark circles and the left hippocampus by the open squares. HCVR is 1. C.: Histological section of the body of a normal hippocampus from a different control subject (obtained at autopsy) (LFB/CV stain, magnification: x17). The pyramidal cell layer of the Ammon's horn and GCDG are normal. The position of the polymorphic layer, between the neurons of the hilus (H) and the GCDG, is indicated by the opposing arrows. The single straight arrow points to CA1, and the curved arrow to CA3.

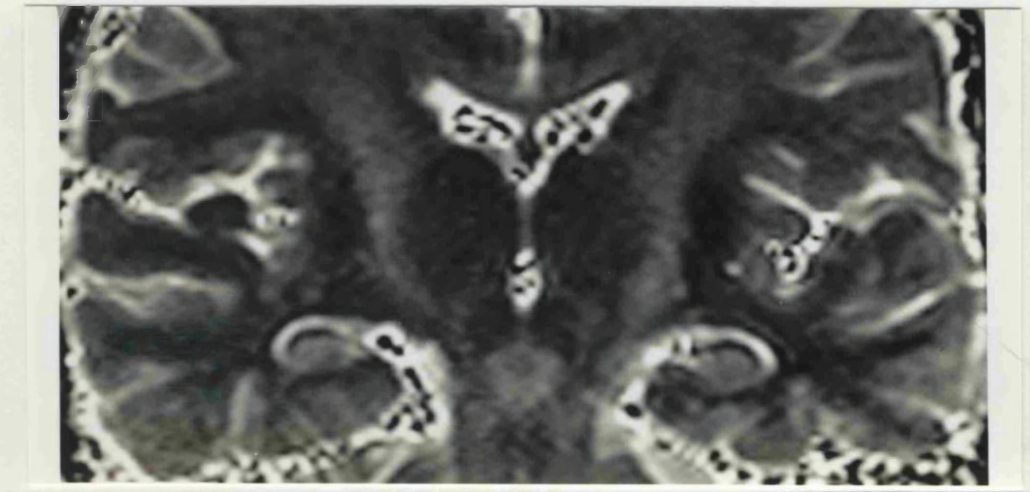

A

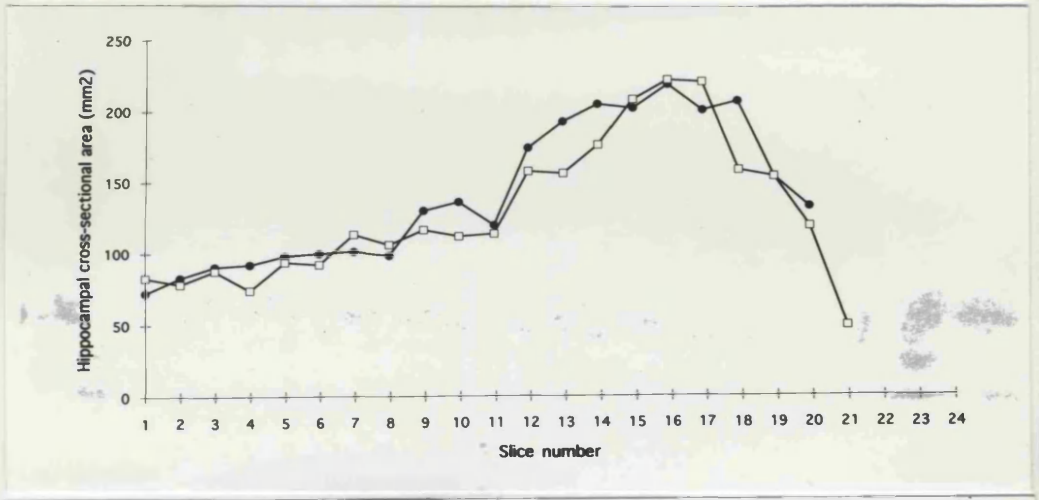

B

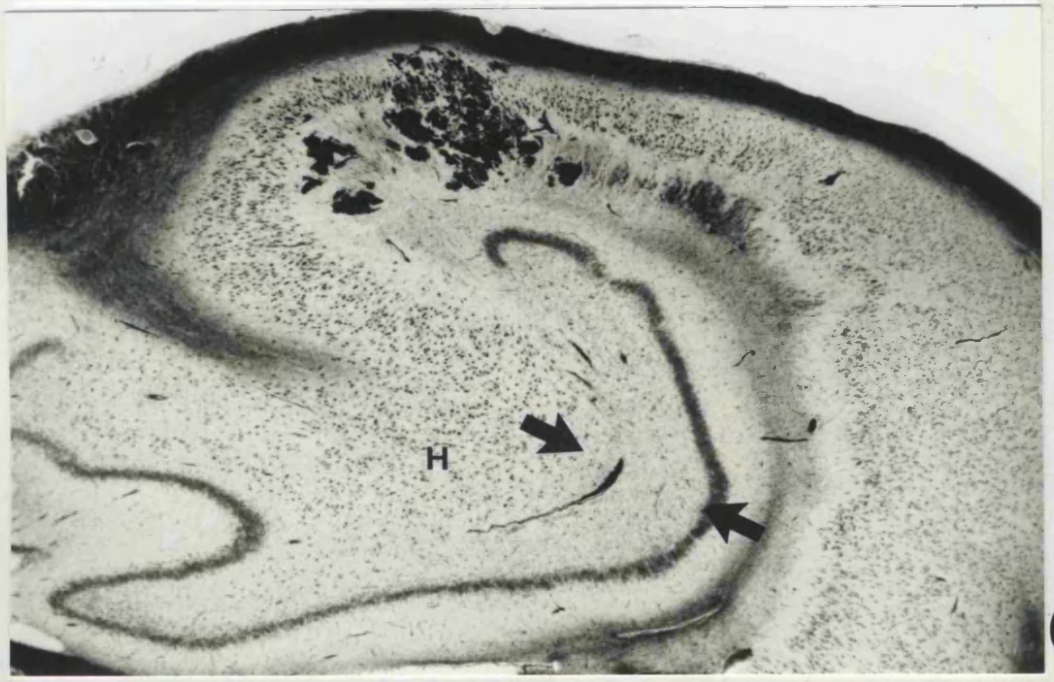

C

Figure 20. Quantitative hippocampal MRI and qualitative pathology of EFS A.: HCT2 maps. The right hippocampus is on the left side of the photograph. Hippocampi are normal on visual inspection, and have a HCT2 of 103 msec bilaterally (Nl ≤ 108 msec). B.: HCV studies. The right hippocampus is represented by the dark circles and the left hippocampus by the open squares. HCVR (L/R) is 0.94. C.: Histological section of the body of the hippocampus (LFB/CV stain, magnification: x17). Surgical specimen of the left hippocampus. CA1-CA3 are normal (CA2 is partly replaced by hemorrhage which occurred during surgery). Due to loss of hilar neurons, the space lying between the GCDG and the remaining neurons of the hilus is widened (opposing straight arrows). The hilus is considerably gliotic (not shown here). [Hospital number: QSB36976]

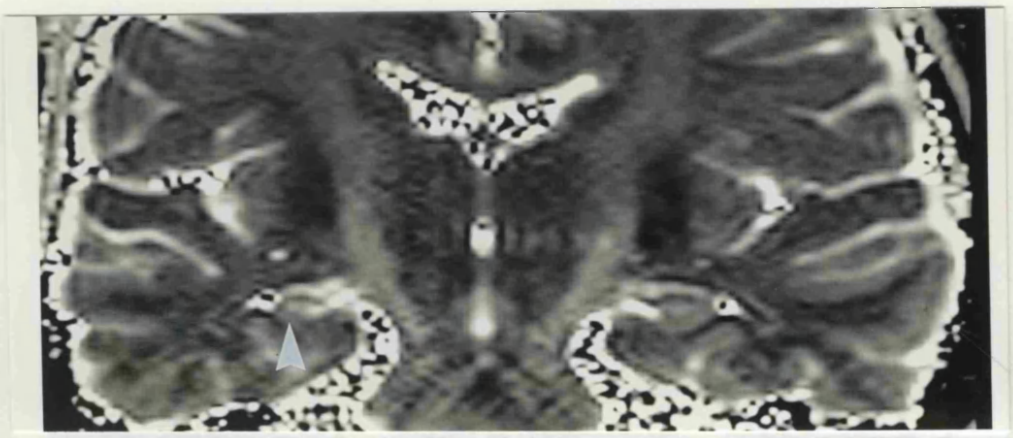

A

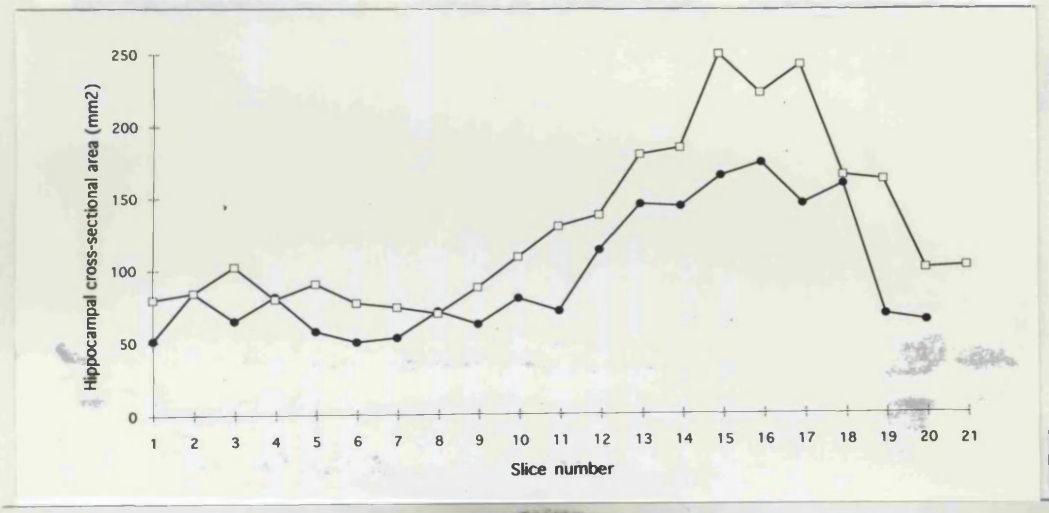

B

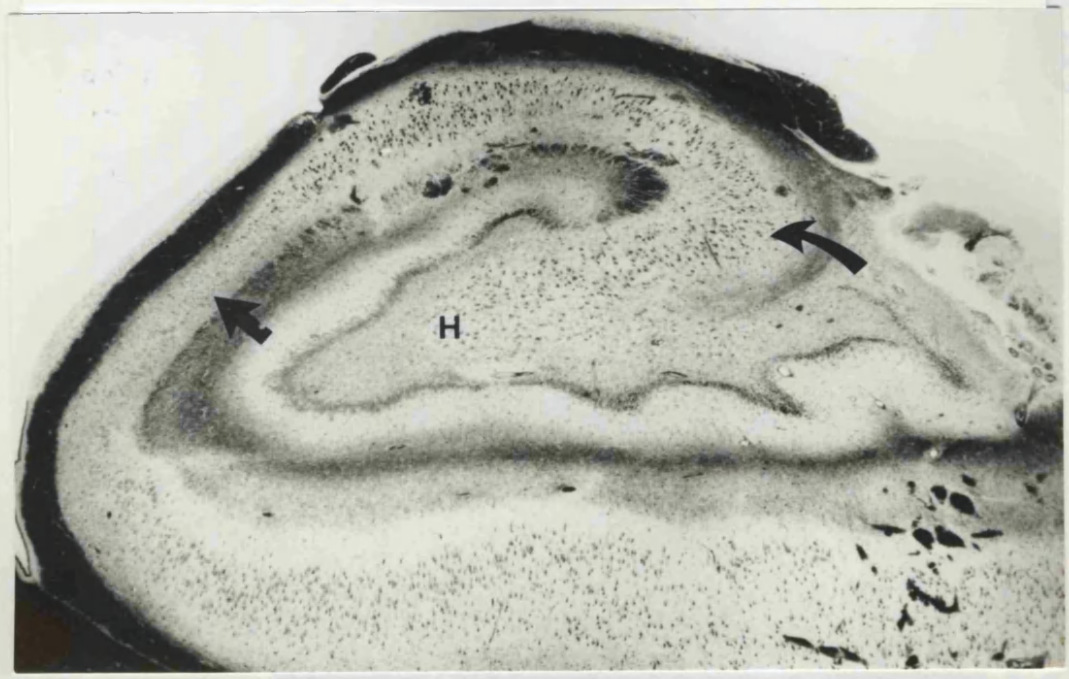

C

Figure 21. Quantitative hippocampal MRI and qualitative pathology of HS. A.: HCT2 maps. The right hippocampus is smaller compared to the left hippocampus and has an increased T2 signal (white arrowhead) which corresponds to a T2 of 116 msec (Nl ≤ 108 msec). The right hippocampus is on the left side of the photograph. B.: HCV studies. The volume of the right hippocampus is 70% of the volume of the left hippocampus. The right hippocampus is represented by the dark circles and the left hippocampus by the open squares. C.: Histological section of the body of the hippocampus (LFB/CV stain, magnification: x17). The pathological specimen of the resected right hippocampus shows HS characterized by neuronal depletion and gliosis affecting mainly CA1 (straight black arrow) and hilus (H) with relative sparing of CA3 (curved black arrow) and CA2 (between CA1 and CA3). The GCDG shows depletion and dispersion. [Hospital number: MVC06063]

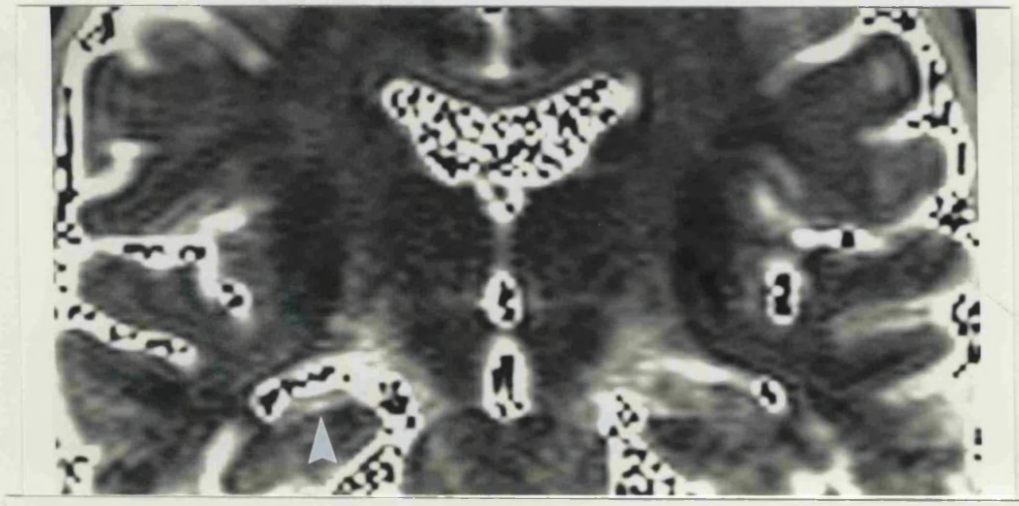

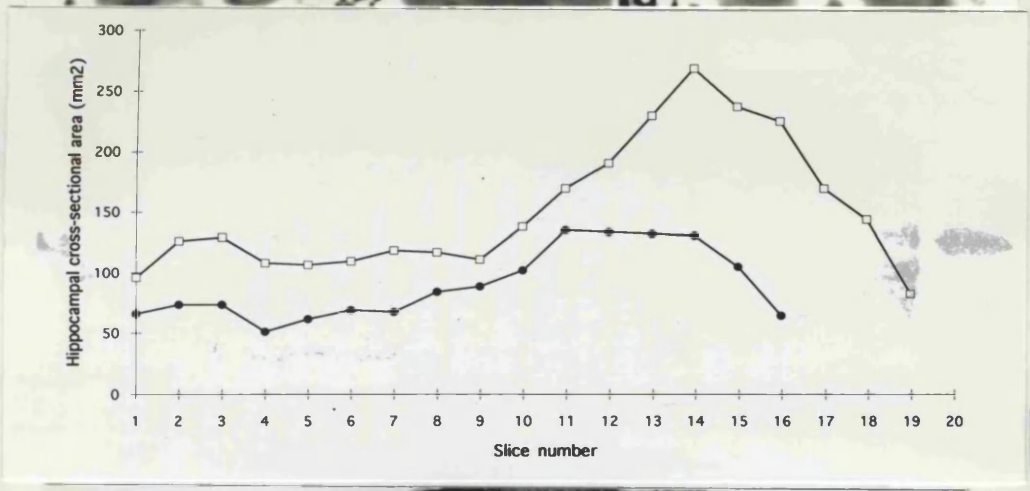

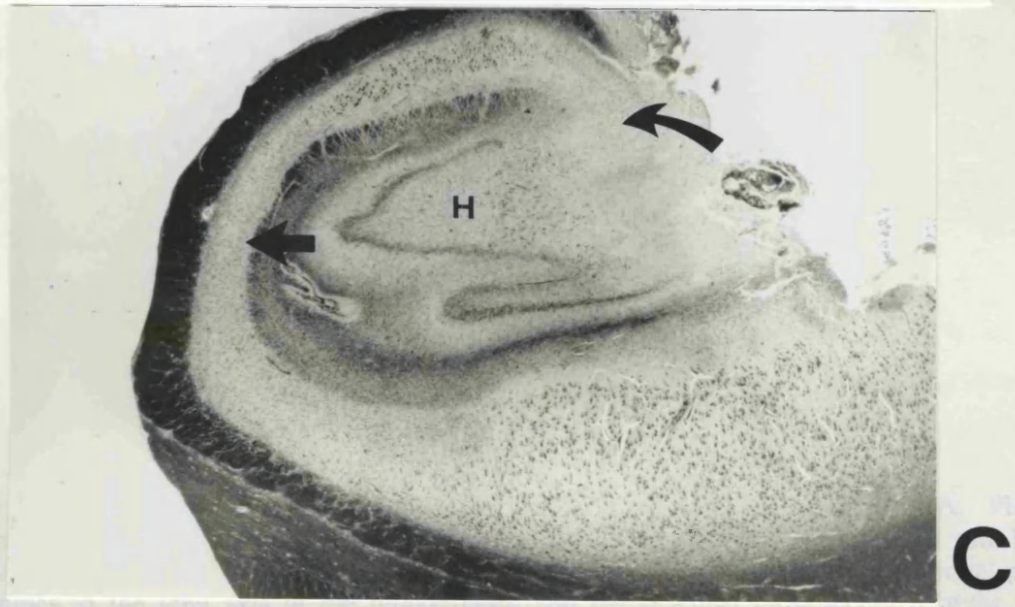

Figure 22. Quantitative hippocampal MRI and qualitative pathology of HS. A.: HCT2 maps. The right hippocampus is on the left side of the photograph. B.: HCV studies. The right hippocampus is represented by the dark circles and the left hippocampus by the open squares. The right hippocampus appears more atrophic and brighter (white arrowhead) than that of the previous example. This was confirmed on quantification with a right HCT2 of 139 msec and HCVR (R/L) of 0.53. C.: Histological section of the body of the hippocampus (LFB/CV stain, magnification: x17). There is severe neuronal loss and gliosis affecting CA1 (straight black arrow), CA3 (curved black arrow) and hilus (H) with relative sparing of CA2. [Hospital number: QSB85154].

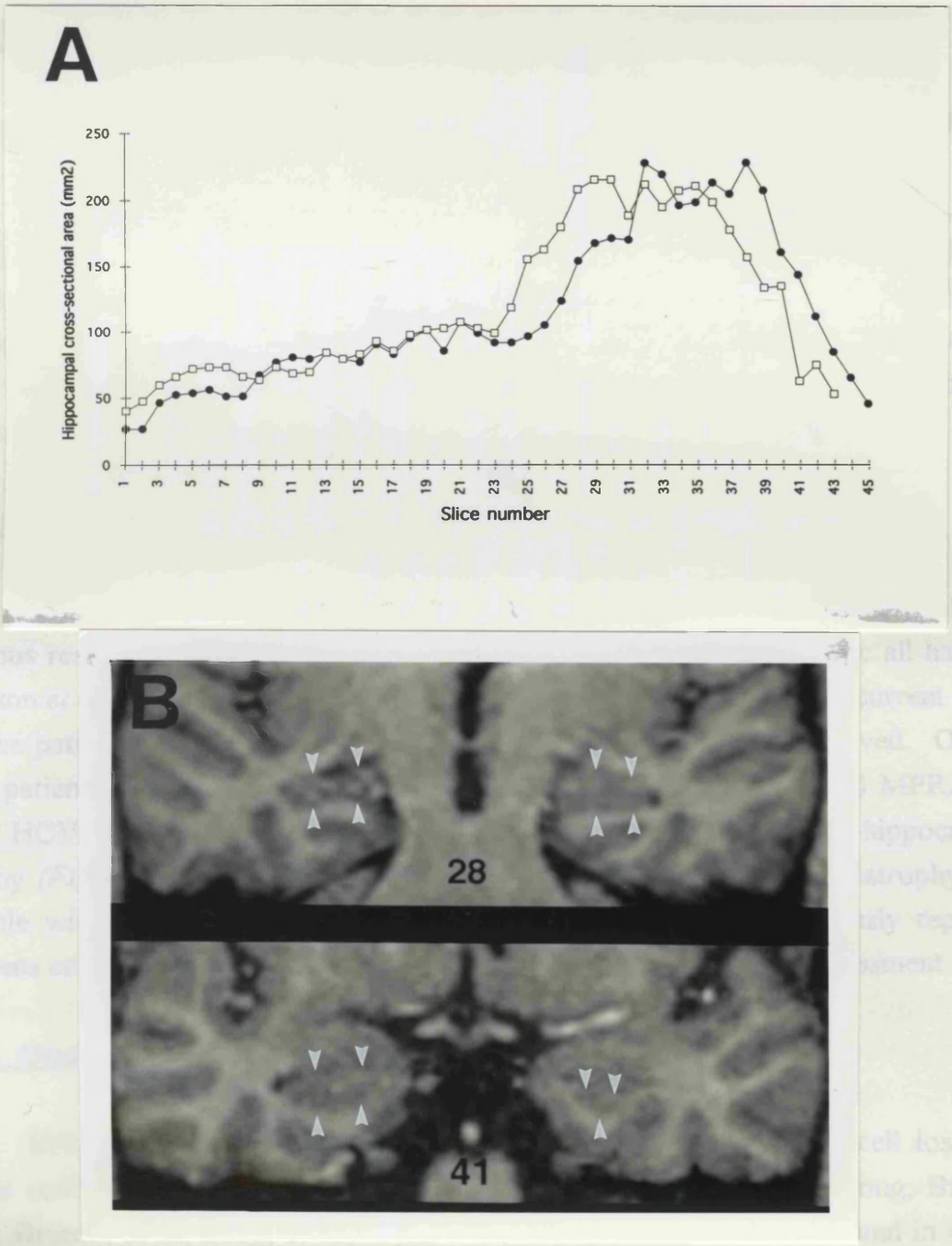

Figure 23: False positive diagnosis of HS using SPGR-based hippocampal volumetry. A. Plot of hippocampal cross-sectional area versus section position for both hippocampi in a patient with EFS. An MPRAGE data set was reformatted into 1 mm thick contiguous sections in a tilted coronal plane at right angles to the long axis of the hippocampus and hippocampal cross-sectional areas were measured on consecutive images. The right hippocampus is represented by the dark circles and the left hippocampus by the open squares. The volume of the right hippocampus is 5034 mm^3 and the volume of the left hippocampus is 5054 mm^3. HCVR is 1. B. Photographs of sections 28 and 41 of the MPRAGE reformatted HCV set. White arrowheads indicate the position of the hippocampi. In section 28, the right (R) hippocampus is smaller than the left. In section 41, the right hippocampus is larger than the left. The amygdalae overlie the heads of the hippocampi and make the difference in size less obvious. Because disarticulation of the hippocampus from amygdala proved too difficult using the SPGR images, due to lower tissue contrast than the MPRAGE images, a spuriously low HCVR (R/L) of 0.83 was obtained. [Hospital number: QSA83367].

3.5. DISCUSSION.

3.5.1. CORRELATION BETWEEN HCT2 AND MR-BASED HIPPOCAMPAL VOLUME.

Quantitative MRI measurements of the hippocampus in patients with intractable TLE were compared and there was a high and significant inverse correlation between HCV or HCVR and HCT2 (Van Paesschen *et al.* 1995d). Higher HCT2 values were associated with a more atrophic hippocampus, and a normal HCT2 with a larger hippocampus. These observations have now been corroborated by others (Pitkänen *et al.* 1996).

3.5.2. QUANTITATIVE AND QUALITATIVE MRI IN HIPPOCAMPAL SCLEROSIS.

An increased T2 signal in an atrophic hippocampus is characteristic of HS. Previous results indicated that patients with HCT2 greater than 116 msec all had HS (Jackson *et al.* 1993b; Grünewald *et al.* 1994a). This is confirmed in the current study but five patients with HS and HCT2 less than 116 msec have been observed. One of these patients had a HCT2 within the normal range. Using an improved MPRAGE-based HCV protocol *(see p 57)*, this patient had predominant anterior hippocampal atrophy *(Figure 37, p 123)*. Reliable visual detection of hippocampal atrophy was possible with a HCVR of 0.85 or lower, which is better than previously reported (Reutens *et al.* 1993), possibly reflecting improved expertise in visual assessment.

3.5.3. QUANTITATIVE MRI IN END FOLIUM SCLEROSIS.

EFS is a rare variant of HS characterized by (mild) neuronal cell loss and gliosis confined to the end-folium (Margerison, Corsellis, 1966; Armstrong, Bruton, 1987; Bruton, 1988; Babb, 1992; Wyler *et al.* 1992). Isolated EFS is found in 4% of patients with intractable TLE who come to surgery (Bruton, 1988; Babb, 1992). It has been hypothesized that EFS might be detectable with T2 relaxometry (Jackson *et al.* 1993b). However, all three patients with EFS in this study had normal HCT2s and normal HCVR. Chan et al (Chan *et al.* 1994) reported four patients with EFS who had an increased hippocampal signal with no atrophy on visual inspection of coronal STIR images. The echo time used in Chan's study was 43 msec, and it is therefore possible that the dominant contrast in the resultant STIR images was T1-based. Differences in severity of EFS, as observed by Sano and Malamud (Sano, Malamud, 1953), may also be a factor, since the pathological specimens in the present study

appeared less severely affected than those reported by Chan et al [personal communication].

3.5.4. BILATERAL INCREASED HCT2S.

Sixteen percent of patients with HS in this study had bilaterally increased HCT2s, confirming previous observations (Jackson *et al.* 1993b; Grünewald *et al.* 1994a). A previous hypothesis was that a contralateral HCT2 between 107 and 115 msec might represent EFS. However, since three patients in this study with EFS had normal HCT2s, and five patients with HS had HCT2s in the 106-115 msec range, it appears more likely that patients with bilateral increased HCT2s have bilateral HS. None of the patients with bilateral increased HCT2s had evidence of seizure onset in the contralateral hippocampus. Post-operative outcome data on this cohort of patients will show whether a raised contralateral HCT2 is an adverse prognostic factor. A retrospective study suggested that a high contralateral HCT2 is associated with a degree of cognitive impairment but not with poor seizure outcome (Incisa della Rocchetta *et al.* 1995).

3.5.5. HIPPOCAMPAL VOLUME RATIO.

An HCVR of 0.91 was used, which is 3 SDs below the mean control value, as a guideline for the detection of unilateral HS. HCVR as measured by different observers is a much more reliable measure than total HCV (Bergin *et al.* 1994). In this study all patients with HS had a low HCVR. However, Jackson et al (Jackson *et al.* 1994c) observed six patients with HS and normal HCVR who had an increased HCT2 on visual inspection of T2-weighted images. Also, patients with bilateral HS may have a normal HCVR. These patients did not undergo surgery, and were therefore not included in this study. Bilateral HS, however, can be detected with normalized absolute HCVs (Free *et al.* 1995; Jack *et al.* 1995) or HCT2 measurement. SPGR-based hippocampal volumetry produced one false-positive result, i.e. a low HCVR in a patient with EFS but not HS. SPGR image data did not allow a clear distinction to be made between amygdala and hippocampus which was crucial in this case due to an anatomical asymmetry of the position of the hippocampal heads with respect to the amygdalae. MPRAGE, which includes an inversion pulse, provided better contrast between gray and white matter, and allowed disarticulation of hippocampus from amygdala. This example illustrates the danger of introducing bias by measuring only part of the hippocampus *(see also discussion of HCV distribution graphs, p 111 and following pages).*

3.5.6. INTRACTABLE MRI-NEGATIVE TEMPORAL LOBE EPILEPSY.

Two patients with EFS were considered MRI-negative including quantification of HCVs and T2 preoperatively. In these patients, the decision to operate was based on results of other tests such as interictal EEG, ictal video-EEG, interictal SPECT and neuropsychology. Another patient with normal qualitative MRI and quantitative hippocampal measures had an increased signal in the amygdala on AT2 mapping and underwent a selective amygdalectomy, with evidence of gliosis in the resected specimen *(see Chapter 8)*. Isolated AS is recognized in intractable TLE (Hudson *et al.* 1993). AS and EFS should therefore be considered in patients with intractable TLE who have normal quantitative MRI hippocampal measures and are otherwise MRI-negative.

3.5.7. QUANTITATIVE MRI IN PATIENTS WITH LESIONS.

Two of four patients with a temporal FTL had a mildly increased HCT2 or mild volume asymmetry. They underwent lesionectomy, and the hippocampus therefore was not available for pathological examination. The combination of a lesion and HS has been well described *(see discussion on dual pathology, p 41 and following page)*. Follow-up studies will be required to determine whether patients with a temporal FTL and (mildly) abnormal hippocampal quantitative measures, and who have a lesionectomy, subsequently require an anterior temporal lobe resection including the hippocampus.

3.5.8. CONCLUSION.

HS was characterized by an increased T2 signal in an atrophic hippocampus, with the exception of one patient with HS who had a normal HCT2 despite a low HCVR. Although atrophy and HCT2 increase represent different aspects of hippocampal pathology, the data presented show that abnormalities in these two measures almost always occurred together in this highly selected group of patients. To gain a better insight into the pathological basis for each of these forms of quantitative MRI, ND and GD were determined, to establish a relationship with these quantitative MRI measures *(see Chapter 5)*.

CHAPTER IV. THE SPECTRUM OF HIPPOCAMPAL SCLEROSIS.

4.1. ABSTRACT

One-hundred patients with intractable TLE and 22 control subjects were scanned on a 1.5 T Siemens SP63 Magnetom scanner. A combination of HCT2 mapping, HCV measurement corrected for ICV and inspection of hippocampal morphology on a HCV distribution graph compared against a control graph revealed previously undetected forms of bilateral HS and 4 false positive diagnoses of HS made on visual inspection of the scans. A physiologic asymmetry in the position of the hippocampi in 41% of control subjects and focal hippocampal atrophies in patients made measurement of the whole length of the hippocampus mandatory. The extent of hippocampal damage in patients with HS correlated with the number of SGS during a patient's lifetime. In contrast to patients with unilateral HS, patients with severe bilateral HS had no history of FCs. Twenty-six patients with intractable TLE had normal hippocampal MRI measures and as a group were significantly older at the onset of habitual epilepsy than patients with HS. In conclusion, a combination of quantitative MRI techniques revealed a spectrum of HS and optimally defined boundaries of hippocampal normality. The spectrum of HS is related to the etiology, to the number of SGS, and to the age at onset of habitual epilepsy.

4.2. INTRODUCTION

In Chapter 3, quantitative MRI findings were described in a highly selected population, i.e. patients with a well defined lesion with concordant investigations such as interictal and ictal EEG, and neuropsychometry, who underwent temporal lobe resection. The majority of these patients had unilateral diffuse HS. A combination of HCVR and HCT2 may be sufficient to describe this highly selected population. Several patients however who had no obvious lesion or were thought to have bilateral HS were not operated upon. Bilateral HS may be more difficult to detect, and can not be demonstrated using HCVR, since there may not be an volume asymmetry. Bilateral HS can be studied using absolute HCVs (Free *et al.* 1995; Gambardella *et al.* 1995; Jack *et al.* 1995; King *et al.* 1995; Lee *et al.* 1995) and using HCT2 mapping. Variants of HS such as diffuse, anterior and posterior atrophy of the hippocampus have been demonstrated using graphs plotting hippocampal cross sectional area (Cook *et al.* 1992; Kim *et al.* 1995b). Further, the definition of normality of hippocampi may require a more refined MR-based hippocampal volumetry protocol in combination with

HCT2 mapping. In this study, the results of a combination of quantitative MRI techniques in 100 consecutive patients with intractable TLE not due to FTLs are reported. The aim was to establish the MRI spectrum of HS, and to correlate this with clinical data (Van Paesschen *et al.* 1997).

4.3. METHODS.

4.3.1. SUBJECTS.

Twenty-two control subjects (M=10, W=12) with median age of 29 years (range: 21-37) and 100 patients (M=44, W=56) with median age of 33 years (range: 16-64) were studied. Selection criteria were historical evidence of TLE that was not controlled with AEDs and concordant interictal EEG findings, and absence of a FTL on visual inspection of standard T1- and T2-weighted MR images. Ictal video-EEG recordings have been obtained in 70 of these patients so far, confirming the diagnosis of TLE. Thirteen of the 100 patients overlapped with those described in Chapter 3 *(see Appendix A, p 222).*

4.3.2. CLINICAL EVALUATION : *see p 52.*

4.3.3. QUANTITATIVE HIPPOCAMPAL MRI PROTOCOL.

4.3.3.1. HIPPOCAMPAL T2 MAPPING: *see p 55.*

4.3.3.2. MPRAGE-BASED HIPPOCAMPAL VOLUMETRY: *see p 57.*

4.4. RESULTS.

4.4.1. CONTROLS.

A dataset consisted of a HCT2 map, HCVR, HCVs corrected for ICV, and a HCV distribution graph *(Figure 24, p 91)*. Mean control HCT2 was 102.4 ± 2.8 msec. The upper limit of the reference range for the control group was taken as 108 msec, i.e. 2 SD above mean control HCT2. Mean uncorrected HCV of men was around 9% larger than that of women ($p= 0.053$) *(Table 6, p 93)*. Uncorrected HCV correlated with ICV ($r= 0.62$; $p<0.001$) *(Figure 13, p 63)*. Mean corrected HCV was comparable between men and women. Mean control uncorrected HCV was 5180 ± 532 mm^3 and corrected for ICV 5180 ± 416 mm^3. The lower limit of the corrected control HCV reference range was defined by 2 SD below the mean control value and was 4348 mm^3. In the remainder of the text, HCV will always refer to HCV corrected for ICV. Mean (±SD) HCVR was 0.96 ± 0.03. The smallest HCVR of the controls was 0.92. A cut-off value of 0.87 was used which is 3 SD below mean control HCVR. Inspection of the HCV distribution graph showed that nine of 22 control subjects (41%) had a difference in length of the hippocampi on reformatting with alignment of the fornices which resulted in an asymmetry of the position of the anterior parts of the hippocampi *(Figure 25, p 92; Figure 23, p 84)*.

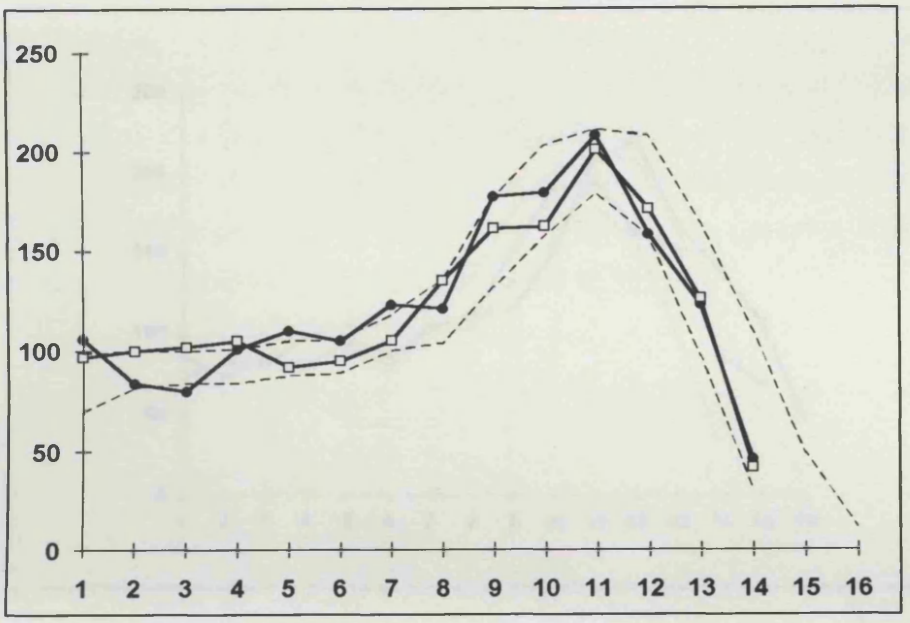

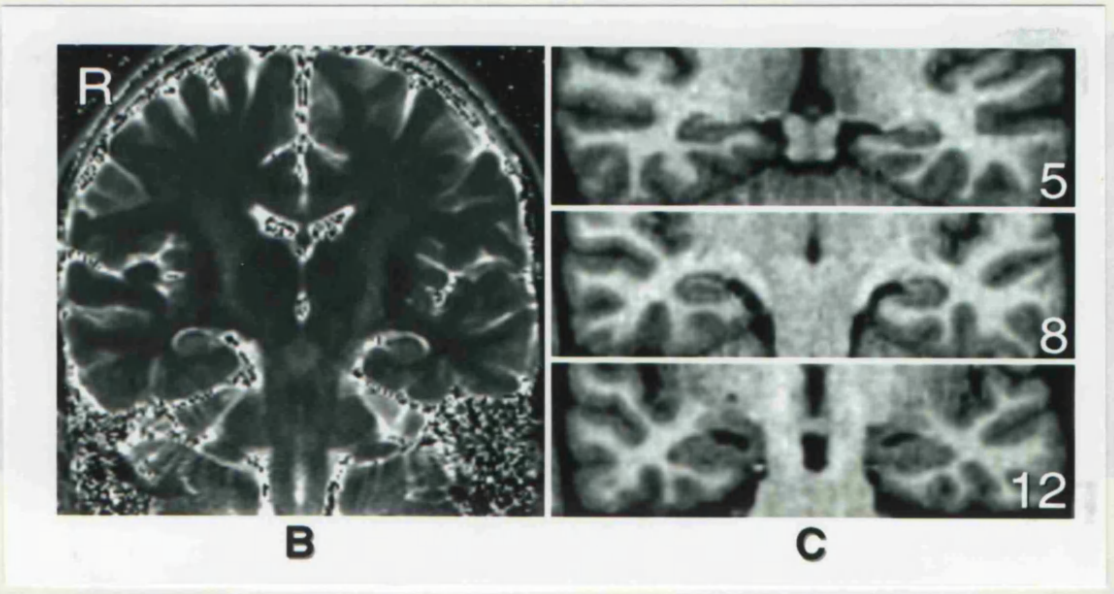

Figure 24 . Control dataset i.e. HCT2, HCV and HCV distribution graph. For all figures, a graph of hippocampal cross-sectional areas (A), HCT2 map (B) and reformatted MPRAGE images (C) are shown. A. Graph plotting hippocampal cross-sectional area (mm^2) as a function of section position. The black circles represent the right and the open squares the left hippocampus. The dashed lines are the upper and lower limit of the control group reference range as defined by ± 2 SD *(see Methods, p 63)*. Section position 1 starts at the tail of the hippocampus and the whole length of the hippocampus was measured. Contiguous sections of 1 mm thickness were acquired. Cross sectional hippocampal area was determined for every third section. B. Coronal 8 mm thick T2 map of the hippocampal body, approximating to MPRAGE sections 7-9 (compare HCT2 map [B] with section 8 of reformatted MPRAGE in C). C. Reformatted MPRAGE images showing the temporal lobe and the hippocampi, which were used for hippocampal volumetry. The white numbers in the lower right corner of the MPRAGE images correspond to the section position on the hippocampal graphs. Selected MPRAGE images highlight the hippocampal abnormality, when present. For this control graph, the hippocampi were symmetric with normal HCVs and HCT2s. The normal appearances of the hippocampus at the level of the hippocampal head (section 12), body (section 8) and more posteriorly (section 5) are illustrated. HCVR(R/L) = 0.98 (Nl ≥ 0.87); HCV right = 5151 mm^3, HCV left = 5070 mm^3 (Nl: ≥ 4348 mm^3); HCT2 right = 105 msec, HCT2 left = 99 msec (Nl ≤ 108 msec).

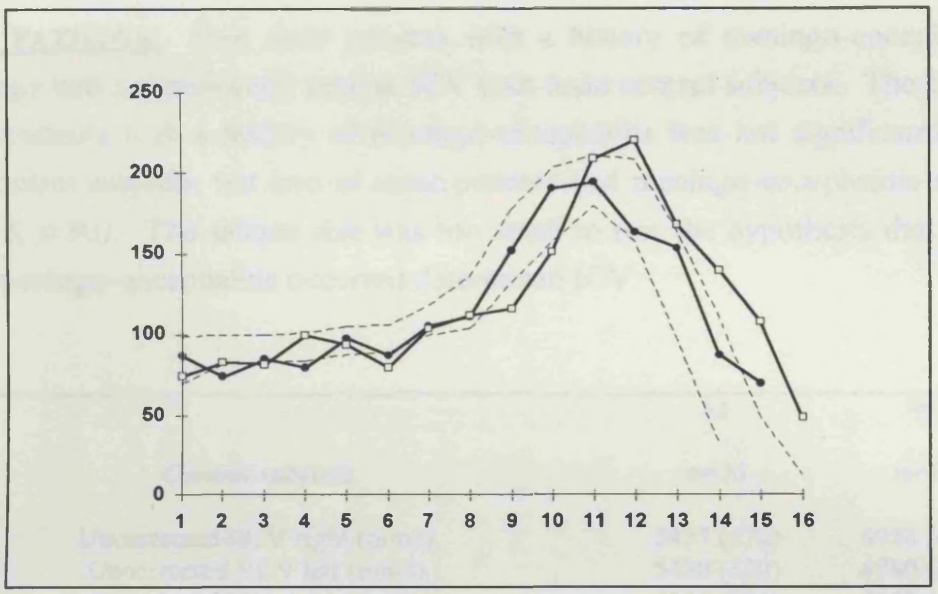

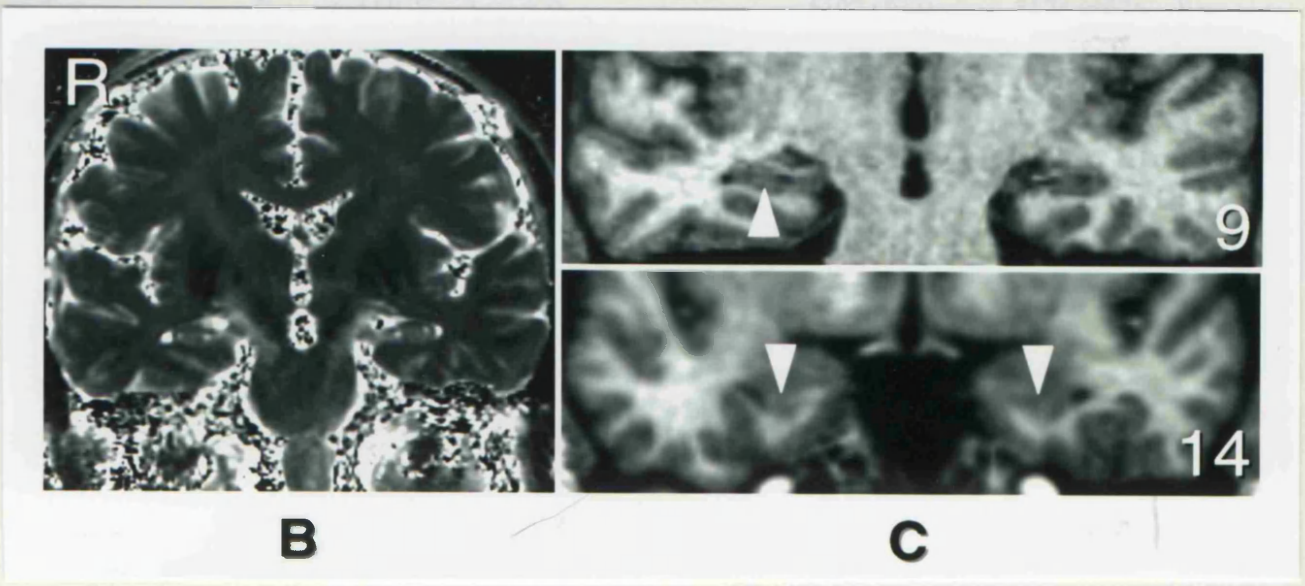

Figure 25. Physiologic asymmetry in position of hippocampi of control subject. For this control subject, the HCV distribution graph (A) showed that the left hippocampus was 3 mm longer than the right, after reformatting and alignment of the fornices. This led to an asymmetry in the position of the hippocampi. On section 9 of the reformatted MPRAGE (C), the right hippocampus appeared larger than the left, which was easily visualized because the amygdalae did not overlie the hippocampi at this level (white arrow). On section 14, the reverse was true, and the left hippocampus was larger than the right (white arrows). Because the overlying amygdalae make the visual assessment of the hippocampi more difficult at this level, the danger exists that a false positive diagnosis of left sided atrophy and HS is made, which happened in this control subject on a blinded assessment of hard copies of the scan *(see also Figure 23, p 84)*. The HCT2 values (B) were normal. HCVR(R/L) = 0.93 (Nl $\geq$ 0.87); HCV right = 5251 mm^3, HCV left = 5639 mm^3 (Nl: $\geq$ 4348 mm^3); HCT2 right = 99 msec, HCT2 left = 99 msec (Nl $\leq$ 108 msec). On the HCV distribution graph, the black circles represent the right hippocampus and the open squares the left hippocampus.

4.4.2. PATIENTS. Five male patients with a history of meningo-encephalitis at a young age had a significantly smaller ICV than male control subjects. The ICV of five female patients with a history of meningo-encephalitis was not significantly different from control subjects, but two of these patients had meningo-encephalitis as an adult *(Table 6, p 93)*. The sample size was too small to test the hypothesis that the age at which meningo-encephalitis occurred determined ICV.

	M	W
Control subjects	n=10	n=12
Uncorrected HCV right (mm3)	5437 (472)	4958 (432)
Uncorrected HCV left (mm3)	5428 (630)	4980 (447)
Corrected HCV right (mm3)	5206 (379)	5152 (362)
Corrected HCV left (mm3)	5197 (502)	5174 (467)
ICV (cm3)	1570 (111)	1393 (109)
Patients with no history of meningo-encephalitis	n=40	n=50
ICV (cm3)	1509 (112)	1335 (99)
Patients with history of meningo-encephalitis	n=5	n=5
ICV (cm3)	1355 (169)	1267 (177)

Table 6. Gender differences in uncorrected HCV, and ICV in controls and patients with epilepsy. A two-way ANOVA of the uncorrected HCV showed that gender ($F = 3.98$, $p = 0.053$) almost reached statistical significance and that side (i.e. right or left hippocampus) was not a significant factor ($F = 0.00$, $p = 0.96$). After correcting HCV for ICV, the effect of gender ($p = 0.97$) was no longer apparent. The ICV of the normal group was compared with each of the two patient groups (those with and those without a history of meningo-encephalitis) using Student's t-test. The two genders were treated separately. The difference between the male control subjects and male patients with a history of meningo-encephalitis was significant ($p = 0.02$ compared with a critical value of 0.05/2). The remaining differences did not achieve significance.

The patients were subdivided on the basis of quantitative hippocampal MRI measures *(Figure 26, p 94)*. Firstly, on the basis of hippocampal asymmetry using HCVR, then according to HCT2 and HCV findings, and thirdly, on the basis of HCV distribution obtained from the hippocampal graphs.

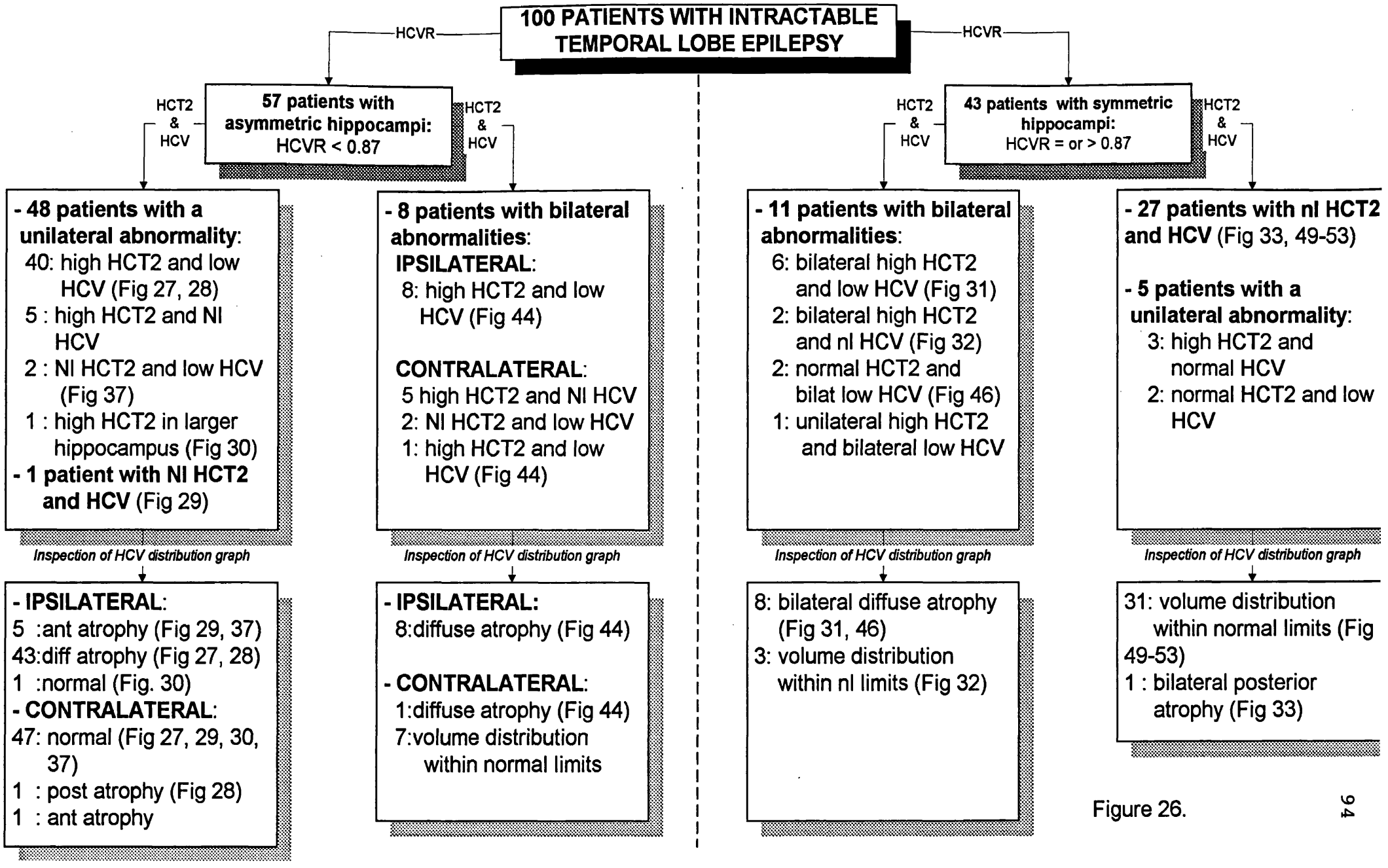
100 PATIENTS WITH INTRACTABLE TEMPORAL LOBE EPILEPSY
HCVR
HCVR
57 patients with asymmetric hippocampi: HCVR < 0.87
43 patients with symmetric hippocampi: HCVR = or > 0.87
HCT2 & HCV
HCT2 & HCV
HCT2 & HCV
HCT2 & HCV
- 48 patients with a unilateral abnormality:
40: high HCT2 and low HCV (Fig 27, 28)
5 : high HCT2 and NI HCV
2 : NI HCT2 and low HCV (Fig 37)
1 : high HCT2 in larger hippocampus (Fig 30)
- 1 patient with NI HCT2 and HCV (Fig 29)
- 8 patients with bilateral abnormalities:
IPSILATERAL:
8: high HCT2 and low HCV (Fig 44)
CONTRALATERAL:
5 high HCT2 and NI HCV
2: NI HCT2 and low HCV
1: high HCT2 and low HCV (Fig 44)
- 11 patients with bilateral abnormalities:
6: bilateral high HCT2 and low HCV (Fig 31)
2: bilateral high HCT2 and nl HCV (Fig 32)
2: normal HCT2 and bilat low HCV (Fig 46)
1: unilateral high HCT2 and bilateral low HCV
- 27 patients with nl HCT2 and HCV (Fig 33, 49-53)
- 5 patients with a unilateral abnormality:
3: high HCT2 and normal HCV
2: normal HCT2 and low HCV
Inspection of HCV distribution graph
Inspection of HCV distribution graph
Inspection of HCV distribution graph
Inspection of HCV distribution graph
- IPSILATERAL:
5 :ant atrophy (Fig 29, 37)
43:diff atrophy (Fig 27, 28)
1 :normal (Fig. 30)
- CONTRALATERAL:
47: normal (Fig 27, 29, 30, 37)
1 : post atrophy (Fig 28)
1 : ant atrophy
- IPSILATERAL:
8:diffuse atrophy (Fig 44)
- CONTRALATERAL:
1:diffuse atrophy (Fig 44)
7:volume distribution within normal limits
8: bilateral diffuse atrophy (Fig 31, 46)
3: volume distribution within nl limits (Fig 32)
31: volume distribution within normal limits (Fig 49-53)
1 : bilateral posterior atrophy (Fig 33)

Figure 26.

4.4.2.1. DIVISION ACCORDING TO THE PRESENCE OF HIPPOCAMPAL ASYMMETRY USING HCVR. Patients were divided into 2 groups according to HCVR. Fifty-seven patients had a HCVR < 0.87 and 43 patients had a HCVR ≥ 0.87.

4.4.2.2. SUBDIVISIONS ACCORDING TO THE PRESENCE OF BILATERAL HIPPOCAMPAL ABNORMALITIES USING HCT2 AND HIPPOCAMPAL VOLUME. Each of the two groups was further divided into two subgroups according to the presence of bilaterally abnormal HCT2s, HCVs, or both.

4.4.2.2.1. The group of 57 patients with asymmetric hippocampi.

4.4.2.2.1.1. Unilateral or no abnormalities of HCT2, HCV or both. Forty-eight of these 57 patients had a unilateral hippocampal abnormality of HCT2, or HCV or both. In 40 patients this consisted of a high HCT2 (median = 122 msec, range: 109 - 144 msec) in an atrophic hippocampus (median: 3611 mm^3, range: 2407 - 4174 mm^3) *(Figure 27, p 96; Figure 28, p 97)*. The median HCV of the contralateral and larger hippocampus of these 40 patients was 5157 mm^3 (range: 4379 - 6249 mm^3), and within normal limits.

Five patients had an increased HCT2 (median: 114 msec, range: 109 to 130 msec) in the smaller hippocampus, of which the HCV was in the normal range (median: 4417 mm^3, range: 4353 to 5142 mm^3). The median HCV of the contralateral and larger hippocampus of these five patients was 6155 mm^3 (range: 5526 to 6439 mm^3) which was significantly larger than that of the contralateral hippocampus in the 40 patients with unilateral HS whose HCV on the sclerotic side was more than 2 SD below the mean control value (Mann-Whitney U test: $p = 0.0034$). This indicates that HS can exist in a hippocampus with an HCV within the normal range and high HCT2, presumably because its original size was large.

Two patients had a low HCV and normal HCT2s *(Figure 29, p 98; Figure 37, p 123)*. One patient had an increased HCT2 in the larger hippocampus *(Figure 30, p 99)*.

One patient with HCVR of 0.76 had normal HCT2s and HCVs within the normal limits. She had atrophy exclusively of the hippocampal head *(Figure 29, p 98)*.

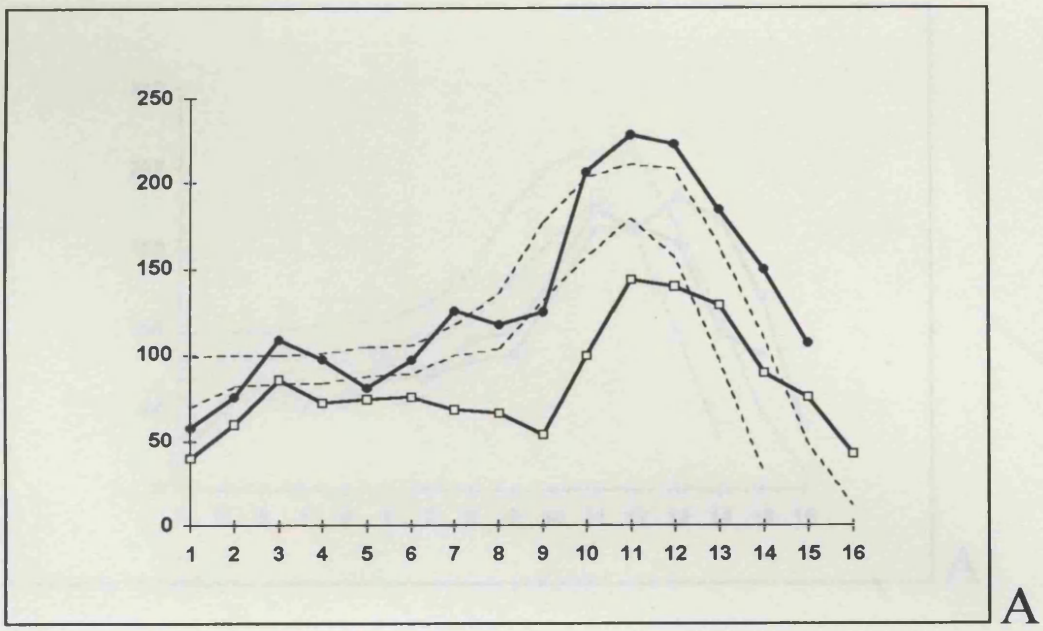

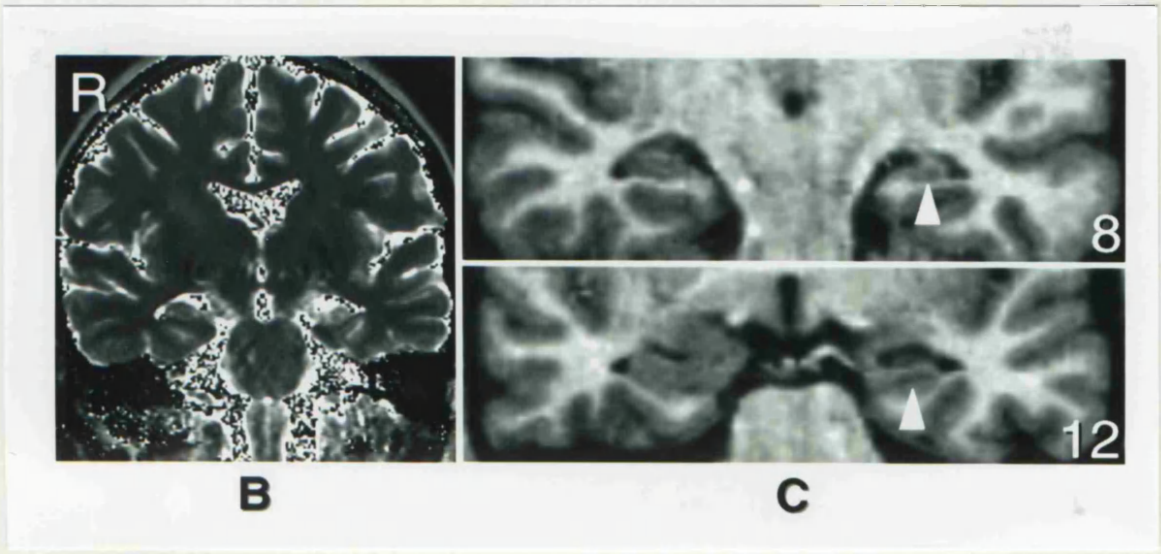

Figure 27. Unilateral diffuse HS. The patient was a 20 year old woman who had been well till the age of 16 years. At that time, she probably had viral encephalitis with high fever and SGS. CSF examination showed 2 white cells, protein was 190 mg% and glucose was normal. High serum and CSF titers of Herpes Simplex antibodies were documented. Subsequently, she developed intractable TLE with a clear left temporal focus on interictal and ictal EEG. The left hippocampus was diffusely atrophic (A) (white arrows on section 8 and 12 in C) with a high T2 signal visible on the HCT2 map (B) (white arrow), which is characteristic of HS. HCVR(L/R) = 0.67 (Nl $\geq$ 0.87); HCV right = 5915 mm^3, HCV left = 3928 mm^3 (Nl: $\geq$ 4348 mm^3); HCT2 right = 102 msec, HCT2 left = 129 msec (Nl $\leq$ 108 msec). On the HCV distribution graph, the black circles represent the right hippocampus and the open squares the left hippocampus. [Hospital number: QSC23691].

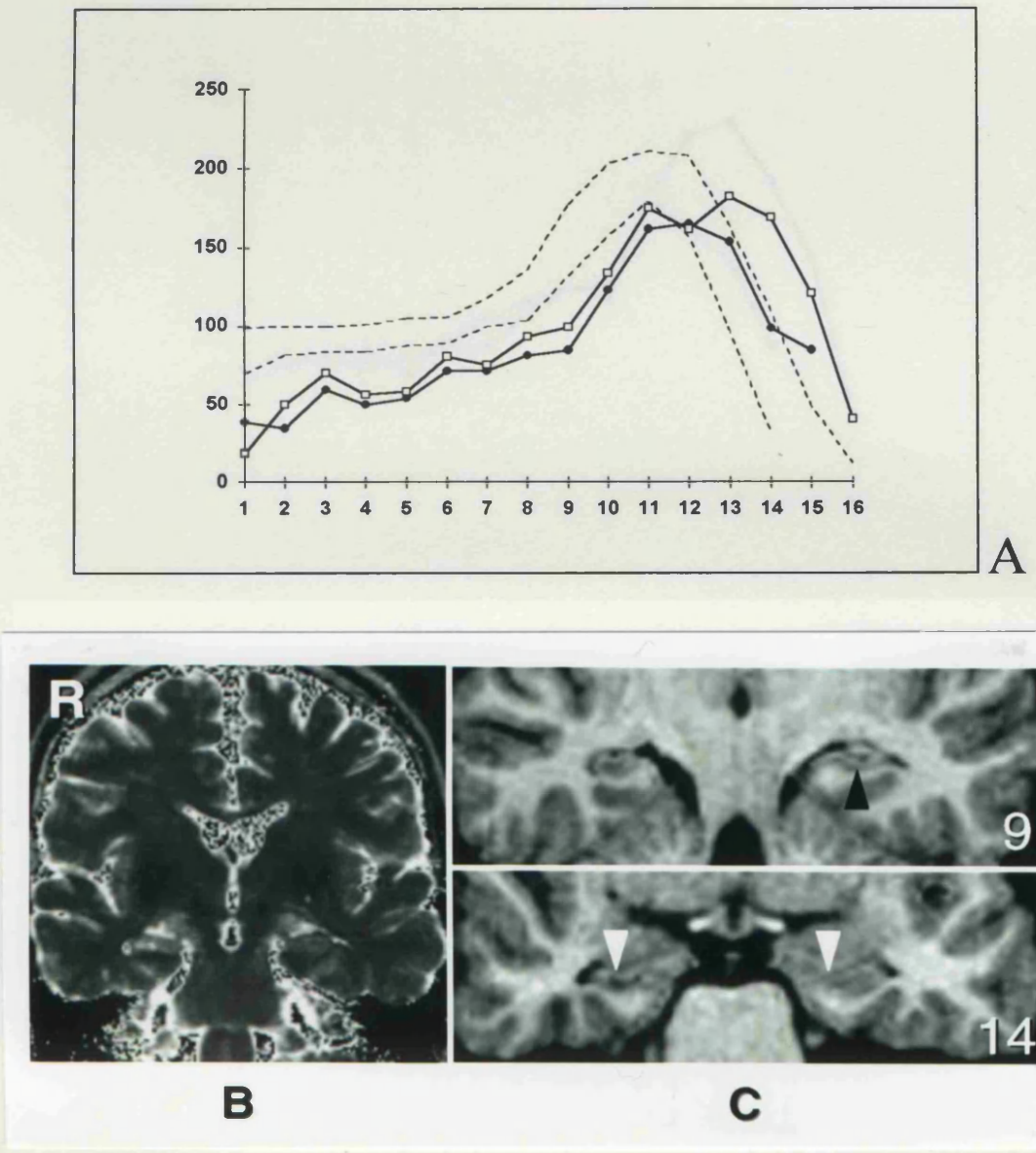

Figure 28. Diffuse HS on the right in combination with posterior atrophy of the left hippocampus. Patient was a 41 year old man, with a history of prolonged FC lasting more than four hours following measles vaccination at the age of 1 year. He had intractable TLE with CPS and secondary generalization. Interictal EEG showed generalized spike wave discharges and a right temporal lobe focus. On the hard copies of the standard MRI scan, the hippocampi appeared more or less symmetric, with a bright signal on the right. On closer examination of the MPRAGE however, the right hippocampus was smaller on all sections, and markedly so at the level of the head (white arrows on section 14 in C). Notice also the hypodense signal in the right hippocampus on the MPRAGE in section 9 and 14, consistent with a diagnosis of HS. Inspection of the HCV distribution graph (A) showed diffuse atrophy of the right hippocampus and in addition posterior atrophy of the left hippocampus compared to the control graph (black arrow on section 9 in C). HCVR(R/L) = 0.80 (Nl $\geq$ 0.87); HCV right = 3938 mm^3, HCV left = 4877 mm^3 (Nl: $\geq$ 4348 mm^3); HCT2 right = 130 msec (white arrow on HCT2 map), HCT2 left = 102 msec (Nl $\leq$ 108 msec). On the HCV distribution graph, the black circles represent the right hippocampus and the open squares the left hippocampus. [Hospital number: QSC23479].

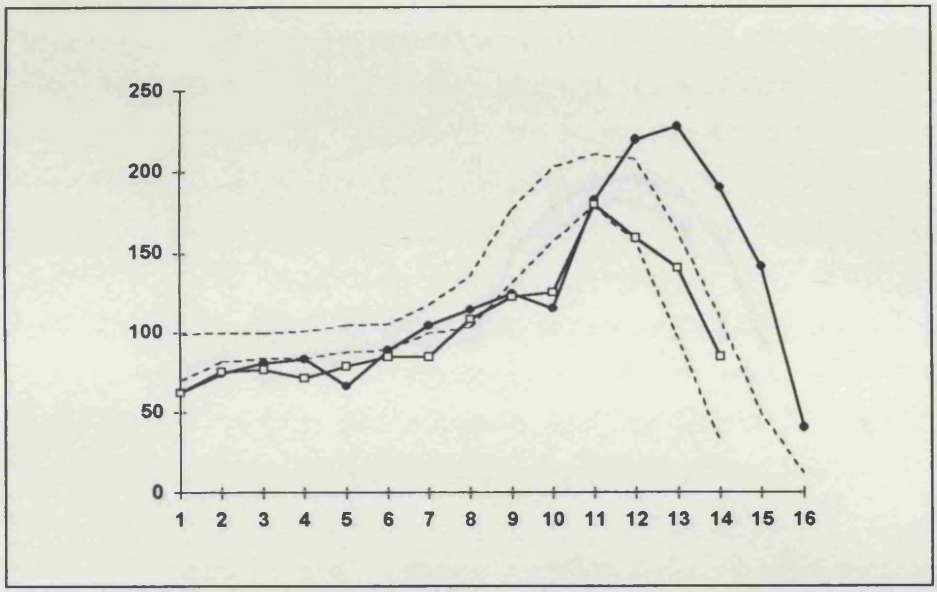

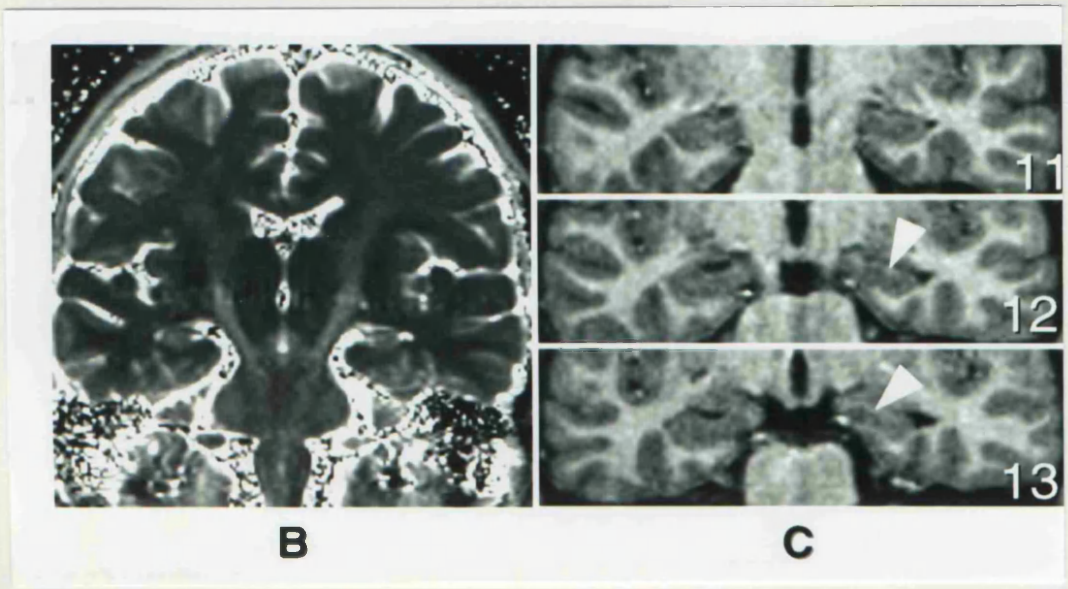

Figure 29. Anterior HS. Patient was a 26 year old woman with a history of FC at the age of 1 year. Habitual epilepsy started at the age of 11 years and was refractory to medication. She had on average two CPS a week, and had a total of three SGS during her lifetime. A clear left antero-temporal focus was demonstrated on interictal and ictal EEGs. The tail and body of the hippocampi were symmetric up to section 11 (A and black arrows on section 11 in C). The anterior 1.5 cm of the hippocampus was severely atrophic compared to the right side (see section 12 and 13, white arrows). The HCT2 signal was normal which could be explained because the HCT2 map (B) was obtained at the level of the body, posterior to the region of hippocampal damage. She underwent a left anterior temporal lobe resection with resection of the anterior part of the hippocampus, with pathological confirmation of HS of the hippocampal head. HCVR(L/R) = 0.76 (Nl $\geq$ 0.87); HCV right = 5746 mm^3, HCV left = 4349 mm^3 (Nl: $\geq$ 4348 mm^3); HCT2 right = 101 msec, HCT2 left = 102 msec (Nl $\leq$ 108 msec). On the HCV distribution graph, the black circles represent the right hippocampus and the open squares the left hippocampus. [Hospital number: QSC26823].

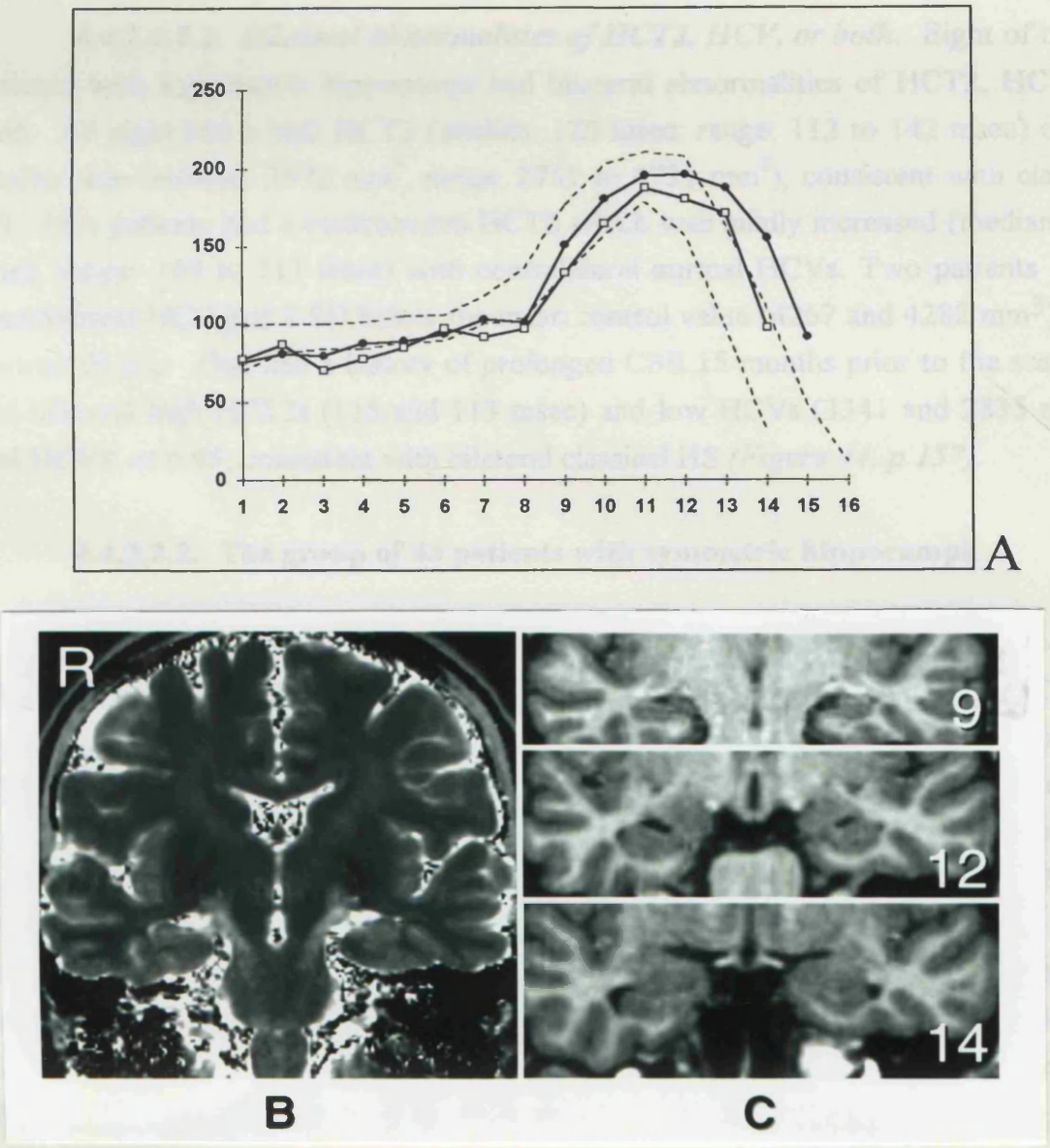

Figure 30. Probable dysgenesis of right hippocampus. Patient was a 27 year old woman with epilepsy since the age of 11 years. There was no history of FC or meningo-encephalitis. Clinically, she had TLE which was confirmed on video-EEG. Dystonic posturing of the left arm and automatisms of the right arm suggested right temporal onset. Interictal and ictal EEG showed a clear right temporal focus. Visual assessment of her MRI scan was unrevealing. The quantitative MRI however was unusual. The anterior part of the right hippocampus appeared larger than the left (A) (see sections 9,12, and 14 in C) and had an increased HCT2, which was not sufficiently prolonged to be evident on visual assessment of the HCT2 map (B). These findings would be unusual for HS, and may represent dysgenesis of the right hippocampus. HCVR(L/R) = 0.86 (Nl $\geq$ 0.87); HCV right = 5584 mm^3, HCV left = 4830 mm^3 (Nl: $\geq$ 4348 mm^3); HCT2 right = 112 msec, HCT2 left = 106 msec (Nl $\leq$ 108 msec). On the HCV distribution graph, the black circles represent the right hippocampus and the open squares the left hippocampus. [Hospital number: QSC37619].

4.4.2.2.1.2. Bilateral abnormalities of HCT2, HCV, or both. Eight of the 57 patients with asymmetric hippocampi had bilateral abnormalities of HCT2, HCV, or both. All eight had a high HCT2 (median: 120 msec, range: 112 to 142 msec) on the smaller side (median: 3572 mm^3, range: 2751 to 4731 mm^3), consistent with classical HS. Five patients had a contralateral HCT2 which was mildly increased (median: 109 msec, range: 109 to 113 msec) with contralateral normal HCVs. Two patients had a contralateral HCV just 2 SD below the mean control value (4267 and 4282 mm^3) with normal HCT2s. One had a history of prolonged CSE 15 months prior to the scan and had bilateral high HCT2s (115 and 113 msec) and low HCVs (3341 and 2835 mm^3), and HCVR of 0.85, consistent with bilateral classical HS *(Figure 44, p 157)*.

4.4.2.2.2. The group of 43 patients with symmetric hippocampi.

4.4.2.2.2.1. Bilateral abnormalities of HCT2, HCV, or both. Eleven of the 43 patients with symmetric hippocampi had bilateral abnormalities of HCT2s, HCVs or both. Six of these patients had bilaterally small HCVs (median: 3089 mm^3, range: 2611 to 3703 mm^3) and increased HCT2s (median: 118 msec, range: 112 to 140 msec) *(Figure 31, p 101)*. Two patients had bilaterally increased HCT2s (median: 112 msec, range: 110 to 114 msec) and normal HCVs (median: 4767 mm^3, range: 4383 to 5374 mm^3) *(Figure 32, p 102)*, two had bilaterally small HCVs (median: 3913 mm^3, range: 3465 to 4344 mm^3), with normal HCT2s (median: 104 msec, range: 100 to 106 msec) *(Figure 46, p 162)* and one had bilaterally small HCVs (HCV right = 2816 and HCV left = 2838 mm^3) with a unilateral increased HCT2 (HCT2 right = 118 msec and HCT2 left = 106 msec).

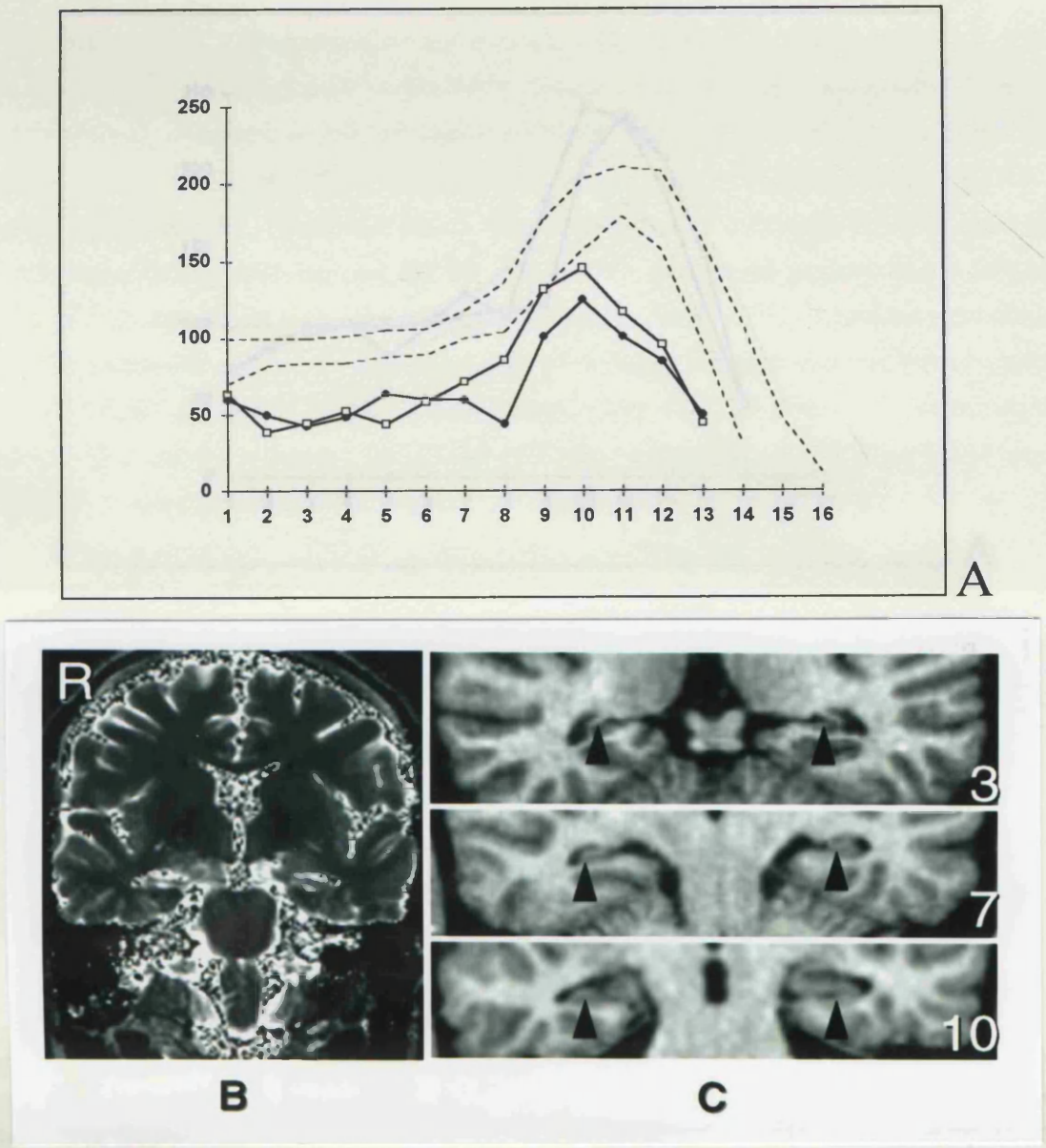

Figure 31. Bilateral severe diffuse HS. The patient was a 25 year old man with TLE since the age of 11 years. A few months prior to the onset of the epilepsy, he sustained a cerebral trauma with brief loss of consciousness. Interictal EEGs never showed any epileptic features, despite intractable TLE with on average 1 CPS per week, and a total of around 200 SGS during his lifetime. Both hippocampi were diffusely very small (A) (black arrows on sections 3, 7 and 10 in C) with high HCT2 signals. HCVR(R/L) = 0.89 (Nl ≥ 0.87); HCV right = 2789 mm^3, HCV left = 3109 mm^3 (Nl: ≥ 4348 mm^3); HCT2 right = 124 msec, HCT2 left = 115 msec (Nl ≤ 108 msec). On the HCV distribution graph, the black circles represent the right hippocampus and the open squares the left hippocampus. [Hospital number: QSC15042].

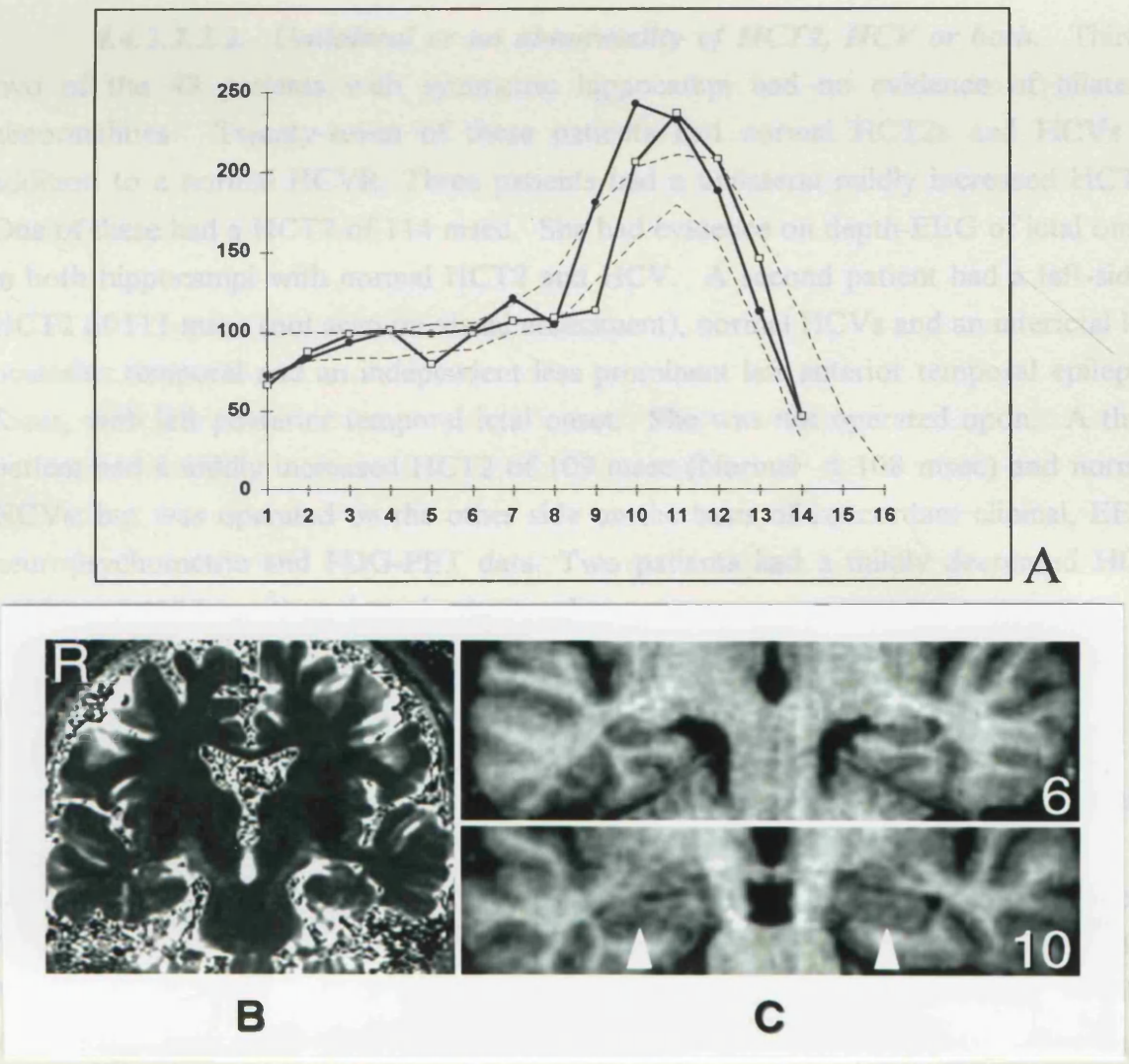

Figure 32. Bilaterally increased HCT2s with normal HCVs. Patient was a 32 year old man with intractable TLE since the age of 14 years, one year after cerebral trauma with loss of consciousness for three hours. He had several admissions because of prolonged complex partial status epilepticus (CPSE), which were documented on video-EEG. On some occasions, CPSE originated from the left temporal lobe, but on other occasions from the right temporal lobe. The hippocampal heads were relatively prominent (A and white arrows on section 10 in C) compared with more posterior levels (section 6). HCT2s were increased bilaterally, which was difficult to appreciate on visual assessment of the HCT2 map (B). This could represent bilateral hippocampal dysgenesis (*compare with Figure 30, p 99*), or relative atrophy of posterior hippocampal regions of hippocampi that originally were of large volume. HCVR(R/L) = 0.93 (Nl ≥ 0.87); HCV right = 5374 mm^3, HCV left = 4986 mm^3 (Nl: ≥ 4348 mm^3); HCT2 right = 113 msec, HCT2 left = 114 msec (Nl ≤ 108 msec). On the HCV distribution graph, the black circles represent the right hippocampus and the open squares the left hippocampus. [Hospital number: MVP18163].

4.4.2.2.2.2. Unilateral or no abnormality of HCT2, HCV or both. Thirty-two of the 43 patients with symmetric hippocampi had no evidence of bilateral abnormalities. Twenty-seven of these patients had normal HCT2s and HCVs in addition to a normal HCVR. Three patients had a unilateral mildly increased HCT2. One of these had a HCT2 of 114 msec. She had evidence on depth-EEG of ictal onset in both hippocampi with normal HCT2 and HCV. A second patient had a left-sided HCT2 of 111 msec (not seen on visual assessment), normal HCVs and an interictal left posterior temporal and an independent less prominent left anterior temporal epileptic focus, with left posterior temporal ictal onset. She was not operated upon. A third patient had a mildly increased HCT2 of 109 msec (Normal $\leq$ 108 msec) and normal HCVs, but was operated on the other side on the basis of concordant clinical, EEG, neuropsychometric and FDG-PET data. Two patients had a mildly decreased HCV (4050 and 4327 mm^3) as the only abnormality.

4.4.2.3. INSPECTION OF HIPPOCAMPAL VOLUME DISTRIBUTION GRAPHS.

4.4.2.3.1. Patients with hippocampal asymmetry and unilateral hippocampal damage. In the 49 patients with hippocampal asymmetry and no evidence of bilateral abnormalities using HCT2 or HCV, 43 had diffuse atrophy *(Figure 27, p 96; Figure 28, p 97)* and five had anterior atrophy *(Figure 29, p 98; Figure 37, p 123)* on the smaller side. Of these five patients with anterior atrophy, three had a normal and two had an increased HCT2 (112 and 114 msec). The single patient with high T2 in the larger hippocampus had a normal volume distribution *(Figure 30, p 99)*. Isolated unilateral posterior atrophy was not observed in any patient. Unexpectedly, the graphs showed that in addition to diffuse HS there was an abnormality on the contralateral side in two patients. One patient had posterior atrophy *(Figure 28, p 97)* and one patient had anterior atrophy.

4.4.2.3.2. Patients with hippocampal asymmetry and bilateral hippocampal damage. All eight patients with asymmetric hippocampi and bilateral abnormalities on HCT2, HCV, or both, had diffuse atrophy on the more affected side. On the contralateral side, one patient had diffuse atrophy *(Figure 44, p 157)*, and the other seven had a HCV distribution within the normal range.

4.4.2.3.3. Patients with symmetric hippocampi and bilateral hippocampal damage. Of the 11 patients with symmetric hippocampi and bilateral abnormalities, 8 had bilateral diffuse atrophy *(Figure 31, p 101)* and 3 had a volume distribution within normal limits.

4.4.2.3.4. Patients with symmetric hippocampi and no apparent hippocampal damage. Of the 32 patients with symmetric hippocampi and no evidence of bilateral disease, one graph unexpectedly showed bilateral posterior atrophy *(Figure 33, p 105)*.

4.4.3. NEUROPATHOLOGICAL CORRELATES.

Thirty-six of the 57 patients (63%) with hippocampal asymmetry underwent a temporal lobe resection including the hippocampus, on the side of the smaller hippocampus, with pathological confirmation of HS in all. Four of the 43 patients (9%) with symmetric hippocampi were operated upon. The hippocampus was removed in two of these patients, who had normal quantitative MRI hippocampal measures. Neuropathologic examination revealed EFS.

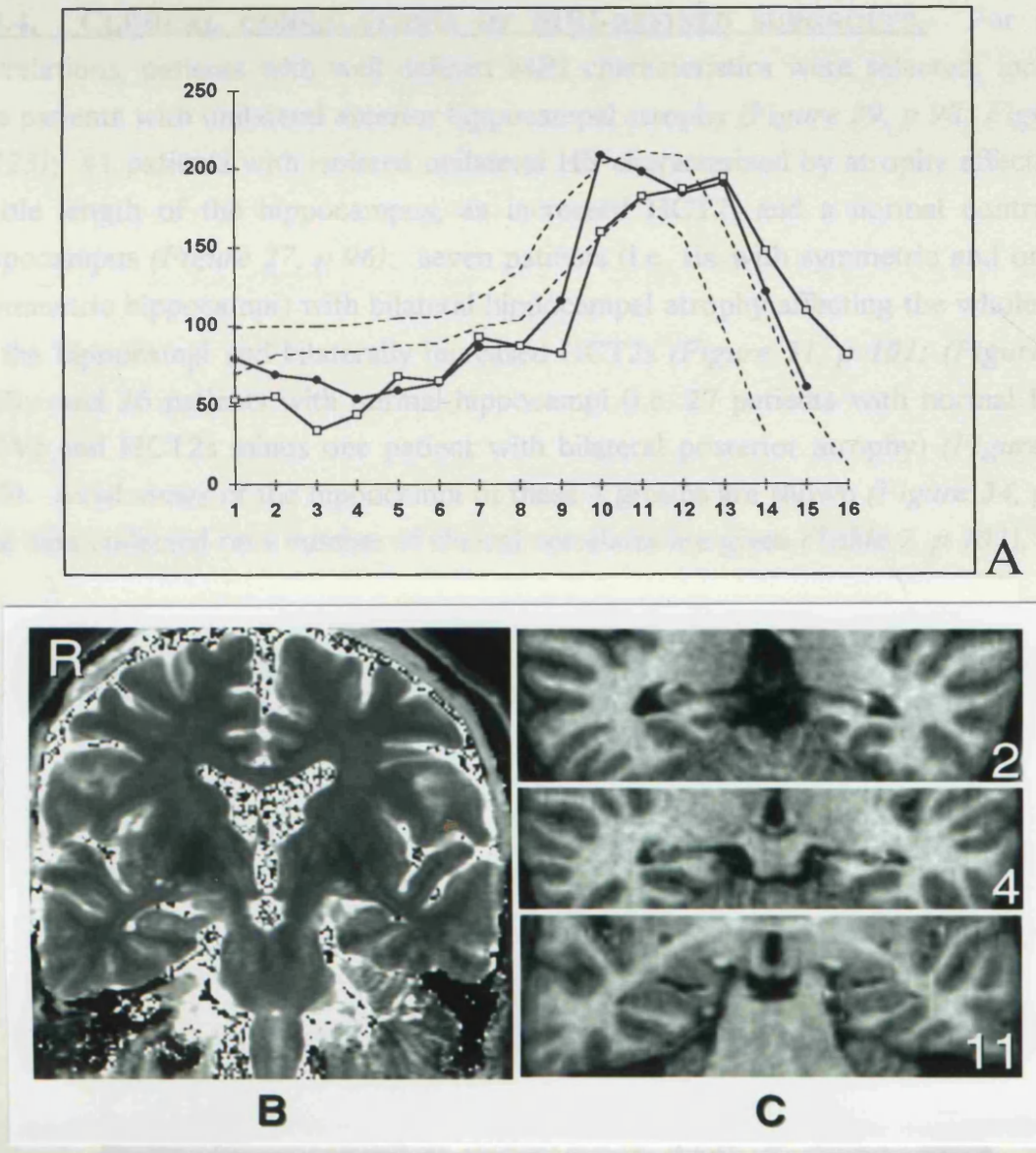

Figure 33. Bilateral posterior atrophy. Patient was a 28 year old man with intractable TLE since the age of 16 years, with no significant prior history. HCVs, HCT2s (B) and HCVR were within normal limits, but inspection of the HCV distribution graph (A) suggested bilateral smallness of the posterior hippocampi. HCVR(R/L) = 0.99 (Nl $\geq$ 0.87); HCV right = 4983 mm^3, HCV left = 4932 mm^3 (Nl: $\geq$ 4348 mm^3); HCT2 right = 104 msec, HCT2 left = 95 msec (Nl $\leq$ 108 msec). On the HCV distribution graph, the black circles represent the right hippocampus and the open squares the left hippocampus. [Hospital number: QSC28503].

4.4.4. CLINICAL CORRELATIONS OF MRI-DEFINED SUBGROUPS. For clinical correlations, patients with well defined MRI characteristics were selected, including: five patients with unilateral anterior hippocampal atrophy *(Figure 29, p 98; Figure 37, p 123)*; 41 patients with isolated unilateral HS characterized by atrophy affecting the whole length of the hippocampus, an increased HCT2, and a normal contralateral hippocampus *(Figure 27, p 96)*; seven patients (i.e. six with symmetric and one with asymmetric hippocampi) with bilateral hippocampal atrophy affecting the whole length of the hippocampi and bilaterally increased HCT2s *(Figure 31, p 101; (Figure 44, p 157)*; and 26 patients with normal hippocampi (i.e. 27 patients with normal HCVR, HCVs and HCT2s minus one patient with bilateral posterior atrophy) *(Figure 53, p 190)*. Axial views of the hippocampi of these 4 groups are shown *(Figure 34, p 106)*. The data collected on a number of clinical correlates are given *(Table 7, p 107)*.

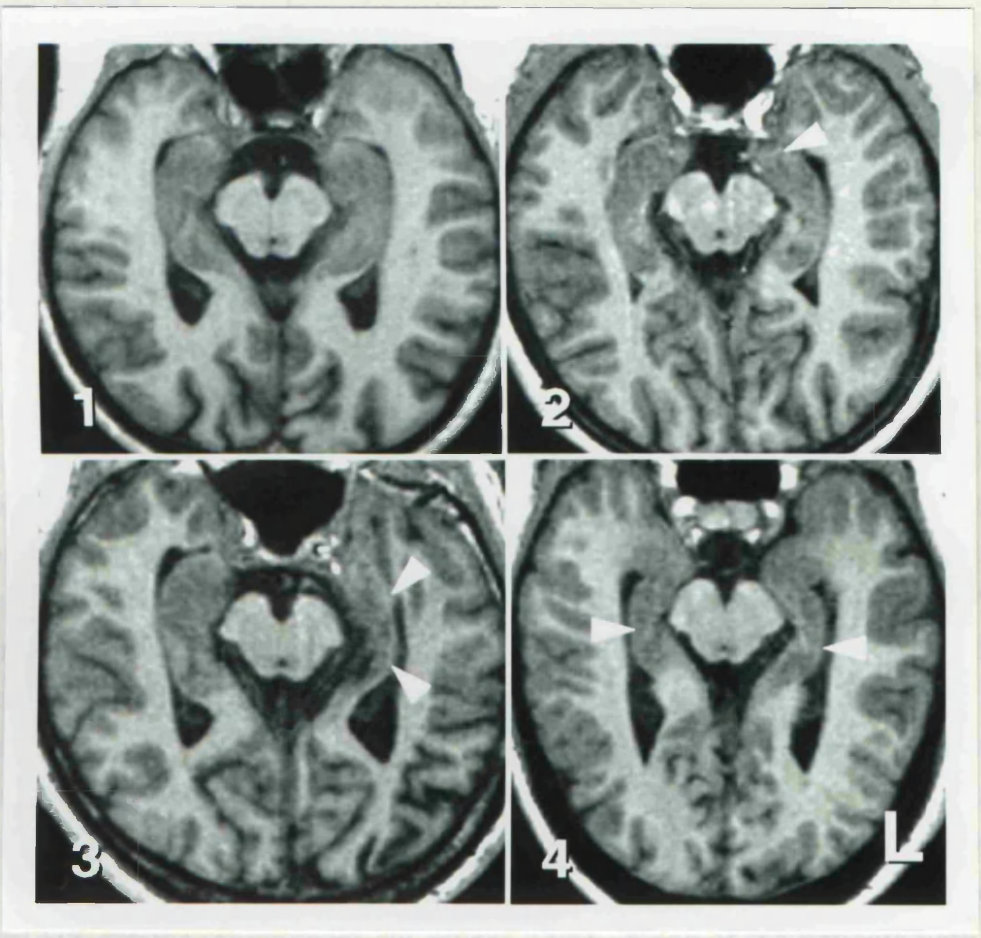

Figure 34. Axial views of the hippocampi demonstrating the spectrum of HS. MPRAGE images reformatted in a tilted axial plane showing the full length of the hippocampi *(see Figure 2, 27; Figure 11, p 58)*. 1. Normal hippocampi. 2. Anterior atrophy of left hippocampal head (white arrow). This is the same patient as in Figure 29, p 98. 3. Unilateral diffuse left HS (white arrows) [Hospital number: MV47675]. 4. Bilateral diffuse HS (white arrows) [Hospital number: QSB71558].

	Anterior hippocampal atrophy	Unilateral diffuse hippocampal sclerosis	Bilateral diffuse hippocampal sclerosis	Normal hippocampi on quantitative MRI
Number of patients	5	41	7	26
Age (years)	26 (19-34)	31 (16-51)	30 (18-37)	38 (24-64)
Age of onset of habitual epilepsy (years)	12 (6)	10 (9)	5 (7)	16 (7)
Duration of epilepsy (years)	15 (10-17)	20 (1-42)	28 (1-36)	21 (7-40)
Febrile convulsions	4 (80%)	21 (50%)	0 (0%)	2 (8%)
Meningo-encephalitis	0 (0%)	5 (12%)	3 (43%)	2 (8%)
First degree relative with FC or epilepsy	2 (40%)	6 (14%)	0 (0%)	5 (19%)
Average number of CPS/week over last year	4 (2-7)	2 (0.25-30)	2 (1-8)	2 (0-25)
> 10 SGS during lifetime	0 (0%)	19 (46%)	5 (71%)	11 (42%)

Table 7. Clinical correlations of MRI-defined subgroups.

There was a significant difference between the patient groups with respect to both their age at the time of study (Kruskal-Wallis ANOVA: $p = 0.02$), and age at the onset of their habitual epilepsy. The normal MRI group was significantly older than the groups with unilateral ($p = 0.01$) and bilateral HS ($p < 0.001$) at the age of onset of habitual epilepsy. The age difference between the normal MRI group and those with anterior hippocampal atrophy was not significant. A history of FC was obtained in four patients (80%) with anterior hippocampal atrophy and 21 patients (50%) with unilateral diffuse HS, but in none of the patients (0%) with bilateral HS and only two patients (8%) with normal hippocampi (Fisher's Exact test: $p = 0.00002$). The low number of patients with a history of FC in the normal MRI group was strikingly different compared with the three HS groups combined (component chi-square = 12.08 compared with a total chi-square = 21.70 (Everitt, 1992)). Also, the absence of FC in the bilateral HS group contrasted with the high frequency of FC in the combined unilateral HS groups (component chi-square 7.98). None of the patients with anterior atrophy had a history of more than 10 SGS in their lifetime, in contrast to five of seven patients (72%) with bilateral HS who had more than 10 SGS (Fisher's Exact test restricted to the three groups with HS: $p = 0.05$). The absence of patients with more than 10 SGS in the anterior hippocampal atrophy group contrasted with the higher number of patients with more than 10 SGS in the combined unilateral and bilateral diffuse HS groups (component chi-square = 4.56 compared with the total chi-square =

6.09). The difference in number of patients with more than 10 SGS between the unilateral and bilateral diffuse HS groups was less marked (component chi-square = 1.52). Duration of epilepsy, frequency of a history of meningo-encephalitis or family history of FC or epilepsy in a first degree relative, and average number of CPS per week did not differ significantly between the groups.

The cause of meningo-encephalitis in three patients with bilateral HS was measles virus, one not further specified cause, and one which with hindsight of autopsy results might not have been meningo-encephalitis *(Figure 44, p 157)* and in five with unilateral HS Herpes Simplex virus *(Figure 27, p 96)*, mumps virus, Haemophilus Influenzae, and two not further specified meningitides respectively.

4.5. DISCUSSION

A combination of HCVR, HCT2 mapping, HCVs corrected for ICV and a HCV distribution graph compared against a control graph were used to establish the MRI spectrum of HS.

4.5.1. HIPPOCAMPAL VOLUMETRY.

Hippocampal volumetry is the most frequently used MR method to study the hippocampus quantitatively (Jack, Jr. *et al.* 1988; Jack, Jr. *et al.* 1990; Cascino *et al.* 1991; Cook *et al.* 1992; Lencz *et al.* 1992; Watson *et al.* 1992; Bhatia *et al.* 1993; Cendes *et al.* 1993b; Kuks *et al.* 1993; Kuzniecky *et al.* 1993; Spencer *et al.* 1993; Adam *et al.* 1994; Kim *et al.* 1994). A significant difference in HCV expressed as a difference or ratio has been shown to indicate the presence of HS on the smaller side, which is confirmed in this study. Thirty-eight patients with a HCVR less than 0.87 and concordant clinical and functional data were operated on so far. Neuropathological examination of the resected specimens confirmed the presence of HS in all cases. Several studies have shown that these patients do well after surgery (Jack, Jr. *et al.* 1992; Kuzniecky *et al.* 1993; Garcia *et al.* 1994), and demonstration of unilateral HS with concordant functional tests obviates the need for invasive EEG studies (Baulac *et al.* 1994; Fish, 1994a; Thadani *et al.* 1995).

The main disadvantage of the HCVR method is its inability to detect bilateral HS. The mean HCVR of seven patients in this study with bilateral HS characterized by bilateral low HCVs and increased HCT2s was 0.90 ± 0.03, which is within normal limits. Even a significant volume difference does not rule out bilateral HS *(Figure 44, p 157)*. Also, HCVR can be falsely lateralising. One patient had seizure onset from the temporal lobe with the larger hippocampus, which had an increased HCT2 signal. This is not consistent with HS but may represent hippocampal dysgenesis. Hippocampal volumetry is time consuming, although the protocol used in this study reduces this to 20 minutes of operator time.

4.5.2. HCT2 MAPPING.

HCT2 mapping was first described by Jackson et al (Jackson *et al.* 1993b). The main advantages of this technique are that the HCT2 values are absolute values which can be compared immediately against control values, with no gender differences, and do not need manipulations or corrections for interpretation, and can be measured

within a few seconds. Further, HCT2 reflects pathology of the tissue which may be other than sclerosis, and not necessarily accompanied by atrophy, although hippocampal pathology underlying intractable TLE is mainly sclerosis. In the current study, all three patients with HCVR less than 0.87 and normal HCT2 had anterior atrophy. This illustrates one of the disadvantages of the HCT2 map as described in this paper, which consists of a single section of 8 mm through the body of the hippocampus. In anterior atrophy, the most severely affected part of the hippocampus probably falls outside the part of the hippocampus covered by the standard HCT2 map. Measuring HCT2 in several coronal sections covering the entire hippocampus may obviate this problem (Duncan *et al.* 1996).

Five patients with unilateral HS confirmed on pathology had an increased HCT2 but normal HCV. In these patients, there was however an abnormal HCVR, with the contralateral HCV being larger than usual. If these patients were to develop bilateral HS, the HCVR and HCVs would be within the normal range, and only HCT2 mapping might be able to give a clue to its presence. Two patients in this study had such a combination of bilaterally increased HCT2s and normal HCVs and HCVR. These might represent forms of bilateral HS, but pathological confirmation was not available.

4.5.3. CORRECTION OF HIPPOCAMPAL VOLUME FOR INTRACRANIAL VOLUME.

Correction of HCV for ICV using a covariance method was described by Jack et al (Jack, Jr. *et al.* 1990) and Free et al (Free *et al.* 1995). The main advantages of correcting HCV for ICV are that gender differences are abolished, and according to Free et al, the increased sensitivity to detect bilateral hippocampal atrophy because the SD of the mean control HCV becomes smaller. Jack et al (Jack, Jr. *et al.* 1990) reported a correlation coefficient between control HCV and ICV of 0.57, and Free et al (Free *et al.* 1995) one of 0.63, which is similar to the value of 0.62 in this study. This correction method assumes that ICV between control subjects and patients with epilepsy are of equal magnitude. A potentially confounding factor for such a correction occurs in HS caused by meningo-encephalitis, since this may be associated with a significantly smaller ICV than that of control subjects. In these cases however, correcting HCV for ICV did not bring small HCVs into the normal range, and was clinically usable.

4.5.4. HIPPOCAMPAL VOLUME DISTRIBUTION GRAPH.

An HCV distribution graph allows identification of unilateral diffuse, anterior and posterior atrophy (Cook *et al.* 1992). A graph plotting mean control values for each section position may be useful to demonstrate bilateral HS (Kim *et al.* 1995b). Two graphs at 2 SD from this mean control graph were constructed, which gives a better indication of the boundaries of normality. The present findings concur with those of Kim et al (Kim *et al.* 1995b) and Bronen et al (Bronen *et al.* 1995) that diffuse atrophy is the most frequent HS variant. Cook et al (Cook *et al.* 1992) and Kuks et al (Kuks *et al.* 1993) however reported that a majority of patients had anterior atrophy. This discrepancy might be explained by different patient selection criteria, by the fact that Cook et al and Kuks et al did not reformat their 3D-volume set and therefore did not correct for headtilt, and differences in interpretation of graphs; this is illustrated by the example of anterior atrophy given by Kuks et al (Kuks *et al.* 1993), which could be interpreted as diffuse atrophy when the hippocampal heads are aligned, and which would be more in keeping with the reported HCVR of 0.54. Unilateral posterior atrophy (Cook *et al.* 1992) was not seen in the present study. The HCV distribution graphs were useful to demonstrate the combination of focal and diffuse atrophies.

Bronen et al (Bronen *et al.* 1995) found in a study using visual assessment that the hippocampal body was the most frequently affected part of the hippocampus. From this quantitative study however, it can be concluded that the hippocampal head is the most frequently involved part. One mm thin sections were used and an MPRAGE 3-D volume acquisition sequence, which has an inversion pre-pulse and which allowed a better assessment of the hippocampal head, than was possible in the study of Bronen et al, due to improved contrast and resolution compared to the 5 mm thick sections without inversion pre-pulse that were used in that investigation.

Jackson et al (Jackson *et al.* 1994c) described six patients with unilateral HS who had undetectable volume loss on MRI, but who had other MR features of HS. Using the improved HCV measurement technique described in this text, it appears unlikely that HS does exist without detectable HCV loss on MRI with the exception of those cases with bilateral hippocampal damage and normal HCVs and HCV distribution graph.

Forty-one percent of controls had an asymmetric position of the hippocampi. This can lead to a false positive diagnosis of unilateral hippocampal atrophy on visual inspection of the scan, which happened in four subjects in this study, one of which was

also described in Chapter 3 *(Figure 23, p 84).* It is therefore mandatory to measure the whole length of the hippocampus, in contrast to the conclusion of Kim et al (Kim *et al.* 1994) and King et al (King *et al.* 1995) that it is sufficient to measure only the hippocampal body.

4.5.5. CLINICAL CORRELATIONS.

The present study corroborates the strong association of prolonged FC and predominantly unilateral HS, for both the anterior and diffuse atrophy variants (Cavanagh, Meyer, 1956; Falconer *et al.* 1964; Falconer, 1974; Annegers *et al.* 1987; Duncan, Sagar, 1987; Rocca *et al.* 1987; Sagar, Oxbury, 1987; Bruton, 1988; Cendes *et al.* 1993a; Harvey *et al.* 1995; Maher, McLachlan, 1995; Mathern *et al.* 1995a). Kuks et al (Kuks *et al.* 1993) on the other hand reported a history of FC in only three of 26 patients (12%) with focal atrophy. Methodological differences in MR techniques and interpretation of graphs commented on earlier, and different patient selection criteria might explain these discrepant findings. None of the seven patients with bilateral HS had a history of FC, which suggests that the etiology of this form of HS may be different than that of unilateral HS.

Free et al (Free *et al.* 1995), and Gambardella et al (Gambardella *et al.* 1993) reported an association of bilateral HS with a history of meningo-encephalitis. In the present study, the percentages of each group having had meningo-encephalitis suggested an association between bilateral disease and meningo-encephalitis, but the differences were statistically not significant, which could be explained by the small numbers of patients with bilateral HS in the present study. A previous episode of meningo-encephalitis therefore should not in itself be taken as indicative of bilateral HS. This supports the observation of Marks et al (Marks *et al.* 1992) who reported that meningitis at a young age was commonly associated with unilateral HS. Also, Ounsted et al (Ounsted *et al.* 1985) described two patients with intractable TLE due to unilateral HS after meningitis who became seizure free after surgery.

Extent of HS was related to the number of SGS. None of five patients with anterior atrophy had more than ten SGS in their lifetime, in agreement with the observation of Cook et al (Cook *et al.* 1992), in contrast to five of seven patients (72%) with bilateral HS, who had more than ten SGS. From this study, it is not clear if bilateral HS predisposes to frequent SGS, or if frequent SGS cause progression to bilateral HS. A longitudinal quantitative MRI follow-up study will be required to answer this question *(see Chapter 7).*

4.5.6. MRI-NEGATIVE TLE.

Normal hippocampal quantitative MRI measures were found in 26 patients (i.e. 27 patients with normal HCVR, HCT2s and HCVs minus one patient with bilateral posterior atrophy) despite a long history of medically refractory TLE. In about 50% of these MRI-negative patients, an amygdala abnormality was detected with AT2 mapping and FLAIR *(see isolated lesions of the amygdala, p 181)*. In seven of the remaining MRI-negative patients, single voxel ^{1}H MRS was obtained, and a low ratio of NAA/(Cho+Cr) was found in five of these patients, which may indicate diffuse neocortical disease *(see Chapter 9)*.

The decision to remove a temporal lobe and hippocampus which appear normal on MRI should take into account the fact that memory function may deteriorate (Scoville, Milner, 1957; Penfield, Milner, 1958; Penfield, Mathieson, 1974; Zola-Morgan *et al.* 1989; Lencz *et al.* 1992; Trenerry *et al.* 1993a) and the observation that removal of a pathologically normal temporal lobe does not generally cure the epilepsy (Falconer, Serafetinides, 1963; Green, Scheetz, 1964; Jensen, Klinken, 1976; Armstrong, Bruton, 1987; Duncan, Sagar, 1987; Bruton, 1988; Berkovic *et al.* 1991) and may lead to a psychosocial deterioration (Bruton, 1988). In hippocampal surgery for epilepsy, the preoperative ascertainment of a normal hippocampus is as important as that of an abnormal hippocampus. The strength of combining different quantitative MRI techniques lies in its better ability to define normal and abnormal.

CHAPTER V. QUANTITATIVE NEUROPATHOLOGY AND QUANTITATIVE MRI OF THE HIPPOCAMPUS IN TEMPORAL LOBE EPILEPSY.

5.1. ABSTRACT.

The aims of this study were to examine the relationships of HCT2 relaxation time and MR-based HCV to ND and GD of hippocampal neuronal cell layers, and to obtain a better clinico-pathological definition of HS and EFS. Fifty-three hippocampi with HS, six with EFS and six control hippocampi were studied. Pathologically, the HS group had a significantly higher logarithm GD/ND than the controls in all hippocampal subregions, and than the EFS group in all subregions except the GCDG. The EFS group had a significantly higher logarithm GD/ND than the control group only in the GCDG. Clinical correlations suggested that EFS may be the consequence of temporal lobe seizures and not an epileptogenic entity. Cell density variables accounted for 65% of the variation in HCT2 and 45% of the variation in HCV. Hippocampal atrophy in HS is associated with neuronal cell depletion in CA1 and also hilus, CA2 and CA3. An increased HCT2 is associated with damage in CA1 and also hilus. This work validates pathologically the use of in vivo quantitative MRI of the hippocampus in the presurgical evaluation of TLE and longitudinal studies.

5.2. INTRODUCTION.

The aims of this study were 1. to establish a 3-D cell counting technique to quantify ND and GD of hippocampal subregions, 2. to examine the relationship between HCT2 relaxation times and MR-based HCV with GD and ND of different hippocampal subregions, and 3. to obtain a better clinico-pathological definition of the range of HS and EFS (Van Paesschen *et al.* 1996d) *(see discussion of HS and EFS, p 32 and following page).*

5.3. METHODS.

5.3.1. DESCRIPTION OF STUDY POPULATION.

Fifty-nine patients (23 men and 36 women; median age: 28 years, range: 17 to 51) with intractable localization-related epilepsy were included in the study. Median duration of epilepsy was 21 years (range: 4 to 42). These patients had a median of 3

CPSs (range: 0.25 to 30) a week in the year preceding surgery. Twenty-three (39%) had more than 10 SGS during their lifetime. All patients had interictal EEGs, ictal video-EEG recordings (n=58) , neuropsychological assessment and standard T1- and T2-weighted images of the brain on a 1.5T GE Signa MRI scanner. Fifty-eight patients had TLE and one had extratemporal epilepsy.

The body of one hippocampus of all these patients was available for neuropathological examination, and was obtained during surgery for epilepsy in 58 and at autopsy in one. Fifty-three patients had MRI-evidence of unilateral HS, that was diffuse in 52 and predominantly anterior in one. The hippocampus affected by HS was available for 52 of these patients, and the hippocampus contralateral to the side affected by HS was obtained at autopsy in one patient. The decision to operate on patients with unilateral HS was based on concordance of imaging, clinical, neurophysiological and neuropsychological data. Two patients had a structural lesion other than HS on MRI. One patient with TLE had a probable DNET near the hippocampus, which was removed during surgery, and one patient with a lifelong hemiparesis and extratemporal seizures due to a large middle cerebral artery infarct underwent a functional hemispherectomy including the hippocampus. Finally, four patients with normal MRI underwent anterior temporal lobe resection including the hippocampus on the basis of concordant clinical data, seizure semiology, interictal and ictal EEG, and interictal SPECT in one, and interictal PET in another. Median post-surgical follow-up of the operated patients was 738 days (range: 222 to 1825).

Six control hippocampi of persons (three men and three women; median age: 31 years, range: 14 to 52) who had died from non-neurological causes were obtained at autopsy.

5.3.2. QUANTITATIVE MR IMAGING.

5.3.2.1. HCT2 MAPPING: *see p 55.*

5.3.2.2. MR-BASED HCV MEASUREMENT: *see p 57.*

5.3.3. NEUROPATHOLOGY.

5.3.3.1. HISTOPATHOLOGICAL PREPARATION OF SPECIMENS. Hippocampi were removed en bloc during surgery and were fixed immediately in formalin where they

remained for 1 week. After fixation both the temporal lobe and hippocampus were cut in approximately 3 to 5 mm thick tissue blocks. The macroscopic appearance of the specimens were described and documented with photographs. Five to 7 µm thick sections of each block were stained with the haematoxylin and eosin (H&E) and luxol fast-blue/cresyl violet (LFB/CV) methods and with an antibody to glial fibrillary acidic protein (GFAP) for neuropathological assessment. For ND 20 µm thick sections of the hippocampus were stained with LFB/CV. The 20 µm section thickness was chosen because this was technically possible and allowed for comfortable margins for a counting box of 10 µm height. Tissue sections of 7 µm thickness stained with GFAP (Eng, 1985) and counterstained with solochrome cyanin (SC) were used for determining GD. The reason for using this method was that it considerably facilitated the recognition of hippocampal boundaries at high magnification. The 7 µm slide thickness was chosen for the following two reasons: 1.) this is the minimum height recommended for the 3-D cell counting technique (Williams, Rakic, 1988) and 2.) thicker tissue sections made it impossible to properly visualize reactive astrocytes and their delicate cytoplasmic processes because of the dense network of overlapping glial fibers present in severe cases of HS.

5.3.3.2. MICROSCOPIC QUALITATIVE ASSESSMENT OF THE HIPPOCAMPUS. The histological sections were used for neuropathological assessment and establishing the presence of HS and other pathological processes. HS was defined by neuronal cell loss and reactive gliosis affecting the hippocampal subregions in a typical distribution. EFS was defined as (mild) pyramidal cell loss and reactive gliosis confined to the hilus with preservation of the pyramidal cell layer of the CA1, CA2 and CA3 (Margerison, Corsellis, 1966; Armstrong, Bruton, 1987; Babb, Brown, 1987; Sagar, Oxbury, 1987; Bruton, 1988; Wyler *et al.* 1992).

5.3.3.3. DESCRIPTION OF THE MICROSCOPE AND THE COUNTING BOX. A direct 3-D counting method was used (Williams, Rakic, 1988; West, Gundersen, 1990). A Zeiss research microscope was fitted with a Zeiss drawing tube and a digital length gauge (Heidenhain MT12) with a sensitivity of 0.5 µm *(Figure 35, p 117)*. An oil immersion objective (magnification x100) with a numerical aperture of 1.3 and depth of field of 0.22 µm was used (Williams, Rakic, 1988). For measurement of ND in the CA1 hippocampal subregion (ND_{CA1}) and ND_{CA2}, CA3 and hilus a counting box of 90x90x10 µm and for ND of the GCDG (ND_{DG}) a counting box of 20x20 x10 µm was used. For GD a counting box of 50x50x5 µm was used for all hippocampal subregions. The main consideration in choosing a particular cross-sectional area for a counting box was the ease of counting cells, e.g. the median number of neurons per

counting box in control hippocampi was 1.5 for CA1, 2.3 for CA2, 1.4 for CA3, 1.0 for the hilus and 1.6 for the GCDG. For the neuronal counts, the bottom plane of the counting box was 5 µm above the bottom plane of the tissue section and for glial cell counts 0.5 to 1 µm.

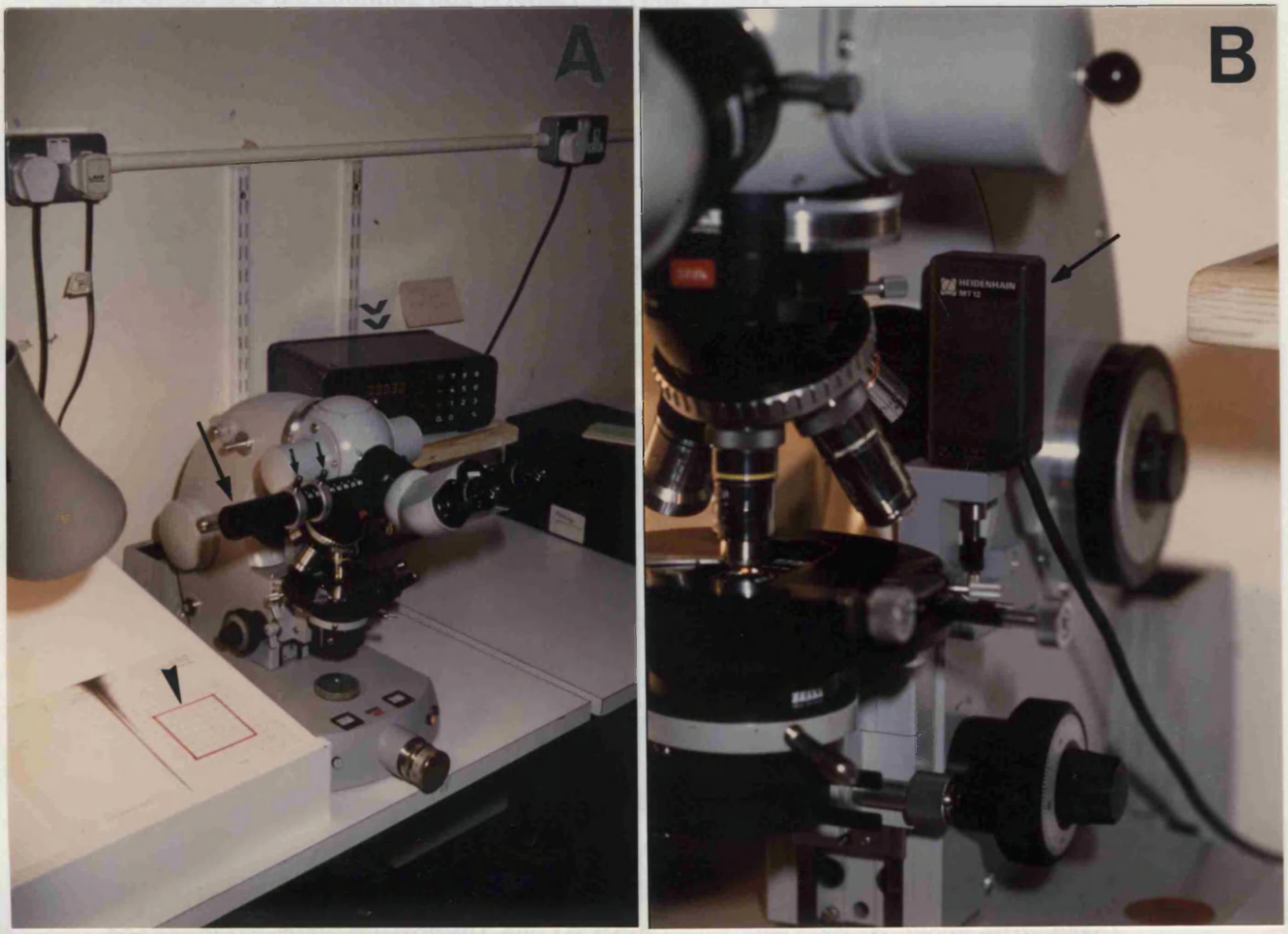

Figure 35 . Microscope, drawing tube, display unit and digital length gauge. A Zeiss microscope was fitted with a drawing tube (A, long arrow). A grid (A, single arrowhead) was projected via this drawing tube into the eye pieces of the microscope and provided 2 dimensions of the counting box. The calibration, which was checked before each measurement, was done by means of a slide micrometer and the calibration screws on the drawing tube (A, small arrows). A Heidenhain MT12 digital length gauge (B, long arrow) was attached to the stage and measured displacements of the stage (and hence in focal plane) in the Z-axis with an accuracy of 0.5 µm, which was displayed on a digital display unit (A, double arrow heads). This measurement of change in focal plane provided the third dimension of the counting box.

5.3.3.4. COUNTING RULES. By focusing from the bottom to top plane of the counting box, cells that came into focus were counted according to the counting rules recommended by Williams and Rakic (Williams, Rakic, 1988) and West et al (West, Gundersen, 1990). Cell nuclei completely inside the counting box were counted, and

cell nuclei completely outside the counting box were not counted. Cell nuclei that touched the forbidden planes i.e. bottom, front and left side of the counting box were also excluded. Cell nuclei that touched the top, right side and back side of the counting box were counted, provided they did not touch any of the forbidden planes, in- or outside the counting box (Gundersen *et al.* 1988).

5.3.3.5. DEFINITION OF COUNTED CELLS. A neuron was defined as a large cell, pyramidal-shaped in the CA1 to CA3 hippocampal subregions and multipolar or triangular-shaped in the hilus, with Nissl substance in the cytoplasm and a vesicular nucleus containing a prominent nucleolus. A granule cell of the dentate gyrus was a small and round cell. An astrocyte was defined as a cell with a nucleus and GFAP-positive cytoplasm and processes *(Figures 36, p 118; Figure 38, p 126)*.

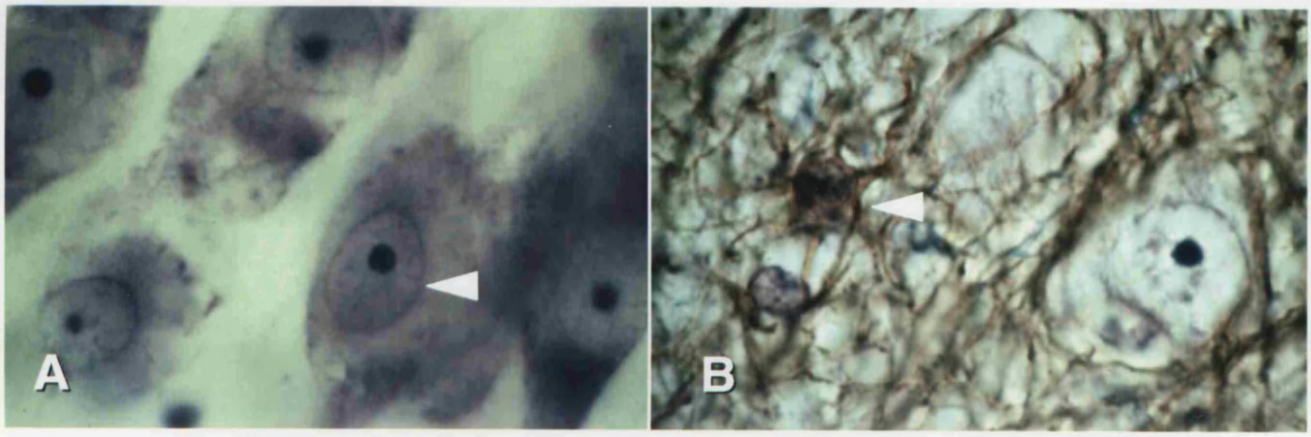

Figure 36 . Definition of counted cells. Pyramidal cells in the CA1 hippocampal subregion (A, white arrowhead), and GFAP-positive glial cells (B, white arrowhead).

5.3.3.6. DEFINITION OF THE NEURON CONTAINING LAYERS OF THE HIPPOCAMPUS. For the definition of the neuron containing layers of the hippocampus, descriptions of Lorente de Nó (Lorente de Nó, 1934), Duvernoy (Duvernoy, 1988) and Amaral and Insausti (Amaral, Insausti, 1990) were used. ND and GD were determined for the neuronal cell layer of CA1, CA2, CA3, hilus and the GCDG *(Figure 1, p 22; Figure 5, p 33)*. A section of the body of the hippocampus with the characteristic C-shaped appearance of the cell layers was used. The neuronal cell layers were identified by their position and shape, cell characteristics, and, in HS, by the typical distribution of damage. The pyramidal cell layer of the CA1 hippocampal subregion was situated between the subiculum and the CA2 hippocampal subregion medial to the temporal horn of the lateral ventricle. In the control hippocampus, the CA1 pyramidal cells were triangular and small, and less densely packed than those of the CA2. The

transition zone between subiculum and CA1, and CA1 and CA2 was characterized by a change in width of the pyramidal cell layer, easily identifiable for the CA1-CA2 transition, and somewhat arbitrary for the CA1-subiculum transition. In HS, the CA1 subregion with neuronal cell depletion was easily identified as it was situated between the preserved subiculum and relatively preserved CA2 subregion. The lateral borders of CA1 were well outlined on the LFB/CV and GFAP/SC stained sections by the myelin containing layers. The pyramidal cells of the CA2 subregion were large and densely packed, and the CA2 pyramidal cell layer was the narrowest of the hippocampus. The margin between the CA2 and CA3 subregions was not clearly discernible in the control hippocampus, and the CA3 hippocampal subregion in these cases was identified by its position at the curve or genu of the hippocampus, which is somewhat arbitrary. In HS, CA3 was usually more severely affected than CA2, which facilitated the delineation of the borders. Part of the CA3 was enclosed by the GCDG. The neuronal cells of the hilus were large, ovoid and more loosely arranged than in CA1, CA2 and CA3 hippocampal subregions. Lorente de Nó (Lorente de Nó, 1934) and Duvernoy (Duvernoy, 1988) considered the neuronal cells in the hilus of the dentate gyrus as part of the hippocampus proper and described it as the CA4 hippocampal subregion, separated by a thin polymorphic layer from the GCDG. This is a very complex region, and recent evidence suggests that this CA4 hippocampal subregion may be part of the dentate gyrus rather than the hippocampus proper, and a better name therefore may be hilus of the dentate gyrus (Amaral, 1978; Amaral, Insausti, 1990). For this study, hilar neurons were defined as those cells lying within the hilus of the dentate gyrus, avoiding cells of the CA3 entering the hilus, and staying away 1 counting box (i.e. 90 μm) from the GCDG, which coincides more or less with the polymorphic layer as defined by Lorente de Nó (Lorente de Nó, 1934) and Duvernoy (Duvernoy, 1988). The GCDG was an easily identifiable structure appearing as a small C-shaped ribbon of densely, small and round nerve cells, the granule cells, surrounding the hilus.

5.3.3.7. NUMBER OF COUNTING BOXES TO DETERMINE CELL DENSITY OF AN HIPPOCAMPAL SUBREGION. At the beginning of the quantitation it was necessary to determine the number of counting boxes required to determine cell densities in hippocampal subregions. For this purpose a pilot study was carried out using hippocampi of 4 control subjects in which neurons of the CA1 hippocampal subregion were counted using different number of counting boxes. ND_{CA1} of 4 control subjects were obtained using successively 200, 100, 50, 25, and 10 counting boxes and these measurements were carried out twice. The RC was similar for the sampling strategy using 50, 100 and 200 counting boxes, but was not as good for the strategies using 25

and 10 boxes *(Table 8, p 120)*. The conclusion of the pilot study was that 50 counting boxes gave an acceptable intrarater variability with no clear improvement with double or quadruple counting effort.

Number of counting boxes	Mean ND (n=4)	SD	mean Δ	RC
200	17045	1542	-2666	3437
100	18411	1975	-1966	4250
50	18271	2583	-2796	3044
25	19568	3227	-6505	10207
10	18339	4927	206	8203

Table 8. Pilot study to determine number of counting boxes to measure cell density in each hippocampal subregion. N counting boxes are the number of counting boxes used to determine ND_{CA1} in 4 control hippocampal sections. Mean ND is the sum of ([ND on first measurement + ND on second measurement]/2) divided by the total number of samples i.e. 4. SD is the standard deviation of this mean ND. Mean Δ is the mean difference between remeasurements i.e. ([ND on first measurement - ND on second measurement]/2) divided by the total number of samples i.e. 4. RC is 2 SD of this mean Δ, and indicates that 5% of remeasurements will fall outside this range.

5.3.3.8. SAMPLING STRATEGY. At magnification 4x the cross-sectional area of the CA1-CA3 hippocampal subregions and hilus were determined using a point counting technique (Gundersen *et al.* 1988). This cross-sectional area was divided by the cross-sectional area of one counting box, which gave the total number of counting boxes which could be fitted within a particular hippocampal field. In the above described pilot study it was decided to use 50 counting boxes to count one hippocampal subregion. The total number of counting boxes which could be fitted in a particular subregion were divided by 50 to obtain a number x (ranging from 1 to 15). This number x gave the ratio of boxes to count/boxes not to count (1/x). Then the counting box was placed at one end of a field. A random number y from 1 to x was generated and the counting box was moved y counting-box-distances in the field to obtain a non-biased starting point. From there, the counting box was moved in a systematic fashion counting every x^{th} counting box. The counting box was moved in successive rows or columns. At the border of the field, the box was moved in the opposite direction after moving it one box-distance perpendicular to the original direction of movement. Sampling and counting therefore was carried out in a systematic and unbiased way. Similarly, the width and length of the GCDG were estimated in order to sample the GCDG systematically. A counting box of 20x20x10 μm was placed randomly at one end of the GCDG and moved across the GCDG at 90 degrees to the long axis of the cell layer at that location. The counting boxes in the GCDG were placed side-by-side and all were counted. These "crossings" were repeated until 50 boxes were counted.

The number of crossings were at equal distances and in the order of 5-15 depending on the width of the GCDG. The whole width of the GCDG was counted, also when there was dispersion of granule cells (Houser *et al.* 1992; Mello *et al.* 1992). Determination of GD or ND for one hippocampal subregion took around 30 minutes.

5.3.3.9. INTRA-RATER TEST-RETEST REPEATABILITY OF NEURONAL CELL AND GLIAL CELL DENSITIES, AND THE RATIO OF GD/ND. ND and GD were determined twice for seventy-eight hippocampal subregions of controls and patients with an interval of weeks to months. To assess repeatability, graphs plotting the difference between the first and second measurement as a function of the mean of these two measurements were used (Bland, Altman, 1986). Because the scatter of the differences increased as the mean increased, the data were log-transformed, as suggested by Bland and Altman (Bland, Altman, 1986). For ND, GD and the ratio GD/ND the mean difference of the log-transformed data was 0, and the RC, i.e. 2 SD of the mean difference between repeated measurements was 20% for ND, 30% for GD and 35% for the ratio GD/ND. These repeatability studies indicated that 5% of individual ND and GD remeasurements were different from the first measurement by more than 20% and 30% respectively.

5.4. RESULTS.

5.4.1. QUALITATIVE ASSESSMENT OF THE RESECTED HIPPOCAMPI AND CLINICAL CORRELATIONS.

Six hippocampi showed EFS. Pre-operative MRI was normal in four of these cases and showed a large infarct in the middle cerebral artery distribution of the fifth patient. The sixth case was obtained at autopsy on the side contralateral to HS. Fifty-three hippocampi showed HS. Pre-operative MRI showed isolated HS in 52 of these patients, and in one patient a probable DNET near the hippocampus, which appeared normal on MRI.

Thirty-two of the 52 patients (62%) with isolated HS had a history of FC compared with none of the 4 patients with isolated EFS (p=0.03; Fisher's Exact test). The median age of onset of habitual epilepsy for the 52 patients with HS was 7 years (range: 0 to 30) compared with the median age of 15.5 years (range: 13 to 23) of the 4 patients with isolated EFS (Mann-Whitney U test: p=0.02). Forty-two patients with isolated HS had a post-surgical follow-up of more than one year (median: 952 days; range: 404 to 1825) and also the 4 patients with isolated EFS (median: 905 days; range: 387 to 1136). Thirty-four of these 42 patients (81%) with HS had been seizure free or had only experienced SPSs during the last year of follow-up compared to only one of four patients (25%) with isolated EFS (p=0.04; Fisher's Exact test).

5.4.2. QUANTITATIVE HIPPOCAMPAL MRI.

The median HCT2 of the resected hippocampi with HS (n=53) was 125 msec (range: 106 to 144 msec [Nl: ≤ 108 msec]). Two patients with HS had a normal HCT2, one with a DNET (MR-based HCV not available) and another patient with predominantly anterior atrophy *(Figure 37, p 123)*. The other 30 patients with HS who had MR-based HCV measurements all had diffuse atrophy affecting the whole length of the hippocampus and an increased HCT2 *(see Figure 21, p 82; Figure 22, p 83, but note that an SPGR-based HCV measurement protocol was used in this study)*. The median HCT2 (n=5) of patients with EFS was 107 msec (range: 103 to 108 msec) *(Figure 20, p 81)*. The median HCV (n=31) of patients with HS was 3678 mm^3 (range: 2407 to 5037 [Nl: > 4348 mm^3]). The HCV of 4 patients with HS was within normal limits, i.e. > 4348 mm^3. The median HCVR of patients with HS was 0.70 (range: 0.46 to 0.82 [Nl: ≥ 0.87]). HCV and HCVR for two patients with EFS were normal.

Figure 37: *see p 124.* HS and normal HCT2. Patient was a 34 year old woman with a history of prolonged FC lasting more than 40 minutes at the age of 9 months. A sister and a niece also had a history of FCs. Habitual epilepsy started at the age of 23 years and was refractory to medication. She had on average two CPS a week, and had a total of ten SGS during her lifetime. A clear left antero-temporal focus was demonstrated on interictal and ictal EEGs. She underwent a left temporal lobe resection including the hippocampus, and has been seizure free for more than two years. A graph of hippocampal cross-sectional areas (A) and HCT2 map (B) are shown. A. Graph plotting hippocampal cross-sectional area (mm^2) as a function of section position. The graph demonstrates that there was atrophy of the left hippocampus, predominantly affecting the head. The black circles represent the right hippocampus and the open squares the left hippocampus. B. Coronal 8 mm thick T2 map of the hippocampal body. The left sided hippocampal atrophy is visible on the HCT2 map, and corresponds approximately with section position 6-8 on the HCV distribution graph. The HCT2 values were normal. HCVR(L/R) = 0.67 (Nl $\geq$ 0.87); HCV right = 5431 mm^3, HCV left = 3609 mm^3 (Nl: $\geq$ 4348 mm^3); HCT2 right = 104 msec, HCT2 left = 106 msec (Nl $\leq$ 108 msec). The histological section of the body of the hippocampus (not shown) corresponded to the level of the HCT2 map. There was classical HS with marked dispersion of the GCDG. GD/ND_{CA1} = 91,429/9,652 = 9.5; GD/ND_{CA2} = 17,959/16,296 = 1.1; GD/ND_{CA3} = 84,694/7,901 = 10.7; GD/ND_{hilus} = 73,469/3951 = 18.6; GD/ND_{DG}= 54,400/155,000 = 0.35 *(see Table 9, p 125 for comparison).* [Hospital number: QSC13829].

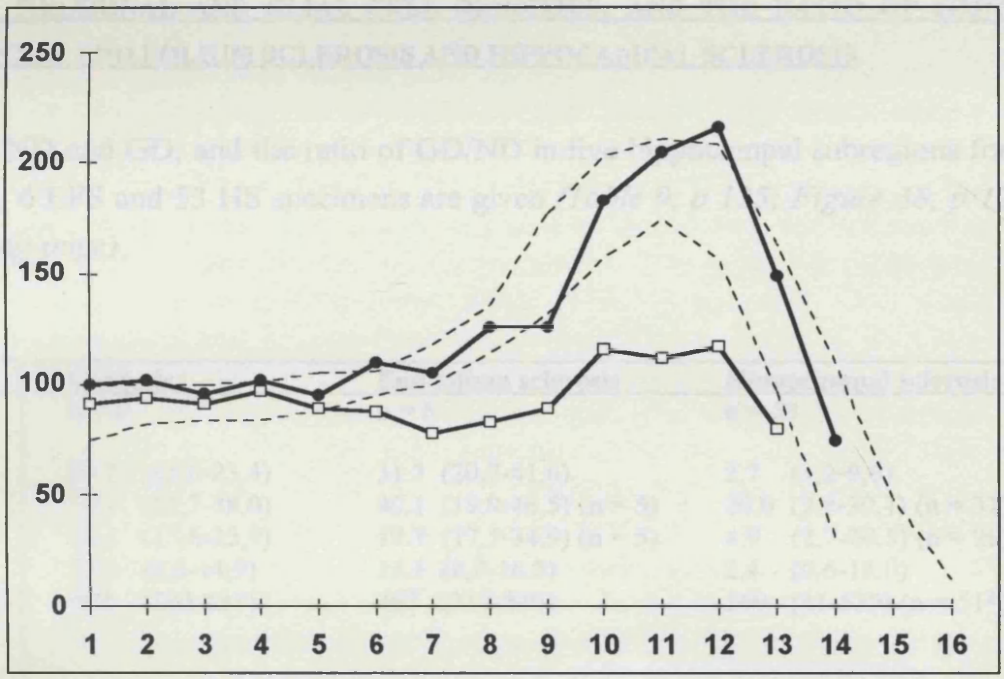

A

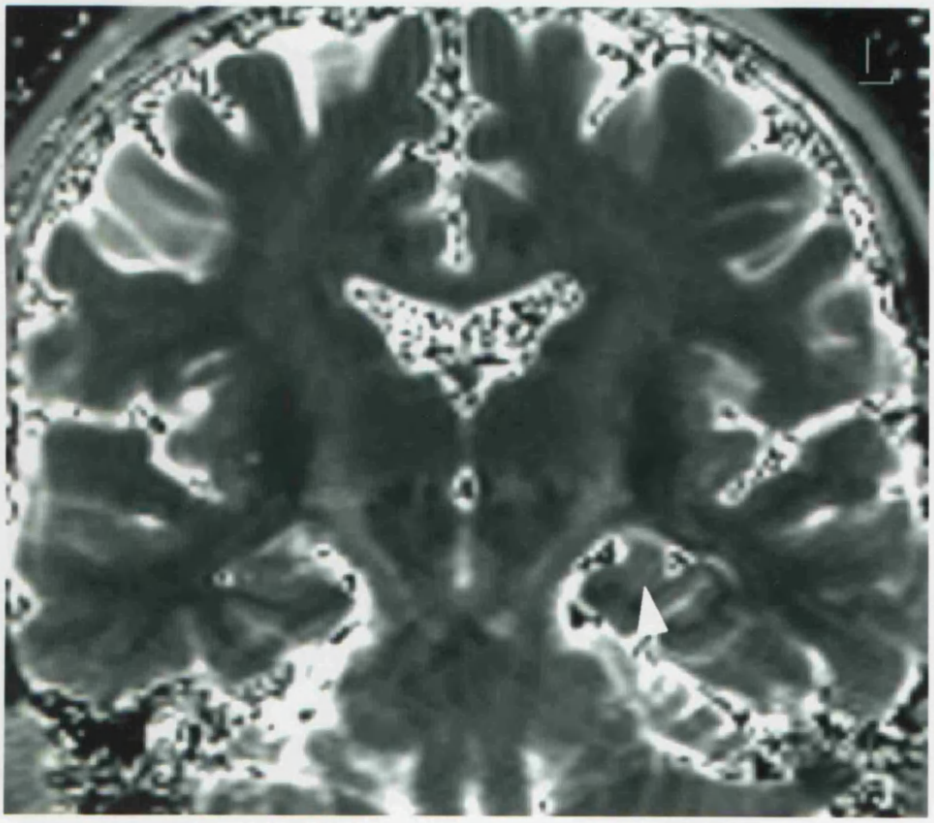

B

5.4.3. NEURONAL AND GLIAL CELL DENSITIES, AND THE RATIO OF GD/ND IN CONTROLS, END FOLIUM SCLEROSIS AND HIPPOCAMPAL SCLEROSIS.

ND and GD, and the ratio of GD/ND in five hippocampal subregions for the 6 control, 6 EFS and 53 HS specimens are given *(Table 9, p 125; Figure 38, p 126 and following page)*.

	Controls	End folium sclerosis	Hippocampal sclerosis
	n = 6	n = 6	n = 53
ND			
CA1	20.3 (15,6-23,4)	31.3 (20,7-41,6)	2.7 (1,2-9,6)
CA2	30.2 (25,7-38,0)	40.1 (19,9-46,5) (n = 5)	20.0 (9,8-30,4) (n = 31)
CA3	16.4 (15,6-25,9)	19.7 (17,5-34,9) (n = 5)	4.9 (2,7-20,5) (n = 29)
H	12.0 (8,6-14,9)	11.1 (8,7-16,8)	2.4 (0,6-18,0)
GCDG	482 (295-635)	407 (342-540)	160 (41-530) (n = 51*)
GD			
CA1	1.4 (0,5-16,0)	10.9 (9,6-11,2)	134 (43-205)
CA2	6.1 (1,0-9,6)	12.8 (6,8-24,4) (n = 5)	38 (3-110) (n = 31)
CA3	16.6 (3,0-25,6)	29.3 (3,9-38,4) (n = 5)	62 (3-144) (n = 29)
H	25.1 (16,3-32,5)	53.0 (40,0-64,0)	89 (36-176)
GCDG	14.6 (1,0-32,0)	40.6 (30,4-77,1)	54 (21-152) (n = 51*)
GD/ND			
CA1	0.09 (0.02-0.69)	0.34 (0.25-0.54)	52 (9-115)
CA2	0.18 (0.04-0.30)	0.40 (0.23-0.53)	1.8 (0.2 - 4.0)
CA3	1.01 (0.14-1.09)	1.10 (0.20-1.67)	11.3 (0.2-198.5)
H	2.27 (1.09-3.33)	4.70 (2.95-5.89)	36 (6-232)
GCDG	0.028 (0.002-0.108)	0.11 (0.06-0.20)	0.35 (0.08-1.64)

Table 9. ND, GD and the ratio of GD/ND of 5 hippocampal subregions for control, EFS, and HS specimens. The CA2 and CA3 hippocampal subregions were available for 5 EFS specimens, and 31 and 29 HS specimens respectively. In the other specimens, those regions were damaged during surgical removal and therefore not available for quantitative neuropathological studies. In 2 HS specimens, the GCDG was almost completely destroyed and technically difficult to count (*). ND and GD are number of cells x $10^3/mm^3$. Cell densities and ratio's are expressed as median (range).

Boxplots of the logarithm (log) of the GD/ND for the five hippocampal subregions of controls, EFS and HS are shown *(Figure 39, p 128 and following page)*. The HS group differed significantly from the controls in all hippocampal subregions, and from the EFS in all hippocampal subregions except for the GCDG. The EFS group differed significantly from the control group only in the GCDG *(The Gabriel statistic is given in Table 10, p 130)*.

Figure 38: *see p 127.* Neuropathology of a control hippocampus, EFS, and HS. Control hippocampus (1), EFS (2) and HS (3), overview (A), CA1 hippocampal subregion (B), hilus (C) and GCDG (D). All sections were 7 μm thick and GFAP/CV stained, as used for GD determination in this study. The magnification of the overviews was approximately x13, and for all other views approximately x1,300. In the control specimen (1A), the hilus (H) contained more GFAP staining cells than the other hippocampal subregions, which was clearly visible as a brown staining of the hilus, more marked near the GCDG (arrowhead). The same but more pronounced pattern was seen in the EFS specimen (2A). The HS specimen (3A) was atrophic compared to control and EFS specimens, with a striking collapse of the CA1 (arrow) and a marked GFAP staining of the neuronal layers of the hippocampus, except CA2 (arrowhead). At high magnification, pyramidal cells (arrows) appeared well preserved in the control (1B) and EFS (2B) CA1 subregions, but depleted in HS (3B). Notice that the CA1 pyramidal cells of the EFS specimen were dark, which is a surgical artifact. The nucleolus of these dark neurons, easily seen in 1B (arrows), could be visualized with bright illumination. No GFAP-positive glial cells could be seen in this photograph of control (1B) and EFS (1C) CA1. In the HS CA1 subregion (3B), on the other hand, there was chronic, dense reactive gliosis. In 3B, two GFAP-positive glial cell were in focus (arrowheads). In both the control (1C) and EFS (2C) hilus, neuronal cells (arrows) and GFAP-positive cells (arrowheads) were readily identified. These GFAP-positive astrocytes in the control hilus were small, had finer processes and less GFAP staining compared with the reactive astrocytes in the EFS hilus. In the HS hilus (3C), no neuronal cells were identified, and there was chronic dense reactive gliosis (two GFAP-positive glial cells were in focus (arrowheads). The high magnification views of the GCDG (D) showed that only a few granule cells were in focus, which illustrated the narrow field of depth of an oil-immersion lens (arrows in D). In the control GCDG (1D), a few GFAP-positive fibers but no glial cells could be seen. On the other hand, in the EFS (2D) and HS (3D) GCDG, large numbers of GFAP-positive fibers and some prominent reactive astrocytes (arrowheads) were present. Note that the EFS specimen is the same as in Figure 20, p 81 and the HS specimen the same as in Figure 22, p 83.

Fig 38

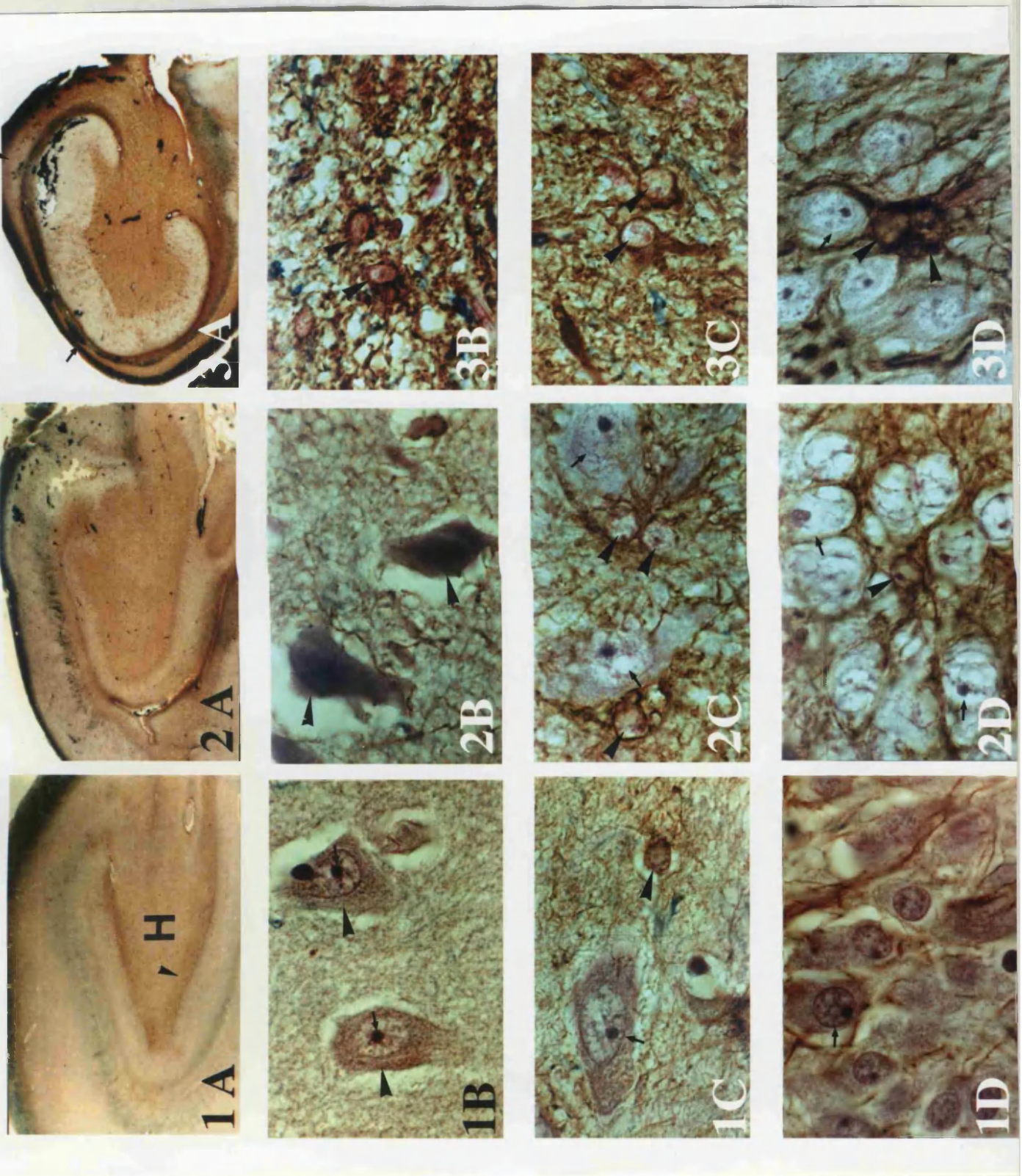

Figure 39: *see p 129*. Boxplots of the logarithm of the GD/ND of five hippocampal subregions of control, EFS and HS specimens. A boxplot shows the median, 25^{th} and 75^{th} percentile, and the largest and smallest observed values that are not outliers. N indicates the number of specimens for which the hippocampal subregion was counted. The boxplots illustrate the typical distribution of damage in HS, with the CA1 as the most severely affected hippocampal subregion, followed by the hilus of the dentate gyrus and CA3 hippocampal subregion, and with less damage to the CA2 hippocampal subregion and the GCDG.

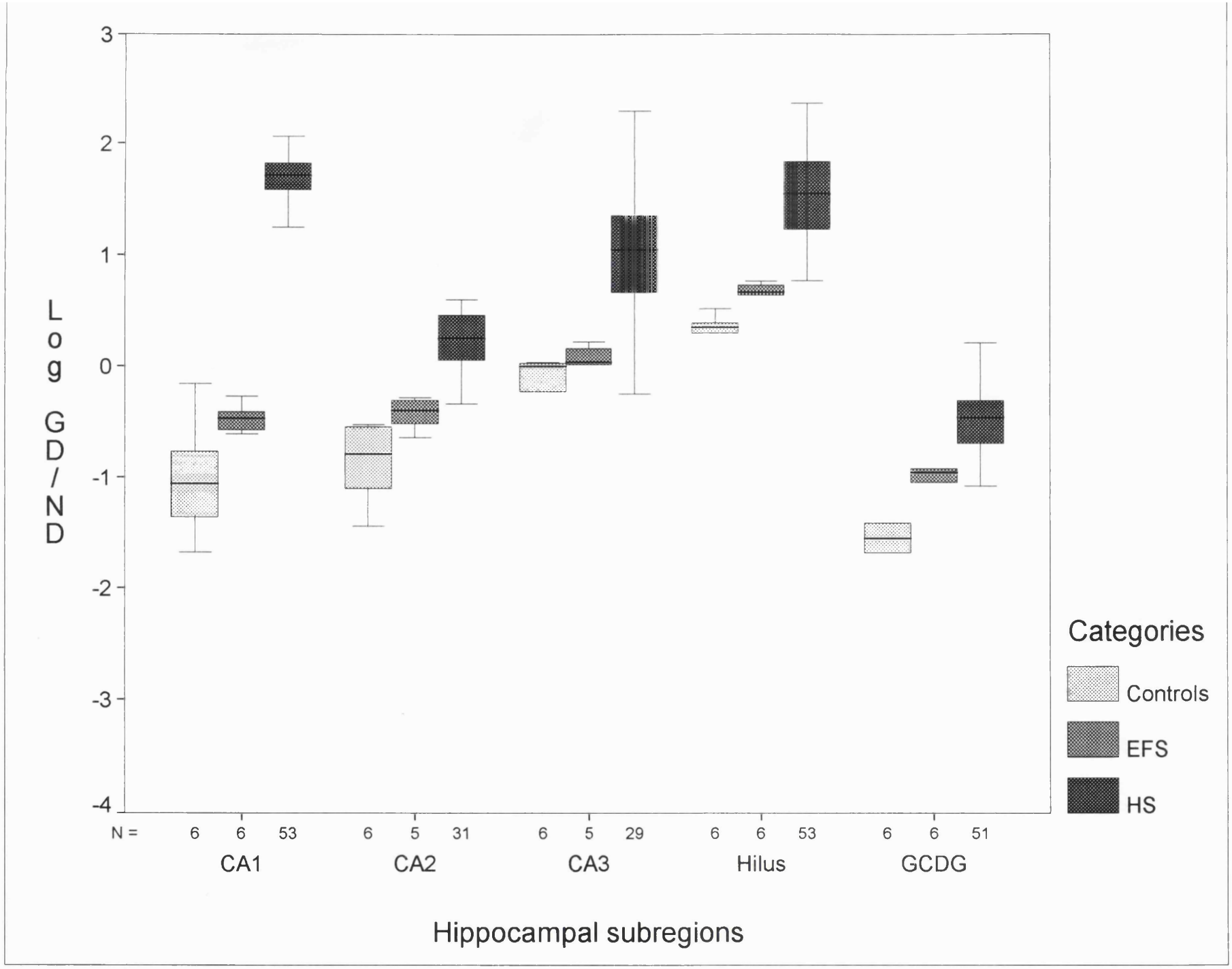
3
2
1
0
-1
-2
-3
-4
Log GD/ND
N = 6 6 53 6 5 31 6 5 29 6 6 53 6 6 51
CA1
CA2
CA3
Hilus
GCDG
Hippocampal subregions
Categories
Controls
EFS
HS

Categories	Single variables CA1	CA2	CA3	hilus	GCDG
Controls-EFS-HS	**.93****	**.64****	**.45****	**.68****	**.61****
Controls-EFS	.18	.13	.00	.09	**.24***
Controls-HS	**.91****	**.61****	**.36****	**.64****	**.60****
EFS-HS	**.84****	**.32****	**.28****	**.42****	.16

Table 10. Single variable maximum characteristic root statistics (Gabriel, 1968) for all subsets of groups, calculated from the log GD/ND ratios for each of the 5 hippocampal subregions *(see Methods, p 72)*. A value of 0.22 or more is significant at the 0.05 level (indicated by *), while a value of 0.28 or more is significant at the 0.01 level (indicated by **). The analysis is performed using only those subjects for which the cell count data are complete, i.e. 6 control, 5 EFS, and 25 HS specimens. All patterns of differences between the three groups achieve significance on at least one of the single variables. Consequently, the table is restricted to the single variable results.

5.4.4. HIPPOCAMPAL SUBREGIONS THAT DETERMINE HIPPOCAMPAL T2 AND VOLUME.

Correlations of HCT2 and HCV with log GD/ND of each hippocampal subregion are shown *(Table 11, p 131)* together with a number of relevant partial correlations. The magnitude of the correlations indicates that no single cell density variable accounts for the total variance in the MRI parameters. For example, the largest correlation coefficient of 0.77 which was between HCT2 and log GD/ND_{CA1} indicates that only approximately 60% of the variance in HCT2 is explained. A regression calculation from all five hippocampal subregions accounted for 65% of the variation in HCT2. Similarly, the largest correlation coefficient obtained for HCV was between HCV and log GD/ND_{CA1}. The value obtained was -0.59, indicating that only 34% of the variance in HCV is accounted for by CA1. Inclusion of all five cell density variables accounted for 45% of the total variance in HCV.

	log GD/ND	r	r partialling out log $GD/ND_{CA1, hilus}$	r partialling out log $GD/ND_{CA2,}$ CA3, GCDG
HCT2	CA1	0.77	-	0.72
	CA2	0.45	0.006	-
	CA3	0.50	0.2	-
	hilus	0.51	-	0.35
	GCDG	0.11	-0.28	-
HCV	CA1	-0.59	-	-0.36
	CA2	-0.53	-0.35	-
	CA3	-0.34	-0.11	-
	hilus	-0.47	-	-0.33
	GCDG	-0.24	0.17	-

Table 11. Correlations between quantitative hippocampal MRI and quantitative hippocampal neuropathology. Only complete datasets were used in these calculations (HCT2: n=29 [4 EFS and 25 HS] and HCV: n=19 [2 EFS and 17 HS]). The first column gives the correlation coefficients (r) between HCT2 or HCV and log GD/ND in the 5 hippocampal subregions. The second column contains partial correlation coefficients between HCT2 or HCV and log GD/ND obtained by partialling out log GD/ND_{CA1} and log GD/ND_{hilus}. The third column contains partial correlation coefficients between HCT2 or HCV and log GD/ND obtained by partialling out log $GD/ND_{CA2,}$ CA3 and GCDG

Factor analysis was used in order to elucidate the relationship between the quantitative hippocampal MR findings and the neuropathological variables. Factor analysis seeks to find an explanation for the pattern of correlations among a set of observed variables in terms of a number of factors or underlying latent processes which are not directly measurable. An initial analysis was performed using the log GD/ND ratios on their own. A number of models were investigated and the most satisfactory model was that in which three processes appear to underlie the observed changes in the cell density ratios *(Table 12, p 132)*. According to this model the first latent process (P1) mainly affects regions CA1 and the hilus, while a second process (P2) predominantly affects CA2 and CA3. The third process (P3) affects the GCDG and has relatively little effect on the remaining regions.

log GD/ND	Process 1	Process 2	Process 3
CA1	**0.80**	0.41	0.33
CA2	0.44	**0.75**	0.37
CA3	0.31	**0.90**	0.17
hilus	**0.81**	0.37	0.35
GCDG	0.36	0.25	**0.90**

Table 12. Three-factor model pattern loadings. The table gives the pattern loadings obtained from a three-factor model (Varimax solution). Each loading is equal to the correlation between the observed variable (i.e. neuropathological variable) and the factor or latent process. High loadings are shown in bold. According to this factor solution, three latent processes drive the observed hippocampal changes, the first mainly affecting CA1 and hilus, the second having the greatest effect on CA2 and CA3, while the third process predominantly affects the GCDG.

Using this model, the relationship between quantitative hippocampal MRI and neuropathological variables was examined. Correlations were obtained between the MRI parameters and the three underlying processes. The results suggest that HCT2 changes are mainly associated with P1, while HCV change, although predominantly driven by P1, also has some contribution from P2. These conclusions are reflected in the pattern of (partial) correlations between HCT2 or HCV and neuropathological variables *(Table 11, p 131)*. The following observations can be made: firstly, the relatively high correlation between HCT2 and log GD/ND_{CA1}, together with the observation that this is not abolished by partialling out the variables log GD/ND_{CA2}, CA3, and GCDG is consistent with a model in which both HCT2 and CA1 changes are driven predominantly by P1, and that this process has relatively less effect on CA2, CA3 and GCDG. Secondly, the lack of correlation between HCT2 and log GD/ND_{GCDG}, and between HCV and log GD/ND_{GCDG} is consistent with the

model, since GCDG changes are driven mainly by P3, while this process has little effect on the MRI variables. Finally, the pattern of correlations and partial correlations between HCT2 and log $GD/ND_{CA1, CA2, CA3 \text{ and hilus}}$ is different to that observed with HCV. In particular, the correlations between HCV and both log GD/ND_{CA2} and log GD/ND_{CA3} are less affected than the corresponding HCT2 correlations when log GD/ND_{CA1} and log GD/ND_{hilus} are partialled out. This arises because P2 affects HCV, and log $GD/ND_{CA2 \text{ and } CA3}$, but has little effect on HCT2. The P2 driven changes in HCV remain after partialling out log GD/ND_{CA1} and hilus.

These observations are summarized in the latent processes model outline *(Table 13, p 133)* that deals with the strongest associations (corresponding to the larger loadings *(Table 12, p 132)*) between the observed variables and the underlying process.

Process 1	Process 2	Process 3	Unique process
HCT2	HCV	GCDG	HCT2
HCV	CA2, CA3		HCV
CA1, H			CA1, CA2, CA3, H, GCDG

Table 13. This table gives an outline of a factor model for the hippocampal changes that occur in TLE. This outline is derived from the factor solution obtained from an analysis of the neuropathological variables, together with the pattern of the HCT2 and HCV correlations and partial correlations given in Table 3. Processes 1, 2 and 3 are latent processes that, in part, underlie the observed changes in HCT2, HCV and neuropathological variables. Listed under each process are the MRI parameters together with the neuropathological variables that are most tightly coupled with the process. Unique process refers to all those processes that are responsible for the unexplained variation in each of the observed variables. HCT2: hippocampal T2, HCV: hippocampal volume, H: hilus, GCDG: granule cell layer of dentate gyrus.

5.4.5. CONTRIBUTIONS OF NEURONAL AND GLIAL CELL DENSITIES OF THE CA1 HIPPOCAMPAL SUBREGION TO HCT2.

The correlation coefficient between HCT2 and $1/ND_{CA1}$ was 0.75 ($p<0.001$), and HCT2 and GD_{CA1} 0.44 ($p= 0.001$). However, the partial correlation coefficient between HCT2 and GD_{CA1} partialling out $1/ND_{CA1}$ was 0.12 (p = NS), and between HCT2 and $1/ND_{CA1}$ partialling out GD_{CA1} 0.68 ($p < 0.001$), indicating that in the sample of this study the high correlation between HCT2 and GD/ND_{CA1} was related to ND *(Figure 40, p 134).*

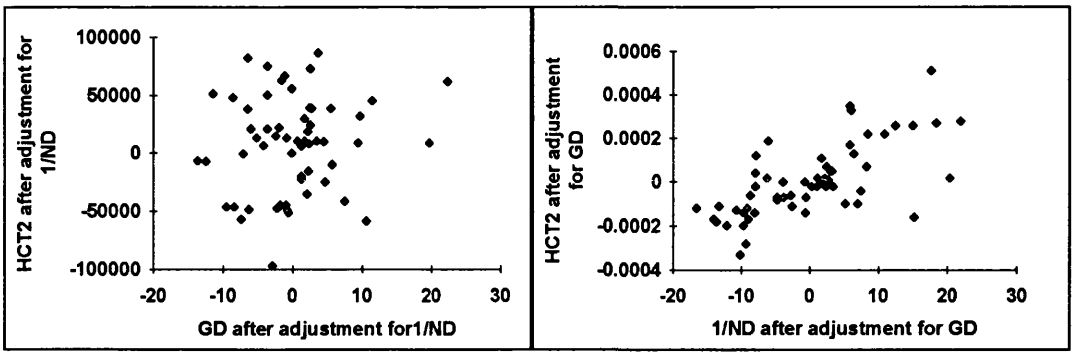

A B

Figure 40. Correlation between HCT2 and GD_{CA1} partialling out $1/ND_{CA1}$ (A) and HCT2 and $1/ND_{CA1}$ partialling out GD_{CA1} (B). The partial correlation coefficient between HCT2 and GD_{CA1} controlling for $1/ND_{CA1}$ is 0.12 (p=NS) (A). This is obtained by plotting the residuals of two regression equations, the first predicting HCT2 from $1/ND_{CA1}$, the second predicting GD_{CA1} from $1/ND_{CA1}$. The partial correlation coefficient between HCT2 and $1/ND_{CA1}$ controlling for GD_{CA1} is 0.68 ($p< 0.001$). This is obtained by plotting the residuals of two regression equations, the first predicting HCT2 from GD_{CA1}, the second predicting $1/ND_{CA1}$ from GD_{CA1}.

5.5. DISCUSSION.

5.5.1. REACTIVE GLIOSIS.

Reactive gliosis (Hirano, 1994) is a response to nerve cell injury and is characterized by reactive astrocytes that are distinguished from resting astrocytes by their large size (Krishnan *et al.* 1994), longer and thicker processes, increased synthesis of GFAP (Eng, 1988) (the major glial intermediate filament protein (Eng, 1985)), and production of neuropeptides, cytokines and growth factors (McMillan *et al.* 1994). Reactive gliosis may be the most sensitive index of neuronal damage in vivo (O'Callaghan, 1993). GFAP has been shown to be a sensitive quantitative marker of neuronal cell injury and is used to screen for selective vulnerability of neuronal cell populations (Brock, O'Callaghan, 1987; Norton *et al.* 1992; O'Callaghan, 1993). The typical distribution of hippocampal damage in HS, illustrated in the present study, is believed to be related to selective vulnerability of hippocampal neuronal populations to glutamate-mediated excitotoxicity (Gloor, 1992b). The use of GD/ND of each hippocampal subregion may therefore be a good indicator of the amount of damage to a given hippocampal subregion. GD/ND is dimensionless and has the advantage of being independent of changes in reference volume due to disease processes, such as HS and tissue processing (Haug, 1986), and can be used to quantify hippocampal specimens that were processed in different ways, as were most of the control specimens in this study.

5.5.2. THE REFERENCE TRAP.

Equating ND with total number of neuronal cells and a decrease in ND with loss of neuronal cells without knowing the reference volume in which the neurons were counted may lead to false conclusions (Brændgaard, Gundersen, 1986; West, Gundersen, 1990; Oorschot, 1994; Coggeshall, Lekan, 1996; Saper, 1996). ND_{GCDG} of controls in the present study was 24x larger than ND_{CA1}, yet the total number of CA1 pyramidal cells in humans has been reported to be larger than that of granule cells in the dentate gyrus (West, Gundersen, 1990). ND_{CA1} in the EFS specimens in this study was 50% higher than in the control specimens, which is best explained by a larger degree of tissue shrinkage in the EFS specimens. Granule cell dispersion is frequently observed in HS (Houser *et al.* 1992; Mello *et al.* 1992), which increases the reference volume and hence decreases ND_{GCDG}. From this density measure, therefore, it is unclear whether there is granule cell loss.

5.5.3. 2D VERSUS 3D COUNTING TECHNIQUES.

The median control ND_{GCDG} determined with the 3-D technique in the present study was around $5x10^5$ cells/mm^3 and higher than that of the previously reported 2-D technique, which was around $3x10^5$ cells/mm^3 (Dam, 1979; Babb *et al.* 1984a; Kim *et al.* 1990; Lee *et al.* 1995), which can be explained by the better resolution of the densely packed granule cells provided by the high magnification used in the 3-D technique.

5.5.4. END FOLIUM SCLEROSIS: A CLINICO-PATHOLOGICAL ENTITY ?

EFS was present in 6 specimens in this study, two in association with another lesion, and four as an isolated finding. These four patients with isolated EFS had later onset of habitual epilepsy, no history of early childhood convulsions, and poorer surgical outcome compared with patients with HS, corroborating previous observations *(see sclerosis of other areas of the hippocampus, p 34)* (Armstrong, Bruton, 1987). In control hippocampi the hilus contained more GFAP-positive astrocytes than other hippocampal subregions, and the GD/ND_{hilus} was 25 times higher than the GD/ND_{CA1}, a finding which should be taken into account when evaluating hippocampi resected from patients with intractable TLE. In EFS, GD/ND did not differ significantly from controls in CA1, CA2, CA3 and the hilus. Qualitatively, however, the EFS specimens appeared more gliotic than control hippocampi. In conclusion, there is reactive gliosis in the EFS specimens with hypertrophy of existing astrocytes and no significant neuronal cell loss in CA1, CA2, CA3 and the hilus. This supports the view that hypertrophy, and not hyperplasia, may be the dominant response of astrocytes to neuronal injury and may occur with neuronal injury that is not apparent on routine histology (O'Callaghan, 1993).

The difference in GD/ND_{GCDG} between controls and EFS specimens was significant and due to an increase in GFAP-positive glial cells in the GCDG in the EFS group. Whether there was a concomitant loss of granule cells is not clear from density measures. Since the GCDG was the only region which differed from controls in these patients, dentate sclerosis (DS) may be an appropriate name to describe the neuropathological changes in the specimens which were called EFS in this study. From the clinical correlations in this study and observations reported by Armstrong and Bruton (Armstrong, Bruton, 1987) it appears that EFS or DS may be a

consequence, rather than a cause of TLE. The observation that EFS is not visible on MRI *(see quantitative hippocampal MRI in EFS, p 79)* (Van Paesschen *et al.* 1995d) is consistent with a model in which changes in the GCDG are not associated with changes on MRI.

5.5.5. CORRELATION OF HCT2 WITH QUANTITATIVE NEUROPATHOLOGY.

An increased HCT2 signal is characteristic of HS, and can be seen throughout the hippocampus on visual inspection (Kuzniecky *et al.* 1987; Berkovic *et al.* 1991; Jackson *et al.* 1993a). This has been confirmed on measurement of HCT2 signal on HCT2 maps using a circular ROI which covers all hippocampal subregions (Jackson *et al.* 1993b; Grünewald *et al.* 1994a; Van Paesschen *et al.* 1995d; Pitkänen *et al.* 1996; Van Paesschen *et al.* 1997). Also, the HCT2 signal has been shown to be increased on a pixel by pixel basis (Jackson *et al.* 1993b). The visibility of the increased signal on a FLAIR image and the observation that HS with increased T2 signal can have a HCV within the normal range (Van Paesschen *et al.* 1997) indicate that this increased signal is due to pathological changes, and not due to partial volume effects of an atrophic hippocampus with CSF, which should be minimal with the orientation of the HCT2 map at right angles to the long axis of the hippocampus.

The present pathological study should be ideal to elucidate the pathological nature of the HCT2 changes in HS, since a tissue section was examined in the same position and orientation as the HCT2 map in vivo. From the (partial) correlations of HCT2 with quantitative hippocampal neuropathology, it appears that both HCT2 and pathological changes in the CA1 and hilus are affected by a process that has less effect on pathological changes in the CA2 and CA3. GD/ND changes in themselves cannot be directly causative of increased HCT2 since some of the HCT2 partial correlation coefficients are small. Therefore the high correlation between HCT2 and pathological changes in CA1 and hilus indicate the presence of an underlying but unidentified abnormality that causes both GD/ND and the HCT2 to increase in HS. This pathological abnormality could be GFAP content (O'Callaghan, 1993), density of glial cell processes (Hawrylak *et al.* 1993), size of glial cells (Krishnan *et al.* 1994) or relative increase in extracellular space.

Although GD/ND is a better index than cell density measures, there is information to be obtained by looking at the relationship of GD_{CA1} and ND_{CA1} with HCT2. Increased T2 relaxation time is caused by increased water mobility, and it has been postulated previously that this may be in some way associated with gliosis.

However, in the present study HCT2 correlated more strongly with ND than GD, and did not correlate with the latter after partialling out ND. Therefore, the hypothesis that HCT2 reflects gliosis, at least with GD as a measure, can not be confirmed (Kuzniecky *et al.* 1987; Jackson *et al.* 1993a). This might be due to the absence of a sufficiently wide range of degrees of gliosis in the available samples, resulting in an inability to identify any correlation between HCT2 and GD. This situation arises because a majority of the patients in this study were operated on because they had evidence of HS with atrophy and a high T2 signal on MRI, with concordant functional tests, which may have biased the study towards more severe forms of HS. For this reason, a majority of specimens for which HCT2 data were available had severe gliosis. HCT2 data were not available for control hippocampi. Alternatively, it is possible that glial cell body density is not a good measure of gliosis in this context, as discussed above.

Two patients with HS had a GD/ND_{CA1} of 9 and had a normal HCT2. This indicates that a normal HCT2, as defined in this study, does not rule out a diagnosis of HS. In one of these two patients, there was predominantly anterior atrophy. Although hippocampal asymmetry was still visible on the HCT2 map, the most severely affected part of the hippocampus was not covered by the HCT2 map (Van Paesschen *et al.* 1997) *(see Chapter 4)*.

5.5.6. CORRELATION OF MR-BASED HIPPOCAMPAL VOLUME WITH QUANTITATIVE NEUROPATHOLOGY.

MRI-based HCV has been reported to correlate with NDs of several hippocampal subregions (Bronen *et al.* 1991; Lencz *et al.* 1992; Lee *et al.* 1995). The quantitative neuropathological measures in the present study accounted for only 45% of the variation in MR-based HCV. All but two patients who had MR-based HCV measurements, however, were selected because unilateral atrophy was present. This selection bias towards HS could obscure a correlation between MR-based HCV and quantitative neuropathology. Also, the GD/ND ratios in one hippocampal section may not be the best pathological correlates of total HCV. Total number of neurons per hippocampal subregion may better correlate with MR-based HCV, but could not be obtained because the hippocampus was resected only partially (West, Gundersen, 1990).

5.5.7. CONCLUSION.

Whilst the MRI parameters HCV and HCT2 are not entirely explained by the measured pathological variables of ND and GD in the hippocampal subregions, it can be concluded that quantitative HCT2 relaxation times and volumes are related to the severity of HS. These quantitative hippocampal MRI measures can be used in the presurgical evaluation of patients with intractable TLE, and for the assessment of progressive hippocampal changes in longitudinal studies.

CHAPTER VI. A QUANTITATIVE HIPPOCAMPAL MRI STUDY OF NEWLY DIAGNOSED LOCALIZATION-RELATED EPILEPSIES IN ADULTS: ETIOLOGY AND EARLY PROGNOSIS.

6.1. ABSTRACT.

Sixty-three adult patients with newly diagnosed localization-related epilepsy underwent a MRI scan of the brain including hippocampal quantitation. Seventy-six percent of patients had normal MRI findings, 10% had HS and 14% had MRI abnormalities other than HS. Patients with HS had a worse early prognosis than patients with other MRI findings with respect to seizures. The extent of hippocampal damage appeared an important mediating factor in frequency of seizures, secondary generalization, and resistance to AED treatment. Because MRI provides prognostic information and can alter management of the individual patient, a high resolution MRI scan should be obtained in all patients with newly diagnosed localization-related epilepsy.

6.2. INTRODUCTION.

The prognosis for seizure control in newly diagnosed epilepsy is good for about two thirds of patients, and is largely established during the first 2-3 years of AED treatment (Annegers *et al.* 1979; Shorvon, Reynolds, 1982; Goodridge, Shorvon, 1983; Elwes *et al.* 1984; Beghi *et al.* 1988; Sander, 1993; Cockerell *et al.* 1995). Remission of epilepsy in around 70% of cases explains the discrepancy between the cumulative incidence of epilepsy which is around 4% (Crombie *et al.* 1960; Juul-Jensen, Foldspang, 1983; Hauser *et al.* 1993) and the prevalence rate of active epilepsy which is about 0.5% (Hauser, Kurland, 1975; Hauser *et al.* 1991; Hopkins, Shorvon, 1995).

To explain why epilepsies become chronic in some patients, Gowers (Gowers, 1881) postulated that recurrent seizures facilitate the occurrence of subsequent seizures. The observation that the number of pre-treatment seizures and poor response to treatment during the first years of the epileptic condition are important indicators of seizure outcome appears to support this hypothesis (Shorvon, Reynolds, 1982; Reynolds *et al.* 1983; Elwes *et al.* 1984; Reynolds, 1987; Reynolds, 1995). An alternative hypothesis is that the underlying etiology determines the prognosis of a specific epilepsy syndrome (O'Donoghue, Sander, 1996). Some localization-related

epilepsy syndromes, e.g. benign childhood epilepsy with centro-temporal spikes, have a good prognosis, other syndromes, e.g. chronic progressive epilepsia partialis continua, may have a less favorable prognosis (Commission on classification and terminology of the International League Against Epilepsy, 1989). Also, several epidemiological studies have shown that patients grouped according to broad etiologies have different prognoses (Annegers *et al.* 1979; Cockerell *et al.* 1995).

The prognosis of newly diagnosed localization-related epilepsy as a function of MRI-based etiologies has not been studied. In particular, the prognosis and incidence of HS in adults with newly diagnosed localization-related epilepsy are not known.

This is a prospective study of adults with newly diagnosed localization-related epilepsy using MRI and hippocampal quantitation. The aims were to establish MRI-based etiologies and their prognostic significance and to assess how the information affected the management of the individual patient (Connelly *et al.* 1996).

6.3. METHODS.

6.3.1. SELECTION CRITERIA.

Patients aged between 15 and 50 years with newly diagnosed localization-related epilepsy (Commission on classification and terminology of the International League Against Epilepsy, 1989) who had an MRI scan of the brain as soon as possible after diagnosis of localization-related epilepsy were included in the study. All patients had a history of at least two seizures. Partial seizures, generalized seizures without clear partial onset but with focal EEG, or a combination of the two were accepted (Commission on classification and terminology of the International League Against Epilepsy, 1981). Patients with acute symptomatic seizures were excluded. All patients had an interictal EEG. Patients with a history of FC were not excluded.

6.3.2. STUDY PROTOCOL.

All patients were recruited from the epilepsy clinic at the National Hospital for Neurology and Neurosurgery or from neurologists who were asked to refer suitable patients. The patients were evaluated clinically. In addition to the evaluation of patients described on p 52, the following data were recorded. Date and age at first seizure and index seizure (i.e. the seizure that led to the diagnosis), total number of each seizure type, and medication started were ascertained. Patients were asked to

keep a seizure diary. Reports of interictal EEGs were obtained. Patients underwent an MRI scan including standard T1- and T2-weighted images and imaging to enable HCT2 mapping and HCV measurements. Management of the patients and prescription of AEDs was at the discretion of the referring physicians.

6.3.3. QUANTITATIVE MR IMAGING.

6.3.3.1. HCT2 MAPPING: *see p 55.* For this study, the upper limit of the reference range for the control group was taken as 111 msec, i.e. 3 SDs above mean control HCT2. This was done to increase the specificity of the test.

6.3.3.2. HCV MEASUREMENT: *see p 57.* To increase the specificity of the diagnosis of HS the lower limit of the control HCV reference range was defined by 3 SD below the mean control value and was 3932 mm^3, instead of 2 SD.

6.3.4. STATISTICS: *see p 72.*

6.4. RESULTS.

6.4.1. DESCRIPTION OF SUBJECTS.

Sixty-three patients (31 men and 32 women) with median age of 26 years (range: 14 to 50) with newly diagnosed localization-related epilepsy were included. The median interval between the first seizure of the habitual epilepsy and the MRI scan was 12 months (range: 1 to 288 months) and between the index seizure and MRI scan was 6 months (range: 1 to 25). Six patients (10%) had a history of FC and six (10%) had a first degree relative with epilepsy or a history of FC. The first seizure of the habitual epilepsy was a partial seizure (SPS or CPS) in 33 patients (52%) and a SGS in 30 patients (48%). The index seizure was a CPS in 20 patients (32%) and a SGS in 43 patients (68%). The first seizure was the index seizure for 33 patients (52%). The median number of CPS before the MRI scan was 6 (range: 0 to 400) and of SGS was 2 (range: 0 to 50). Forty patients (63%) had an abnormal interictal EEG. Twenty-five patients had focal epileptiform abnormalities, localized to the temporal lobes in 22. Eleven patients had focal slowing (theta or delta waves) as the sole interictal EEG abnormality, localized to the temporal lobes in 10. Four patients had generalized interictal epileptiform activity, which was interpreted as secondary bilateral synchrony.

6.4.2. MRI-BASED ETIOLOGIES OF NEWLY DIAGNOSED LOCALIZATION-RELATED EPILEPSIES.

Eight patients (12.5%) had a lesion other than HS *(Figure 41, p 144)*. Interictal EEG showed concordant epileptiform abnormalities in 5 (62.5%) and was normal in the other three (37.5%). The immediate management of one patient was changed by the information provided by MRI. This patient had a giant aneurysm of the left internal carotid artery with mass effect on the amygdala, and concordant interictal epileptiform abnormalities *(Figure 41.2)*. This aneurysm was not detected on X-ray CT scan. The aneurysm was clipped, and the patient has been without neurological deficit and seizure free for more than 2 years. All patients with lesions other than HS (n=8) had quantitative hippocampal measures within normal limits, i.e. none had evidence of dual pathology.

Six patients (10%) had hippocampal abnormalities more than 3 SD outside the mean control values consistent with HS *(Figure 42, p 145)*. Five of these six patients with HS had concordant interictal epileptiform abnormalities and the sixth had a normal EEG.

One patient (1.5%) was scanned two months after an episode of CSE and had an increased HCT2 of 115 msec in the larger hippocampus, consistent with edema. Forty-eight of the 63 patients (76%) had normal standard MR imaging and hippocampal quantitative measures.

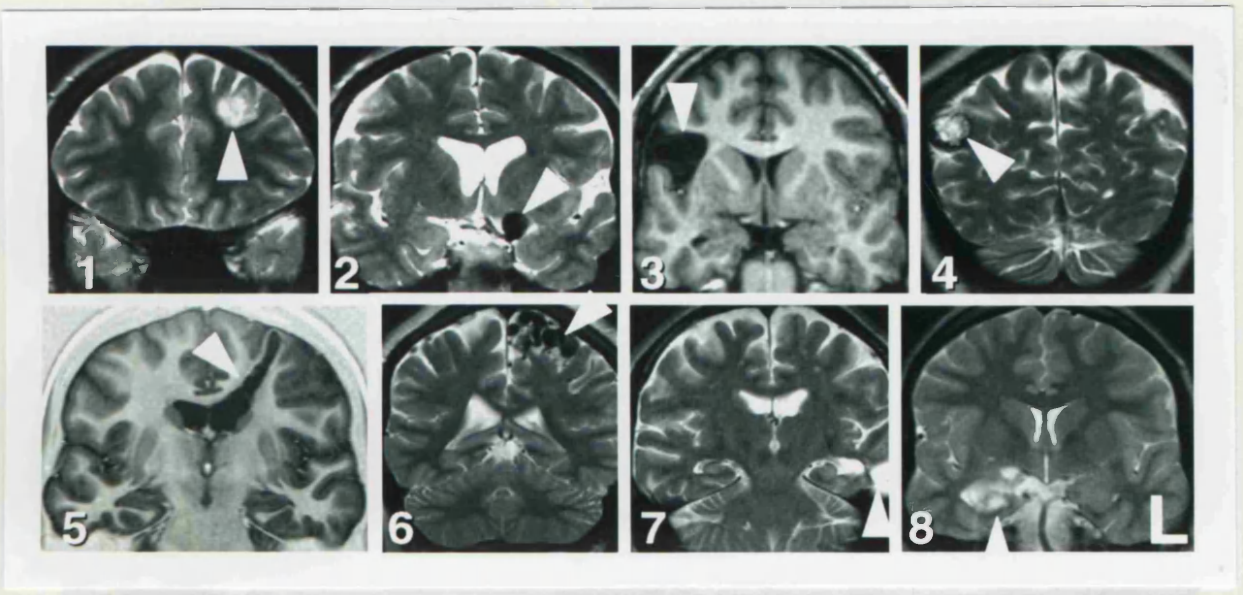

Figure 41. Lesions other than HS in adults with newly diagnosed localization-related epilepsy. All lesions are indicated by white arrows. 1, 2, 4,6-8: T2-weighted images (TE = 80 msec), 3 and 5: IR T1-weighted images. 1. Mass lesion in left frontal lobe, possibly a DNET [Hospital number: QSC16548]. 2. Giant aneurysm of the left terminal internal carotid [Hospital number: QSC23328]. 3. Widening of the sylvian fissure returning signal similar to CSF suggesting an extrinsic lesion such as an arachnoid cyst or a cisternal epidermoid. 4. Cavernous angioma. 5. Patient with stroke-like episode with sudden onset aphasia resolving over 8 weeks, and first right adversive seizure with secondary generalization 7 months later. The MRI shows an unusual prominent linear abnormality extending from the pial surface to the ependyma which is associated with tissue loss. The appearance suggests brain damage of uncertain cause, possibly an unusual infarct [Hospital number: QSC30152]. 6. Arteriovenous malformation. 7. Post traumatic scar. 8. Mass lesion involving right mesial temporal structures, possibly low-grade glioma or DNET [Hospital number: QSC27119].

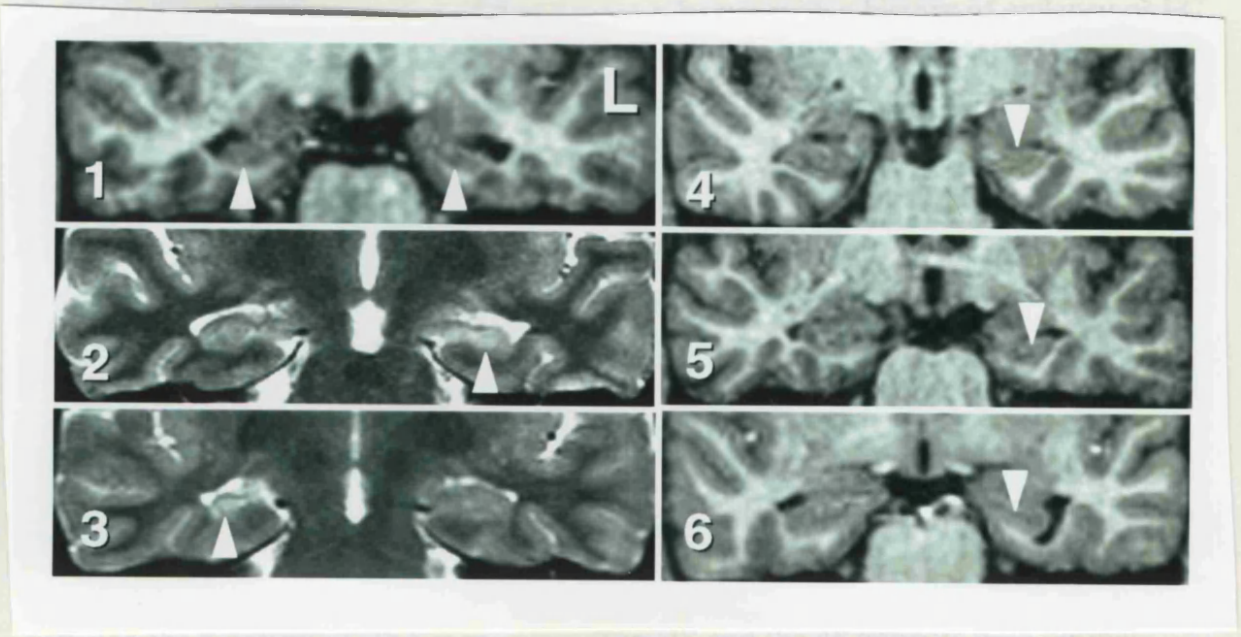

Figure 42. HS in adults with newly diagnosed localization-related epilepsy. Involved hippocampi are indicated by white arrows. 1, 4-6: reformatted MPRAGE images, 2 and 3: T2-weighted images (TE = 80 msec). Median HCVR of these 6 patients was 0.77 (range: 0.67 to 0.82). Normal values: HCVR ≥ 0.87, HCV > 3932 mm^3, HCT2 ≤ 111 msec. 1. Bilateral diffuse hippocampal atrophy with normal HCT2s *(see also Figure 44, p 157)* (HCV left = 3446 mm^3 and HCV right = 2802 mm^3) with normal HCT2s (HCT2 right = 105 msec, HCT2 left = 108 msec) [Hospital number: QSC24608]. 2. Left diffuse hippocampal atrophy with increased HCT2 (HCT2 left = 119 msec, HCV left = 3901 mm^3). 3. Right diffuse hippocampal atrophy with increased HCT2 (HCT2 right = 120 msec, HCV right = 3616 mm^3) [Hospital number: QSC27812]. 4. Diffuse left hippocampal atrophy with normal HCT2 (HCT2 left = 104 msec, HCV left = 3772 mm^3) and posterior atrophy of right hippocampus (not shown). 5 and 6. Left anterior hippocampal atrophy with normal HCT2 (patient 5: HCT2 left = 107 msec, HCV left = 4101 mm^3; patient 6: HCT2 left = 108 msec, HCV left = 4423 mm^3) [Hospital number: QSC26386]. Hippocampal atrophy in these last two cases only affected the head of the hippocampus i.e. at the level of the amygdala.

6.4.3. COMPARISON OF PATIENTS WITH HS AND PATIENTS WITH OTHER MRI FINDINGS: WORSE EARLY PROGNOSIS FOR PATIENTS WITH HS WITH RESPECT TO SEIZURES.

The six patients with HS were compared with the 57 patients with other MRI findings. Age, gender, number of first degree relatives with a history of epilepsy or FC and interval between first or index seizure and MRI scan did not differ between these two groups. Three of the six patients (50%) with HS had a history of prolonged FC compared to three of 57 patients (5%) with other MRI findings (p=0.0004; Fisher's Exact test). The early prognosis differed significantly between the two groups *(Table 14, p 146)*. Patients with HS had more CPS and SGS compared to the other group before the MRI scan, and at 1 year follow-up after the baseline scan the same pattern was observed, with recurrent seizures in all 6 patients with HS (100%) compared to 27 of 57 patients (51%) with other MRI findings. The total number of CPS and SGS at around 1 year follow-up was known for 5 patients with HS and 51 patients with other MRI findings and was significantly higher in the HS group. All patients with HS and 52 of 57 patients (90%) of the other group were prescribed AEDs from the time of diagnosis. There were no differences in terms of epilepsy history and early prognosis between the 8 patients with lesions other than HS and the 48 patients with normal MRI.

	Hippocampal sclerosis	Other MRI findings	p
n	6	57	
No of CPS before first MRI	70 (0 to 700)	4 (0 to 300)	0.05 (a)
No of SGS before first MRI	4 (1 to 50)	2 (0 to 7)	0.005 (a)
No of patients with recurrent seizures of follow-up	6 (100%)	27 (51%)	0.03 (b)
No of CPS on follow-up¶	12 (2 to 120)*	0 (0 to 180)**	0.004 (a)
No of SGS on follow-up¶	4 (0 to 376)*	0 (0 to 14)**	0.0009 (a)

Table 14. Early prognosis with respect to seizures in patients with HS compared with patients with other MRI findings. a: Mann-Whitney U test, b: Fisher's Exact test, *: n = 5, **: n = 51, ¶: follow-up of approximately 1 year.

6.5. DISCUSSION.

6.5.1. MRI IN NEWLY DIAGNOSED LOCALIZATION-RELATED EPILEPSY.

MRI has been reported to detect an abnormality in 85% of patients with intractable localization-related epilepsy (Fish, 1994b), most often HS (Jackson *et al.* 1990; Van Paesschen *et al.* 1997). In the present study of newly diagnosed localization-related epilepsy, however, MRI including hippocampal quantitation revealed an abnormality in only 15 of 63 adult patients (24%). No cases of CD were detected. This study included patients who were referred to neurology clinics, and was not community-based, which would be more likely to have more patients with milder forms of epilepsy.

6.5.2. HIPPOCAMPAL SCLEROSIS AND NEWLY DIAGNOSED LOCALIZATION-RELATED EPILEPSY.

HS was found in 10% of adults with newly diagnosed localization-related epilepsy. Four of the six patients (67%) with HS on HCV criteria had a normal HCT2 compared with six of 66 patients (9%) of a previously reported group of patients with HS and longstanding TLE with onset in childhood (Van Paesschen *et al.* 1997) ($p=0.003$; Fisher's Exact test). This could mean that patients with lesser degrees of HS have onset of habitual epilepsy at an older age, or that HS progresses, or both. In that retrospective study of patients with intractable longstanding TLE, it was found that patients with unilateral anterior HS had a later onset of habitual epilepsy compared with patients with unilateral diffuse or bilateral HS. The findings of this previous study (Van Paesschen *et al.* 1997) together with this present work are consistent with the dentate lamellar hypothesis *(see dentate lamellar hypothesis, p 50)* (Sloviter, 1994; Sloviter, Brisman, 1995), which postulates that the length of hippocampus in which hippocampal lamellae have lost the ability to inhibit neighboring lamellae, rendering the GCDG hyperexcitable, determines the length of the "silent period" i.e. the time from an early insult such as prolonged FC to the onset of habitual epilepsy.

6.5.3. ETIOLOGY AND EARLY PROGNOSIS IN NEWLY DIAGNOSED LOCALIZATION-RELATED EPILEPSY.

This study confirms the observation that the number of pre-treatment seizures is an important indicator of early prognosis with respect to seizure control (Shorvon, Reynolds, 1982; Reynolds *et al.* 1983; Elwes *et al.* 1984; Reynolds, 1987; Reynolds,

1995). The presence of HS was associated with significantly more seizures before MRI and at one year follow-up after the MRI, which coincided approximately with the first year of treatment. All patients with HS had recurrent seizures at one year follow-up in comparison with about half of the patients with other MRI findings. Within this group of patients with HS, the patient with the worst hippocampal damage, i.e. bilateral diffuse hippocampal atrophy, had the most CPS and SGS. This corroborates the observation that extent of hippocampal damage is associated with the frequency of SGS during the lifetime of patients with longstanding intractable TLE *(see clinical correlations of MRI-defined subgroups, p 106)* (Van Paesschen *et al.* 1997), and the suggestion that an individual's seizure threshold is inversely proportional to the degree of HS (Sloviter, 1994). This is an argument to obtain a high resolution MRI scan in all adults with newly diagnosed localization-related epilepsy to identify patients with HS early, to follow these patients more closely, and treat them more vigorously. Also, MRI may alter the management of the individual patient with other lesions, such as the patient with the giant aneurysm that was clipped, rendering the patient seizure free. In view of these findigs, AED trials of newly diagnosed epilepsy should be stratified for HS and other etiologies (Walker, Sander, 1996). HS may also be an adverse risk factor for seizure recurrence in patients in whom the epilepsy is in remission and AED withdrawal is considered. Drug withdrawal studies should include an MRI-based etiologic classification.

This study shows that the etiology of newly diagnosed localization-related may be an important determinant factor with regard to early seizure prognosis. The possibility that recurrent seizures facilitate the occurrence of subsequent seizures can not be excluded. Whether recurrent seizures cause progressive hippocampal damage will be determined in a longitudinal quantitative hippocampal MRI study of this cohort *(see Chapter 7)*.

CHAPTER VII. A LONGITUDINAL QUANTITATIVE HIPPOCAMPAL MRI STUDY OF NEWLY DIAGNOSED LOCALIZATION-RELATED EPILEPSIES IN ADULTS: ONE YEAR FOLLOW-UP RESULTS

7.1. ABSTRACT.

Thirty-six adult patients with newly diagnosed localization-related epilepsy underwent a MRI scan of the brain including hippocampal quantitation and had a follow-up quantitative MRI scan around 1 year after the baseline MRI scan. At baseline, four patients (11%) had HS, four (11%) had abnormalities other than HS, and 28 had a normal MRI scan (78%). There was no MRI evidence of progressive hippocampal damage with continued seizures over 1 year in the three groups of patients compared with a control group. However, three individual patients had significant changes of hippocampal quantitative measures, possibly reflecting ongoing hippocampal damage. Worsening of seizure pattern, defined as onset of habitual epilepsy with SPS or CPS and followed later by SGS, was associated with quantitative MRI defined hippocampal damage (i.e. HS or significant hippocampal changes on follow-up). Follow-up of this cohort over several years will be required to settle the question of whether there is progressive hippocampal damage in TLE.

7.2. INTRODUCTION.

HS is the most common cause of longstanding intractable TLE (Falconer *et al.* 1964; Margerison, Corsellis, 1966; Babb, Brown, 1987; Bruton, 1988). The incidence, natural history and prognosis of HS in adults with newly diagnosed localization-related epilepsy are not known. It is unclear whether HS is present from the outset of habitual epilepsy, whether HS can be the consequence of repeated seizures, or whether HS can progress as a consequence of repeated seizures. Several studies addressing the question of progression of HS were cross-sectional and retrospective, and therefore inconclusive (Dam, 1980; Sagar, Oxbury, 1987; Cendes *et al.* 1993c; Trenerry *et al.* 1993b; Saukkonen *et al.* 1994; Mathern *et al.* 1995a; Meencke, 1995; Van Paesschen *et al.* 1997).

Status epilepticus and more particularly prolonged FC have been associated with hippocampal damage and unilateral HS in about 50-60% of cases of TLE (Cavanagh, Meyer, 1956; Falconer *et al.* 1964; Duncan, Sagar, 1987; Sagar, Oxbury, 1987; Bruton, 1988; Cendes *et al.* 1993a; Kuks *et al.* 1993; Grünewald *et al.* 1994a;

Harvey *et al.* 1995; Maher, McLachlan, 1995; Mathern *et al.* 1995a; Van Paesschen *et al.* 1997). Acute hippocampal pathological changes after CSE include pyramidal cell necrosis and edema (Corsellis, Bruton, 1983). Chronic changes are hippocampal atrophy, gliosis (Falconer *et al.* 1964; Margerison, Corsellis, 1966; Jensen, Klinken, 1976; Babb, Brown, 1987; Bruton, 1988; Armstrong, 1993; Kim *et al.* 1995a) and mossy fiber sprouting (Sutula *et al.* 1989; Babb *et al.* 1991). MRI features of hippocampal changes after CSE have been reported in a total of six patients (Nohria *et al.* 1994; Jackson *et al.* 1995; Tien, Felsberg, 1995), and in animals with kainic acid-induced limbic seizures (Tanaka *et al.* 1993). In the acute stages, the affected hippocampus was enlarged with an increased T2 signal, consistent with edema, which resolved over weeks to months. Several months after CSE, hippocampal atrophy with normal or increased T2 signal was observed.

This study describes the one-year follow-up results of a longitudinal, prospective study of adults with newly diagnosed localization-related epilepsy using MRI and hippocampal quantitation. The aim was to establish whether there is progression of hippocampal disease (Van Paesschen *et al.* 1996c).

7.3. METHODS.

7.3.1. SELECTION CRITERIA.

Patients aged between 15 and 50 years with newly diagnosed localization-related epilepsy (Commission on classification and terminology of the International League Against Epilepsy, 1989) who had a baseline MRI scan of the brain as soon as possible after diagnosis and who had a follow-up scan one year later were included in the study. Partial seizures, generalized seizures without clear partial onset but with focal EEG, or a combination of the two were accepted (Commission on classification and terminology of the International League Against Epilepsy, 1981). Patients with acute symptomatic seizures were excluded. All patients had an interictal EEG.

7.3.2. STUDY PROTOCOL.

All patients were recruited from the epilepsy clinics at the National Hospital for Neurology and Neurosurgery or were referred by neurologists who were asked to refer suitable patients. The patients were evaluated clinically *(see p 52 and p 141)*. Reports of interictal EEGs were obtained. Patients were asked to keep a seizure diary between baseline and follow-up MRI scan. Patients underwent a baseline standard MRI scan of

the brain including T1- and T2-weighted images. Imaging for HCT2 mapping and HCV measurements were obtained at baseline and at follow-up of at least one year. At follow-up, record was made of the number and type of seizures between the two scans. Management of the patients and prescription of AEDs was at the discretion of the referring physicians.

Control subjects with no history of neurologic or psychiatric illness and of similar age to the patients underwent the same MRI protocol as the patients, but the interval between the scans was longer, i.e. they were scanned before the study and rescanned after the one year follow-up scan of the patients.

7.3.3. QUANTITATIVE MR IMAGING.

7.3.3.1. HCT2 MAPPING: *see p 55.* To increase the specificity of the diagnosis of HS the upper limit of the reference range for the control group was taken as 111 msec, i.e. 3 standard deviations (SD) above mean control HCT2.

7.3.3.2. HIPPOCAMPAL VOLUMETRY: *see p 57.* Images for hippocampal volumetric studies were obtained using an MPRAGE sequence . The same parameters including FOV were used for baseline and follow-up MPRAGE. The baseline and follow-up MPRAGE datasets were reformatted in an identical way during the same session into 1 mm thick contiguous sections in a tilted coronal plane that was perpendicular to the long axis of the hippocampus. Hippocampal cross-sectional areas of all 1 mm sections of the HCV datasets of one subject were measured by the same person during the same session. The order of measurement, i.e. baseline MRI measured first and then the follow-up scan or vice versa, was blinded. The HCV was calculated by summing the hippocampal cross-sectional areas (Cavalieri's principle) (Mayhew, Olsen, 1991). HCVs were corrected for ICV and HCV distribution graphs were constructed. In these graphs, one datapoint represented the average hippocampal cross-sectional area of three consecutive sections. To increase the specificity of the diagnosis of HS the lower limit of the control HCV reference range was defined by 3 SD below the mean control value and was 3932 mm^3.

7.3.4. STATISTICS: *see p 72.*

Statistical analysis was performed using SPSS for Windows, release 6 (SPSS Inc., Chicago, Ill., USA) (Norusis, 1993). For group comparisons, repeated measures analysis of variance with number of seizures between the two MRI scans as a covariate

were used. For these group comparisons, patients were divided in several ways, namely 1. all patients together, 2. patients with HS, other abnormalities, and normal MRI, 3. patients with TLE. The mean HCT2 or HCV of both hippocampi at baseline were compared with the mean value at follow-up. In a further analysis, hippocampal measures on the side of the EEG focus in patients with TLE were also compared with the control subjects.

To compare the results of individual patients with the control group, the limits of agreement for repeated measures of HCT2 and HCV in the control group were calculated. The limits of agreement in this study were defined as the mean difference (d) of HCT2 or HCV at baseline minus HCT2 or HCV at follow-up $\pm$ 3 standard deviations (SD) of this mean difference (Bland, Altman, 1986).

7.4. RESULTS.

7.4.1. DESCRIPTION OF SUBJECTS.

7.4.1.1. CONTROL SUBJECTS AND LIMITS OF AGREEMENT. Twelve control subjects (5 men and 7 women) with median age of 29 years (range: 21 to 38) underwent baseline and follow-up quantitative MRI. The median interval between baseline and follow-up scan was 643 days (range: 385 to 1024). The mean difference d_{HCT2} (± SD) of baseline minus follow-up HCT2 (n=22) was 0 ± 3 msec. The limits of agreement (Bland, Altman, 1986) for HCT2 mapping defined in this study as d_{HCT2} ± 3 SD were therefore ± 9 msec. The mean difference d_{HCV} (± SD) of baseline minus follow-up HCV (n=24) was 91 ± 151 mm^3. The limits of agreement for the HCV defined as d_{HCV} ± 3 SD were therefore +554 and -362 mm^3, i.e. a decrease of HCV on follow-up of more than 554 mm^3 was considered significant.

7.4.1.2. PATIENTS. Thirty-six patients (15 men and 21 women) with median age of 26 years (range: 14 to 50) with newly diagnosed localization-related epilepsy were included. The median interval between the first seizure of the habitual epilepsy and the MRI scan was 17 months (range: 1 to 288 months) and between the index seizure and MRI scan was 7 months (range: 1 to 25). Four patients (11%) had a history of FC. The first seizure of the habitual epilepsy was a partial seizure (SPS or CPS) in 19 patients (53%) and a SGS in 17 patients (47%). The index seizure was a CPS in 11 patients (31%) and a SGS in 25 patients (69%). At the time of baseline MRI scan, 14 patients (39%) had a seizure pattern characterized by SPS or CPS followed later by SGS and 22 (61%) with other patterns such as only SPS or CPS, only SGS or SGS followed by partial seizures without generalization. The median number of CPS before the MRI scan was 12 (range: 0 to 400) and of SGS was 2 (range: 0 to 40). Nineteen patients (53%) had an epileptic abnormality on interictal EEG. Three patients (8%) had focal slowing (theta or delta waves) as the sole interictal EEG abnormality. Fourteen patients (39%) had a normal interictal EEG. Taking all information, i.e. clinical, EEG and MRI into account, twenty-two patients had TLE, three had extratemporal epilepsy and for eleven patients the location of the epileptogenic zone was unclear.

7.4.2. MRI-BASED ETIOLOGIES AT BASELINE.

Three patients (8%) had a lesion on standard MRI (DNET, cavernous angioma, AVM) and normal hippocampi *(Figure 41 [1, 4, 6], p 144)*. Four patients (11%) had hippocampal abnormalities more than 3 SD outside the mean control values consistent with HS *(Figure 42 [1-4], p 145)*. One patient (3%) had an increased HCT2 of 115 msec in the larger hippocampus, consistent with edema *(Figure 43, p 155)*. Twenty-eight patients (78%) had normal standard MR imaging and hippocampal quantitative measures.

7.4.3. FOLLOW-UP QUANTITATIVE HIPPOCAMPAL MEASURES.

The median interval between baseline and follow-up MRI scans for the 36 patients was 394 days (range: 287 to 776). Repeated measures analysis of variance did not reveal significant differences in HCV or HCT2 between control and patient groups *(see Statistics, p 151)*, taking into account the number of CPS and SGS between the two scans. However, three individual patients had changes in quantitative hippocampal measures which fell outside the limits of agreement *(Figures 43, p 155; Figure 44, p 157; Figure 45, p 159)*.

7.4.4. ASSOCIATION OF PROGRESSIVE SEIZURE HISTORY WITH MRI-BASED HIPPOCAMPAL DAMAGE.

Fourteen of the 36 patients (39%) presented at the time of baseline MRI with a seizure history characterized by SPS or CPS followed later by SGS *(for examples of this seizure pattern, see Figure 43, p 155 and Figure 45, p 159)*. Five of the six patients with MRI evidence of hippocampal damage at follow-up (i.e. three with HS and two with progressive changes) had such a seizure history compared with 9 of 30 patients (30%) with other MRI findings ($p = 0.024$; Fisher's Exact test).

Figure 43: *see p 156.* Case report 1. A 35 year old man had 9 CPSs during the 18 months prior to the baseline scan. He had a first SGS four months prior to the baseline scan, and two months later a prolonged SGS lasting more than 20 minutes. Since this prolonged SGS he had memory difficulties. A interictal EEG was normal. He was rescanned one year after the baseline MRI scan. On medication, he had two brief partial seizures between the two scans.

The HCT2 map at baseline (A) shows an increased T2 signal in the right (larger) hippocampus (HCT2 right = 115 msec, HCT2 left = 102 msec [Nl: ≤ 111 msec]) (white arrow in A). B and C show images of the baseline and follow-up MPRAGE volume sets that were reformatted in an identical fashion into 1 mm thick contiguous sections. The number on the left-hand side represents the section position starting from the tail of the hippocampus with section 1 being the section in which the fornix was seen in its full profile. These numbers correspond to the section position numbers on the HCV distribution graphs. The HCV distribution graphs (D-G) plot hippocampal cross-sectional area (mm^2) as a function of section position. The dashed lines are the upper and lower limit of the control group reference range as defined by ± 2 SD. Section position 1 starts at the tail of the hippocampus and the whole length of the hippocampus was measured. D plots hippocampal cross sectional areas of right (RHC_B, black circles) and left (LHC_B, open squares) hippocampus of the baseline MRI. E plots hippocampal cross sectional areas of right hippocampus at follow-up (RHC_{FU}, black circles) and left hippocampus at follow-up (LHC_{FU}, open squares). E compares RHC_B (full black line) with RHC_{FU} (dotted black line), and G compares LHC_B (full black line) with LHC_{FU} (dotted black line). At baseline, HCVs were borderline normal: HCVR(R/L) = 0.87 (Nl ≥ 0.87); HCV right = 4797 mm^3, HCV left = 4174 mm^3 (Nl ≥ 3932 mm^3) (B and D). On follow-up there was a significant decrease in right HCV of 583 mm^3 (Nl: < 554 mm^3) (white and black arrow in B and C, and F) and normalization of HCT2. On follow-up the quantitative hippocampal measures were: HCVR(R/L) = 0.87 (Nl ≥ 0.87); HCV right = 4214 mm^3, HCV left = 3718 mm^3 (Nl ≥ 3932 mm^3); HCT2 right = 106 msec, HCT2 left = 100 msec (Nl: ≤ 111 msec).

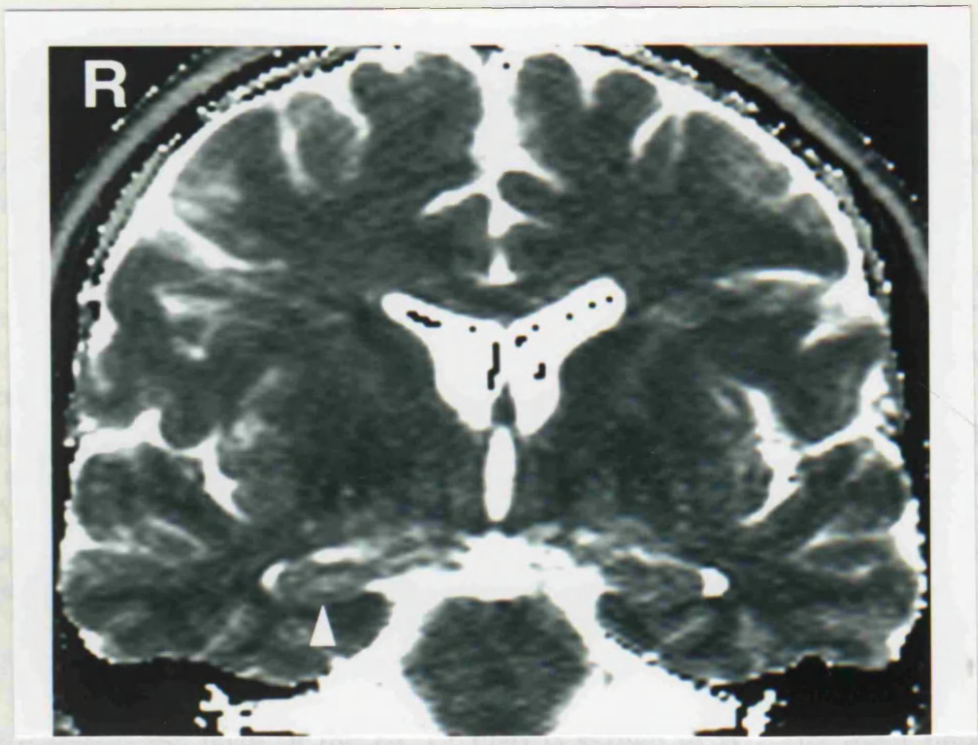
R
A

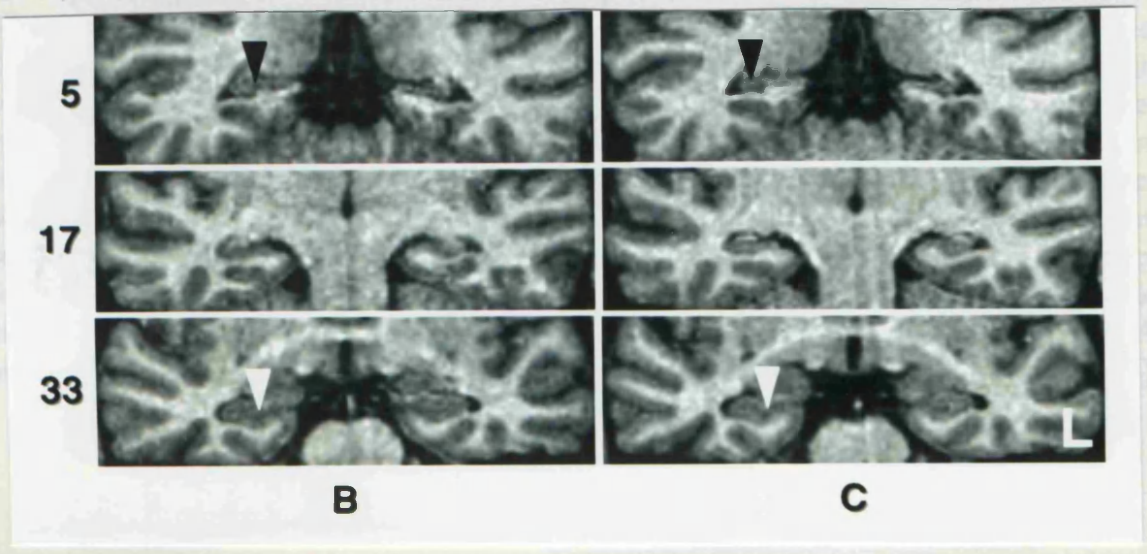
5
17
33
L
B
C

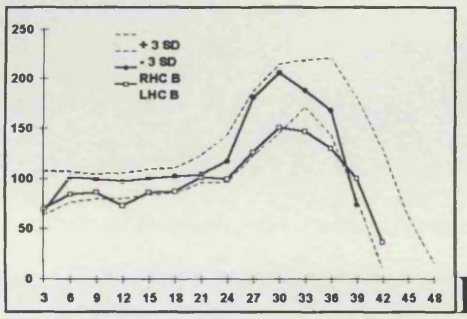
+ 3 SD
- 3 SD
RHC B
LHC B
D

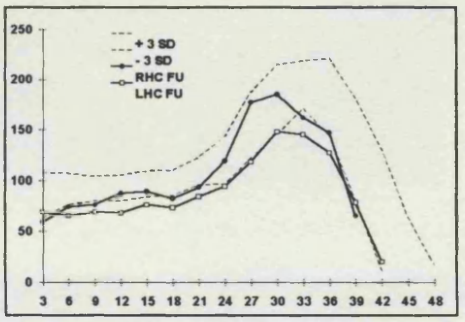
+ 3 SD
- 3 SD
RHC FU
LHC FU
E

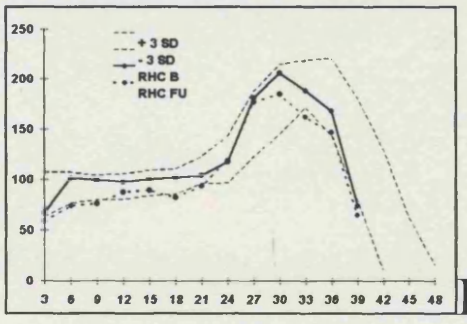
+ 3 SD
- 3 SD
RHC B
RHC FU
F

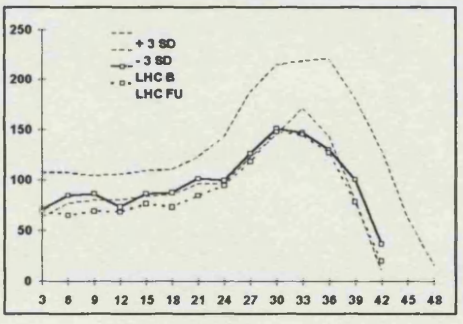
+ 3 SD
- 3 SD
LHC B
LHC FU
G

Figure 44: *see p 158.* Case report 2. An 18 year old woman presented with convulsive status epilepticus for which no cause was established. Since that time, she had intractable TLE with daily CPS and frequent secondary generalization.

The baseline MRI was 8 months after seizure onset and revealed bilateral asymmetric hippocampal atrophy (A). HCVR(L/R) = 0.81 (Nl: ≥ 0.87), HCV right = 3446 mm^3, HCV left = 2802 mm^3 (Nl: >3932 mm^3). The HCT2 on the right was 105 msec and on the left 108 msec (Nl ≤ 111 msec). She was rescanned at 7 months follow-up, prior to vagal nerve stimulator implantation. Between the two scans, she had an estimated 120 CPS and 376 SGS despite a combination of high doses of all major AEDs. At follow-up, the HCT2 value on the left was 113 msec (Nl: < 111 msec) and on the right 115 msec, which was increased 10 msec (Nl: ≤ 9 msec) compared to baseline HCT2 (B). There was no significant HCV loss.

She died a sudden, unexpected death following a CPS 7 months after the second MRI scan. The macroscopic view of the coronal section of the brain corresponding to the level of the HCT2 map is shown in B. The main finding was bilateral HS (black arrowheads) with clear atrophy of the CA1 hippocampal subregion (black arrow). C. Neuropathological section of the hippocampi (GFAP/SC stain, magnification x13). On the left (L), the typical distribution of damage of HS was seen, with severe damage of CA1 (between the two white arrows), and hilar neuronal cell loss and reactive gliosis. In the right hippocampus, the hilar region showed moderate neuronal cell loss and reactive gliosis, and the CA1 subregion showed focal neuronal cell loss and reactive gliosis (white arrow). The CA2 and CA3 hippocampal subregions and GCDG were well preserved. On a RCA 120 lectin stained hippocampal section several macrophages and microglia were present in the left CA1 hippocampal subregion, suggestive of recent damage. [Hospital number: QSC24608].

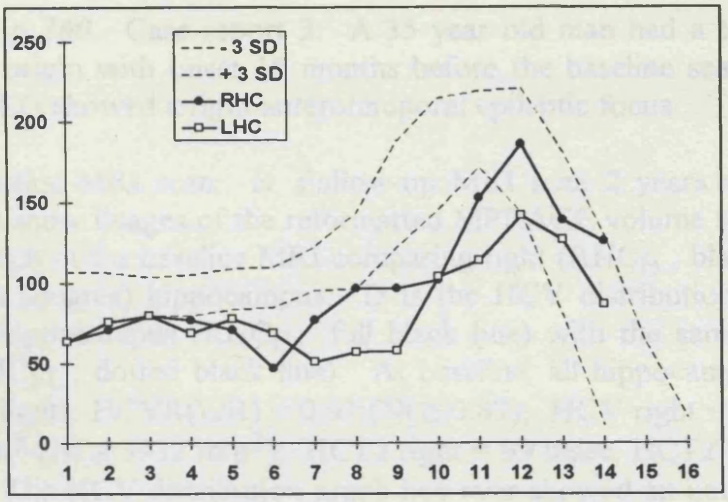
250
200
150
100
50
0
1 2 3 4 5 6 7 8 9 10 11 12 13 14 15 16
- - - - 3 SD
- - - - + 3 SD
RHC
LHC

A

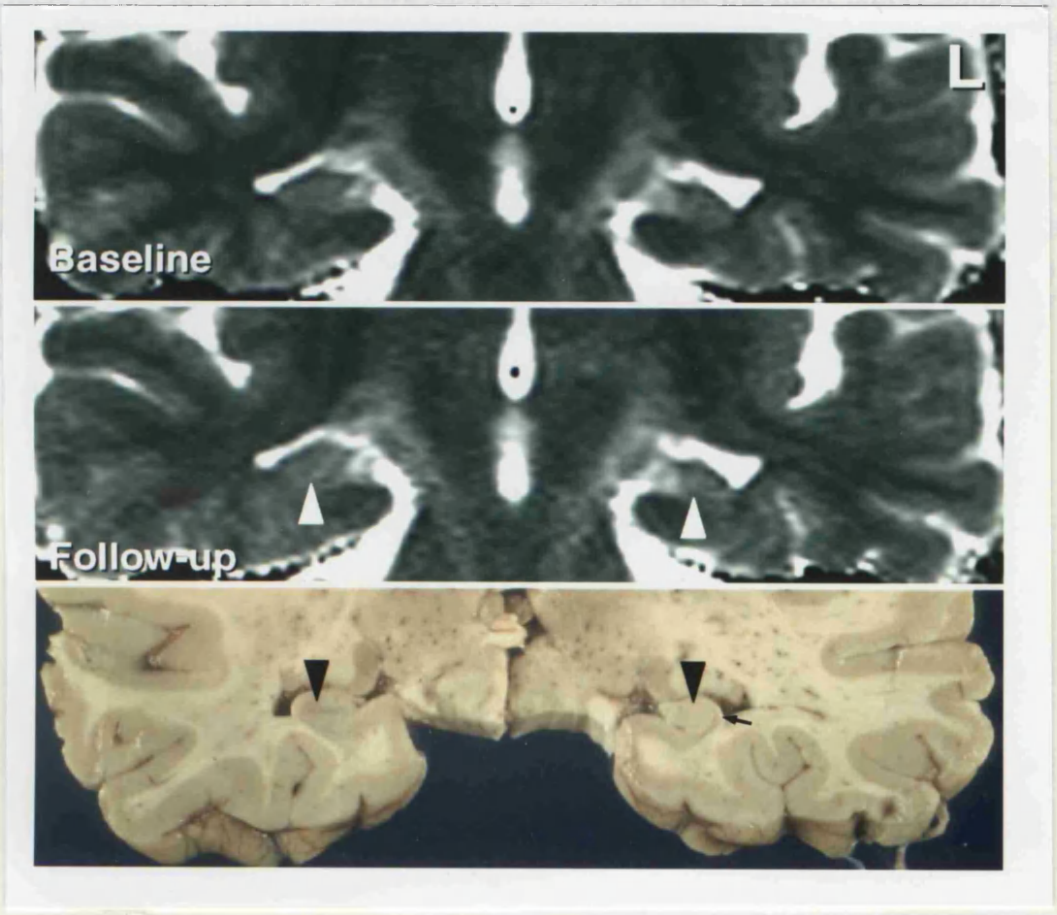
L
Baseline
Follow-up

B

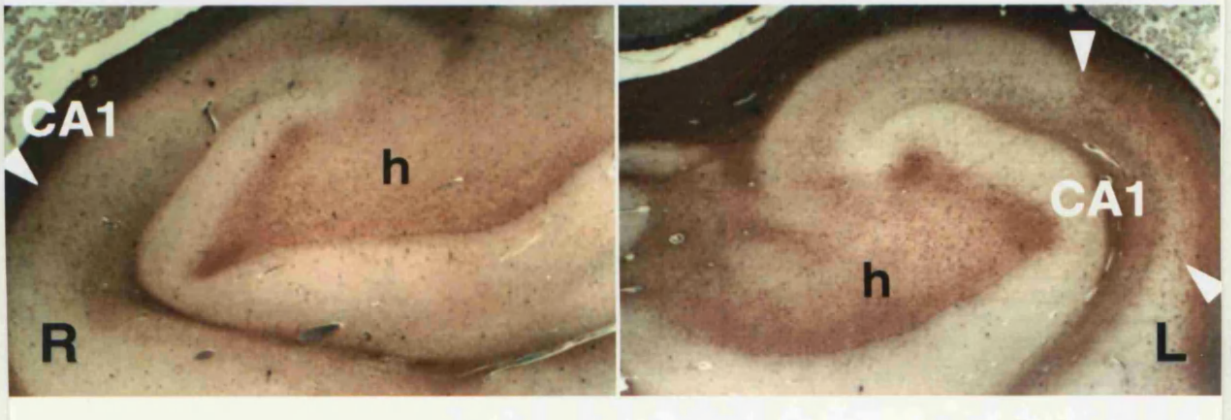
CA1
h
R
CA1
h
L

C

Figure 45: *see p 160.* Case report 3. A 35 year old man had a total of 25 CPS of temporal lobe origin with onset 18 months before the baseline scan, and three SGS. An interictal EEG showed a right anterotemporal epileptic focus.

A. Baseline MRI scan. B. Follow-up MRI scan 2 years after baseline MRI scan. A and B show images of the reformatted MPRAGE volume sets. C is the HCV distribution graph of the baseline MRI comparing right (RHC_B , black circles) and left (LHC_B , open squares) hippocampus. D is the HCV distribution graph comparing baseline right hippocampus (RHC_B, full black line) with the same hippocampus on follow-up (RHC_{FU}, dotted black line). At baseline, all hippocampal measures were within normal limits: HCVR(L/R) = 0.93 (Nl $\geq$ 0.87); HCV right = 5599 mm^3 , HCV left = 5144 mm^3 (Nl $\geq$ 3932 mm^3); HCT2 right = 99 msec, HCT2 left = 97 msec (Nl $\leq$ 111 msec). The HCV distribution graph however showed an unusual asymmetry at the level of the body of the hippocampus indicating that the right hippocampus was too large compared to the control population, and that the left was not atrophic, which had been the interpretation of visual inspection (black arrow in section 21 of B and C). On medication, he had one CPS over the next two years. On the follow-up MRI, there was a significant reduction in right HCV of 661 mm^3 (Nl: < 554 mm^3) mainly due to volume loss at the level of the hippocampal head (A and B: white arrows). Despite this volume loss, there were no MRI features of HS on the follow-up scan, and quantitative measures were within normal limits: HCVR(L/R) = 0.99 (Nl $\geq$ 0.87); HCV right = 4939 mm^3, HCV left = 4907 mm^3 (Nl $\geq$ 3932 mm^3); HCT2 right = 97 msec, HCT2 left = 92 msec (Nl $\leq$ 111 msec).

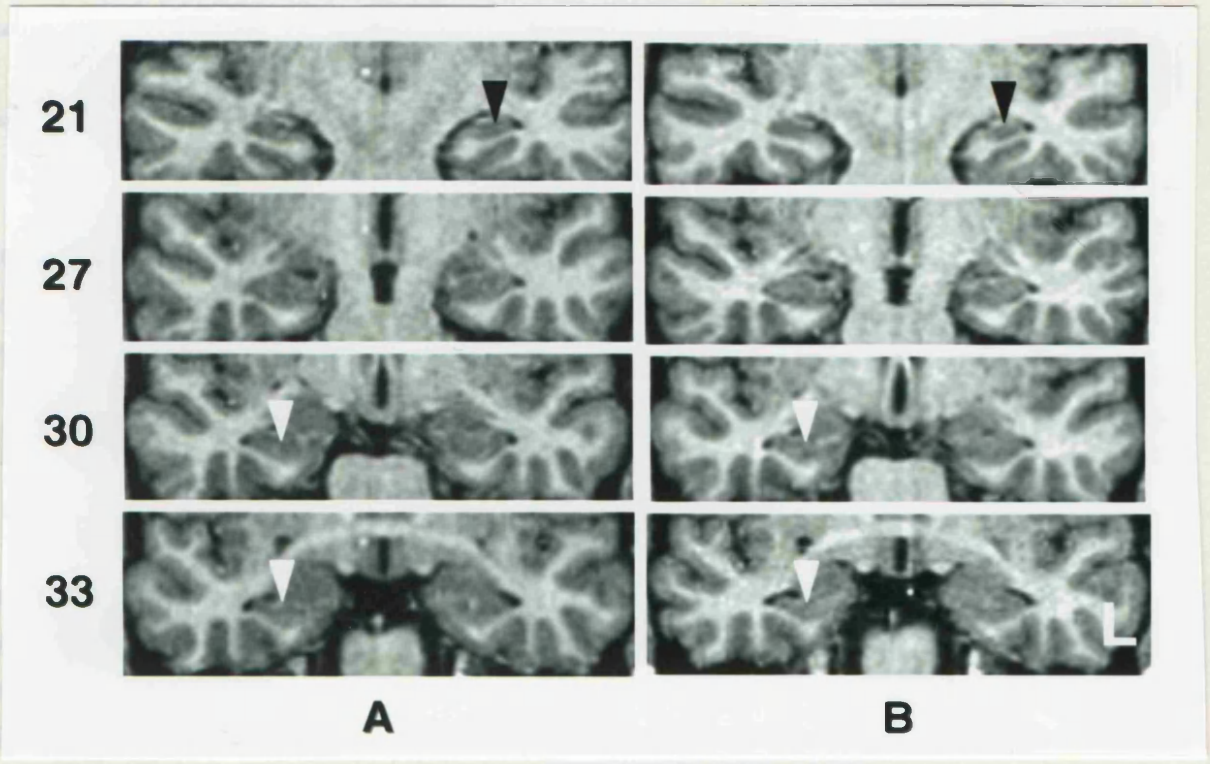
21
27
30
33
L
A
B

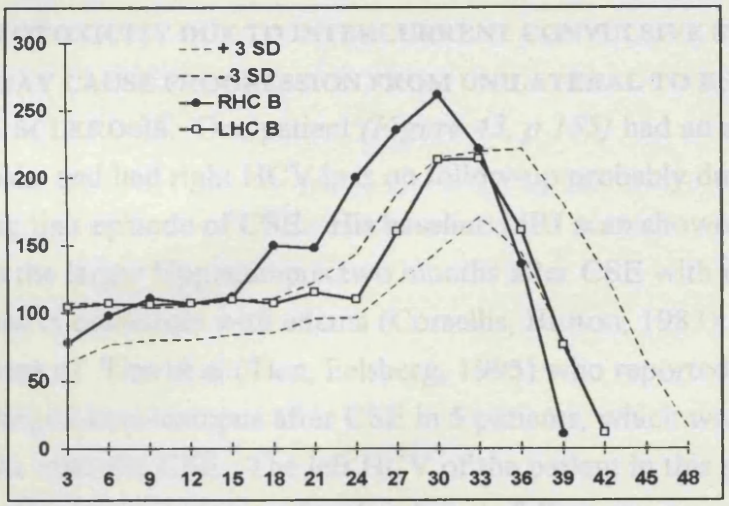
+ 3 SD
- 3 SD
RHC B
LHC B
300
250
200
150
100
50
0
3 6 9 12 15 18 21 24 27 30 33 36 39 42 45 48

C

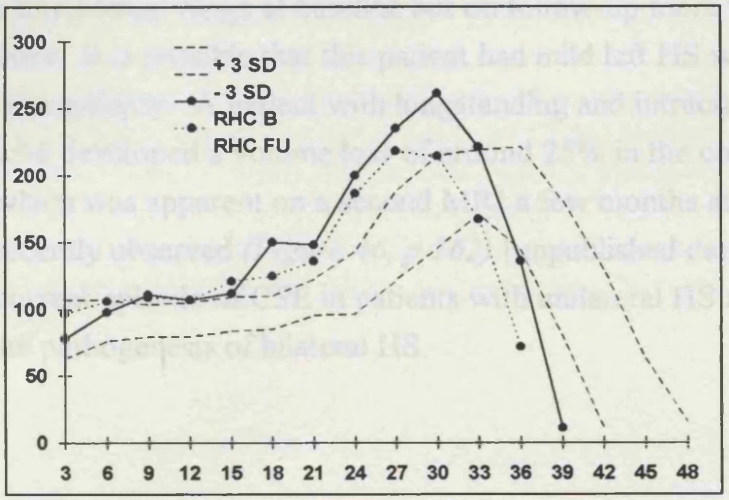
+ 3 SD
- 3 SD
RHC B
RHC FU
300
250
200
150
100
50
0
3 6 9 12 15 18 21 24 27 30 33 36 39 42 45 48

D

7.5. DISCUSSION.

7.5.1. LIMITATIONS OF THE STUDY.

This work is a prospective MRI-based study designed to address the issue of progressive hippocampal changes in localization-related epilepsies. Follow-up was only one year for most patients and the HS group was small. The conclusions of the study therefore can only be preliminary.

7.5.2. PROGRESSIVE HIPPOCAMPAL CHANGES.

Comparison of groups of patients did not provide evidence of progressive hippocampal damage with continued seizures over 1 year time. To gain insight into possible mechanisms of progressive hippocampal damage, it is therefore important to study each individual patient separately. Three patients had hippocampal changes that fell outside the limits of agreement.

7.5.2.1. EXCITOTOXICITY DUE TO INTERCURRENT CONVULSIVE STATUS EPILEPTICUS MAY CAUSE PROGRESSION FROM UNILATERAL TO BILATERAL HIPPOCAMPAL SCLEROSIS. One patient *(Figure 43, p 155)* had an episode of CSE prior to diagnosis, and had right HCV loss on follow-up probably due to damage sustained during that episode of CSE. His baseline MRI scan showed an increased HCT2 signal in the larger hippocampus two months after CSE with normalization on follow-up, which is consistent with edema (Corsellis, Bruton, 1983). This supports the MRI observations of Tien et al (Tien, Felsberg, 1995) who reported an increased T2 signal in an enlarged hippocampus after CSE in 5 patients, which was still visible in one patient 2 months after the CSE. The left HCV of the patient in this study *(Figure 43, p 155)* was in the low normal range at baseline but on follow-up more than 3 SD smaller than control values. It is possible that this patient had mild left HS which was responsible for the epilepsy. A patient with longstanding and intractable TLE and unilateral HS, who developed a volume loss of around 25% in the contralateral hippocampus, which was apparent on a second MRI a few months after an episode of CSE was also recently observed *(Figure 46, p 162)* [unpublished data]. Excitotoxicity due to an intercurrent episode of CSE in patients with unilateral HS may therefore be a mechanism in the pathogenesis of bilateral HS.

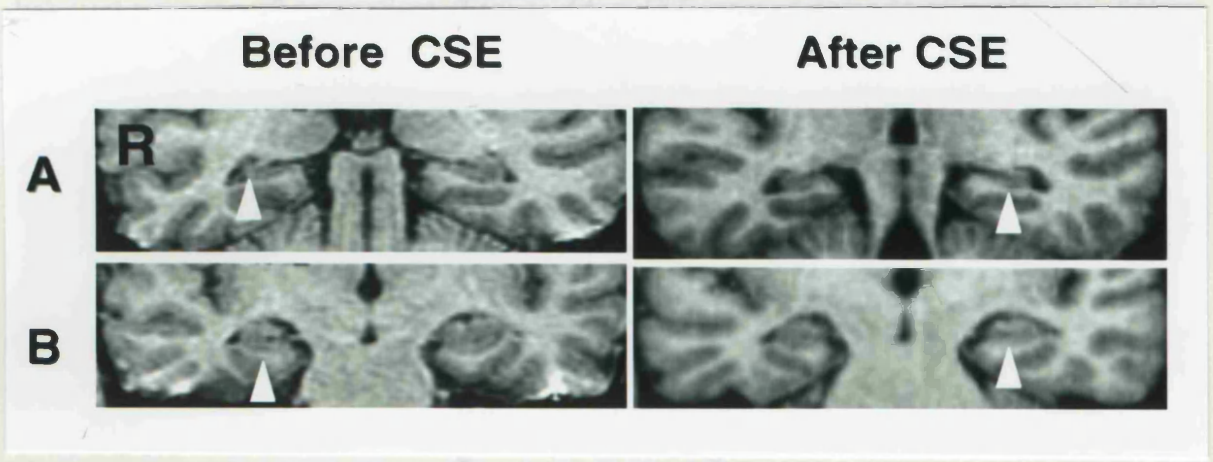

Figure 46. Progression from unilateral to bilateral HS. The patient was a 46 year old right handed man whose birth and early development were normal. The onset of habitual epilepsy was at the age of 4 years. There was no history of meningitis or FCs. The first seizure was an episode of CSE with left sided predominance, left sided Todd's paresis and right sided EEG focus. At the age of 12, he had 4 SGS with left sided predominance and no recovery of consciousness between seizures. He had a left Todd's paresis which resolved over one day. He had on average 4 SGS a year and was seizure free for 9 years from the age of 28 to 37 years. At the age of 35, he developed CPS with no aura, characterized by a vocalization, followed by staring, smacking movements of the mouth and swallowing, and dystonic posturing of the left arm with occasional SGS. The seizures continued at a frequency of 2 to 3 per year. At the age of 46 years, MRI of the brain (GE Signa 1.5 T, SPGR volume acquisition) showed right hippocampal atrophy without signal abnormality (white arrows in "before CSE"). Right HCV was 2877 mm^3 which was 5 SD below mean control values (5180 $\pm$ 416 mm^3) and the left HCV was 4095 mm^3, which was 2 SD below mean control values. The HCVR (R/L) was 0.70. Several interictal EEGs consistently showed right sided temporal delta activity without epileptiform activity. One month after the MRI, he had an episode of CSE, characterized by 9 serial SGS over 12 hours with no recovery of consciousness between seizures. Four months later, he had another episode of CSE with 5 serial SGS and without recovery of consciousness between seizures. After this episode of CSE, he complained of severe memory difficulties. An MRI was repeated 4 months after the last episode of CSE (Siemens SP63 Magnetom, 1.5 T, MPRAGE volume acquisition) and showed bilateral and symmetric hippocampal atrophy. Right HCV was 2951 mm^3 and comparable to the previous measurement, but the left HCV had decreased by 25% to 2998 mm^3 (white arrows in "after CSE"). HCT2s were 106 msec bilaterally and within normal limits (Nl$\leq$ 108 msec). [Hospital number: MVP12799].

7.5.2.2. PROGRESSIVE QUANTITATIVE HIPPOCAMPAL CHANGES IN A PATIENT WITH BILATERAL HIPPOCAMPAL ATROPHY: AN UNUSUAL CASE REPORT. The onset of habitual epilepsy of one patient *(Figure 44, p 157)* was an episode of prolonged status epilepticus at the age of 18 years, for which no cause was established. Bilateral HS was the main neuropathological finding at autopsy two years later. This clinico-pathological description bears a resemblance to the toxic encephalopathy caused by domoic acid (Teitelbaum *et al.* 1990; Cendes *et al.* 1995a). Several of these patients had status epilepticus in the acute stages of domoic acid intoxication, and were left with severe residual memory impairment, as did the patient in the present study. Cendes et al (Cendes *et al.* 1995a) reported a patient who developed TLE with a silent period of 1 year after the intoxication, and had evidence of bilateral HS on MRI. Bilateral HS was the main finding on neuropathological examination in 5 of these patients who came to autopsy (Teitelbaum *et al.* 1990; Cendes *et al.* 1995a). Domoic acid is an excitotoxin analogous to kainic acid and structurally related to glutamate, and induces limbic status epilepticus in animals (Olney *et al.* 1974; Nadler *et al.* 1978; Sperk *et al.* 1983; Ben-Ari, 1985; Olney *et al.* 1986). These induced prolonged seizures, and not a direct neurotoxic effect have been shown to cause bilateral HS, which in turn result in spontaneous hippocampal seizures. It may therefore be that the etiology of the first status epilepticus of the patient in this study was an unidentified excitotoxin similar to domoic acid or kainic acid. The presence of macrophages and microglia in the CA1 hippocampal subregion suggests that the damage was of relatively recent onset, and is consistent with the view that the HS was the result of the first episode of status epilepticus. Bilateral HS was most likely the etiology of the ensuing TLE. In this patient, frequent seizures between the 2 MRI scans was associated with changes in quantitative hippocampal measures. The HCT2s were normal at baseline and became abnormal on both sides on follow-up, with an increase of more than 9 msec on one side. Reversible T2 hyperintensities following single seizures have been described primarily in the posterior vascular boundary zones, probably due to edema (Yaffe *et al.* 1995). Grünewald et al (Grünewald *et al.* 1994b) did not find an increased HCT2 in 4 patients immediately after status epilepticus. The patient in this study had a seizure immediately before the first scan but not the second. If the increased HCT2 was due to edema one would expect an increase in HCV, which was not the case. HCT2 has a high inverse correlation with the amount of pyramidal cell damage in the CA1 hippocampal subregion (Van Paesschen *et al.* 1995c). Therefore, in the patient of the present study, progression of hippocampal damage is a more likely explanation for the increased HCT2 than edema. Although it is not clear whether an intrinsic progressive hippocampal disease caused the seizures or whether the seizures caused progressive hippocampal damage, kindling studies in animals have

provided evidence that seizure activity per se can cause progressive hippocampal damage and HS (Bertram *et al.* 1990; Cavazos, Sutula, 1990; Cavazos *et al.* 1994). This case is therefore consistent with the hypothesis that HS may be both the cause and consequence of seizures originating in the temporal lobe (Pringle *et al.* 1993; Sloviter, 1994).

7.5.2.3. UNEXPLAINED HIPPOCAMPAL VOLUME LOSS. One patient *(Figure 45, p 159)* had an unusual asymmetry of the hippocampal bodies at baseline and progressive HCV loss of the larger hippocampus on follow-up despite good seizure control. It is unclear what the underlying pathology or mechanism of HCV loss is, or whether this could progress to HS.

7.5.3. THE ASSOCIATION OF A PROGRESSIVE SEIZURE HISTORY AND HIPPOCAMPAL DAMAGE.

Glaser (Glaser, 1987) and French et al (French *et al.* 1993) observed that seizures in mesial TLE may progressively become worse and suggested that this may be indicative of a progressive disease. Hauser (Hauser, 1992) estimated that between 5-10% of patients with newly identified CPS will not be controlled on AED and may progress. Elwes et al (Elwes *et al.* 1988) reported a decreasing interval between SGS in patients who had presented with between two and five untreated SGS, in keeping with an escalating process of epilepsy in the early stages. The data show that a pattern of seizures, characterized by SPS or CPS at onset of the habitual epilepsy followed later by SGS, was associated with MRI-evidence of hippocampal damage. Whether patients with this and other seizure patterns who had a normal baseline and follow-up MRI at 1 year will show hippocampal changes after a longer follow-up period will be determined at the planned 4-year follow-up.

CHAPTER VIII. THE AMYGDALA AND INTRACTABLE TEMPORAL LOBE EPILEPSY: A QUANTITATIVE MAGNETIC RESONANCE IMAGING STUDY

8.1. ABSTRACT.

The aim of this study was to establish a quantitative MRI technique using T2 relaxation time mapping to investigate systematically the amygdalae in patients with intractable TLE. Identification of a focal abnormality on MRI in patients with intractable TLE is important, because outcome from surgery depends largely on the removal of the underlying pathology. HS is the most common cause of intractable TLE, but epileptogenic lesions can be confined to the amygdala. Twenty control subjects and 82 patients with intractable TLE were studied. Patients who had FTLs visible on standard MRI were excluded. All subjects had a HCT2 map and HCV measurement, and an AT2 map. Forty-four of the 82 patients (54%) had an abnormal AT2, which was bilateral in 18. Forty-four patients (54%) had unilateral HS on MRI, 25 (57%) of whom had an abnormal AT2. Seven patients (8%) had bilateral HS, four of whom had an abnormal AT2. Thirty-one patients (38%) had normal quantitative hippocampal measures, 15 of whom had an abnormal AT2, which was bilateral in seven. FLAIR imaging where appropriate confirmed that the increased AT2 signal was due to parenchymal changes. Neuropathological correlates of an increased AT2 included microdysgenesis in one, and gliosis in three patients. A small hypodense lesion in the amygdala of one patient was a DNET. Patients with an isolated AT2 abnormality were significantly older at the onset of habitual epilepsy and rarely had a history of FCs in comparison with patients who had HS. An isolated AT2 abnormality correlated well with interictal EEG findings. In conclusion, the combination of AT2 mapping and FLAIR is a sensitive method to detect lesions which are not seen on standard MRI scans in the amygdalae of patients with intractable TLE. Further correlation studies will be required to define the role of this technique in the presurgical evaluation of patients with intractable TLE.

8.2. INTRODUCTION.

Lesions of mesial temporal structures can cause amygdalohippocampal seizures, which may have characteristic electro-clinical features (Commission on classification and terminology of the International League Against Epilepsy, 1989). The nature of these lesions and the extent of resection determines seizure outcome

after surgery for intractable TLE *(see pathology and outcome with respect to seizures, p 43)*. MRI allows identification of these lesions preoperatively. HS is the most frequently encountered cause of intractable TLE, accounting for 50-70% of cases *(see HS and other pathological lesions, p 40)*. Surgery renders 60-70% of these patients with HS seizure free.

The amygdala is an important source of epileptic seizures but has received less attention than the hippocampus *(see p 44)*. Neuropathological studies have demonstrated isolated lesions confined to the amygdala in patients with intractable TLE. These lesions include small tumors, which have a predilection for the amygdala (Falconer, Cavanagh, 1959), vascular lesions (Falconer, Cavanagh, 1959; Bruton, 1988), AS (Hudson *et al.* 1993; Miller *et al.* 1994), CD (Bruton, 1988), microdysgenesis (Feindel *et al.* 1991) and abnormal glial cells (Bruton, 1988). Further, gliosis affects the ipsilateral amygdala in 50-75% of patients with classical HS (Sano, Malamud, 1953; Falconer *et al.* 1964; Margerison, Corsellis, 1966; Bruton, 1988). These lesions of the amygdala may be detected on MRI (Kuzniecky *et al.* 1987; Feindel *et al.* 1991), but systematic studies using visual assessment found that the detection rate of these lesions was low (Kuzniecky *et al.* 1987; Hudson *et al.* 1993; Miller *et al.* 1994; Bronen *et al.* 1995).

To increase the detection rate of lesions in the amygdala, a quantitative MRI technique was established using T2 relaxometry to study the amygdalae systematically and in a standardized way in patients with intractable TLE. In this study, the results of AT2 mapping in control subjects and patients with intractable TLE are reported (Van Paesschen *et al.* 1996b).

8.3. METHODS.

8.3.1. SUBJECTS.

Twenty controls (M = 9, W = 11) with median age of 27 years (range: 21-37) and 82 patients with median age of 31 years (range: 14 - 64) were included in the study. All patients had clinical evidence of intractable TLE (Commission on classification and terminology of the International League Against Epilepsy, 1989), with concordant interictal EEG findings, and were in various stages of presurgical evaluation. Fifty-six patients (68%) had ictal video-EEG recordings confirming the diagnosis of TLE. All patients had a standard MRI scan *(see p 53)* of the brain that did not reveal a FTL on visual inspection of the hard copies.

8.3.2. CLINICAL EVALUATION: *see p 52.*

8.3.3. MR IMAGING.

8.3.3.1. HCT2 MAP: *see p 55.*

8.3.3.2. HCV MEASUREMENT: *see p 57.*

8.3.3.3. AT2 MAP: *see p 67.*

8.3.3.4. FLAIR: *see p 69.*

An MRI diagnosis of HS was made using a combination of qualitative assessment of T1- and T2-weighted MR images together with quantitative assessment of HCT2, HCV corrected for ICV, HCVR and inspection of a HCV distribution graph compared against a control graph *(see Chapter 4)*.

8.4. RESULTS.

8.4.1. CONTROLS.

The AT2 values were normally distributed in the 20 control subjects examined. The mean control AT2 (± SD) was 99.3 ± 2.5 msec, ranging from 95 to 104 msec. There were no significant gender or right-left differences. The mean difference between left and right AT2 was 0.35 ± 1.42 msec. An AT2 value ≥ 105 msec (i.e. more than 2 SD above the mean control value) or a side-to-side difference of ≥ 5 msec (i.e. 3 SD above mean control values or higher) were considered as abnormal. An abnormal AT2 signal was considered lateralized if there was a unilateral increased AT2 ≥ 105 msec, or if the side-to-side difference was ≥ 5 msec. Test-retest intra rater repeatability was -0.01 ± 0.66 msec and inter rater repeatability was 0.02 ± 0.73 msec.

8.4.2. PATIENTS.

A total of 44 of 82 patients (52%) had an abnormal AT2 map. Thirty-five of these 44 patients (80%) had an AT2 ≥ 105 msec, which was bilateral in 18. The median value of the higher AT2 of these 35 patients was 108 msec (range: 105-113 msec). Eight of these 44 patients (18%) had an AT2 within normal limits, but which

was ≥ 5 msec above that of the other side. One of these 44 patients (2%) had a hypodense lesion in the amygdala.

8.4.3. SUBDIVISION OF PATIENTS ACCORDING TO QUANTITATIVE MRI RESULTS.

Patients were subdivided according to quantitative hippocampal and amygdala measures *(Figure 47, p 169)*.

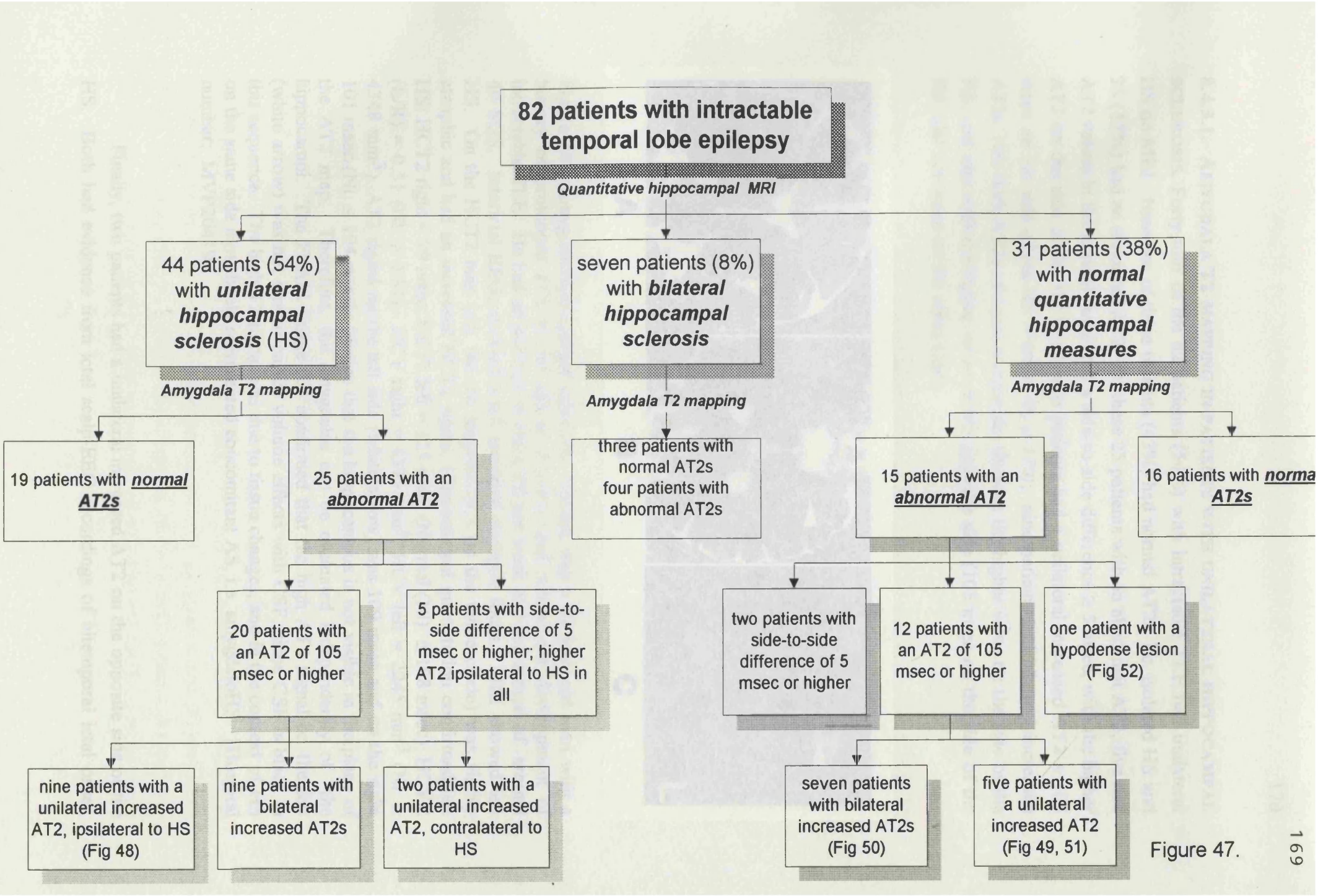
82 patients with intractable temporal lobe epilepsy
Quantitative hippocampal MRI
44 patients (54%) with unilateral hippocampal sclerosis (HS)
seven patients (8%) with bilateral hippocampal sclerosis
31 patients (38%) with normal quantitative hippocampal measures
Amygdala T2 mapping
Amygdala T2 mapping
Amygdala T2 mapping
19 patients with normal AT2s
25 patients with an abnormal AT2
three patients with normal AT2s four patients with abnormal AT2s
15 patients with an abnormal AT2
16 patients with norma AT2s
20 patients with an AT2 of 105 msec or higher
5 patients with side-to-side difference of 5 msec or higher; higher AT2 ipsilateral to HS in all
two patients with side-to-side difference of 5 msec or higher
12 patients with an AT2 of 105 msec or higher
one patient with a hypodense lesion (Fig 52)
nine patients with a unilateral increased AT2, ipsilateral to HS (Fig 48)
nine patients with bilateral increased AT2s
two patients with a unilateral increased AT2, contralateral to HS
seven patients with bilateral increased AT2s (Fig 50)
five patients with a unilateral increased AT2 (Fig 49, 51)

Figure 47.

8.4.3.1. AMYGDALA T2 MAPPING IN PATIENTS WITH UNILATERAL HIPPOCAMPAL SCLEROSIS. Forty-four of the 82 patients (54%) with intractable TLE had unilateral HS on MRI. Nineteen of these patients (43%) had normal AT2s, i.e. isolated HS and 25 (57%) had an abnormal AT2. Of these 25 patients with an abnormal AT2, five had AT2 values in the normal range, but a side-to-side difference ≥ 5 msec, with the higher AT2 on the side of the HS in all; nine patients had a unilateral increased AT2 ≥ 105 msec on the side of the HS *(Figure 48, p 170)*; nine patients had bilateral increased AT2s, two with AT2s of equal magnitude, six with the higher value on the side of the HS, and one with the higher value on the opposite side (105 msec on the side of the HS, and 106 msec on the other side).

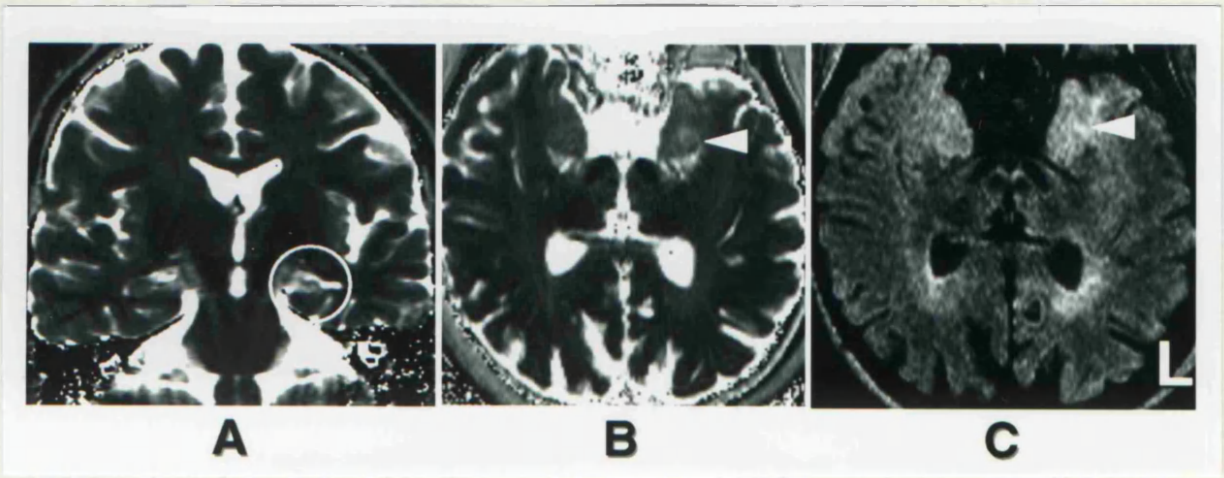

Figure 48. Amygdalohippocampal sclerosis. Patient was a 42 year old man with a history of prolonged FCs at the age of 2 years, and subsequent development of intractable TLE. He had an average of one CPS per week and had a total of around 40 SGS. Interictal EEGs showed a left temporal epileptic focus. MRI showed left HS. On the HCT2 map (A), the left hippocampus (in the white circle) was visibly atrophic and had an increased HCT2 signal. Hippocampal quantitation confirmed left HS: HCT2 right = 99 msec, HCT2 left = 125 msec (Normal (Nl): ≤ 108 msec); HCVR (L/R) = 0.51 (Nl: ≥ 0.87); HCV right = 4375 mm^3, HCV left = 2245 mm^3 (Nl: ≥ 4348 mm^3). AT2 signal on the left side (white arrow) was 109 msec and on the right 101 msec (Nl: ≤ 104 msec). Notice that the hippocampus is not visible in the plane of the AT2 map. Therefore, the amygdalae can be evaluated independently of the hippocampi. The FLAIR image (C) confirmed that the high AT2 signal on the left (white arrow) was not due to partial volume effects with CSF, since CSF is black in this sequence. The high T2 signal was due to tissue changes, and in the context of HS on the same side most likely represented concomitant AS, i.e. amygdaloHS. [Hospital number: MVP20419].

Finally, two patients had a unilateral increased AT2 on the opposite side of the HS. Both had evidence from ictal scalp-EEG recordings of bitemporal ictal onset.

Hippocampal quantitative measures were unusual in one of these two patients: HCT2 right = 105 msec, HCT2 left = 114 msec (Nl: ≤ 108 msec), HCVR (L/R) = 0.97 (Nl: ≥ 0.87), HCV right = 4510 mm^3, HCV left = 4371 mm^3 (Nl: ≥ 4348 mm^3), AT2 right = 107 msec, AT2 left = 104 msec (Nl: ≤ 104 msec). This patient probably had left HS (i.e. increased HCT2 signal and HCV in the low normal range), but some damage of the right hippocampus, in view of the hippocampal symmetry, could not be excluded. This patient had depth-EEG studies with recording of three seizures. One seizure started in the left, and two in the right mesial temporal structures, one with the first EEG changes in the right amygdala, the other with the first EEG changes in the right hippocampus.

8.4.3.2. AMYGDALA T2 MAPPING IN PATIENTS WITH BILATERAL HIPPOCAMPAL SCLEROSIS. Seven of the 82 patients (8%) with intractable TLE had bilateral HS on MRI. Three of these patients had normal AT2s, two had bilateral increased AT2s, one had a unilateral increased AT2 and one had AT2s within normal limits, but a side-to-side difference of 5 msec.

8.4.3.3. AT2 MAPPING IN OTHERWISE MRI-NEGATIVE PATIENTS. Thirty-one of the 82 patients (38%) with intractable TLE had a normal standard MRI and normal quantitative hippocampal measures. AT2 mapping was normal in 16 of these 31 patients (52%). AT2 mapping showed an abnormality in 15 of these 31 apparently MRI-negative cases (48%). Twelve of these patients had an AT2 ≥ 105 msec, which was bilateral in seven. Two patients had AT2 values within normal limits but a side-to-side difference ≥ 5 msec, and one patient had a hypodense lesion in one amygdala and exhibited an abnormally low AT2 within this lesion.

8.4.3.3.1. FLAIR and AT2 abnormality. A FLAIR image in the same plane as the AT2 map was useful to confirm that an increased AT2 signal was not due to CSF, and was helpful for the visual assessment of increased AT2 signals. Nine of the 15 patients with normal standard MRI and hippocampal quantitation but abnormal AT2 had a lesion which was detectable on visual assessment of the AT2 map and FLAIR. Five of these had a focal or nodular hyperintense T2 signal in the amygdala *(Figure 49, p 173; Figure 50, p 175)*, three had a more diffuse increased T2 signal throughout the amygdala *(Figure 51, p 176)*, and one had a focal lesion which was hypodense on the AT2 map, and hyperintense on a T1-weighted image *(Figure 52, p 177)*. In the remaining six of these 15 patients, an abnormal AT2 signal was measured, which was not appreciated on visual assessment of AT2 map or FLAIR. The T2 signal

of the small and focal lesions measured with a ROI confined to the lesion was higher than when measured with the larger ROI as defined for this study *(Figure 50, p 175)*.

Figure 49: *see p 174.* Microdysgenesis of the amygdala. Patient was a 25 year old man with onset of TLE at the age of 16 years. There was no history of FCs, meningitis or cerebral trauma. An aura was characterized by a strange cephalic sensation, dizziness, an epigastric rising sensation, a diffuse warm sensation and déjà vu. A CPS was characterized by unresponsiveness, staring and prominent oral automatisms. He had an average of five CPS per week, and never had a SGS. Interictal EEG showed left fronto-temporal epileptic activity. Ictal EEG showed left sided onset without clear localization.

Standard MRI was normal and hippocampal quantitation was normal: HCT2 right = 102 msec, HCT2 left = 108 msec (Nl: ≤ 108 msec), HCVR (L/R) = 0.92 (Nl: ≥ 0.87), HCV right = 5925 mm^3, HCV left = 5471 mm^3 (Nl: ≥ 4348 mm^3). The AT2 map (A) revealed an increased AT2 of 108 msec on the left and a normal AT2 of 102 msec on the right. The FLAIR image (B) - for this patient not in the same plane as the AT2 map- showed a lesion with increased T2 signal in the posterior aspect of the left amygdala (white arrow), which was also visible on the AT2 map, but was initially mistaken for CSF. Patient underwent an anterior temporal lobe resection with amygdalectomy and minimal hippocampal resection. A sagittal section of the unreformatted MPRAGE shows the left hippocampus and amygdala (C; T = tail of hippocampus; B = body of hippocampus). The white box corresponds to the location of the resected specimen shown in (D).

The resected specimen shows the resected left amygdala, cut in the sagittal direction, and the anterior part of the head of the hippocampus (Magnification: x12). Microscopic examination of the posterior aspect of the amygdala (indicated by the white box) revealed abnormal clusters of neurons admixed with primitive neuroblast-like cells (E) (Magnification: x170). This region corresponded to the region of the abnormal AT2 signal. In the resected temporal neocortex, heterotopic neurons were seen in the white matter and the molecular layer. These findings were consistent with a diagnosis of microdysgenesis. Patient has been seizure free for more than two years after surgery. [Hospital number: MVC16347].

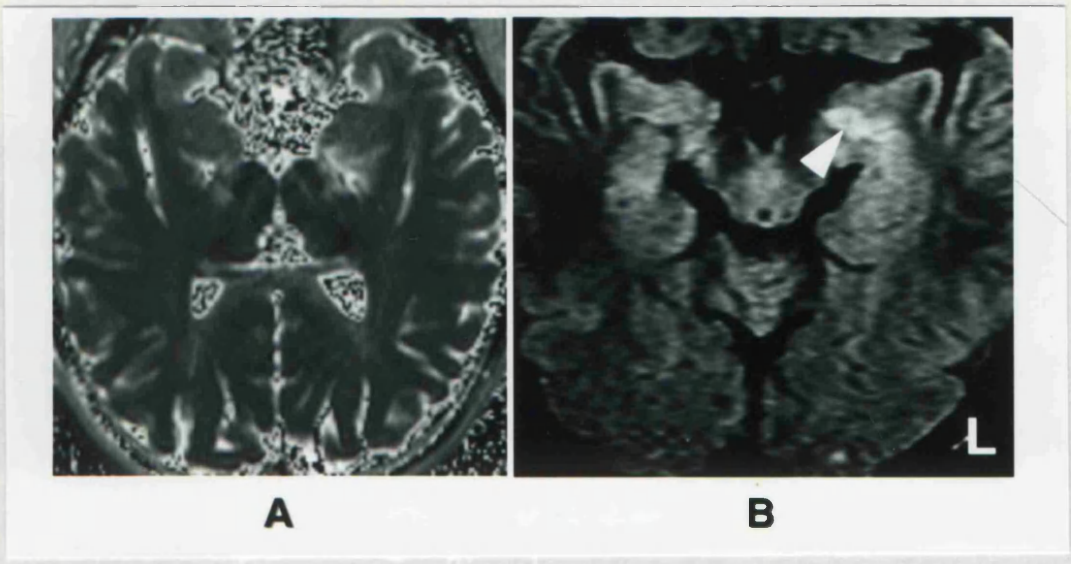
L
A
B

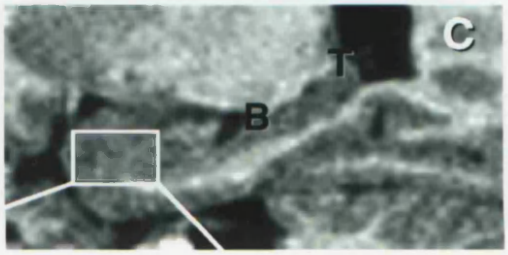
C
T
B

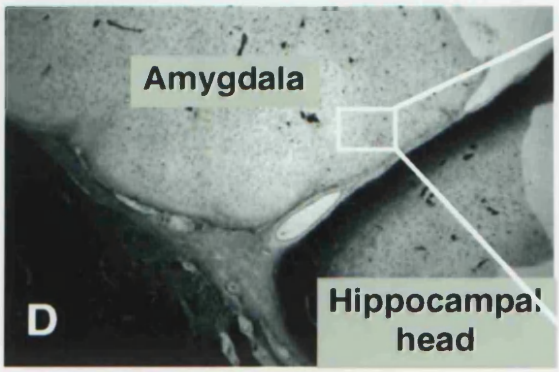
Amygdala
Hippocampal
head
D

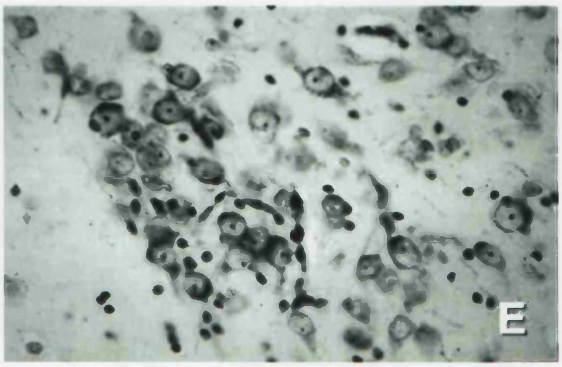
E

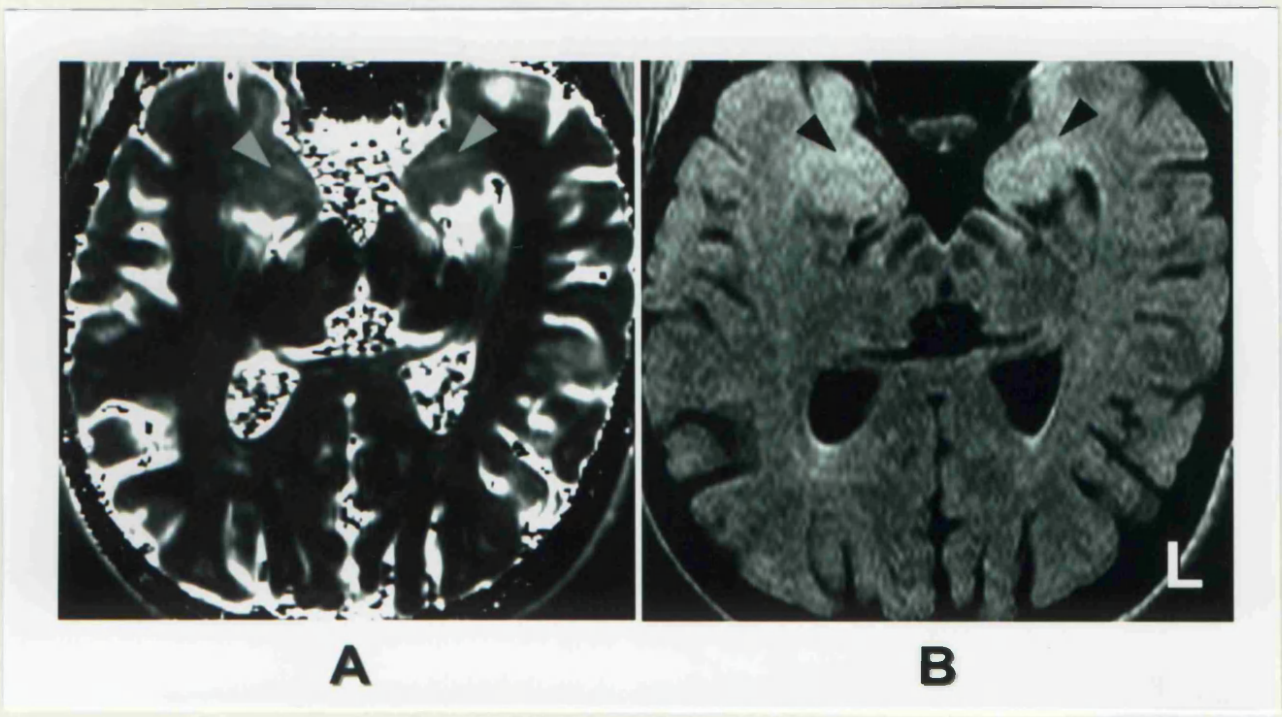

Figure 50. Isolated bilateral AT2 abnormalities. Patient was a 26 year old woman who had a FC at the age of two years and subsequently developed intractable TLE from the age of five years. Auras were characterized by panic, an epigastric rising sensation and déjà vu. Interictal EEGs showed bilateral fronto-temporal epileptiform discharges. A standard MRI was normal and hippocampal quantitation was normal: HCT2 right = 108 msec, HCT2 = 108 msec (Nl: ≤ 108 msec), HCVR = 0.98 (Nl: ≥ 0.87), HCV right = 5530 mm^3, HCV left = 5402 mm^3, (Nl: ≥ 4348 mm^3). The AT2 map (A) showed bilateral increased AT2 values of 109 msec on the right, and 108 msec on the left (Nl: ≤ 104 msec). The T2 values of the brighter regions in the amygdalae (gray arrows), measured with a small circle, were 119 msec on the right and 121 msec on the left. The FLAIR image (B) showed bilateral increased signals in the amygdalae with a streak-like and elongated shape (black arrows), in the same position as those seen on the AT2 map, confirming the tissue origin of the increased signal. [Hospital number: QSC28724].

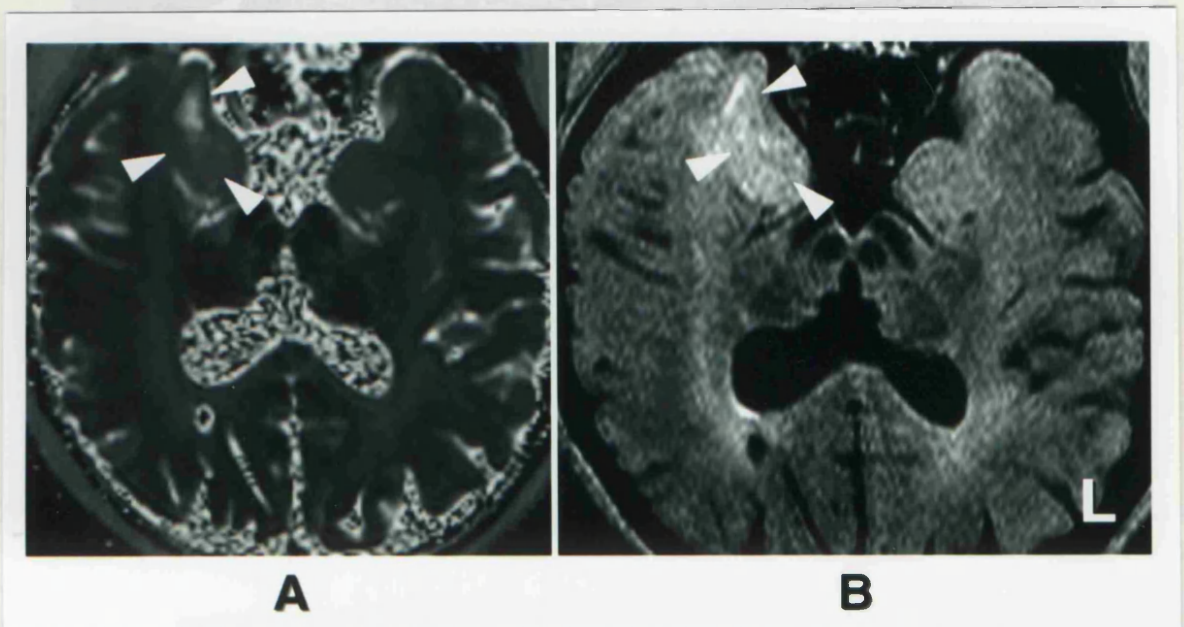

Figure 51. Isolated hyperdense lesion of the amygdala. Patient was a 54 year old man with onset of TLE at the age of 21 years. There was no history of FCs, or meningitis. He had an average of one CPS per month and had a total of four SGS. Interictal EEG showed a clear right antero-temporal epileptic focus. Standard MRIs were all reported as normal. Hippocampal quantitation was normal: HCT2 right = 108 msec, HCT2 left = 104 msec (Nl: ≤ 108 msec), HCVR (R/L) = 0.99 (Nl: ≥ 0.87), HCV right = 5018 mm^3, HCV left = 5079 mm^3 (Nl: ≥ 4348 mm^3). On visual inspection of the AT2 map (A), there was an increased T2 signal throughout the right amygdala, and a triangular shaped region of increased T2 signal anterior to the right amygdala (white arrows). The AT2 on the right was 113 msec, and on the left was 100 msec (Nl: ≤ 104 msec). The FLAIR image (B) confirmed that this increased T2 signal was not due to CSF, but due to tissue changes in this region (white arrows). [Hospital number: QSA77724].

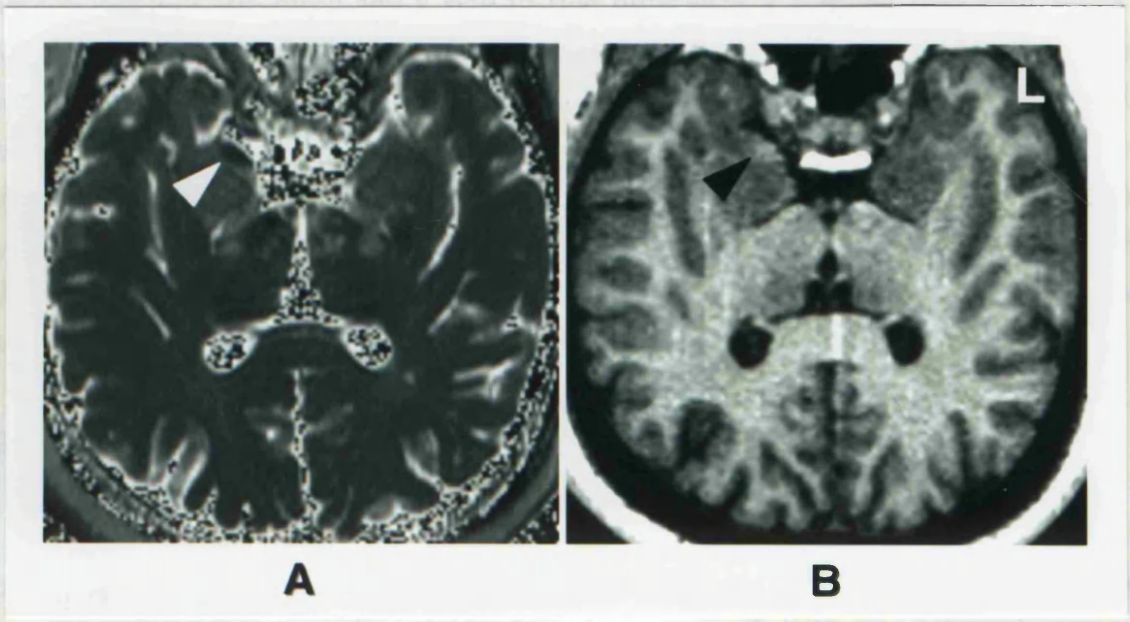

Figure 52. Isolated hypodense lesion of the amygdala. Patient was a 42 year old man with onset of TLE at the age of 9 years. There was no history of FCs, meningitis or cerebral trauma. A typical aura was characterized by a déjà vu, fear, an epigastric rising sensation, gustatory and olfactory hallucinations, and an experiential sensation that time went by 4 times as fast as usual. A CPS was characterized by unresponsiveness, oral automatisms and automatisms of the right arm and hand. He had an average of three CPS per week and never had a SGS. Interictal EEG showed a right antero-temporal epileptic focus, and ictal EEG showed bilateral discharges for the first ten seconds followed by right antero-temporal rhythmic theta waves. A standard MRI was normal and hippocampal quantitation was normal: HCT2 right = 105 msec, HCT2 left = 99 msec (Nl: ≤ 108 msec), HCVR (L/R)= 0.95 (Nl: ≥ 0.87), HCV right = 5321 mm^3, HCV left = 5049 mm^3 (Nl: ≥ 4348 mm^3). The AT2 map (A) showed a hypodense lesion (white arrow) in the right amygdala near the uncinate gyrus. The AT2 as defined for this study was normal in both amygdalae, on the right 100 msec and on the left 98 msec. However, the T2 measured with a ROI which fitted this hypodense lesion was 70 msec. This lesion was also visible as an intra-axial hyperdense lesion (black arrow) on a 1 mm thick T1-weighted section of the reformatted MPRAGE dataset (B), which was used to determine the coordinates of the AT2 map. The patient underwent an anterior temporal lobe resection with amygdalectomy and minimal hippocampal resection. Neuropathological examination of the resected amygdala showed a small DNET. Patient has remained seizure free after surgery. [Hospital number: QSB18240].

8.4.3.3.2. Interictal EEG and isolated amygdala T2 abnormalities. Nine of the 15 patients with normal hippocampi and an abnormal AT2 had a lateralized abnormality on the AT2 map (i.e. five with an unilateral AT2 ≥ 105 msec, two with bilateral AT2s ≥ 105 msec and a side-to-side difference ≥ 5 msec, two with AT2s in the normal range and a side-to-side difference ≥ 5 msec, and one with a hypodense lesion). Eight of these nine patients had an epileptiform abnormality over the concordant temporal lobe, and one had bitemporal slowing. Six patients had a non-lateralized abnormal AT2 map (i.e. bilateral increased AT2s and side-to-side difference < 5 msec). Three of these had a unilateral epileptiform abnormality over the temporal lobe with the higher AT2 signal, and three had bilateral epileptiform abnormalities over the temporal, fronto-temporal and frontal lobes respectively.

8.4.4. NEUROPATHOLOGICAL CORRELATIONS.

So far, three patients with an isolated abnormal AT2 signal underwent an anterior temporal lobe resection with amygdalectomy and minimal hippocampal resection. One of these patients had AS, and one year after the operation, there was a 75% reduction in seizure frequency. The second patient had microdysgenesis (without gliosis) of the resected amygdala and temporal neocortex and has been seizure free for more than two year after surgery *(Figure 49, p 173)*. The third patient had a small DNET and has remained seizure free so far *(Figure 52, p 177)*.

To date, twenty-seven patients with unilateral HS, 14 of whom had an ipsilateral increased AT2 signal, have been operated on. Amygdala specimens of two of these patients were available. The AT2 values of the resected amygdala of these two patients were increased, and were 110 and 112 msec respectively. In both cases, neuropathological examination of a GFAP stained section revealed gliosis of the amygdala.

8.4.5. CLINICAL CORRELATIONS.

Clinical data of patients with isolated unilateral HS, unilateral amygdaloHS, an isolated AT2 abnormality and normal standard and quantitative MRI were compared *(Table 15, p 179)*. A history of FCs was obtained predominantly in the groups with HS with or without concomitant amygdala abnormality. As a group, patients with HS were younger at the onset of their habitual epilepsy and at the age of evaluation than patients with an isolated AT2 abnormality or normal MRI. Duration of habitual epilepsy, seizure types and frequencies, and the frequency of a family history of epilepsy or FCs and history of meningo-encephalitis did not differ between the groups.

	Isolated unilateral HS	Unilateral amygdaloHS	Normal MRI	Isolated AT2 abnormality	p
n	19	23	16	15	
Age	34 (9)	27 (7)	37 (12)	36 (11)	0.01 (a)
Age onset habitual epilepsy	7 (0 to 43)	5 (0 to 30)	14 (6 to 38)	16 (1 to 40)	0.005 (b)
Duration of epilepsy	27 (4 to 40)	19 (1 to 37)	20 (4 to 40)	23 (7 to 34)	NS (b)
Febrile convulsions	11 (58%)	15 (65%)	1 (6%)	2 (13%)	0.00012 (c)
Meningo-encephalitis	2 (10%)	2 (8%)	1 (6%)	0 (0%)	NS (c)
First degree relative with FC or epilepsy	5 (26%)	3 (13%)	3 (18%)	1 (6%)	NS (c)
Number of patients reporting auras	16 (84%)	21 (91%)	14 (88%)	10 (67%)	NS (c)
Number of CPS per week	2 (0.25 to 21)	2 (0.25 to 30)	2 (0 to 25)	1 (0 to 10)	NS (b)
Estimated total number of SGS	7 (0 to 400)	5 (0 to 1800)	6 (0 to 1200)	20 (0 to 900)	NS (b)

Table 15. AT2 mapping and clinical correlations. The data are presented as mean (SD), median (range), or number of patients (percentage of group total).(a): one-way ANOVA, (b): Kruskal-Wallis, (c): Fisher's Exact test.

8.5. DISCUSSION.

8.5.1. METHODOLOGY.

AT2 mapping is a new MRI approach to the study of patients with intractable TLE. It is similar in principle to HCT2 mapping (Jackson *et al.* 1993b), but the orientation is in a tilted axial plane through the amygdala (Kuzniecky, Jackson, 1995). This plane allows the evaluation of the amygdala independently of the hippocampi, which are not visualized in this plane. The standardized determination of the orientation of the amygdala images is of critical importance. The thickness is only 5 mm instead of 8 mm of the HCT2 map, which would be too large for the size of the amygdala. The range of abnormally high AT2 signals (105-113 msec) was considerably smaller than the HCT2 signal range in HS (109-142 msec) *(Chapter 3 and 4)*. The largest circle which could be fitted into the amygdala as a ROI was used to measure the AT2. In patients with small focal lesions with a high T2 signal in the amygdala, the use of a large circle, as defined in the present study, led to a lower AT2 reading than the AT2 value of the lesion itself. The same measurement technique was used for purposes of standardization and reproducibility, which was found to be excellent.

8.5.2. VISUAL ASSESSMENT OF ABNORMAL AMYGDALA T2 SIGNALS.

Detection of an increased AT2 signal is difficult on visual assessment of the MRI. Bronen et al (Bronen *et al.* 1995) reported an increased AT2 signal on visual inspection of MR scans of only two of 48 patients (4%) with HS, and Miller et al (Miller *et al.* 1994) reported an increased AT2 signal in only two of 11 patients (18%) with neuropathological evidence of isolated AS. The sensitivity of detecting an abnormal signal on visual inspection of a hard copy of the image with TE =118 msec (from the set of images used to calculate the AT2 map) was 38% (Van Paesschen *et al.* 1995a).

8.5.3. AMYGDALOHIPPOCAMPAL SCLEROSIS AND ISOLATED HIPPOCAMPAL SCLEROSIS.

Pathological studies have shown AS to be present on the side of classical HS in 50-76% of cases (Sano, Malamud, 1953; Falconer *et al.* 1964; Margerison, Corsellis, 1966; Bruton, 1988). In this current study, an abnormal AT2 signal was detected on the side of classical HS in 23 of 44 patients (52%) with unilateral HS. Cendes et al

(Cendes *et al.* 1993b), using amygdala volumetry, detected atrophy on the side of the smaller hippocampus in a similar percentage of patients. In the present study amygdala volumetry had a poor repeatability, with a RC (Bland, Altman, 1986) of more than 20%, and was therefore not used to study these patients. Neuropathological studies revealed the presence of gliosis of the amygdala in two patients with unilateral HS who had an increased AT2 signal on the same side, which indicates that AT2 mapping is able to detect AS. Amygdala tissue was available for neuropathological examination for only two of the 27 patients with unilateral HS operated on so far, which highlights one of the difficulties which has hampered the study of the role of the amygdala in TLE (Gloor, 1992a; Gloor, 1992b).

Clinical features of patients with isolated HS did not differ significantly from those with amygdaloHS, which is in agreement with the observations of Falconer et al (Falconer *et al.* 1964) and Bruton (Bruton, 1988). Gambardella et al (Gambardella *et al.* 1995) however reported that patients with amygdala atrophy experienced significantly more SGS per year compared to patients with isolated HS. It is possible that the pathologies detected by AT2 mapping and amygdala volumetry are not identical, and clinical characteristics therefore not comparable. Also, differences in reporting SGS frequency might explain this discrepancy.

Two patients had the unusual combination of unilateral HS and a contralateral increased AT2. Other unusual features in these two patients were the late age of onset (26 and 30 years respectively), with no evidence of prior cerebral insult, such as FC or meningitis. One of these had two different types of seizure onset. Further, these were the only patients in the study with unilateral HS and independent bitemporal onset of seizures on ictal scalp-EEG studies. Ictal depth-EEG recordings in one of these patients showed ictal onset in the amygdala with the abnormal AT2.

8.5.4. ISOLATED LESIONS OF THE AMYGDALA.

Thirty-one patients (38%) with intractable TLE had a normal standard MRI and normal quantitative hippocampal measures and were considered MRI-negative. In 15 of these 31 patients (48%) the AT2 map showed an abnormal signal, which was bilateral in 7 (47%). This is a higher rate of bilateral abnormality than was found with HCT2 values, which was observed in 16-29% of patients with HS *(Chapters 3 and 4)*. A FLAIR image was useful to confirm that the high signal was of parenchymal origin and not due to partial volume effects with CSF. FLAIR has already been shown to be

useful to detect abnormalities in the amygdala in patients with TLE, which were not apparent on standard MRI (Bergin *et al.* 1995).

Compared with patients with HS, patients with an isolated abnormality of the amygdala did not have a history of FCs, and had the onset of their habitual epilepsy at a significantly older age, in agreement with previous findings (Cavanagh, Meyer, 1956; Falconer *et al.* 1964; Duncan, Sagar, 1987; Bruton, 1988; Cendes *et al.* 1993a; Kuks *et al.* 1993; Maher, McLachlan, 1995). The results also concur with the observations of Miller et al (Miller *et al.* 1994) in patients with isolated AS. Berkovic et al (Berkovic *et al.* 1995) observed that 36% of patients with TLE and normal standard MRI had a good seizure outcome following temporal lobe resection. This group was characterized on ictal SPECT by a pattern of unilateral anteromesial temporal hyperperfusion, suggesting that the epileptogenic zone was confined to the anteromesial temporal lobe (Ho *et al.* 1995). It is possible that some of these patients might have had a unilateral lesion of the amygdala which was undetected on standard qualitative MRI, but which might have been detected by AT2 mapping and FLAIR imaging.

8.5.5. NEUROPATHOLOGY OF EPILEPTOGENIC LESIONS OF THE AMYGDALA.

A variety of lesions were detectable on visual assessment of the AT2 map and the FLAIR image, ranging from small nodules to a diffuse increase of the AT2 signal. This probably reflects the wide range of lesions that may occur in the amygdalae of patients with intractable TLE, which have been described in the neuropathological literature. Falconer et al (Falconer, Cavanagh, 1959) and Bruton (Bruton, 1988) documented several patients with small tumors and vascular anomalies confined to the amygdala, who became seizure free after temporal lobe resection. They noted that small tumors have a predilection for the amygdala and rarely affect the hippocampus. Bruton (Bruton, 1988) described four patients in his group of 21 patients with indefinite pathology, who had unusually large, hyperchromatic glial cells, resembling giant astrocytes scattered in an otherwise normal amygdala, which possibly represented a subtle glial abnormality. He noted that these four benefited from surgery in contrast to the other patients in this group, who did poorly. Bruton (Bruton, 1988) also reported cortical dysplasia of the amygdala as a cause of intractable TLE.

To date, three patients with an isolated increased AT2 have undergone an anterior temporal lobe resection with amygdalectomy and minimal resection of the hippocampus. One of these three patient had AS, and had a 75% reduction in seizure

frequency after one year. Hudson et al (Hudson *et al.* 1993) reported 11 patients with isolated AS, who represented 10% of the patients who were operated for intractable TLE. Only three of these 11 patients (27%) became seizure free after surgery, which suggested that AS was not the epileptogenic zone. They concluded that AS might be associated with a more widespread epileptogenic abnormality, which was not detected on microscopic examination of the resected temporal lobe.

The second patient who underwent an anterior temporal lobe resection with amygdalectomy and minimal resection of the hippocampus had microdysgenesis of the amygdala and temporal neocortex and has been seizure free for more than two years. Microdysgenesis is the microscopic variant of cortical dysplasia (Meencke, Janz, 1984). Microdysgenesis of the amygdala as a cause of intractable TLE has been reported by Feindel et al (Feindel *et al.* 1991). Microdysgenesis has been reported previously to be not detectable on MRI (Meencke, 1994; Vital *et al.* 1994a; Raymond *et al.* 1995). In the patient in this study however there was a clearly increased T2 signal corresponding to the location of abnormal clusters of neurons admixed with primitive neuroblast-like cells in the posterior aspect of the amygdala.

The third patient had a small DNET and is doing well after surgery. Falconer et al (Falconer, Cavanagh, 1959) and Bruton (Bruton, 1988) reported several patients with small tumors confined to the amygdala, who became seizure free after temporal lobe resection, and noted that small tumors have a predilection for the amygdala.

This neuropathological variety of epileptic lesion of the amygdala is in contrast to the limited range of epileptic lesions of the hippocampus, which is predominantly HS. Atrophy is probably not a feature of a majority of these epileptogenic amygdala lesions. AT2 mapping in combination with FLAIR imaging therefore might be a better technique than amygdala volumetry to detect these lesions.

8.5.6. SURGICAL TECHNIQUES FOR TLE.

Several surgical techniques have been described for patients with TLE (Penfield, Baldwin, 1952; Wieser, Yasargil, 1982; Feindel, Rasmussen, 1991; Rasmussen, Feindel, 1991; Goldring *et al.* 1992). Feindel (Feindel, Rasmussen, 1991) and Rasmussen (Rasmussen, Feindel, 1991) noted that seizure outcome was similar for patients who underwent temporal lobe resection with amygdalectomy and minimal hippocampal resection as for those who underwent a standard temporal lobe resection with major hippocampectomy. They concluded that resection of the amygdala might

be crucial for a good seizure outcome. Goldring et al (Goldring *et al.* 1992) on the other hand reported outcome results similar to those of Feindel and Rasmussen using an anterior temporal lobe resection that spared the amygdala. So far, no guidelines have been formulated for the indications of each of these surgical techniques.

Formulating these guidelines would be important since Milner (Milner, 1978) and Smith and Milner (Smith, Milner, 1981) reported that memory functions of patients who underwent an anterior temporal lobe resection with amygdalectomy and minimal hippocampal resection were significantly better than those of patients who had undergone an operation with major hippocampectomy. Trenerry et al (Trenerry *et al.* 1993a) reported that MRI HCV data provided meaningful information in evaluating the risk for memory impairment following temporal lobe resection, and stressed the detrimental effect on memory functions of removing a non atrophic left hippocampus. Miller et al (Miller *et al.* 1994) reported that the memory functions of patients with isolated AS deteriorated after standard temporal lobe resection, including the intact hippocampus, compared to patients with amygdaloHS, who underwent the same operation. Several other studies have demonstrated the importance of the hippocampus (Scoville, Milner, 1957; Penfield, Milner, 1958; Penfield, Mathieson, 1974; Lencz *et al.* 1992; Miller *et al.* 1993; Rausch, Babb, 1993; Sass *et al.* 1994; Incisa della Rocchetta *et al.* 1995) but not the amygdala (Zola-Morgan *et al.* 1989) for memory functions. With the presented quantitative MRI protocol of mesial temporal structures, it might be possible to provide better presurgical information.

8.5.7. MRI-NEGATIVE INTRACTABLE TLE.

An important subgroup of 16 patients (20%) had intractable TLE with normal standard MRI, hippocampal quantitation and AT2 map. This is in accordance with pathological studies before MRI was available. Corsellis (Corsellis, 1970) reported that no definite structural abnormality could be found in 20% of post-operative specimens of patient with intractable TLE, Green and Scheetz (Green, Scheetz, 1964) found an incidence of 18%, although Jensen and Klinken (Jensen, Klinken, 1976) reported only 3 out of 78 patients (4%) with no structural abnormality. This group should be studied with all modern imaging techniques and neuropathological correlations after surgery in order to further define the epileptogenic lesions in these patients. Before contemplating surgery in such patients, it should be remembered that removal of a pathologically normal temporal lobe does not generally cure the epilepsy and also leads to a worse social and personal outcome (Falconer, Serafetinides, 1963; Bruton, 1988).

8.5.8. CONCLUSION.

AT2 mapping in combination with FLAIR imaging proved a very powerful tool in the systematic study of the amygdalae of patients with intractable TLE, particularly when standard MRI and hippocampal quantitative measures were unremarkable. Outcome studies and correlation studies with functional tests such as EEG (Spencer, 1995), PET (Ho *et al.* 1995), SPECT (Newton, Berkovic, 1995) and neuropsychometry, and neuropathology will be necessary to gain a better understanding of the role of AT2 mapping and the amygdala in intractable TLE.

CHAPTER IX. SINGLE VOXEL ^{1}H MAGNETIC RESONANCE SPECTROSCOPY IN PATIENTS WITH MRI-NEGATIVE INTRACTABLE TEMPORAL LOBE EPILEPSY.

9.1. ABSTRACT.

The nature of an epileptogenic lesion and the extent of its resection are important prognostic factors with respect to seizure outcome after surgery for intractable TLE *(see pathology and outcome with respect to seizures, p 43)*. Around 20% of patients with intractable TLE (with exclusion of FTL) have normal quantitative MRI of hippocampi and amygdala. The aim of this study was to investigate these patients with apparently structural MRI-negative TLE with single voxel ^{1}H MRS. Seven patients with intractable TLE with normal structural imaging underwent single voxel ^{1}H MRS of the temporal lobes. Five of these seven patients had an abnormally low ratio of NAA/(Cho+Cr) and a sixth patient had ratios within normal limits but a large asymmetry of 0.26. These six patients with MRS abnormalities had EEG findings that were not discordant. In conclusion, single voxel ^{1}H MRS of the temporal lobes was abnormal in 6 of 7 patients with apparent MRI-negative intractable TLE and may provide lateralizing information that could not have been obtained otherwise. Neuropathological and surgical outcome studies will be important to further define the role of ^{1}H MRS in patients with MRI-negative intractable TLE.

9.2. INTRODUCTION.

In vivo single voxel ^{1}H MRS of the brain is able to detect signals from lactate, NAA, glutamate, glutamine, GABA, Cr, Cho and a few other metabolites (Howe *et al.* 1993). It is believed that ^{1}H MRS can give cell-type specific information, and that each cell type has a characteristic metabolic pattern which is discernible by ^{1}H MRS (Kauppinen, 1993; Urenjak *et al.* 1993). Immunohistochemical studies have shown that NAA is localized exclusively in neurons and neuronal processes (Moffett *et al.* 1991; Simmons *et al.* 1991). A reduction of NAA is therefore usually interpreted as a loss or dysfunction of neurons. It has however been shown that a subgroup of glial cells, namely the oligodendrocyte-type 2 astrocyte progenitor cells have a high NAA content (Urenjak *et al.* 1993). Increases in Cr and Cho are usually interpreted as reflecting gliosis.

^{1}H MRS temporal lobe aids lateralization of TLE. As a group, patients with intractable TLE have been reported to show a decrease in NAA, and increases in Cr

and Cho in the temporal lobe ipsilateral to the seizure focus (Hugg *et al.* 1993; Cendes *et al.* 1994; Connelly *et al.* 1994; Gadian *et al.* 1994; Ng *et al.* 1994; Vainio *et al.* 1994; Hetherington *et al.* 1995). Data are usually presented as dimensionless ratios such as NAA/(Cho+Cr) and NAA/Cr, because absolute concentration measurements may be technically too difficult. Most MRS studies of patients with epilepsy have reported on groups of patients with intractable TLE regardless of underlying etiology. Cendes et al (Cendes *et al.* 1995b) combined ^{1}H MRS and MR-based HCV measurement. There was good concordance between the presence of HS and ^{1}H MRS abnormalities, but 2 of the 30 patients had a significantly decreased NAA/Cr ratio ipsilateral to the EEG focus despite normal structural imaging, which suggested that MRS is able to provide information that is different from that of structural MR imaging.

Using an MRI protocol combining standard MRI, MR-based HCV measurement, HCT2 mapping, and AT2 mapping in combination with FLAIR, about 20% of patients with intractable TLE and normal standard MRI had normal quantitation of hippocampi and amygdala. The present study was undertaken to investigate the incidence of MRS abnormality in patients who have intractable TLE yet who remain MRI-negative after extensive investigation (Van Paesschen *et al.* 1996a).

9.3. METHODS.

9.3.1. SELECTION CRITERIA.

The inclusion criteria for this study were: intractable TLE; normal standard MRI; normal HCV and HCVR, normal HCT2 and AT2 values, and single voxel ^{1}H MRS of the temporal lobes.

9.3.2. CLINICAL EVALUATION: *see clinical evaluation p 52.*

9.3.3. STRUCTURAL MR IMAGING.

9.3.3.1. STANDARD MR IMAGING: *see p 53.*

9.3.3.2. MR-BASED HIPPOCAMPAL VOLUMETRY: *see p 57.*

9.3.3.3. HIPPOCAMPAL T2 MAPPING: *p 55.*

9.3.3.4. AMYGDALA T2 MAPPING: *see p 67.*

9.3.3.5. FLAIR: *see p 69.*

9.3.3.6. SINGLE VOXEL ^{1}H MAGNETIC RESONANCE SPECTROSCOPY: *see p 70.*

9.4. RESULTS.

9.4.1. DESCRIPTION OF STUDY POPULATION.

Seven patients (three men and four women) with median age of 31 years (range: 25 to 47) with MRI-negative intractable TLE underwent ^{1}H MRS of the temporal lobes. Median age at onset of habitual epilepsy was 13 years (range: 10 to 38 years). One of these 7 patients (14%) had a history of FCs and none had a history of meningo-encephalitis. There was no family history of epilepsy in any of the patients. All experienced auras of temporal lobe origin, and had a median of 2 CPSs (range: 0.25 - 7) per week during the year before the MRS. The median of estimated SGS during their lifetime was six (range: 0 - 1200). All patients had interictal EEGs and four patients had ictal video-EEG recordings.

9.4.2. SINGLE VOXEL ^{1}H MAGNETIC RESONANCE SPECTROSCOPY RESULTS.

Results are given in Table 16, p 189. Five of seven patients (patients 1 to 5) with MRI-negative TLE had a NAA/(Cr+Cho) ratio below 0.72. The values were bilaterally low for two of these patients (patients 3 and 5) *(Figure 53, p 190, and following page)*. One of these two patients with bilaterally abnormal spectra had a lateralized abnormality, i.e. the difference between the two sides was more than 0.05 (patient 3). In addition, one patient with bilateral normal ratios (0.80 and 1.06) showed a side-to-side difference of 0.26 (patient 6).

No	age	gender	HCT2 right	HCT2 left	AT2 right	AT2 left	HCV right	HCV left	HCV ratio	inter ictal EEG	ictal EEG	ratio right	ratio left	Hosp. number
1	25	W	98	97	98	95	5174	4903	0.95	RT		**0.68**	0.88	C38461
2	30	M	105	103	98	95	4466	4455	1.00	LT		0.77	**0.68**	/
3	31	M	102	100	97	96	5246	5055	0.96	BT	RFT	**0.56**	**0.64**	C23971
4	27	W	97	96	100	100	5472	5490	1.00	BT		0.80	**0.48**	/
5	39	M	104	103	101	99	5640	5179	0.92	BT	BT	**0.56**	**0.54**	C21566
6	47	W	106	106	99	102	5115	5243	0.97	LT	LT	1.06	0.81	C07274
7	42	W	106	103	100	100	4432	4451	1.00	LT	LT	0.77	0.78	C15454

Table 16. Single voxel ^{1}H magnetic resonance spectroscopy (MRS) and EEG correlates in patients with TLE and negative MRI including quantitation of hippocampi and amygdalae. The seven patients are indicated with a number (No). HCT2 and AT2 are expressed in msec [HCT2: Nl $\leq$ 108 msec; AT2: Nl $\leq$ 104 msec]. HCV is expressed in mm^3 [HCV: Nl $\geq$ 4348 mm^3; HCVR: Nl $\geq$ 0.87]. Interictal and ictal EEG indicate location of epileptiform abnormality: RT: right temporal, LT: left temporal, BT: bitemporal, RFT: right fronto-temporal. Ratio: NAA/(Cho+Cr) [NAA/(Cho+Cr): Nl $\geq$ 0.72]. The ratios in bold are abnormally low.

Figure 53 *(see also p 191)*. Patient with MRI-negative TLE and abnormal ^{1}H MRS. Patient was a 31 year old man with intractable right TLE *(patient 3, Table 16, p 189)*. A. HCT2 map, B. AT2 map, C. reformatted MPRAGE showing section 7 and 11 that were used to measure the HCV and construct the HCV distribution graph (D). The hippocampi appear symmetric and of normal size. On section 7 two dimensions of the cube (2x2x2 cm), in which the spectrum was measured, are drawn. E. Control spectrum. NAA is higher than the Cho and Cr peaks. F. The spectrum of the right temporal lobe is shown. Notice the decrease in NAA compared with the control spectrum. The NAA/(Cho+Cr) of the right temporal lobe of the patient was 0.56 (Nl ≥ 0.72) and of the left was 0.64. Because the difference was more than 0.05, lateralization was towards the right side *(see Methodology of MRS, p 70)*.

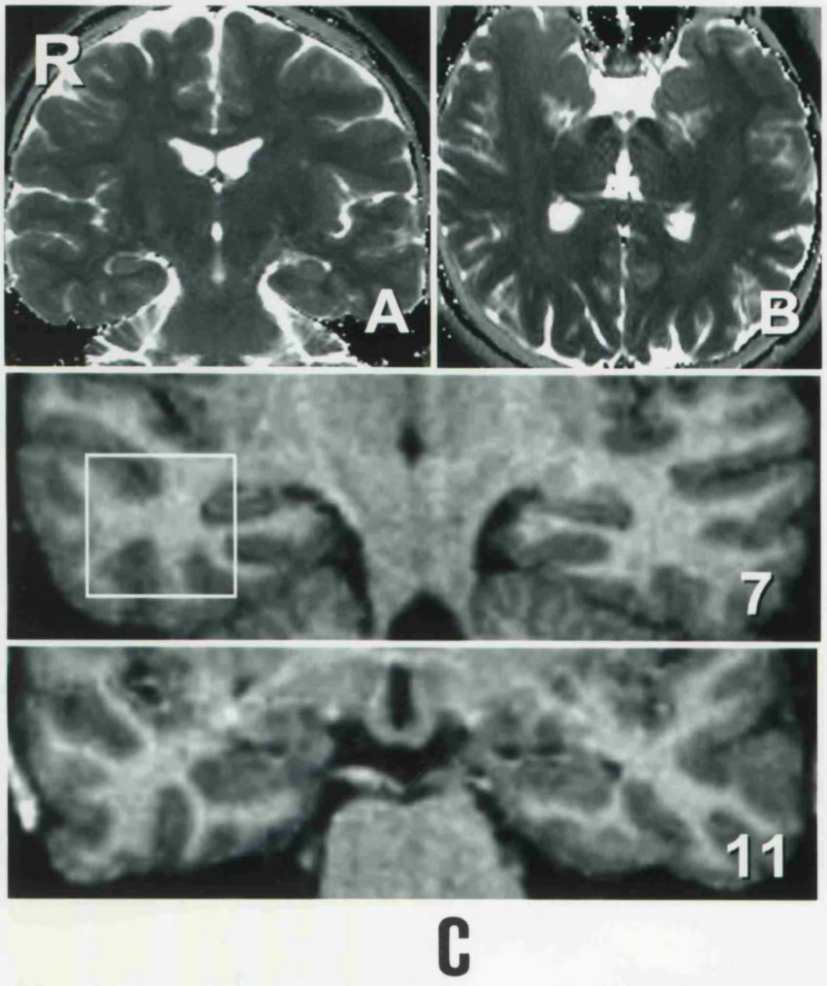

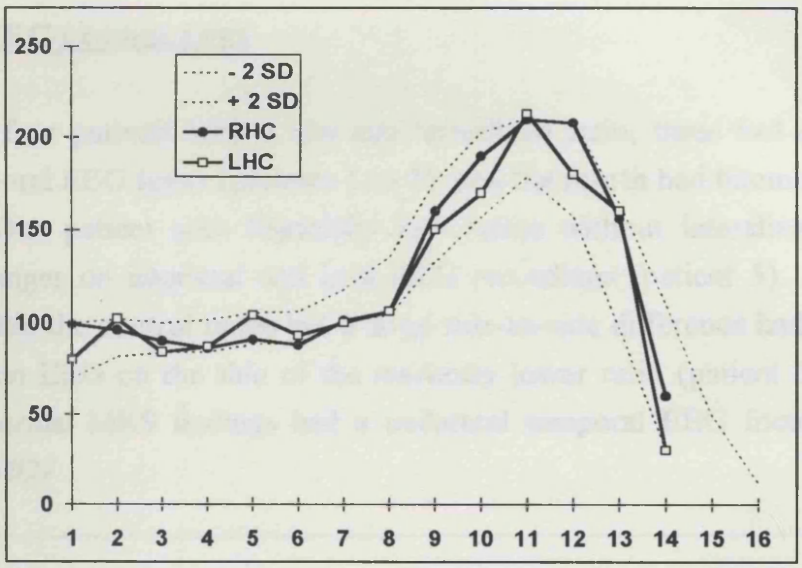
250
200
150
100
50
0
- 2 SD
+ 2 SD
RHC
LHC
1 2 3 4 5 6 7 8 9 10 11 12 13 14 15 16

D

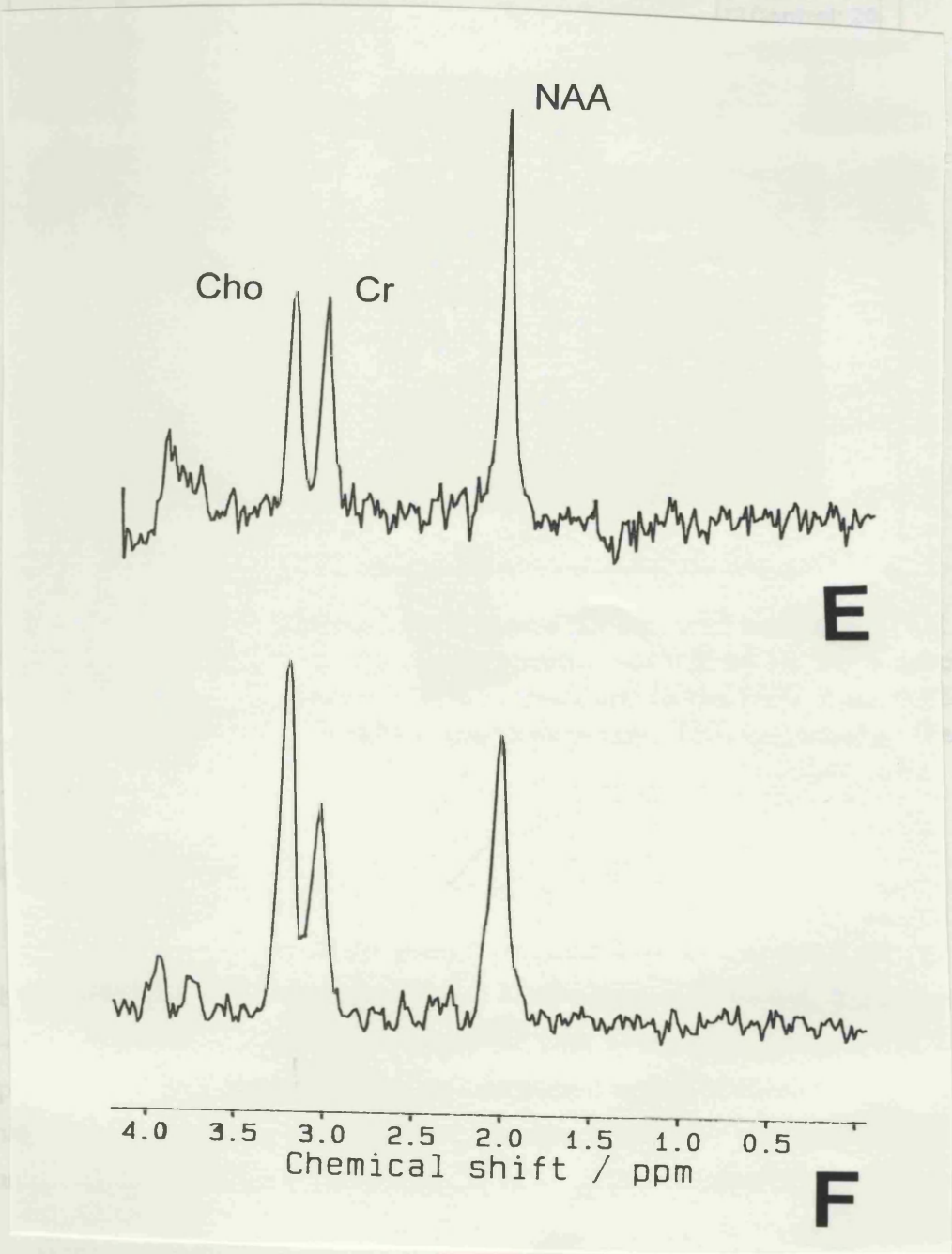
NAA
Cho
Cr
E
4.0 3.5 3.0 2.5 2.0 1.5 1.0 0.5
Chemical shift / ppm
F

9.4.3. MRS-EEG CORRELATES.

Of the four patients with a low and lateralized ratio, three had a concordant unilateral temporal EEG focus (patients 1 to 3), and the fourth had bitemporal changes (patient 4). One patient with bilaterally low ratios without lateralization showed bitemporal changes on interictal and ictal EEG recordings (patient 5). One patient with ratios within the control range but a large side-to-side difference had epileptiform abnormalities on EEG on the side of the markedly lower ratio (patient 6). The only patient with normal MRS findings had a unilateral temporal EEG focus (patient 7) *(Figure 54, p 192)*.

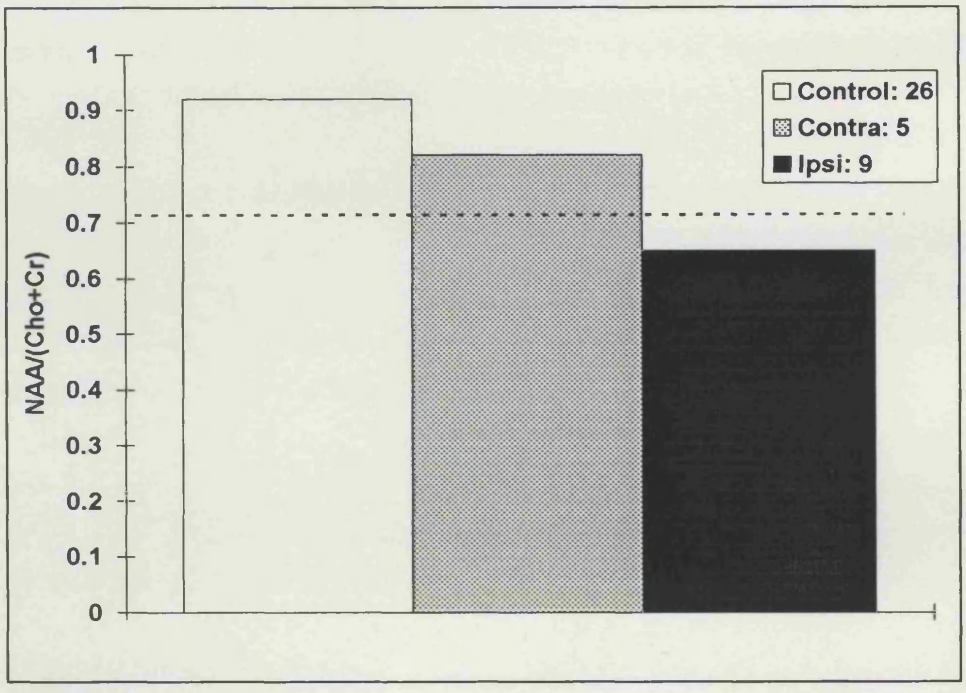

Figure 54. Single voxel ^{1}H MRS in MRI-negative patients with intractable TLE. The mean ratio of NAA/(Cho+Cr) for 26 control spectra was 0.92±0.16, for 5 spectra of patients with MRI-negative intractable TLE contralateral to the EEG focus 0.82±0.15 and for 9 spectra of patients with MRI-negative intractable TLE ipsilateral to the EEG focus 0.65±0.12.

9.5. DISCUSSION.

NAA/(Cr+Cho) ratios of the mesial temporal lobe as measured on ^{1}H MRS were abnormal in five of seven patients with MRI-negative TLE, and showed a large side-to-side difference in one additional patient with bilaterally normal ratios. There were epileptiform EEG changes that were concordant in five of these six patients with abnormal MRS findings, the sixth showing bitemporal changes with a unilateral MRS abnormality. These findings indicate that ^{1}H MRS provides lateralising and localizing

information in patients with intractable TLE, that could not have been provided by other MRI techniques, including quantitative hippocampal and amygdala measurements. The results confirm that ^{1}H MRS detects a widespread abnormality in the temporal lobe which is not necessarily apparent on structural MRI. Neuropathological and surgical outcome studies will be important to further define the role of ^{1}H MRS in patients with MRI-negative intractable TLE.

CHAPTER X. UNANSWERED QUESTIONS AND FUTURE DIRECTIONS.

Ideally, all patients with intractable TLE should be studied with a combination of MRI techniques in addition to standard T1- and T2-weighted images and FLAIR, such as HCV measurement and HCT2 mapping, AT2 mapping and MRS of the temporal lobes. These techniques could give an answer to several questions:

- *Why do only 60-70% of patients with HS become seizure free after surgery* (Falconer, Serafetinides, 1963; Jensen, Klinken, 1976; Duncan, Sagar, 1987; Bruton, 1988; Berkovic *et al.* 1995), *i.e. how can patients who will become seizure free and those who will not benefit be identified presurgically ?*

Possible answers are that the posterior part of the hippocampus was affected by HS and not completely removed, that dual pathology was overlooked, that there was bilateral HS, or that there was progression of the contralateral side to HS. Improved quantitative MRI techniques may help to identify these factors. Further MRI of the hippocampus left in situ may answer this question.

- *Why do late (i.e. after several years without seizures) relapses after surgery occur mainly in patients who had HS* (Berkovic *et al.* 1995; Spencer, 1996)*?*

It may be that the other hippocampus was also affected and that the "silent period" was longer for this hippocampus, which became epileptic at a later date (see also previous question).

- *Is there progression of HS with continued seizures ?*

Our study had a follow-up of only 1 year and is not conclusive. We have obtained funding now to rescan this cohort with a follow-up of 4 years, which will start in September 1997.

- *What surgical technique should be used for TLE ?*

A systematic quantitative MRI study of the temporal lobes will allow a study comparing outcome of different surgical techniques as a function of the quantitative MRI findings.

- Does HS exist before the onset of habitual epilepsy or FC, or is HS the result of prolonged FC or recurrent seizures, or both ?

Prospective quantitative MRI studies of children with FC, several of which are underway (Grünewald *et al.* 1996; VanLandingham *et al.* 1996), and also our longitudinal study in adults (Van Paesschen *et al.* 1996c) may give an answer to this question.

- How can neocortical TLE be better delineated (Walczak, 1995; Burgerman *et al.* 1995) *?*

A correlational study using our protocol of standard MR imaging, quantitative hippocampal MRI, AT2 mapping and MRS of the temporal lobes and other techniques such as EEG, PET, SPECT, pathology and surgical outcome may provide a better understanding of neocortical TLE.

- Does a patient with bilateral HS have bilateral epileptogenic lesions ?

This can be answered with the presented quantitative MRI protocol in combination with repeated ictal SPECT scans, depth EEG studies and surgical outcome studies.

- Is Wada testing for memory function useful ?

The intracarotid amobarbital test, devised by Wada and Rasmussen to determine speech lateralization (1960), was introduced to study short term-memory (Milner *et al.* 1962) after it became apparent that dense anterograde amnesia could result from unilateral temporal lobe resection if the contralateral hippocampus was damaged (Penfield, Milner, 1958). However, the Wada test has never been properly validated since patients who failed the test were usually not operated on. Ten patients however have been reported who failed the test, and were operated on without developing amnesia (Loring *et al.* 1990). Also, the Wada test for memory was introduced after two cases of anterograde amnesia had occurred out of 90 patients operated on. One case came to autopsy and was reported 16 years after the initial

report (Penfield, Mathieson, 1974). This patient who had undergone a left temporal neocortical resection on the basis of clinical and interictal EEG data was not seizure free, underwent a left hippocampectomy despite runs of right temporal 5/sec rhythmic discharges and became amnesic. After this second operation his seizures were unchanged and EEG showed ictal suppression of electrical activity followed by rhythmic theta over the right temporal region. An autopsy several years later revealed right HS, and what remained of the left hippocampus was normal. In other words, the normal hippocampus was removed in a patient with TLE due to right HS, which would not occur in the modern era of preoperative MRI evaluation.

Quantitative MRI in conjunction with EEG and neuropsychological data may provide sufficient information to make the Wada test redundant. Our results have shown that patients with unilateral HS with concordant EEG and neuropsychological data never failed the Wada test, did well after surgery and did not become amnesic. The problem could be redefined as follows: in patients with unilateral HS, removal of the affected hippocampus can be performed with no deterioration or even improvement of memory functions (Baxendale *et al.* 1996), but removal of the normal hippocampus probably causes amnesia. In patients with bilateral normal hippocampi, removal of one hippocampus causes material-specific memory deficits but no amnesia. Memory function or removal of one hippocampus in patients with bilateral HS have not been studied adequately. A quantitative hippocampal MRI protocol is a prerequisite for further studies in this field.

- Are there differences in outcome after surgery in patients with HS associated with CD and HS not associated with CD ?

The association of HS and CD has been reported *(see dual pathology, p 48)* and there is anecdotal evidence that patients with HS and CD do less well after surgery (Raymond *et al.* 1994; Cendes *et al.* 1995c). On the other hand, patients with microdysgenesis in the resected temporal neocortex had a better surgical outcome than patients without (Hardiman *et al.* 1988). Correlational studies using preoperative quantitative MRI, pathology and surgical outcome will clarify this issue.

- What is the pathological nature of the MRS signals NAA, Cr and Cho ?

This could be answered by a correlational study comparing quantitative neuropathology of temporal neocortex and MRS of the temporal lobe.

- What other new MRI techniques could supplement the quantitative MRI techniques described in the present work ?

HCT2 mapping using multiple slices instead of a single slice HCT2 map would be able to give information along the axis of the hippocampus (Duncan *et al.* 1996). The use of phased-array head coils will improve the signal-to-noise ratio and improve the resolution of the MR images (Hayes *et al.* 1993). Functional MRI may be of importance in the near future for the localization of the epileptogenic zone. In functional MRI, images are sensitized to susceptibility effects produced by changes in deoxyhemoglobin concentrations such that focal alterations in cerebral hemodynamics can be visualized (Kwong, 1995). Epilepsy is characterized by a clinical manifestation due to a sudden discharge of a large number of nerve cells of the brain, which is accompanied by an increase in blood flow. This has been observed during surgery for epilepsy (Penfield, 1933), and forms the basis for ictal SPECT, which is a sensitive test for the localization of partial epilepsy (Ho *et al.* 1995; Newton *et al.* 1995; Newton, Berkovic, 1995). Advantages of fMRI compared to ictal SPECT are the repeatability, and the high spatial and temporal resolution. Practical problems of fMRI are that the patient has to stay in the scanner until the occurrence of ictal activity, and that he/she is not allowed to move. Further, there is no need to inject a radioactive isotope. Recently, localization of clinical and subclinical ictal activity by fMRI has been described in 2 case reports (Jackson *et al.* 1994a; Detre *et al.* 1995), and this localization was more accurate than that obtained by invasive EEG in one of these patients. EEG monitoring in the MRI scanner, which would be essential in such studies, has recently been described (Ives *et al.* 1993). EEG-triggered echo-planar fMRI in epilepsy may have the potential to identify brain regions activated during brief focal epileptic discharges (Warach *et al.* 1996).

In this study, single voxel ^{1}H MRS was used. An alternative is Chemical Shift Imaging (Connelly, 1996), which allows the acquisition of several smaller voxels in one session, which has the advantage of providing the spatial distribution of metabolites. MRS of other compounds such as GABA may be possible.

BIBLIOGRAPHY

ADAM C, BAULAC M, SAINT-HILAIRE JM, LANDAU J, GRANAT O, LAPLANE D (1994) Value of magnetic resonance imaging-based measurements of hippocampal formations in patients with partial epilepsy. *Arch Neurol*, **51**, 130-138.

AMARAL DG (1978) A golgi study of cell types in the hilar region of the hippocampus in the rat. *J Comp Neurol*, **182**, 851-914.

AMARAL DG, INSAUSTI R (1990) Hippocampal formation. In: *The human nervous system*. Edited by G Paxinos. San Diego: Academic Press,Inc. 711-755.

AMARAL DG, WITTER MP (1989) The three-dimensional organization of the hippocampal formation: a review of anatomical data. *Neurosci*, **31**, 571-591.

ANDERSEN P, BLISS TVP, SKREDE KK (1971) Lamellar organization of hippocampal excitatory pathways. *Exp Brain Res*, **13**, 222-238.

ANNEGERS JF, HAUSER WA, ELVEBACK LR (1979) Remission of seizures and relapse in patients with epilepsy. *Epilepsia*, **20**, 729-737.

ANNEGERS JF, ALLEN HAUSER W, SHIRTS SB, KURLAND LT (1987) Factors prognostic of unprovoked seizures after febrile convulsions. *N Eng J Med*, **316**, 493-498.

ARMSTRONG DD (1993) The neuropathology of temporal lobe epilepsy. *J Neuropathol Exp Neurol*, **52**, 433-443.

ARMSTRONG DD, BRUTON CJ (1987) What terminology is appropriate for tissue pathology ? How does it predict outcome ? In: *Surgical treatment of the epilepsies*. Edited by J Engel. New York: Raven Press. 541-552.

ARMSTRONG DL, GROSSMAN RG, ZHU Z. (1987) Complex partial epilepsy: evidence of a malformative process in the resected anterior temporal lobes of thirty-three patients. *J Neuropathol Exp Neurol*, **46**, 359 (Abstract).

AWAD IA, ROSENFELD J, AHL J, HAHN JF, LüDERS H (1991) Intractable epilepsy and structural lesions of the brain: mapping, resection strategies, and seizure outcome. *Epilepsia*, **32**, 179-186.

BABB TL, BROWN WJ, PRETORIUS J, DAVENPORT C, LIEB JP, CRANDALL PH (1984a) Temporal lobe volumetric cell densities in temporal lobe epilepsy. *Epilepsia*, **25**, 729-740.

BABB TL, LIEB JP, BROWN WJ, PRETORIUS J, CRANDALL PH (1984b) Distribution of pyramidal cell density and hyperexcitability in the epileptic human hippocampal formation. *Epilepsia*, **25**, 721-728.

BABB TL (1991) Bilateral pathological damage in temporal lobe epilepsy. *Can J Neurol Sci*, **18**, 645-648.

BABB TL, KUPFER WR, PRETORIUS JK, CRANDALL PH, LéVESQUE MF (1991) Synaptic reorganization by mossy fibers in human epileptic fascia dentata. *Neuroscience*, **42**, 351-363.

BABB TL (1992) Research on the anatomy and pathology of epileptic tissue. In: *Epilepsy surgery*. Edited by HO Lüders. New York: Raven Press. 719-727.

BABB TL, PRETORIUS JK, MELLO LE, MATHERN GW, LéVESQUE MF (1992) Synaptic reorganizations in epileptic human and rat kainate hippocampus may contribute to feedback and feedforward excitation. *Epilepsy Res Suppl*, **9**, 193-202.

BABB TL, BROWN WJ (1987) Pathological findings in epilepsy. In: *Surgical treatment of the epilepsies*. Edited by J Engel. New York: Raven Press. 511-540.

BAULAC M, SAINT-HILAIRE JM, ADAM C, MARTINEZ M, FONTAINE S, LAPLANE D (1994) Correlations between magnetic resonance imaging-based hippocampal sclerosis and depth electrode investigation in epilepsy of the mesiotemporal lobe. *Epilepsia*, **35**, 1045-1053.

BAXENDALE SA, VAN PAESSCHEN W, THOMPSON PJ, DUNCAN JS, HARKNESS WF, SHORVON SD. (1996) Prediction of postoperative memory decline in temporal lobectomy: a multivariate approach. *Epilepsia*, **37**, 181 (Abstract).

BEGHI E, TOGNONI G, COLLABORATIVE GROUP FOR THE STUDY OF EPILEPSY (1988) Prognosis of epilepsy in newly referred patients: a multicenter prospective study. *Epilepsia*, **29**, 236-243.

BEN-ARI Y (1985) Limbic seizure and brain damage produced by kainic acid: mechanisms and relevance to human temporal lobe epilepsy. *Neurosci*, **14**, 375-403.

BERGIN PS, RAYMOND AA, FREE SL, SISODIYA SM, STEVENS JM (1994) Magnetic resonance volumetry [letter]. *Neurology*, **44**, 1770-1771.

BERGIN PS, FISH DR, SHORVON SD, OATRIDGE A, DESOUZA NM, BYDDER GM (1995) Magnetic resonance imaging in partial epilepsy: additional abnormalities shown with the fluid attenuated inversion recovery (FLAIR) pulse sequence. *J Neurol Neurosurg Psychiatry*, **58**, 439-443.

BERKOVIC SF, ANDERMANN F, OLIVIER A, ETHIER R, MELANSON D, ROBITAILLE Y, et al (1991) Hippocampal sclerosis in temporal lobe epilepsy demonstrated by magnetic resonance imaging. *Ann Neurol*, **29**, 175-182.

BERKOVIC SF, MCINTOSH AM, KALNINS RM, JACKSON GD, FABINYI GC, BRAZENOR GA, et al (1995) Preoperative MRI predicts outcome of temporal lobectomy: an actuarial analysis. *Neurology*, **45**, 1358-1363.

BERKOVIC SF, MCINTOSH A, HOWELL RA, MITCHELL A, SHEFFIELD LJ, HOPPER JL (1996) Familial temporal lobe epilepsy: a common disorder identified in twins. *Ann Neurol*, **40**, 227-235.

BERTRAM EH, LOTHMAN EW, LENN NJ (1990) The hippocampus in experimental chronic epilepsy: a morphometric analysis. *Ann Neurol*, **27**, 43-48.

BETTLER B, MULLE C (1995) AMPA and kainate receptors. *Neuropharmacol*, **34**, 123-139.

BHATIA S, BOOKHEIMER SY, GAILLARD WD, THEODORE WH (1993) Measurement of whole temporal lobe and hippocampus for MR volumetry: normative data. *Neurology*, **43**, 2006-2010.

BLACKSTAD TW (1956) Commissural connections of the hippocampal region in the rat, with special reference to their mode of termination. *J Comp Neurol*, **105**, 417-537.

BLAND JM, ALTMAN DG (1986) Statistical methods for assessing agreement between two methods of clinical measurement. *Lancet*, **327**, 307-310.

BOUCHET, CAZAUVIEILH (1825) De l'épilepsie considerée dans ses rapports avec l'aliénation mentale. Recherches sur la nature et le siège de ces deux maladies. *Arch Gen Med*, **9**, 510-542.

BRATZ (1899) Ammonshornbefunde bei Epileptischen. *Arch Psychiatr Nervenkr*, **32**, 820-835.

BROCK TO, O'CALLAGHAN JP (1987) Quantitative changes in the synaptic vesicle proteins synapsin I and p38 and the astrocyte-specific protein glial fibrillary acidic protein are associated with chemical-induced injury to the rat central nervous system. *J Neurosci*, **7**, 931-942.

BRONEN RA, CHEUNG G, CHARLES JT, KIM JH, SPENCER DD, SPENCER SS, et al (1991) Imaging findings in hippocampal sclerosis: correlation with pathology. *AJNR*, **12**, 933-940.

BRONEN RA, FULBRIGHT RK, KIM JH, SPENCER SS, SPENCER DD, AL-RHODAN NRF (1995) Regional distribution of MR findings in hippocampal sclerosis. *AJNR*, **16**, 1193-1200.

BROOKS BS, KING DW, ELGAMMAL T (1990) MR imaging in patients with intractable complex partial epileptic seizures. *AJNR*, **11**, 93-99.

BRUSA R, ZIMMERMANN F, KOH D, FELDMEYER D, GASS P, SEEBURG PH, et al (1995) Early-onset epilepsy and postnatal lethality associated with an editing-deficient GluR-B allele in mice. *Science*, **270**, 1677-1680.

BRUTON C (1988) *The neuropathology of temporal lobe epilepsy*. New York: Oxford University Press.

BRæNDGAARD H, GUNDERSEN HJG (1986) The impact of recent stereological advances on quantitative studies of the nervous system. *J Neurosci Meth*, **18**, 39-78.

BURGERMAN RS, SPERLING MR, FRENCH JA, SAYKIN AJ, O'CONNOR MJ (1995) Comparison of mesial versus neocortical onset temporal lobe seizures: neurodiagnostic findings and surgical outcome. *Epilepsia*, **36**, 662-670.

BUTLER LS, SILVA AJ, ABELIOVICH A, WATANABE Y, TONEGAWA S, MCNAMARA JO (1995) Limbic epilepsy in transgenic mice carrying a Ca2+/calmodulin-dependent kinase II alpha-subunit mutation. *Proc Natl Acad Sci USA*, **92**, 6852-6855.

CARPENTER MB (1991) Olfactory pathways, hippocampal formation, and the amygdala. In: *Core text of neuroanatomy*. Edited by MB Carpenter. Baltimore: Williams & Wilkins. 361-389.

CASCINO GD, JACK CR, JR., PARISI JE, SHARBROUGH FW, HIRSCHORN KA, MEYER FB, et al (1991) Magnetic resonance imaging-based volume studies in temporal lobe epilepsy: pathological correlations. *Ann Neurol*, **30**, 31-36.

CASCINO GD, JACK CR, JR., PARISI JE, SHARBROUGH FW, SCHREIBER CP, KELLY PJ, et al (1993) Operative strategy in patients with MRI-identified dual pathology and temporal lobe epilepsy. *Epilepsy Res*, **14**, 175-182.

CASCINO GD, TRENERRY MR, SHARBROUGH FW, SO EL, MARSH WR, STRELOW DC (1995) Depth electrode studies in temporal lobe epilepsy: relation to quantitative magnetic resonance imaging and operative outcome. *Epilepsia*, **36**, 230-235.

CAVANAGH JB, MEYER A (1956) Aetiological aspects of ammon's horn sclerosis associated with temporal lobe epilepsy. *Br Med J*, 1403-1407.

CAVAZOS JE, GOLARAI G, SUTULA TP (1991) Mossy fiber synaptic reorganization induced by kindling: time course of development, progression, and permanence. *J Neurosci*, **11**, 2795-2803.

CAVAZOS JE, DAS I, SUTULA TP (1994) Neuronal loss induced in limbic pathways by kindling: evidence for induction of hippocampal sclerosis by repeated brief seizures. *J Neurosci*, **14**, 3106-3121.

CAVAZOS JE, SUTULA TP (1990) Progressive neuronal loss induced by kindling: a possible mechanism for mossy fiber synaptic reorganization and hippocampal sclerosis. *Brain Res*, **527**, 1-6.

CENDES F, ANDERMANN F, DUBEAU F, GLOOR P, EVANS A, JONES-GOTMAN M, et al (1993a) Early childhood prolonged febrile convulsions, atrophy and sclerosis of mesial structures, and temporal lobe epilepsy: an MRI volumetric study. *Neurology*, **43**, 1083-1087.

CENDES F, ANDERMANN F, GLOOR P, EVANS A, JONES-GOTMAN M, WATSON C, et al (1993b) MRI volumetric measurement of amygdala and hippocampus in temporal lobe epilepsy. *Neurology*, **43**, 719-725.

CENDES F, ANDERMANN F, GLOOR P, LOPES CENDES I, ANDERMANN E, MELANSON D, et al (1993c) Atrophy of mesial structures in patients with temporal lobe epilepsy: cause or consequence of repeated seizures?. *Ann Neurol*, **34**, 795-801.

CENDES F, ANDERMANN F, PREUL MC, ARNOLD DL (1994) Lateralization of temporal lobe epilepsy based on regional metabolic abnormalities in proton magnetic resonance spectroscopic images. *Ann Neurol*, **35**, 211-216.

CENDES F, ANDERMANN F, CARPENTER S, ZATORRE RJ, CASHMAN NR (1995a) Temporal lobe epilepsy caused by domoic acid intoxication: evidence for glutamate receptor-mediated excitotoxicity in humans. *Ann Neurol*, **37**, 123-126.

CENDES F, ANDERMANN F, DUBEAU F, ARNOLD D (1995b) Proton magnetic resonance spectroscopic images and MRI volumetric studies for lateralization of temporal lobe epilepsy. *Magn Res Imag*, **13**, 1187-1191.

CENDES F, COOK MJ, WATSON C, ANDERMANN F, FISH DR, SHORVON SD, et al (1995c) Frequency and characteristics of dual pathology in patients with lesional epilepsy. *Neurology*, **45**, 2058-2064.

CHAN S, SLOVITER RS, GOODMAN RR, et al. (1994) MR imaging of endfolium sclerosis: diagnosis of mesial temporal sclerosis without hippocampal atrophy. *Epilepsia*, **35**, 88 (Abstract).

COCKERELL OC, JOHNSON AL, SANDER JWAS, HART YM, SHORVON SD (1995) Remission of epilepsy: results from the National General Practice Study of Epilepsy. *Lancet*, **346**, 140-144.

COGGESHALL RE, LEKAN HA (1996) Methods for determining numbers of cells and synapses: a case for more uniform standards of review. *J Comp Neurol*, **364**, 6-15.

COMMISSION ON CLASSIFICATION AND TERMINOLOGY OF THE INTERNATIONAL LEAGUE AGAINST EPILEPSY (1981) Proposal for revised clinical and electroencephalographic classification of epileptic seizures. *Epilepsia*, **22**, 489-501.

COMMISSION ON CLASSIFICATION AND TERMINOLOGY OF THE INTERNATIONAL LEAGUE AGAINST EPILEPSY (1989) Proposal for revised classification of epilepsies and epileptic syndromes. *Epilepsia*, **30**, 389-399.

CONNELLY A, JACKSON GD, DUNCAN JS, KING MD, GADIAN DG (1994) Magnetic resonance spectroscopy in temporal lobe epilepsy. *Neurology*, **44**, 1411-1417.

CONNELLY A (1996) Proton magnetic resonance spectroscopy in epilepsy. In: *Neuroimaging in epilepsy: principles and practice*. Edited by GD Cascino, CR Jack, Jr. Butterworth-Heinemann.

CONNELLY A, VAN PAESSCHEN W, STEVENS JM, DUNCAN JS. (1996) Aetiology and early prognosis of newly diagnosed localization-related epilepsies in adults: a quantitative MRI study. *Epilepsia*, **37**, 124 (Abstract).

COOK MJ, FISH DR, SHORVON SD, STRAUGHAN K, STEVENS JM (1992) Hippocampal volumetric and morphometric studies in frontal and temporal lobe epilepsy. *Brain*, **115**, 1001-1015.

CORSELLIS JAN (1970) The neuropathology of temporal lobe epilepsy. In: *Modern trends in neurology*. Edited by D Williams. London: Butterworth. 254-270.

CORSELLIS JAN, BRUTON CJ (1983) Neuropathology of status epilepticus in humans. In: *Status epilepticus*. Edited by AV Delgado-Escueta, CG Wasterlain, DM Treiman, RJ Porter. New York: Raven Press. 129-139.

COTMAN CW, MONAGHAN DT, OTTERSEN OP, STORM-MATHISEN J (1987) Anatomical organization of excitatory amino acid receptors and their pathways. *TINS*, **10**, 273-280.

CROMBIE DL, CROSS KW, FRY J (1960) A survey of the epilepsies in general practice: a report by the Research Committee of the College of General Practitioners. *Br Med J*, **2**, 416-422.

DAM AM (1979) The density of neurons in the human hippocampus. *Neuropath Appl Neurobiol*, **5**, 249-264.

DAM AM (1980) Epilepsy and neuron loss in the hippocampus. *Epilepsia*, **21**, 617-629.

DAM AM (1982) Hippocampal neuron loss in epilepsy and after experimental seizures. *Acta Neurol Scandinav*, **66**, 601-642.

DE LANEROLLE NC, KIM JH, ROBBINS RJ, SPENCER DD (1989) Hippocampal interneuron loss and plasticity in human temporal lobe epilepsy. *Brain Res*, **495**, 387-395.

DELGADO-ESCUETA AV, NASHOLD B, FREEDMAN M, KEPLINGER C, WADDELL G, MILLER P, et al (1979) Videotaping epileptic attacks during stereoelectroencephalography. *Neurology*, **29**, 473-489.

DELGADO-ESCUETA AV, WALSH GO (1985) Type I complex partial seizures of hippocampal origin: excellent results of anterior temporal lobectomy. *Neurology*, **35**, 143-154.

DETRE JA, SIRVEN JI, ALSOP DC, O'CONNER MJ, FRENCH JA (1995) Localization of subclinical ictal activity by functional magnetic resonance imaging: correlation with invasive monitoring. *Ann Neurol*, **38**, 618-624.

DUBINSKY JM (1993) Examination of the role of calcium in neuronal death. *Ann N Y Acad Sci*, **679**, 34-42.

DUNCAN JS, SHORVON SD, FISH DR (1995) *Clinical epilepsy*. New York: Churchill Livingstone.

DUNCAN JS, BARTLETT P, BARKER GJ (1996) Measurement of hippocampal T2 relaxation time - development and implementation of new techniques. *AJNR*, (In Press)

DUNCAN JS, SAGAR HJ (1987) Seizure characteristics, pathology, and outcome after temporal lobectomy. *Neurology*, **37**, 405-409.

DUVERNOY HM (1988) *The human hippocampus. An atlas of applied anatomy*. München: J.F.Bergmann Verlag. 1-166.

EARLE KM, BALDWIN M, PENFIELD W (1953) Incisural sclerosis and temporal lobe seizures produced by hippocampal herniation at birth. *Arch Neurol Psychiatry*, **69**, 27-42.

ELWES RDC, JOHNSON AL, SHORVON SD, REYNOLDS EH (1984) The prognosis for seizure control in newly diagnosed epilepsy. *N Engl J Med*, **311**, 944-947.

ELWES RDC, JOHNSON AL, REYNOLDS EH (1988) The course of untreated epilepsy. *Br Med J*, **297**, 948-950.

ENG LF (1985) Glial fibrillary acidic protein (GFAP): the major protein of glial intermediate filaments in differentiated astrocytes. *J Neuroimmunol*, **8**, 203-214.

ENG LF (1988) Regulation of glial intermediate filaments in astrogliosis. In: *The biochemical pathology of astocytes*. Edited by MD Norenberg, L Hertz, A Schousboe. New York: Alan R. Liss,Inc. 79-90.

ENGEL J (1993) Update on surgical treatment of the epilepsies: summary of the second international Palm Desert conference on the surgical treatment of the epilepsies. *Neurology*, **43**, 1612-1617.

ENGEL J, VAN NESS PC, RASMUSSEN TB, OJEMANN LM (1993) Outcome with respect to epileptic seizures. In: *Surgical treatment of the epilepsies*. Edited by J Engel. New York: Raven Press. 609-621.

ENGEL J, SHEWMON DA (1993) Who should be considered a surgical candidate ? In: *Surgical treatment of the epilepsies*. Edited by J Engel. New York: Raven Press. 23-34.

ERICKSON JC, CLEGG KE, PALMITER RD (1996) Sensitivity to leptin and susceptibility to seizures of mice lacking neuropeptide Y. *Nature*, **381**, 415-418.

EVERITT BS (1992) *The analysis of contingency tables*. London: Chapman and Hall.

FALCONER MA, SERAFETINIDES EA, CORSELLIS JAN (1964) Etiology and pathogenesis of temporal lobe epilepsy. *Arch Neurol*, **10**, 233-248.

FALCONER MA (1974) Mesial temporal (Ammon's horn) sclerosis as a common cause of epilepsy. Aetiology, treatment, and prevention. *Lancet*, 767-770.

FALCONER MA, CAVANAGH JB (1959) Clinico-patholological considerations of temporal lobe epilepsy due to small focal lesions. *Brain*, **82**, 483-503.

FALCONER MA, SERAFETINIDES EA (1963) A follow-up study of surgery in temporal lobe epilepsy. *J Neurol Neurosurg Psychiatry*, **26**, 154-165.

FALCONER MA, TAYLOR DC (1968) Surgical treatment of drug-resistant epilepsy due to mesial temporal sclerosis. *Arch Neurol*, **19**, 353-361.

FEINDEL W, ROBITAILLE Y, TAMPIERI D, GOOSSENS L, LI M, MELANçON D (1991) Electroencephalography, magnetic resonance imaging and pathology in patients treated surgically for temporal lobe epilepsy. *Can J Neurol Sci*, **18**, 577-579.

FEINDEL W, RASMUSSEN T (1991) Temporal lobectomy with amygdalectomy and minimal hippocampal resection: review of 100 cases. *Can J Neurol Sci*, **18**, 603-605.

FELDBLUM S, ACKERMANN R (1987) Increased susceptibility to hippocampal and amygdala kindling following intrahippocampal kainic acid. *Exp Neurol*, **97**, 225-269.

FISH D, ANDERMANN F, OLIVIER A (1991) Complex partial seizures and small posterior temporal or extratemporal structural lesions: surgical management. *Neurology*, **41**, 1781-1784.

FISH DR (1994a) MRI in focal lesions. *Acta Neurol Scand*, **Suppl. 152**, 101-104.

FISH DR (1994b) The anatomical bases of the epilepsies and MRI. In: *Magnetic resonance scanning and epilepsy*. Edited by SD Shorvon, DR Fish, F Andermann, GM Bydder, H Stefan. New York: Plenum Press. 15-20.

FORSGREN L, FAGERLUND M, ZETTERLUND B (1991) Electroencephalographic and neuroradiological findings in adults with newly diagnosed unprovoked seizures. *Eur Neurol*, **31**, 61-67.

FREE SL, BERGIN PS, FISH DR, COOK MJ, SHORVON SD, STEVENS JM (1995) Methods for normalization of hippocampal volumes measured with MR. *AJNR*, **16**, 637-643.

FRENCH JA, WILLIAMSON PD, THADANI VM, DARCEY TM, MATTSON RH, SPENCER SS, et al (1993) Characteristics of medial temporal lobe epilepsy: results of history and physical examination. *Ann Neurol*, **34**, 774-780.

FRIED I, KIM JH, SPENCER DD (1992) Hippocampal pathology in patients with intractable seizures and temporal lobe masses. *J Neurosurg*, **76**, 735-740.

GABRIEL KR (1968) Simultaneous test procedures in multivariate analysis of variance. *Biometrika*, **55**, 489-504.

GADIAN DG, CONNELLY A, DUNCAN JS, CROSS JH, KIRKHAM FJ, JOHNSON CL, et al (1994) 1H magnetic resonance spectroscopy in the investigation of intractable epilepsy. *Acta Neurol Scand*, **Suppl. 152**, 116-121.

GAMBARDELLA A, CENDES F, ANDERMANN F. (1993) Etiologic, genetic, and clinical characteristics of patients with unilateral and with bilateral mesiotemporal atrophy. *Epilepsia*, **34**, 121-122. (Abstract).

GAMBARDELLA A, GOTMAN J, CENDES F, ANDERMANN F (1995) The relation of spike foci and of clinical seizure characteristics to different patterns of mesial temporal atrophy. *Arch Neurol*, **52**, 287-293.

GARCIA PA, LAXER KD, BARBARO NM, DILLON WP (1994) Prognostic value of qualitative magnetic resonance imaging hippocampal abnormalities in patients undergoing temporal lobectomy for medically refractory seizures. *Epilepsia*, **35**, 520-524.

GLASER GH (1987) Natural history of temporal lobe-limbic epilepsy. In: *Surgical treatment of the epilepsies*. Edited by J Engel. New York: Raven Press. 13-30.

GLOOR P (1992a) Role of the amygdala in temporal lobe epilepsy. In: *The amygdala: neurobiological aspects of emotion, memory, and mental dysfunction*. Edited by JP Aggleton. New York: Wiley-Liss, Inc. 505-538.

GLOOR P (1992b) Mesial temporal sclerosis: historical background and an overview from a modern perspective. In: *Epilepsy surgery*. Edited by HO Lüders. New York: Raven Press. 689-703.

GODDARD G, MCINTYRE D, LEECH C (1969) A permanent change in brain function resulting from daily electrical stimulation. *Exp Neurol*, **25**, 295-330.

GOLDRING S, EDWARDS I, HARDING GW, BERNARDO KL (1992) Results of anterior temporal lobectomy that spares the amygdala in patients with complex partial seizures. *J Neurosurg*, **77**, 185-193.

GOODRIDGE DMG, SHORVON SD (1983) Epilepsy in a population of 6000. *Br Med J*, **287**, 641-647.

GOWERS WR (1881) *Epilepsy and other chronic convulsive diseases: their causes, symptoms, & treatment*. London: Churchill,J.&A.

GRAUMANN R, OPPELT A, STETTER E (1986) Multiple-spin-echo imaging with a 2D Fourier method. *Magn Res Med*, **3**, 707-721.

GREBER S, SCHWARZER C, SPERK G (1994) Neuropeptide Y inhibits potassium-stimulated glutamate release through Y2 receptors in rat hippocampal slices in vitro. *Br J Pharmacol*, **113**, 737-740.

GREEN JR, SCHEETZ DG (1964) Surgery of epileptogenic lesions of the temporal lobe. *Arch Neurol*, **10**, 135-148.

GREENAMYRE JT, PORTER RHP (1994) Anatomy and physiology of glutamate in the CNS. *Neurology*, **44**, S7-S13.

GRüNEWALD RA, JACKSON GD, CONNELLY A, DUNCAN JS (1994a) MR detection of hippocampal disease in epilepsy: factors influencing T2 relaxation time. *AJNR*, **15**, 1149-1156.

GRüNEWALD RA, JACKSON GD, CONNELLY A, DUNCAN JS (1994b) MR detection of hippocampal disease in epilepsy: factors influencing T2 relaxation time. *A J N R Am J Neuroradiol*, **15**, 1149-1156.

GRüNEWALD RA, FARROW TFD, MUNDY JVB, RITTEY C, SAGAR HJ. (1996) Preliminary results of university of Sheffield study of complicated early childhood convulsion. *Epilepsia*, **37**, 125 (Abstract).

GUNDERSEN HJG, BENDTSEN TF, KORBO L, MARCUSSEN N, MOLLER A, NIELSEN K, et al (1988) Some new, simple and efficient stereological methods and their use in pathological research and diagnosis. *APMIS*, **96**, 379-394.

HAND DJ, TAYLOR CC (1987) *Multivariate analysis of variance and repeated measures*. London: Chapman & Hall.

HARDIMAN O, BURKE T, PHILLIPS J, MURPHY S, O'MOORE B, STAUNTON H, et al (1988) Microdysgenesis in resected temporal neocortex: incidence and clinical significance in focal epilepsy. *Neurology*, **38**, 1041-1047.

HARVEY AS, GRATTAN SMITH JD, DESMOND PM, CHOW CW, BERKOVIC SF (1995) Febrile seizures and hippocampal sclerosis: frequent and related findings in intractable temporal lobe epilepsy of childhood. *Pediatr Neurol*, **12**, 201-206.

HAUG H (1986) History of neuromorphometry. *J Neurosci Meth*, **18**, 1-17.

HAUSER WA, ANNEGERS JF, KURLAND LT (1991) Prevalence of epilepsy in Rochester, Minnesota: 1940-1980. *Epilepsia*, **32**, 429-445.

HAUSER WA (1992) The natural history of temporal lobe epilepsy. In: *Epilepsy surgery*. Edited by HO Lüders. New York: Raven Press. 133-141.

HAUSER WA, ANNEGERS JF, KURLAND LT (1993) Incidence of epilepsy and unprovoked seizures in Rochester, Minnesota: 1935-1984. *Epilepsia*, **34**, 453-468.

HAUSER WA, KURLAND LT (1975) The epidemiology of epilepsy in Rochester, Minnesota 1935 through 1967. *Epilepsia*, **16**, 1-66.

HAWRYLAK N, CHANG FL, GREENOUGH WT (1993) Astrocytic and synaptic response to kindling in hippocampal subfield CA1. II. Synaptogenesis and astrocytic process increases to in vivo kindling. *Brain Res*, **603**, 309-316.

HAYES CE, TSURUDA JS, MATHIS CM (1993) Temporal lobes: surface MR coil phased-array imaging. *Radiology*, **189**, 918-920.

HETHERINGTON HP, KUZNIECKY RI, PAN JW, VAUGHAN JT, TWIEG DB, POHOST GM (1995) Application of high field spectroscopic imaging in the evaluation of temporal lobe epilepsy. *Magn Res Imag*, **13**, 1175-1180.

HIRANO A (1994) Neurons and astrocytes. In: *Textbook of neuropathology*. Edited by RL Davis, DM Robertson. Baltimore: Williams & Wilkins. 1-94.

HO SS, BERKOVIC SF, BERLANGIERI SU (1995) Comparison of ictal SPECT and interictal PET in the presurgical evaluation of temporal lobe epilepsy. *Ann Neurol*, **37**, 738-745.

HOLLMANN M, HEINEMANN S (1994) Cloned glutamate receptors. *Ann Rev Neurosci*, **17**, 31-108.

HOPKINS A, SHORVON S (1995) Definitions and epidemiology of epilepsy. In: *Epilepsy*. Edited by A Hopkins, S Shorvon, G Cascino. London: Chapman & Hall. 1-21.

HOUSER CR, MIYASHIRO JE, SWARTZ BE, WALSH GO, RICH JR, DELGADO-ESCUETA AV (1990) Altered patterns of dynorphin immunoreactivity suggest mossy fiber reorganization in human hippocampal epilepsy. *J Neurosci*, **10**, 267-282.

HOUSER CR, SWARTZ BE, WALSH GO, DELGADO-ESCUETA AV (1992) Granule cell disorganization in the dentate gyrus: possible alterations of neuronal migration in human temporal lobe epilepsy. *Epilepsy Res Suppl*, **9**, 41-48.

HOWE FA, MAXWELL RJ, SAUNDERS DE, BROWN MM, GRIFFITHS JR (1993) Proton spectroscopy in vivo. *Magn Res Quart*, **9**, 31-59.

HUDSON LP, MUNOZ DG, MILLER L, MCLACHLAN RS, GIRVIN JP, BLUME WT (1993) Amygdaloid sclerosis in temporal lobe epilepsy. *Ann Neurol*, **33**, 622-631.

HUGG JW, LAXER KD, MATSON GB, MAUDSLEY AA, WEINER MW (1993) Neuron loss localizes human temporal lobe epilepsy by in vivo proton magnetic resonance spectroscopic imaging. *Ann Neurol*, **34**, 788-794.

INCISA DELLA ROCCHETTA A, GADIAN DG, CONNELLY A, POLKEY CE, JACKSON GD, WATKINS KE, et al (1995) Verbal memory impairment after right temporal lobe surgery: role of contralateral damage as revealed by 1H magnetic resonance spectroscopy and T2 relaxometry. *Neurology*, **45**, 797-802.

IVES JR, WARACH S, SCHMITT F, EDELMAN RR, SCHOMER DL (1993) Monitoring the patient's EEG during echo planar MRI. *Electroenceph clin Neurophysiol*, **87**, 417-420.

JACK CR, TRENERRY MR, CASCINO GD, SHARBROUGH FW, SO EL, O'BRIEN PC (1995) Bilaterally symmetric hippocampi and surgical outcome. *Neurology*, **45**, 1353-1358.

JACK CR, JR., SHARBROUGH FW, MARSH WR (1988) Use of MR imaging for quantitative evaluation of resection for temporal lobe epilepsy. *Radiology*, **169**, 463-468.

JACK CR, JR., SHARBROUGH FW, TWOMEY CK, CASCINO GD, HIRSCHORN KA, MARSH WR, et al (1990) Temporal lobe seizures: lateralization with MR volume measurements of the hippocampal formation. *Radiology*, **175**, 423-429.

JACK CR, JR., SHARBROUGH FW, CASCINO GD, HIRSCHORN KA, O'BRIEN PC, MARSH WR (1992) Magnetic resonance image-based hippocampal volumetry: correlation with outcome after temporal lobectomy. *Ann Neurol*, **31**, 138-146.

JACK CR, JR. (1994) MRI-based hippocampal volume measurements in epilepsy. *Epilepsia*, **35**, S21-S29.

JACKSON GD, BERKOVIC SF, TRESS BM, KALNINS RM, FABINYI GCA, BLADIN PF (1990) Hippocampal sclerosis can be reliably detected by magnetic resonance imaging. *Neurology*, **40**, 1869-1875.

JACKSON GD, BERKOVIC SF, DUNCAN JS, CONNELLY A (1993a) Optimizing the diagnosis of hippocampal sclerosis using MR imaging. *AJNR*, **14**, 753-762.

JACKSON GD, CONNELLY A, DUNCAN JS, GRüNEWALD RA, GADIAN DG (1993b) Detection of hippocampal pathology in intractable partial epilepsy: increased sensitivity with quantitative magnetic resonance T2 relaxometry. *Neurology*, **43**, 1793-1799.

JACKSON GD, CONNELLY A, CROSS JH, GORDON I, GADIAN DG (1994a) Functional magnetic resonance imaging of focal seizures. *Neurology*, **44**, 850-856.

JACKSON GD, CROSS JH, CONNELLY A, NEVILLE BGR, GADIAN DG. (1994b) Hippocampal T2 relaxometry in intractable childhood epilepsy reveals a

substantial subgroup with severe bilateral hippocampal sclerosis. *Epilepsia*, **35**, 20 (Abstract).

JACKSON GD, KUZNIECKY RI, CASCINO GD (1994c) Hippocampal sclerosis without detectable hippocampal atrophy. *Neurology*, **44**, 42-46.

JACKSON GD, FITT GJ, MITCHELL LA, CHAMBERS BR, BERKOVIC SF. (1995) Hippocampal sclerosis developing in adults: progression of hippocampal MR findings. *Epilepsia*, **36**, S249 (Abstract).

JENSEN I, KLINKEN L (1976) Temporal lobe epilepsy and neuropathology: histological findings in resected temporal lobes correlated to surgical results and clinical aspects. *Acta Neurol Scand*, **54**, 391-414.

JUUL-JENSEN P, FOLDSPANG A (1983) Natural history of epileptic seizures. *Epilepsia*, **24**, 297-312.

KANDEL ER, SCHWARTZ JH (1991) Directly gated transmission at central synapses. In: *Principles of neural science*. Edited by ER Kandel, JH Schwartz, TM Jessell. New York: Elsevier. 153-172.

KAUPPINEN RA (1993) 1H nuclear magnetic resonance spectroscopy identifies neural cell types: a promising step for neuroimaging ? *TINS*, **16**, 384-386.

KIM JH, GUIMARAES PO, SHEN MY, MASUKAWA LM, SPENCER DD (1990) Hippocampal neuronal density in temporal lobe epilepsy with and without gliomas. *Acta Neuropathol*, **80**, 41-45.

KIM JH, TIEN RD, FELSBERG GJ, OSUMI AK, LEE N (1994) MR measurements of the hippocampus for lateralization of temporal lobe epilepsy: value of measurements of the body vs the whole structure. *AJR*, **163**, 1453-1457.

KIM JH, KRAEMER DL, SPENCER DD (1995a) The neuropathology of epilepsy. In: *Epilepsy*. Edited by A Hopkins, S Shorvon, G Cascino. London: Chapman & Hall Medical. 243-267.

KIM JH, TIEN RD, FELSBERG GJ, OSUMI AK, LEE N, FRIEDMAN AH (1995b) Fast spin-echo MR in hippocampal sclerosis: correlation with pathology and surgery. *AJNR*, **16**, 627-636.

KING D, SPENCER SS, MCCARTHY G, LUBY M, SPENCER DD (1995) Bilateral hippocampal atrophy in medial temporal lobe epilepsy. *Epilepsia*, **36**, 905-910.

KRISHNAN B, ARMSTRONG DL, GROSSMAN RG, ZHU ZQ, RUTECKI PA, MIZRAHI EM (1994) Glial cell nuclear hypertrophy in complex partial seizures. *J Neuropathol Exp Neurol*, **53**, 502-507.

KUKS JBM, COOK MJ, FISH DR, STEVENS JM, SHORVON SD (1993) Hippocampal sclerosis in epilepsy and childhood febrile seizures. *Lancet*, **342**, 1391-1394.

KUZNIECKY R, DE LA SAYETTE V, ETHIER R, MELANSON D, ANDERMANN F, BERKOVIC S, et al (1987) Magnetic resonance imaging in temporal lobe epilepsy: pathological correlations. *Ann Neurol*, **22**, 341-347.

KUZNIECKY R, BURGARD S, FAUGHT E, MORAWETZ R, BARTOLUCCI A (1993) Predictive value of magnetic resonance imaging in temporal lobe epilepsy surgery. *Arch Neurol*, **50**, 65-69.

KUZNIECKY RI, JACKSON GD (1995) *Temporal lobe epilepsy*. New York: Raven Press.

KWONG KK (1995) Functional magnetic resonance imaging with echo planar imaging. *Magn Reson Q*, **11**, 1-20.

LEE N, TIEN RD, LEWIS DV, FRIEDMAN AH, FELSBERG GJ, CRAIN B, et al (1995) Fast spin-echo, magnetic resonance imaging-measured hippocampal volume: correlation with neuronal density in anterior temporal lobectomy patients. *Epilepsia*, **36**, 899-904.

LENCZ T, MCCARTHY G, BRONEN RA, SCOTT TM, INSERNI JA, SASS KJ, et al (1992) Quantitative magnetic resonance imaging in temporal lobe epilepsy: relationship to neuropathology and neuropsychological function. *Ann Neurol*, **31**, 629-637.

LéVESQUE MF, NAKASATO N, VINTERS HV, BABB TL (1991) Surgical treatment of limbic epilepsy associated with extrahippocampal lesions: the problem of dual pathology. *J Neurosurg*, **75**, 364-370.

LORENTE DE Nó R (1934) Studies on the stucture of the cerebral cortex. II: Continuation of the study of the Ammonic system. *J Psychol Neurol*, **46**, 113-177.

LORING DW, LEE GP, MEADOR MD, MM M, L L, P P, et al (1990) The intracarotid amobarbital procedure as a predictor of memory failure following unilateral temporal lobectomy. *Neurology*, **40**, 605-610.

MAHER J, MCLACHLAN RS (1995) Febrile convulsions: is seizure duration the most important predictor of temporal lobe epilepsy ? *Brain*, **118**, 1521-1528.

MALDONADO HM, DELGADO-ESCUETA AV, WALSH GO, SWARTZ BE, RAND RW (1988) Complex partial seizures of hippocampal and amygdalar origin. *Epilepsia*, **29**, 420-433.

MARGERISON JH, CORSELLIS JAN (1966) Epilepsy and the temporal lobes. A clinical, electroencephalographic and neuropathological study of the brain in epilepsy with particular reference to the temporal lobes. *Brain*, **89**, 499-530.

MARKS DA, KIM J, SPENCER DD, SPENCER SS (1992) Characteristics of intractable seizures following meningitis and encephalitis. *Neurology*, **42**, 1513-1518.

MATHERN GW, BABB TL, VICKREY BG, MELENDEZ M, PRETORIUS JK (1995a) The clinical-pathogenic mechanisms of hippocampal neuron loss and surgical outcomes in temporal lobe epilepsy. *Brain*, **118**, 105-118.

MATHERN GW, PRETORIUS JK, BABB TL (1995b) Quantified patterns of mossy fiber sprouting and neuron densities in hippocampal and lesional seizures. *J Neurosurg*, **82**, 211-219.

MAYHEW TM (1992) A review of recent advances in stereology for quantifying neural structure. *J Neurocytol*, **21**, 313-328.

MAYHEW TM, OLSEN DR (1991) Magnetic resonance imaging (MRI) and Cavalieri estimates of brain volume. *J Anat*, **178**, 133-144.

MCMILLAN MK, THAI L, HONG JS, O'CALLAGHAN JP, PENNYPACKER KR (1994) Brain injury in a dish: a model for reactive gliosis. *TINS*, **17**, 138-142.

MEENCKE HJ (1985) Neuron density in the molecular layer of the frontal cortex in primary generalized epilepsy. *Epilepsia*, **26**, 450-454.

MEENCKE HJ (1994) Minimal developmental disturbances in epilepsy and MRI. In: *Magnetic resonance scanning and epilepsy*. Edited by SD Shorvon, DR Fish, F Andermann, G Bydder, H Stefan. New York: Plenum Press. 127-136.

MEENCKE HJ (1995) Pathological findings in childhood absence epilepsy. In: *Typical absences and related epileptic syndromes*. Edited by JS Duncan, CP Panayiotopoulos. London: Churchill Communications Europe. 122-132.

MEENCKE HJ, JANZ D (1984) Neuropathological findings in primary generalised epilepsies: a study of eight cases. *Epilepsia*, **25**, 8-21.

MEENCKE HJ, VEITH G (1991) Hippocampal sclerosis in epilepsy. In: *Epilepsy surgery*. Edited by HO Lüders. New York: Raven Press. 705-727.

MELDRUM BS, BRUTON CJ (1992) Epilepsy. In: *Greenfield's neuropathology*. Edited by J Hume, LW Duchen. London: Edward Arnold. 1246-1283.

MELLO LEAM, CAVALHEIRO EA, TAN AM, PRETORIUS JK, BABB TL, FINCH DM (1992) Granule cell dispersion in relation to mossy fiber sprouting, hippocampal cell loss, silent period and seizure frequency in the pilocarpine model of epilepsy. *Epilepsy Res*, **Suppl. 9**, 51-60.

MILLER LA, MUNOZ DG, FINMORE M (1993) Hippocampal sclerosis and human memory. *Arch Neurol*, **50**, 391-394.

MILLER LA, MCLACHLAN RS, BOUWER MS, HUDSON LP, MUNOZ DG (1994) Amygdalar sclerosis: preoperative indicators and outcome after temporal lobectomy. *J Neurol Neurosurg Psychiatry*, **57**, 1099-1105.

MILNER B, BRANCH C, RASMUSSEN T (1962) Study of short-term memory after intracarotid injection of Sodium Amytal. *Trans Am Neurol Ass*, **87**, 224-226.

MILNER B (1978) Clues to the cerebral organization of memory. In: *Cerebral correlates of conscious experience*. Edited by PA Buser, A Rougeul-Buser. Amsterdam: Elsevier/North Holland Biomedical Press. 139-153.

MOFFETT JR, ARYAN MA, NAMBOODIRI MAA, CANGRO CB, NEALE JH (1991) Immunohistochemical localization of N-acetylaspartate in rat brain. *Neuroreport*, **2**, 131-134.

MONAGHAN DT, HOLETS VR, TOY DW, COTMAN CW (1983) Anatomical distribution of four pharmacologically distinct 3H-L-glutamate binding sites. *Nature*, **306**, 176-179.

MUNOZ DG (1990) The distribution of chromogranin A-like immunoreactivity in the human hippocampus coincides with the pattern of resistance to epilepsy-induced neuronal damage. *Ann Neurol*, **27**, 266-275.

NADLER JV, PERRY BW, COTMAN CW (1978) Intraventricular kainic acid preferentially destroys hippocampal pyramidal cells. *Nature*, **271**, 676-677.

NEWTON MR, BERKOVIC SF, AUSTIN MC, ROWE CC, MCKAY WJ, BLADIN PF (1995) SPECT in the localisation of extratemporal and temporal seizure foci. *J Neurol Neurosurg Psychiatry*, **59**, 26-30.

NEWTON MR, BERKOVIC SF (1995) Ictal SPECT. In: *Recent advances in epilepsy*. Edited by TA Pedley, BS Meldrum. Edinburgh: Churchill Livingstone. 41-55.

NG TC, COMAIR YG, XUE M, SO N, MAJORS A, KOLEM H, et al (1994) Temporal lobe epilepsy: presurgical localisation with proton chemical shift imaging. *Radiology*, **193**, 465-472.

NIH CONSENSUS PANEL. (1990) Consensus conference on surgery for epilepsy. *JAMA*, **264**, 729-733.

NOEBELS JL (1996) Targeting epilepsy genes. *Neuron*, **16**, 241-244.

NOHRIA V, LEE N, TIEN RD, HEINZ ER, SMITH JS, DELONG GR, et al (1994) Magnetic resonance imaging evidence of hippocampal sclerosis in progression: a case report. *Epilepsia*, **35**, 1332-1336.

NORTON WT, AQUINO DA, HOZUMI I, CHIU FC, BROSNAN CF (1992) Quantitative aspects of reactive gliosis: a review. *Neurochem Res*, **17**, 877-885.

NORUSIS MJ (1993) *SPSS for Windows: base system user's guide, release 6.* USA: SPSS Inc.

O'CALLAGHAN JP (1993) Quantitative features of reactive gliosis following toxicant-induced damage of the CNS. *Ann N Y Acad Sci*, **679**, 195-210.

O'DONOGHUE M, SANDER JWAS (1996) Does early anti-epileptic drug treatment alter the prognosis for remission of the epilepsies ? *J R Soc Med*, **89**, 245-248.

OLNEY JW, RHEE V, HO OL (1974) Kainic acid: a powerful neurotoxic analogue of glutamate. *Brain Res*, **77**, 507-512.

OLNEY JW (1978) Neurotoxicity of excitatory amino acids. In: *Kainic acid as a tool in neurobiology*. Edited by EG McGeer, JW Olney, PL McGeer. New York: Raven Press. 95-121.

OLNEY JW, DE GUBAREFF T, LABRUYERE J (1983) Seizure-related brain damage induced by cholinergic agents. *Nature*, **301**, 520-522.

OLNEY JW, COLLINS RC, SLOVITER RS (1986) Excitotoxic mechanisms of epileptic brain damage. *Adv Neurol*, **44**, 857-877.

OORSCHOT DE (1994) Are you using neuronal densities, synaptic densities or neurochemical densities as your definitive data ? There is a better way to go. *Prog Neurobiol*, **44**, 233-247.

OUNSTED C, GLASER GH, LINDSAY J, RICHARDS P (1985) Focal epilepsy with mesial temporal sclerosis after acute meningitis. *Arch Neurol*, **42**, 1058-1060.

PENFIELD W (1933) The evidence for a cerebral vascular mechanism in epilepsy. *Ann Intern Med*, **7**, 303-310.

PENFIELD W, BALDWIN M (1952) Temporal lobe seizures and the technics of subtotal temporal lobectomy. *Ann Surg*, **136**, 625-634.

PENFIELD W, MATHIESON G (1974) Memory. Autopsy findings and comments on the role of hippocampus in experiential recall. *Arch Neurol*, **31**, 145-154.

PENFIELD W, MILNER B (1958) Memory deficit produced by bilateral lesions in the hippocampal zone. *Arch Neurol Psychiatry*, **79**, 475-497.

PITKäNEN A, LAAKSO M, KäLVIäINEN R, PARTANEN K, VAINIO P, LEHTOVIRTA M, et al (1996) Severity of hippocampal atrophy correlates with the prolongation of MRI T2 relaxation time in temporal lobe epilepsy but not in Alzheimer's disease. *Neurology*, **46**, 1724-1730.

PLATE KH, WIESER HG, YASARGIL MG, WIESTLER OD (1993) Neuropathological findings in 224 patients with temporal lobe epilepsy. *Acta Neuropathol Berl*, **86**, 433-438.

PLUMMER DL (1992) DispImage, a display and analysis tool for medical images. *Rev Neuroradiol*, **5**, 489-495.

PRINGLE CE, BLUME WT, MUNOZ DG, LEUNG LS (1993) Pathogenesis of mesial temporal sclerosis. *Can J Neurol Sci*, **20**, 184-193.

QUESNEY LF (1986) Clinical and EEG features of complex partial seizures of temporal lobe origin. *Epilepsia*, **27**, S27-S45.

RASMUSSEN T, FEINDEL W (1991) Temporal lobectomy: review of 100 cases with major hippocampectomy. *Can J Neurol Sci*, **18**, 601-602.

RAUSCH R, BABB TL (1993) Hippocampal neuron loss and memory scores before and after temporal lobe surgery for epilepsy. *Arch Neurol*, **50**, 812-817.

RAYMOND AA, FISH DR, STEVENS JM, COOK MJ, SISODIYA SM, SHORVON SD (1994) Association of hippocampal sclerosis with cortical dysgenesis in patients with epilepsy. *Neurology*, **44**, 1841-1845.

RAYMOND AA, FISH DR, SISODIYA SM, ALSANJARI N, STEVENS JM, SHORVON SD (1995) Abnormalities of gyration, heterotopias, tuberous sclerosis, focal cortical dysplasia, microdysgenesis, dysembryoplastic neuroepithelial tumour and dysgenesis of the archicortex in epilepsy. Clinical, EEG and neuroimaging features in 100 adult patients. *Brain*, **118**, 629-660.

REUTENS D, COOK M, KINGSLEY D. (1993) Volumetric MRI is essential for reliable detection of hippocampal asymmetry. *Epilepsia*, **34**, 138 (Abstract).

REYNOLDS EH, ELWES RDC, SHORVON SD (1983) Why does epilepsy become intractable ? Prevention of chronic epilepsy. *Lancet*, 952-954.

REYNOLDS EH (1987) Early treatment and prognosis of epilepsy. *Epilepsia*, **28**, 97-106.

REYNOLDS EH (1995) Do anticonvulsants alter the natural course of epilepsy ? Treatment should be started as early as possible. *Br Med J*, **310**, 176-177.

RIBAK CE, SERESS L, AMARAL DG (1985) The development, ultrastructure and synaptic connections of the mossy cells of the dentate gyrus. *J Neurocytol*, **14**, 835-857.

RIMMINGTON JE, PORTER DA. (1996) Anomalous T2 measurement behaviour using a slice selective phase alternating phase shift (PHAPS or CPMG/CP) sequence. *Proc Soc Magn Res*, 1561 (Abstract).

ROCCA WA, SHARBROUGH FW, HAUSER WA, ANNEGERS JF, SCHOENBERG BS (1987) Risk factors for complex partial seizures: a population-based case-control study. *Ann Neurol*, **21**, 22-31.

RUSH E, MORRELL MJ. (1993) Cortical dysplasia with mesiotemporal sclerosis: evidence for kindling in humans. *Epilepsia*, **34**, 15 (Abstract).

SAGAR HJ, OXBURY JM (1987) Hippocampal neuron loss in temporal lobe epilepsy: correlation with early childhood convulsions. *Ann Neurol*, **22**, 334-340.

SANDER JWAS (1993) Some aspects of prognosis in the epilepsies: a review. *Epilepsia*, **34**, 1007-1016.

SANO K, MALAMUD N (1953) Clinical significance of sclerosis of the cornu ammonis. *Arch Neurol Psychiatry*, **70**, 40-53.

SAPER CB (1996) Any way you cut it: a new journal policy for the use of unbiased counting methods. *J Comp Neurol*, **364**, 5

SASS KJ, WESTERVELD M, BUCHANAN CP, SPENCER SS, KIM JH, SPENCER DD (1994) Degree of hippocampal neuron loss determines severity of verbal memory decrease after left anteromesiotemporal lobectomy. *Epilepsia*, **35**, 1179-1186.

SAUKKONEN A, KäLVIäINEN R, PARTANEN K, VAINIO P, RIEKKINEN P, PITKäNEN A (1994) Do seizures cause neuronal damage? A MRI study in newly diagnosed and chronic epilepsy. *Neuroreport*, **6**, 219-223.

SCOVILLE WB, MILNER B (1957) Loss of recent memory after bilateral hippocampal lesions. *J Neurol Neurosurg Psychiatry*, **20**, 11-21.

SHORVON SD, REYNOLDS EH (1982) Early prognosis of epilepsy. *Br Med J*, **285**, 1699-1701.

SIMMONS ML, FRONDOZA CG, COYLE JT (1991) Immunocytochemical localization of N-acetyl-aspartate with monoclonal antibodies. *Neuroscience*, **45**, 37-45.

SLOVITER RS (1987) Decreased hippocampal inhibition and a selective loss of interneurons in experimental epilepsy. *Science*, **235**, 73-76.

SLOVITER RS (1991) Permanently altered hippocampal structure, excitability, and inhibition after experimental status epilepticus in the rat: the "dormant basket cell" hypothesis and its possible relevance to temporal lobe epilepsy. *Hippocampus*, **1**, 41-66.

SLOVITER RS, SOLLAS AL, BARBARO NM, LAXER KD (1991) Calcium-binding protein (calbindin-D28K) and parvalbumin immunocytochemistry in the normal and epileptic human hippocampus. *J Comp Neurol*, **308**, 381-396.

SLOVITER RS (1994) The functional organization of the hippocampal dentate gyrus and its relevance to the pathogenesis of temporal lobe epilepsy. *Ann Neurol*, **35**, 640-654.

SLOVITER RS, BRISMAN JL (1995) Lateral inhibition and granule cell synchrony in the rat hippocampal dentate gyrus. *J Neurosci*, **15**, 811-820.

SMITH ML, MILNER B (1981) The role of the right hippocampus in the recall of spatial location. *Neuropsychologia*, **19**, 781-793.

SO N, GLOOR P, QUESNEY LF, JONES-GOTMAN M, OLIVIER A, ANDERMANN F (1989) Depth electrode investigations in patients with bitemporal epileptiform abnormalities. *Ann Neurol*, **25**, 423-431.

SOMMER W (1880) Erkrankung des Ammonshorns als aetiologisches Moment der Epilepsie. *Arch Psychiatr Nervenkr*, **10**, 631-675.

SPENCER SS, MCCARTHY G, SPENCER DD (1993) Diagnosis of medial temporal lobe seizure onset: relative specificity and sensitivity of quantitative MRI. *Neurology*, **43**, 2117-2124.

SPENCER SS (1995) MRI and epilepsy surgery. *Neurology*, **45**, 1248-1250.

SPENCER SS (1996) Long-term outcome after epilepsy surgery. *Epilepsia*, **37**, 807-813.

SPERK G, LASSMANN H, BARAN H, KISH SJ, SEITELBERGER F, HORNYKIEWICZ O (1983) Kainic acid induced seizures: neurochemical and histopathological changes. *Neurosci*, **10**, 1301-1315.

SPERLING MR, WILSON C, ENGEL JJ, BABB TW, PHELPS M, BRADLEY W (1986) Magnetic resonance imaging in intractable partial epilepsy: correlative studies. *Ann Neurol*, **20**, 57-62.

SPIELMEYER W (1927) Die Pathogenese des epileptischen Krampfes. *Z Dtsch Ges Neurol Psychiatr*, **109**, 501-520.

STERIO DC (1984) The unbiased estimation of number and sizes of arbitrary particles using the disector. *J Microsc*, **134**, 127-136.

SUTULA T, HARRISON C, STEWARD O (1986) Chronic epileptogenesis induced by kindling in the entorhinal cortex: the role of the dentate gyrus. *Brain Res*, **385**, 291-299.

SUTULA T, CASCINO G, CAVAZOS J, PARADA I, RAMIREZ L (1989) Mossy fiber synaptic reorganization in the epileptic human temporal lobe. *Ann Neurol*, **26**, 321-330.

SUTULA TP (1990) Experimental models of temporal lobe epilepsy: new insights from the study of kindling and synaptic reorganization. *Epilepsia*, **31 Suppl 3**, S45-54.

TANAKA S, TANAKA T, KONDO S, HORI T, FUKUDA H, YONEMASU Y, et al (1993) Magnetic resonance imaging in kainic acid-induced limbic seizure status in cats. *Neurol Med Chir Tokyo*, **33**, 285-289.

TEITELBAUM JS, ZATORRE RJ, CARPENTER S, GENDRON D, EVANS AC, GJEDDE A, et al (1990) Neurologic sequelae of domoic acid intoxication due to the ingestion of contaminated mussels. *N Engl J Med*, **322**, 1781-1787.

THADANI VM, WILLIAMSON PD, BERGER R, SPENCER SS, SPENCER DD, NOVELLY RA, et al (1995) Successful epilepsy surgery without intracranial EEG recording: criteria for patient selection. *Epilepsia*, **36**, 7-15.

TIEN RD, FELSBERG GJ (1995) The hippocampus in status epilepticus: demonstration of signal intensity and morphologic changes with sequential fast spin-echo MR imaging. *Radiology*, **194**, 249-256.

TRENERRY MR, JACK CR, JR., IVNIK RJ, SHARBROUGH FW, CASCINO GD, HIRSCHORN KA, et al (1993a) MRI hippocampal volumes and memory function before and after temporal lobectomy. *Neurology*, **43**, 1800-1805.

TRENERRY MR, JACK CR, JR., SHARBROUGH FW, CASCINO GD, HIRSCHORN KA, MARSH WR, et al (1993b) Quantitative MRI hippocampal volumes: association with onset and duration of epilepsy, and febrile convulsions in temporal lobectomy patients. *Epilepsy Res*, **15**, 247-252.

URENJAK J, WILLIAMS SR, GADIAN DG, NOBLE M (1993) Proton nuclear magnetic resonance spectroscopy unambiguously identifies different neural cell types. *J Neurosci*, **13**, 981-989.

VAINIO P, USENIUS JP, VAPALAHTI M, PARTANEN K, KäLVIäINEN R, RINNE J, et al (1994) Reduced N-acetylaspartate concentration in temporal lobe epilepsy by quantitative 1H MRS in vivo. *Neuroreport*, **5**, 1733-1736.

VAN HOESEN GW (1995) Anatomy of the medial temporal lobe. *Magn Res Imag*, **13**, 1047-1055.

VAN PAESSCHEN W, CONNELLY A, JOHNSON CL, DUNCAN JS. (1995a) Clinical and pathological correlations of amygdala T2 mapping. *Epilepsia*, **36**, 247 (Abstract).

VAN PAESSCHEN W, CONNELLY A, JOHNSON CL, DUNCAN JS. (1995b) Bilateral hippocampal sclerosis: a quantitative MRI study. *Proc Soc Magn Res*, **2**, 1231 (Abstract).

VAN PAESSCHEN W, REVESZ T, SISODIYA S, CONNELLY A, JACKSON GD, DUNCAN JS. (1995c) Quantitative neuropathology and quantitative magnetic

resonance imaging of the hippocampus of patients with intractable temporal lobe epilepsy. *Epilepsia*, **36**, S96 (Abstract).

VAN PAESSCHEN W, SISODIYA S, CONNELLY A, DUNCAN JS, FREE SL, RAYMOND AA, et al (1995d) Quantitative hippocampal MRI and intractable temporal lobe epilepsy. *Neurology*, **45**, 2233-2240.

VAN PAESSCHEN W, CONNELLY A, DUNCAN JS, JOHNSON CL, PORTER DA, GADIAN DG. (1996a) Single voxel 1H Magnetic Resonance Spectroscopy in patients with MRI-negative intractable temporal lobe epilepsy. *Proc Soc Magn Res*, **1**, 139 (Abstract).

VAN PAESSCHEN W, CONNELLY A, JOHNSON CL, DUNCAN JS (1996b) The amygdala and intractable temporal lobe epilepsy: a quantitative magnetic resonance imaging study. *Neurology*, **47**, 1021-1031.

VAN PAESSCHEN W, DUNCAN JS, CONNELLY A. (1996c) Progression of hippocampal disease in newly diagnosed localization-related epilepsy: a longitudinal quantitative MRI study. *Epilepsia*, **37**, 191 (Abstract).

VAN PAESSCHEN W, REVESZ T, CONNELLY A, DUNCAN JS. (1996d) Quantitative MRI of the hippocampus: neuropathological validation. *Epilepsia*, **37**, 24 (Abstract).

VAN PAESSCHEN W, CONNELLY A, KING MD, JACKSON GD, DUNCAN JS (1997) The spectrum of hippocampal sclerosis: a quantitative magnetic resonance imaging study. *Ann Neurol*, **41**, 41-51.

VANLANDINGHAM KE, TIEN RD, CAVAZOS JE, HEINZ ER, LEWIS DV. (1996) MRI hippocampal volume and signal abnormalities following complex febrile convulsions. *Epilepsia*, **37**, 113 (Abstract).

VITAL A, MARCHAL C, LOISEAU H, ROUGIER A, PEDESPAN JM, RIVEL J, et al (1994a) Glial and neuronoglial malformative lesions associated with medically intractable epilepsy. *Acta Neuropathol*, **87**, 196-201.

VITAL A, RIVEL J, LOISEAU H, MARCHAL C, ROUGIER A, VITAL C (1994b) Histopathologie de 110 cortectomies pour epilepsie pharmacoresistante. *Rev Neurol Paris*, **150**, 33-38.

VOGT O (1925) Der Begriff der Pathoklise. *J Psychol Neurol (Leipzig)*, **31**, 245-255.

WALCZAK TS (1995) Neocortical temporal lobe epilepsy: characterizing the syndrome. *Epilepsia*, **36**, 633-635.

WALKER MC, SANDER JWAS (1996) The impact of new antiepileptic drugs on the prognosis of epilepsy: seizure freedom should be the ultimate goal. *Neurology*, **46**, 912-914.

WARACH S, IVES JR, SCHLAUG G, PATEL MR, DARBY DG, THANGARAJ V, et al (1996) EEG-triggered echo-planar functional MRI in epilepsy. *Neurology*, **47**, 89-93.

WATSON C, ANDERMANN F, GLOOR P, JONES GOTMAN M, PETERS T, EVANS A, et al (1992) Anatomic basis of amygdaloid and hippocampal volume measurement by magnetic resonance imaging. *Neurology*, **42**, 1743-1750.

WEST MJ, GUNDERSEN HJG (1990) Unbiased stereological estimation of the number of neurons in the human hippocampus. *J Comp Neurol*, **296**, 1-22.

WIESER HG (1988) Human limbic seizures: EEG studies, origin, and patterns of spread. In: *Anatomy of epileptogenesis*. Edited by BS Meldrum. London: John Libbey. 127-138.

WIESER HG (1991) Ictal manifestations of temporal lobe epilepsy. In: *Advances in neurology*. Edited by D Smith, D Treiman, M Trimble. New York: Raven Press. 301-315.

WIESER HG, YASARGIL MG (1982) Selective amygdalohippocampectomy as a surgical treatment of mesiobasal limbic epilepsy. *Surg Neurol*, **17**, 445-457.

WILLIAMS RW, RAKIC P (1988) Three-dimensional counting: an accurate and direct method to estimate numbers of cells in sectioned material. *J Comp Neurol*, **278**, 344-352.

WILLIAMSON PD, FRENCH JA, THADANI VM, KIM JH, NOVELLY RA, SPENCER SS, et al (1993) Characteristics of medial temporal lobe epilepsy: interictal and ictal scalp electroencephalography, neuropsychological testing, neuroimaging, surgical results, and pathology. *Ann Neurol*, **34**, 781-787.

WOLF HK, CAMPOS MG, ZENTNER J, HUFNAGEL A, SCHRAMM J, ELGER CE, et al (1993) Surgical pathology of temporal lobe epilepsy. Experience with 216 cases. *J Neuropathol Exp Neurol*, **52**, 499-506.

WOLF HK, WIESTLER OD (1993) Surgical pathology of chronic epileptic seizure disorders. *Brain Pathol*, **3**, 371-380.

WYLER AR, DOHAN FC, SCHWEITZER JB, BERRY AD (1992) A grading system for mesial temporal pathology (hippocampal sclerosis) from anterior temporal lobectomy. *J Epilepsy*, **5**, 220-225.

YAFFE K, FERRIERO D, BARKOVICH AJ, ROWLEY H (1995) Reversible MRI abnormalities following seizures. *Neurology*, **45**, 104-108.

ZENTNER J, HUFNAGEL A, WOLF HK, OSTERTUN B, BEHRENS E, CAMPOS MG, et al (1995) Surgical treatment of temporal lobe epilepsy: clinical, radiological, and histopathological findings in 178 patients. *J Neurol Neurosurg Psychiatry*, **58**, 666-673.

ZOLA-MORGAN S, SQUIRE LR, AMARAL DG (1989) Lesions of the amygdala that spare adjacent cortical regions do not impair memory or exacerbate the impairment following lesions of the hippocampal formation. *J Neurosci*, **9**, 1922-1936.

Appendix A

Legend: initials: initials of the patient; hospital number: National Hospital for Neurology hospital number; Gend = gender; M = man, W = woman; Categ = category; Category: 1: patient with localization-related epilepsy, 0: control subject; Ch 3, Ch 4, Ch 5, Ch 6, Ch 7, Ch 8, Ch 9: Chapter 3, 4, 5, 6, 7, 8, 9: x indicates which patients were used for a particular study; MRI: hard disk on which MRI is stored at the Great Ormond Street Hospital.

Initials	Hospital number	Gend	Categ	Ch. 3	Ch. 4	Ch. 5	Ch. 6	Ch. 7	Ch. 8	Ch. 9	MRI
P.K.	QSB85154	M	1	x		x					V2A
D.F.	MVC 06063	W	1	x		x					V2B
A.W.	QSB36976	W	1	x		x					V2B
K.L.	MVP20497	W	1	x		x					V2B
G.L.	QSC10954	W	1	x		x					V2B
H.O.	QSB91555	W	1	x		x					V2B
A.S.	MVC05847	M	1	x		x					V2A
G.P.	MV 99857	M	1	x		x					V3A
M.C.	MVP 23055	W	1	x		x					V1B
C.P.	B71679	M	1	x		x					V2A
R.T.	QSB82506	M	1	x		x					V1B
S.C.	MVC14609	W	1	x		x					AR1
J.H.	MVP21487	W	1	x		x					V2B
D.L.	QSB64404	M	1	x		x					AR1
P.W.	QSC04082	W	1	x		x					V2B
K.A.	QSB 93870	W	1	x		x					V2B
K.M.	MVC07277	M	1	x		x					V2B
A.B.	MVP24607	M	1	x		x					V3A
J.H.	MVP24605	W	1	x							V2B
L.G.	QSB97295	W	1	x							V2A
E.K.	B99878	M	1	x							V2B
L.B.	QSC02138	W	1	x							V4A
V.H.	QSB92230	W	1	x							V1B
K.L.	QSB 36531	W	1	x							V2A
K.C.	QSB00779	W	1	x							V2B
N.A.	QSB92544	M	1	x							V1B
M.B.	QSB76280	M	1	x							AR1A
S.M.	QSC13498	W	1	x	x	x			x		AR2A
C.G.	QSB89363	W	1	x	x	x			x		AR2A
J.M.	MVP13421	M	1	x	x	x			x		AR1A
J.P.	QSA34752	W	1	x	x	x			x		V4A
N.S.	QSA83367	M	1	x	x	x					AR1B
R.N.	MV95228	M	1	x	x	x					AR1B
E.D.	MVP06823	W	1	x	x	x					AR1B
L.T.	QSC13829	W	1	x	x	x					AR2A
C.C.	QSB48898	W	1	x	x	x					AR1
T.E.	QSC22940	W	1	x	x				x		AR1B
A.H.	MVC20080	W	1	x	x				x		AR1B
R.S.	MVC09566	M	1	x	x						AR1A
S.B.	QSC00388	W	1	x	x						AR1A
D.B.	QSA58244	W	1			x					Wrm1A

L.F.	QSC28566	W	1	x			
S.W.	QSC58148	W	1	x			
K.C.	QSB00779	W	1	x			
J.A.	CX802336	W	1		x	x	AR2B
J.G.	CX492573	W	1		x		AR2A
J.M.	W267794	W	1		x	x	FVKRB
S.M.	CX803715	W	1		x	x	AR2B
A.S.	QSC25404	M	1		x	x	AR2B
J.B.	QSC26534	W	1		x	x	AR2B
M.C.	QSC27119	W	1		x		AR2B
C.M.	CX802641	W	1		x	x	AR2B
C.C.		M	1		x		AR1A
A.M.	QSC26386	M	1		x		AR2B
T.B.	CX802660	M	1		x	x	AR2B
R.R.	CX795452	W	1		x		AR2B
J.H.	QSC27474	W	1		x	x	AR2B
J.B.	CX810851	W	1		x	x	AR2B
C.S.	CX803723	M	1		x		AR2B
S.W.	CX810161	M	1		x		AR2B
A.S.		M	1		x		AR3A
P.C.	MVC21216	M	1		x		AR1B
E.H.		W	1		x		V3A
A.V.		M	1		x	x	AR1A
F.M.		M	1		x	x	V4B
R.G.		M	1		x		FVKRB
M.E.		M	1		x		AR1A
M.D.		M	1		x		AR1B
J.E.		M	1		x		
S.D.	QSC 16548	W	1		x	x	AR1A
D.C.	QSC17456	W	1		x	x	VA4
S.A.	QSC17386	W	1		x		
M.M.	QSC18108	M	1		x	x	AR1B
P.W.		M	1		x	x	AR1B
C.W.		M	1		x	x	AR1B
O.S.		M	1		x	x	AR1B
G.L.		M	1		x		AR1B
B.I.		M	1		x	x	AR2A
D.D.	CX802006	M	1		x	x	AR2B
L.P.	QSC23328	W	1		x		AR2A
J.O.	QSC23870	M	1		x		AR2A
S.B.	CX784946	W	1		x	x	AR1A
S.M.		M	1		x	x	AR1B
B.C.	QSC22158	W	1		x		AR2B
C.K.	QSC18500	M	1		x		AR1B
E.H.	QSC24391	M	1		x		V4B
M.J.		M	1		x	x	AR1B
D.S.		W	1		x		AR1B
M.M.	CX788901	W	1		x	x	AR1A
A.S.	CX781159	W	1		x	x	AR1A
C.K.	MVC14020	W	1		x	x	AR1B
C.N.		W	1		x	x	AR2A
J.S.	QSC24630	W	1		x		V3A
L.C.		W	1		x	x	V3A
A.R.	QSC29737	W	1		x		V4B
R.R.	W818063	W	1		x	x	V3A

J.J.		W	1			x	x			V4B
Z.R.	QSC28490	W	1			x	x			V4B
I.D.	QSC29190	M	1			x				VB4
D.B.		M	1			x	x			V4B
J.H.	QSC30963	M	1			x				V3A
N.C.	QSC30152	W	1			x				V4B
J.D.	QSB50619	M	1					x		46A
N.H.	QSC32643	W	1					x		CP-B
D.M.	MVC20738	W	1					x		FVKRB
A.D.	QSC33075	M	1					x		FVKRB
C.V.	QSC28964	W	1					x		46A
C.B.	QSC38461	W	1					x	x	CP-B
T.B.	QSB94839	W	1					x		FVKRB
G.H.	A93520	W	1		x					V1A
A.W.	MVC 12279	M	1		x					AR1
L.V.	QSB58226	M	1		x					V2A
D.B.	QSB59961	W	1		x					V1A
D.D.	MP23340	M	1		x					V2A
P.P.	A51942	W	1		x					V1A
R.L.		W	1			x	x			V3A
R.T.		M	1			x	x			AR1A
R.D.	QSC15601	M	1			x	x			AR1
K.D.	QSC28724	W	1					x		FVKRB
W.S.	QSC25407	W	1					x		FVKRB
A.H.	QSB17400	M	1	x	x			x		V3A
G.C.	QSC10874	W	1	x	x			x		V3A
S.M.	QSC23220	W	1	x	x			x		V3A
P.W.	MV47675	M	1	x	x			x		SDB
P.C.	QSC24120	W	1	x	x			x		V3A
T.K.	MVC14031	W	1	x	x			x		V4A
N.M.	QSC25336	W	1	x	x			x		V3A
A.H.	QSB92575	W	1	x	x			x		AR2A
F.P.	MVC 11255	M	1	x	x			x		AR2A
S.C.	QSB90962	M	1	x	x			x		V4B
M.T.	QSC25216	W	1	x	x			x		FVK-RB
L.K.Y.	QSC23221	W	1	x	x			x		V3A
A.C.	MVP24943	W	1	x				x		V4A
K.M.	MVP17779	W	1	x	x			x		V4A
S.L.	QSB78001	W	1	x	x			x		AR2B
T.K.	QSC15345	W	1	x	x			x		V4A
S.B.	QSC22465	M	1	x	x			x		V4A
D.M.	QSC25408	M	1	x	x					FVKRB
P.D.	MVC12731	M	1	x	x					AR2
G.W.	MVC17357	M	1	x	x					AR2
M.B.	QSB68324	W	1	x	x					V3A
R.H.	MV38101	M	1	x	x					V4B
E.M.	QSC24608	W	1	x		x	x	x		AR2B
D.C.	QSC27812	W	1	x		x	x	x		AR2B
A.B.	QSC15042	M	1	x				x		AR2
M.B.	QSA97347	M	1	x				x		AR2B
J.S.	QSC18721	M	1	x				x		AR2
J.C.	A04671	W	1	x				x		AS2
R.M.	QSC32158	M	1	x				x		FVKRB
P.H.		M	1	x				x		FVKRB

D.L.	QSC23479	M	1	x	x		V4A
A.B.	QSC28306	M	1	x	x		
S.M.	QSB92221	W	1	x	x		AR2A
P.B.	QSC22926	W	1	x	x		AR2B
G.H.	QSC24488	M	1	x	x		FVKRB
S.C.		W	1	x	x	x	V4A
J.D.	MVP23032	W	1	x	x		FVKRB
D.F.	QSB38167	M	1	x	x		V4A
C.M.	QSB00577	W	1	x	x		V4A
B.M.	QSB71558	W	1	x	x		AR2B
I.P.	MVC16347	M	1	x	x		ARBU
J.L.	QSC14322	W	1	x	x		FVKRB
M.H.	QSC23695	W	1	x	x		V4A
J.H.	QSC23691	W	1	x	x		AR2B
J.J.	QSB62546	W	1	x	x		AR1B
P.G.	QSC30562	M	1	x	x		FVKRB
P.B.	QSC28562	M	1	x	x		FVKRB
L.F.	QSB88547	W	1	x	x		AR1A
J.T.	MV90280	W	1	x	x		VB4
P.G.	QSC28503	M	1	x	x		FVKRB
G.B.	QSA89114	W	1	x	x		AR1
S.B.	QSC15454	W	1	x	x	x	V4A
P.M.	MVC21566	M	1	x	x	x	V4B
S.B.	QSC24635	W	1	x	x		V3A
D.J.	QSA77724	M	1	x	x		V4B
S.P.	QSB33045	M	1	x	x		V3A
D.T.	MVP12799	M	1	x	x		V4B
M.H.	QSB98961	M	1	x	x	x	V3A
T.C.	QSC15490	M	1	x	x		V3A
T.H.	MVP13745	M	1	x	x		VB4
K.B.	MVP23016	M	1	x	x		V3A
P.B.	QSC30136	M	1	x	x		V3A
R.S.	QSB10061	M	1	x	x		V4B
C.H.	QSB63341	M	1	x	x		AR2B
H.T.	QSC30548	W	1	x	x		V3A
T.W.	MVP20469	W	1	x	x		FVKRB
S.W.	QSC12128	W	1	x	x		V4B
D.R.	QSC26823	W	1	x	x		V3A
R.W.	QSB18240	M	1	x	x		V4A
T.K.	QSC23971	M	1	x	x	x	V3A
R.S.	QSB77838	M	1	x	x		V3A
C.W.	MVC07274	W	1	x	x	x	FVKRB
D.J.	MVC06745	M	1	x			V2B
T.R.	QSA83773	M	1	x			V4B
K.C.	QSC29562	W	1	x			V3A
C.G.	QSC18458	W	1	x			AR1B
M.W.	QSC27808	W	1	x			V3A
D.C.	QSC10307	M	1	x			AR2B
H.H.	MVC17788	W	1	x			V3A
A.W.	QSC14874	M	1	x			AR2B
S.O.	QSB31053	W	1	x			FVKRB
T.G.	QSC37619	W	1	x			FVKRB
J.R.	B50606	W	1	x			AR1B
S.W.	MVP 18163	M	1	x			V4A
J.R.	MVC15457	W	1	x			AR2

J.S.	MVC13148	W	1	x				AR2
M.H.	QSC34154	W	1	x				FVKRB
S.N.		W	0		x			
R.D.L.		W	0		x			
O.		M	0		x			
B.A.		M	0		x			
		W	0		x			
Y.A.		M	0		x			
V.H.		W	0			x	Y	V4B
A.C.		M	0			x		S1B
C.J.		W	0			x		S1B
C.B.		W	0			x		
K.W.		W	0				x	AR2B
M.G.		M	0				x	
N.P.		M	0	x		x	x	AR2A
G.P.		W	0	x		x	x	AR2A
A.W.		M	0	x		x	x	AR2A
A.B.		W	0	x		x	x	AR2A
C.H.		W	0	x		x	x	AR2A
G.S.		M	0	x		x	x	AR1B
R.E.		M	0	x		x	x	AR1B
C.B.		W	0	x		x	x	AR2A
L.N.		M	0	x			x	AR2A
S.F.		M	0	x			x	AR1B
C.M.		W	0	x			x	AR2A
M.S.		M	0	x			x	AR2A
K.S.		W	0	x			x	AR2B
P.O.		M	0	x			x	AR2A
K.B.		W	0	x			x	AR2A
L.L.		W	0	x			x	AR2B
A.F.		W	0	x			x	AR2A
R.G.		M	0	x				
L.T.		W	0	x				AR1A1
L.N.		W	0	x				ARBuB
N.V.		W	0	x				AR1A